AD NUMBER
AD881610
LIMITATION CHANGES
TO: **Approved for public release; distribution is unlimited.**
FROM: **Distribution authorized to U.S. Gov't. agencies and their contractors; Critical Technology; JAN 1971. Other requests shall be referred to Army Air Mobility Research and Development Laboratory, Fort Eustis, VA 23604. This document contains export-controlled technical data.**
AUTHORITY
USAAML ltr, 23 Apr 1971

USAAVLABS TECHNICAL REPORT 70-66

MODE OF FAILURE INVESTIGATIONS OF HELICOPTER TRANSMISSIONS

By

C. W. Bowen
L. L. Dyson
R. D. Walker

January 1971

EUSTIS DIRECTORATE
U. S. ARMY AIR MOBILITY RESEARCH AND DEVELOPMENT LABORATORY
FORT EUSTIS, VIRGINIA

CONTRACT DAAJ02-69-C-0061
BELL HELICOPTER COMPANY
FORT WORTH, TEXAS

364

Disclaimers

The findings in this report are not to be construed as an official Department of the Army position unless so designated by other authorized documents.

When Government drawings, specifications, or other data are used for any purpose other than in connection with a definitely related Government procurement operation, the United States Government thereby incurs no responsibility nor any obligation whatsoever; and the fact that the Government may have formulated, furnished, or in any way supplied the said drawings, specifications, or other data is not to be regarded by implication or otherwise as in any manner licensing the holder or any other person or corporation, or conveying any rights or permission, to manufacture, use, or sell any patented invention that may in any way be related thereto.

Trade names cited in this report do not constitute an offical endorsement or approval of the use of such commercial hardware or software.

Disposition Instructions

Destroy this report when no longer needed. Do not return it to the originator.

DEPARTMENT OF THE ARMY
EUSTIS DIRECTORATE
U.S. ARMY AIR MOBILITY RESEARCH AND DEVELOPMENT LABORATORY
FORT EUSTIS, VIRGINIA 23604

This report represents a continuing effort to review and analyze the causes of transmission failures to determine those areas requiring research to derive the design technology necessary to produce more reliable helicopter transmission systems. Presented herein are the results of a comprehensive effort to evaluate and analyze two existing Army transmission systems, in overhaul at USARADMAC, Corpus Christi, Texas. The major contributing factors which prohibit the continuous use of components are identified herein.

This directorate concurs with the findings reported herein.

Task 1G162203D14414
Contract DAAJ02-69-C-0061
USAAVLABS Technical Report 70-66
January 1971

MODE OF FAILURE INVESTIGATIONS OF HELICOPTER TRANSMISSIONS

Bell Helicopter Report 299-099-479

By

C. W. Bowen
L. L. Dyson
R. D. Walker

Prepared by

BELL HELICOPTER COMPANY
Fort Worth, Texas

for

EUSTIS DIRECTORATE
U.S. ARMY AIR MOBILITY RESEARCH AND DEVELOPMENT LABORATORY
FORT EUSTIS, VIRGINIA

SUMMARY

This report presents the results of a program of review and analysis of failed parts rejected during UH-1 and CH-47 transmission overhaul at ARADMAC. The program was conducted to identify the modes of failure and to reveal areas requiring additional research or development to improve engineering design capability.

Rejected components were inspected and relevant failure data entered on log sheets by an on-site inspection team comprised of BHC transmission design and test engineers. Primary failure components as well as the log sheets were forwarded to BHC for further evaluation.

Log sheet data were keypunched and entered into a computer storage file. A second file of pertinent operational characteristics and design data was established from analytical review of the detail design drawings. Various interrogative computer programs were employed for correlation studies between these two data files.

The review and analysis included:

- The statistical treatment of observed failure rates.
- Metallurgical and metrological examination of failed components.
- Identification of failure modes.
- Correlation testing of failure rates with accepted stress indices and design techniques.
- The comparison of real failure modes with those predicted by diagnostic methods used at time of non-scheduled transmission removals.
- The examination of failure modes with respect to tribological considerations.
- The evaluation of relative quality control levels as they influence generic failures.

The study revealed that overhaul life is limited by a small number of gears, bearings, and spacers whose characteristic failure rates exceed the mean by over an order of magnitude. While this fact suggests that longer periods of operation could be expected after design improvements in these components, it was also shown that conventional design methods appear inadequate to predict life in these cases. Recommendations for improving design methods and development testing techniques are included.

FOREWORD

This report presents the results of a study conducted by Bell Helicopter Company (BHC) for the Eustis Directorate, U. S. Army Air Mobility Research and Development Laboratory under contract DAAJ02-69-C-0061 (Task 1G162203D14414). The study was based upon investigations performed on selected Bell UH-1 and Vertol CH-47 helicopter transmissions during overhaul at the U. S. Army Overhaul Facility, ARADMAC, Corpus Christi, Texas.

USAAVLABS technical direction was provided by Mr. Wayne A. Hudgins.

Principal investigators at BHC were Mr. L. L. Dyson, Mr. R. D. Walker, and Mr. C. W. Bowen. Mr. Dyson was project engineer for the study.

The on-site inspection team at ARADMAC consisted of Messrs. F. A. Green, C. A. Turner, J. H. Drennan, and D. J. Ward of the BHC Transmission Design Group.

Metallurgical studies were principally conducted by Mr. P. A. Finn and Mr. M. L. Marx of the Transmission Process Laboratories of BHC. Supporting analyses were performed by Battelle Memorial Institute, The Fafnir Bearing Company, and Wear Check International. Acknowledgement for technical contribution is also due Mr. T. Mundheim of the BHC Engineering Computing Group.

TABLE OF CONTENTS

Page

APPENDIXES

LIST OF ILLUSTRATIONS

Figure		Page

Figure		Page

LIST OF TABLES

INTRODUCTION

Transmission system components represent a major cost item in the overall life cycle of Army helicopters. Components now in service have scheduled overhaul periods (TBO) of from 600 to 1600 hours, with the largest population near the 1100- to 1200-hour interval. However, the mean time to removal and hence overhaul (MTBR) for selected units range from several hundred to near fifteen hundred hours with a probable mean population in the 900-hour level, far short of the airframe life cycle. Average time on UH-1D airframes undergoing overhaul at the Army's major overhaul facility at Lake Charles, Louisiana, is approximately 3300 hours. Since many of the transmission components undergo complete life cycles of numerous overhauls, it is not unreasonable to expect attainment of several thousand hours MTBR's through improvement of capabilities in selected areas. Technological improvements in transmission design which could increase overhaul life would greatly reduce the helicopter life cycle cost to the Army.

Such improvements cannot be accomplished in future helicopters without access to improved stress-life functions and design techniques. These improvements are necessary not only for increased design life capability but to increase the confidence levels as well, so that rapid attainment of specified TBO levels can be implemented.

All of the transmissions operating at today's TBO level were introduced into service at far lower levels and were periodically increased as service experience dictated that adequate confidence levels were attained. The deliberate design and development of a transmission to achieve the required TBO at time of introduction has heretofore not been accomplished.

The objectives of this program are to identify failure modes and to cite specific design technology disciplines which restrict overhaul lives and are consequently in need of research-fostered advances in order to permit the attainment of greatly increased overhaul periods in future generation helicopters. Additional subtasks involve the identification of failure modes, the generation of failure rates, and the testing of those rates for correlation with accepted design methods.

The task of obtaining documentation for identifying life-limiting factors was implemented through comprehensive inspection of transmissions as received for overhaul at the Army's overhaul facility, USARADMAC, Corpus Christi, Texas.

Components considered for this report were Bell UH-1 main transmissions and Vertol CH-47 forward, aft, and combining transmissions. An on-site team from BHC was selected and trained to conduct this phase of the program. The on-site team was familiarized with types of transmissions to be studied and the types of failures to be expected.

The team spent five months at the ARADMAC facility collecting data and representative failed parts, which were subsequently returned to BHC for analysis.

The representative failed parts were selectively distributed to BHC Process Laboratory, Battelle Institute, and Fafnir Bearing Company for detailed failure and metallurgical analysis for later correlation with analytical predictions of failure modes.

An engineering design analysis of the gear and bearing elements in each transmission was performed based on operating power conditions. The resulting stress-life predictions were then cataloged in the computerized file.

The final task of identifying areas of design technology that proved to be inadequate for predicting accurate stress-life relationships was implemented through statistical analysis of failure information in comparison to calculated predictions.

The transmissions selected for review were those used in the Bell UH-1 (Figure 1) and Vertol CH-47 (Figure 2), since they alone were available in sufficient sample size to place the necessary confidence in statistical evaluation of the observations. The ARADMAC facility, Corpus Christi, Texas, was selected for the overhaul survey in order to provide the best statistical data from the Army-user standpoint. Although the Bell Helicopter Company and the Vertol Division of the Boeing Company perform in-house overhaul of these same components, the data extracted at these facilities must to some degree be influenced by environmental factors not present at ARADMAC.

Detailed information about the condition of each component part in each transmission was recorded and cataloged. The cataloged information subsequently was entered on a computerized file system designed for rapid information retrieval.

A concurrent effort resulted in a parallel computerized file, which comprised engineering design data relative to each bearing and gear element involved in the overhaul review.

Figure 1. Bell UH-1 Helicopter.

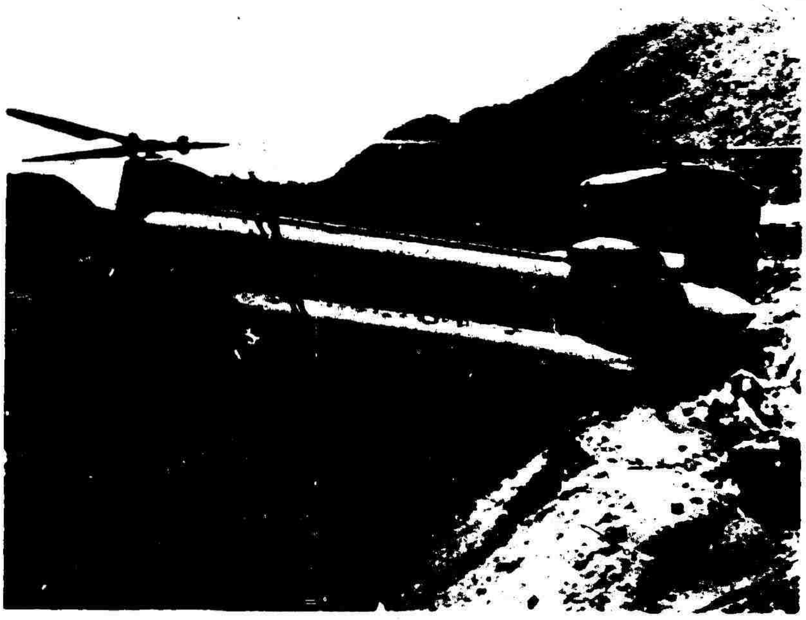

Figure 2. Vertol CH-47 Helicopter.

A third portion of the computer programming effort resulted in an analytical section designed specifically to extract statistical information from the overhaul information file while meeting prescribed criteria established by the engineering data file.

Utilization of the program provided the ability to determine inadequacies in predictions of operating stress conditions through observation of failures in comparison to stress life predictions.

DESCRIPTION OF TRANSMISSIONS

Section views representing the transmissions studied in this program are shown in Figures 3 through 6. Figure 3 is the main transmission used on the UH-1, and Figures 4, 5, and 6 are respectively the forward, aft, and combining transmissions used on the CH-47. The Item No. code shown on these figures will subsequently be used in this report in the component failure discussion given in Results. Specifically excluded from this study are the Bell UH-1 42° and 90° tail rotor gearboxes, and the Vertol CH-47 engine nose boxes and the aft pylon rotor thrust bearing assembly.

The Bell UH-1 has a 1400-hp T-53 gas turbine engine, flat rated at the transmission design level of 1100 hp. The transmission shown in Figure 3 accepts 1100 hp @ 6600 rpm from the engine via the input drive shaft and delivers required power to the single 2-bladed main rotor @324 rpm, to the 2-bladed tail rotor through the sump case output at 4300 rpm, and to various accessory pads at 4300 to 8000 rpm. The main rotor speed reduction of 20.384:1 is accomplished by the series array of a 62:29 90° spiral bevel gear set and two simple fixed ring, sun input, carrier output spur gear planetary drives of 3.087:1 each. An overrunning clutch is located between the input drive shaft and the 29-tooth spiral bevel pinion. The first or lower planetary stage uses four planet idler gears, and the second or upper stage uses eight. The tail rotor output is taken through a 55:41 spur gear drive from the lower end of the 62-tooth bevel gear shaft down into the sump assembly and then out through a 90° bevel set of 27:26 ratio. The transmission cases or housings act as the primary structural support between the main rotor and the fuselage.

The Vertol CH-47 employs two 2650-hp T-55 gas turbines, flat rated at a total power level of 3636 hp at the combining transmission. The combining transmission drives the two 3-bladed main rotors through interconnect shaft to the forward and aft transmissions, which are each design rated at 2170 hp (60% of the combining transmission output).

Each engine drives through a 43:34 90° spiral bevel gear reduction nose box into opposite sides of a combining transmission. The combining transmission input spiral bevel pinions drive a single gear which delivers power to the forward and aft transmissions. The combining gearbox encompasses a disengaging mechanism, which is used to mechanically disengage the forward rotor drive from the aft rotor drive. A

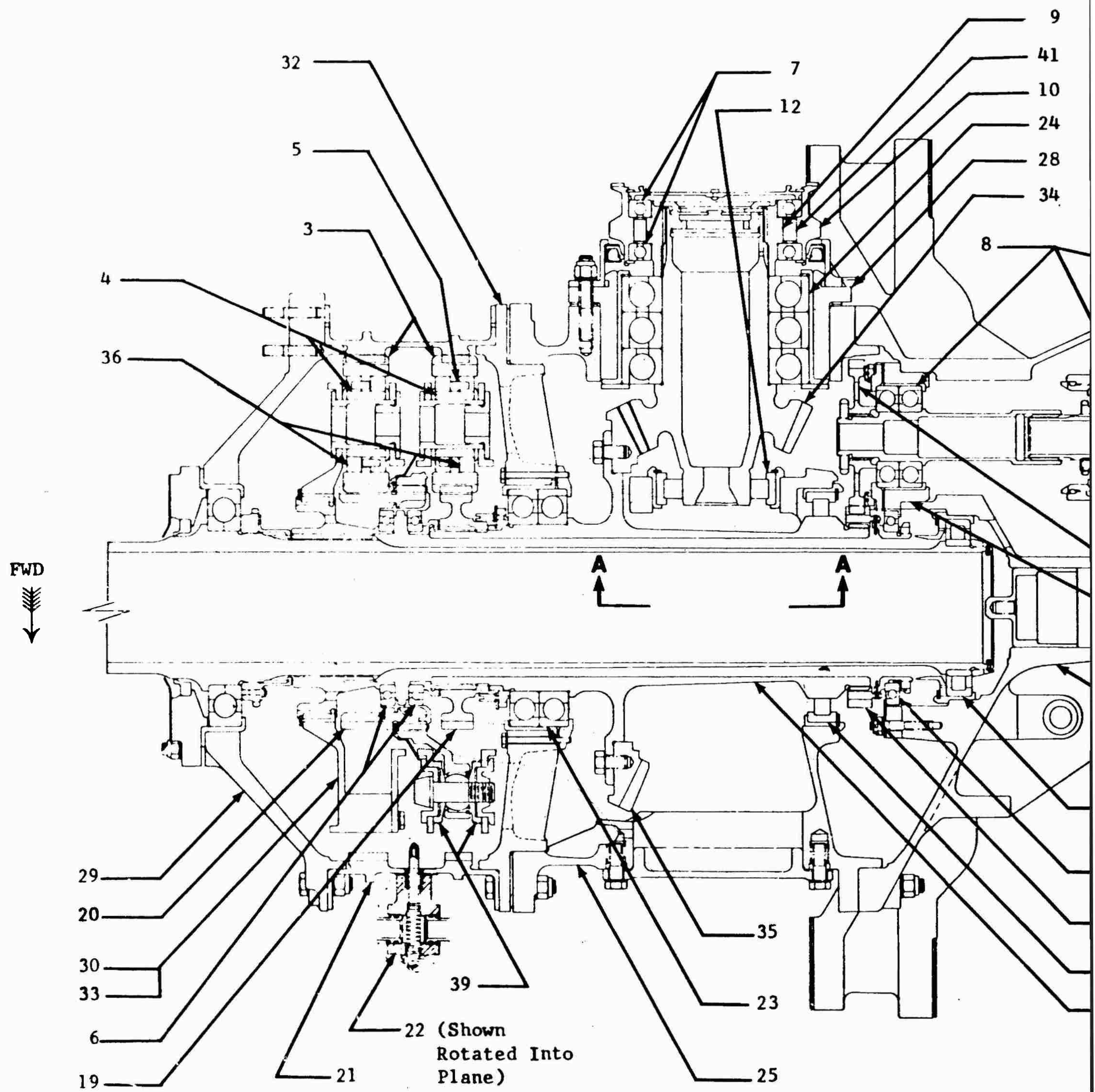

Figure 3. Bell Transmission.

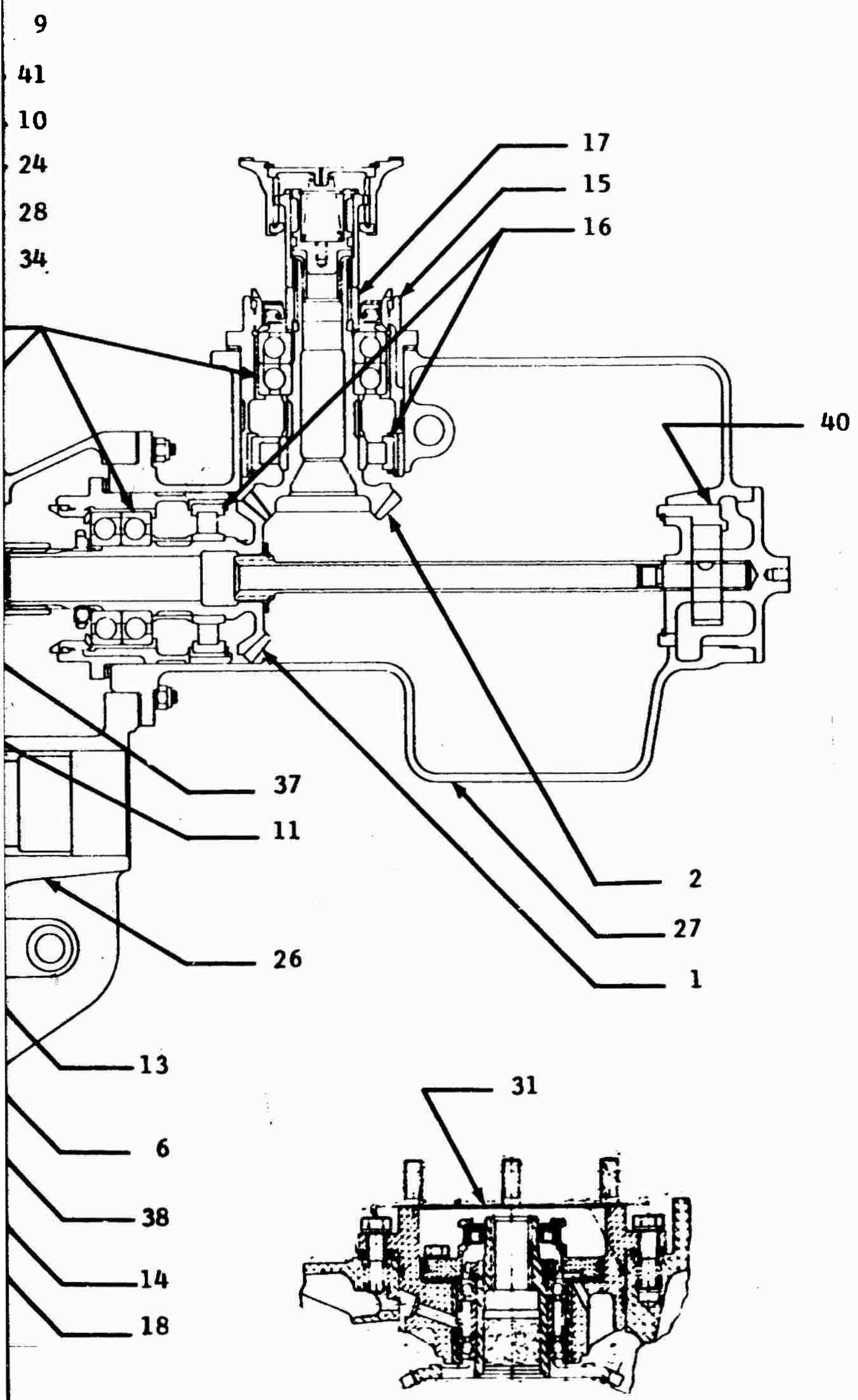

SECTION A—A

ITEM NO.	PART NUMBER	PART NAME
1	204-040-103	Gear
2	204-040-104	Pinion
3	204-040-108	Pinion
4	204-040-132	Race
5	204-040-133	Retainer
6	204-040-135	Bearing
7	204-040-142	Bearing
8	204-040-143	Bearing
9	204-040-190	Race
10	204-040-191	Race
11	204-040-250	Sleeve
12	204-040-269	Bearing
13	204-040-270	Bearing
14	204-040-271	Bearing
15	204-040-305	Sleeve
16	204-040-310	Bearing
17	204-040-313	Spacer
18	204-040-324	Shaft
19	204-040-329	Gear
20	204-040-330	Gear
21	204-040-331	Ring Gear
22	204-040-339	Manifold
23	204-040-345	Bearing
24	204-040-346	Bearing
25	204-040-353	Case
26	204-040-354	Case
27	204-040-355	Case
28	204-040-356	Sleeve
29	204-040-359	Case
30	204-040-360	Planetary Assy
31	204-040-379	Quill Assy
32	204-040-386	Case
33	204-040-397	Spider
34	204-040-700	Pinion
35	204-040-701	Gear
36	204-040-725	Roller Set
37	204-040-762	Pinion
38	204-040-763	Gear
39	204-040-789	Washer
40	GC1669	Oil Pump
41	X-131720	Freewheeling Clutch

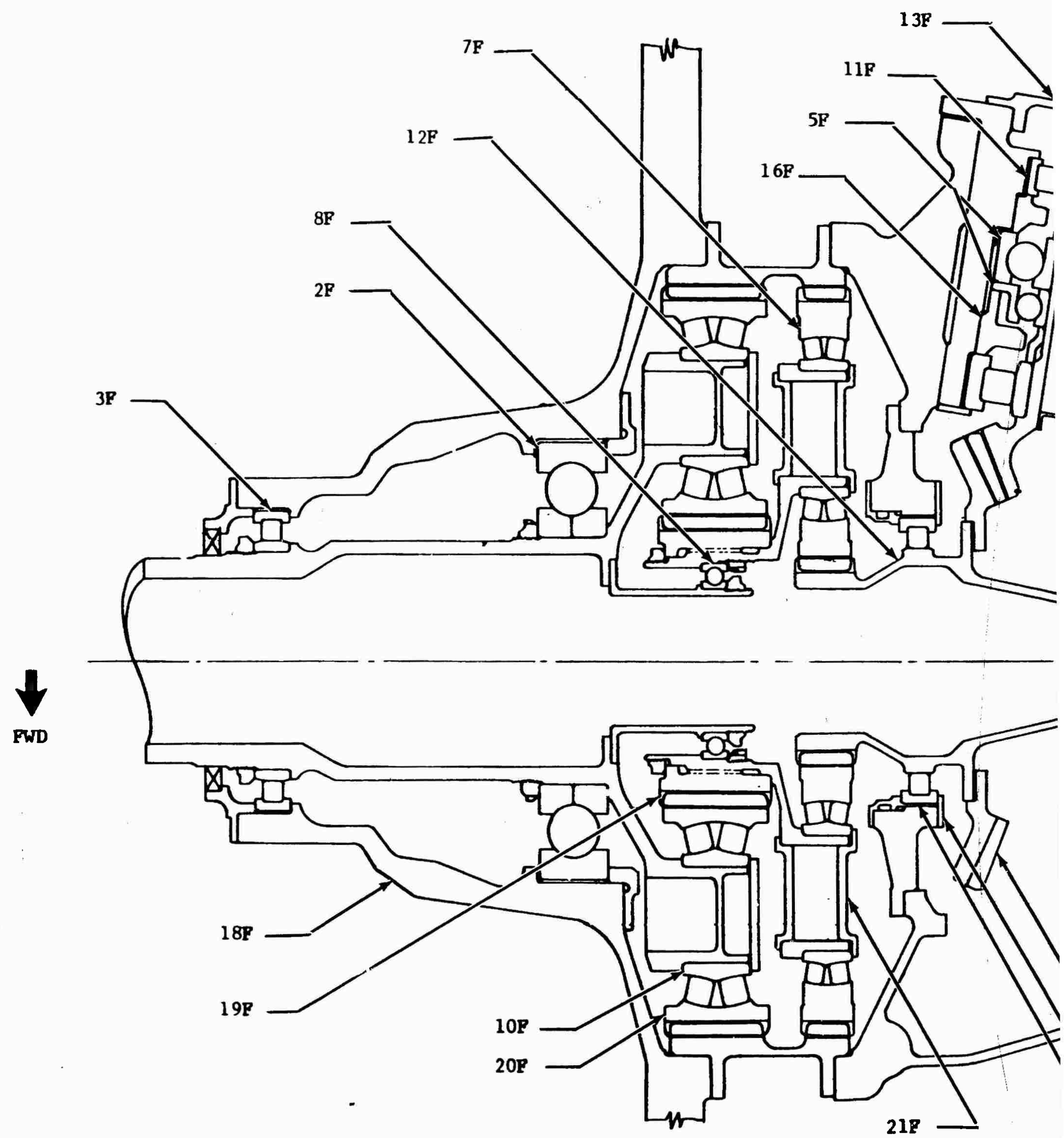

Figure 4. Vertol Forward Transmission.

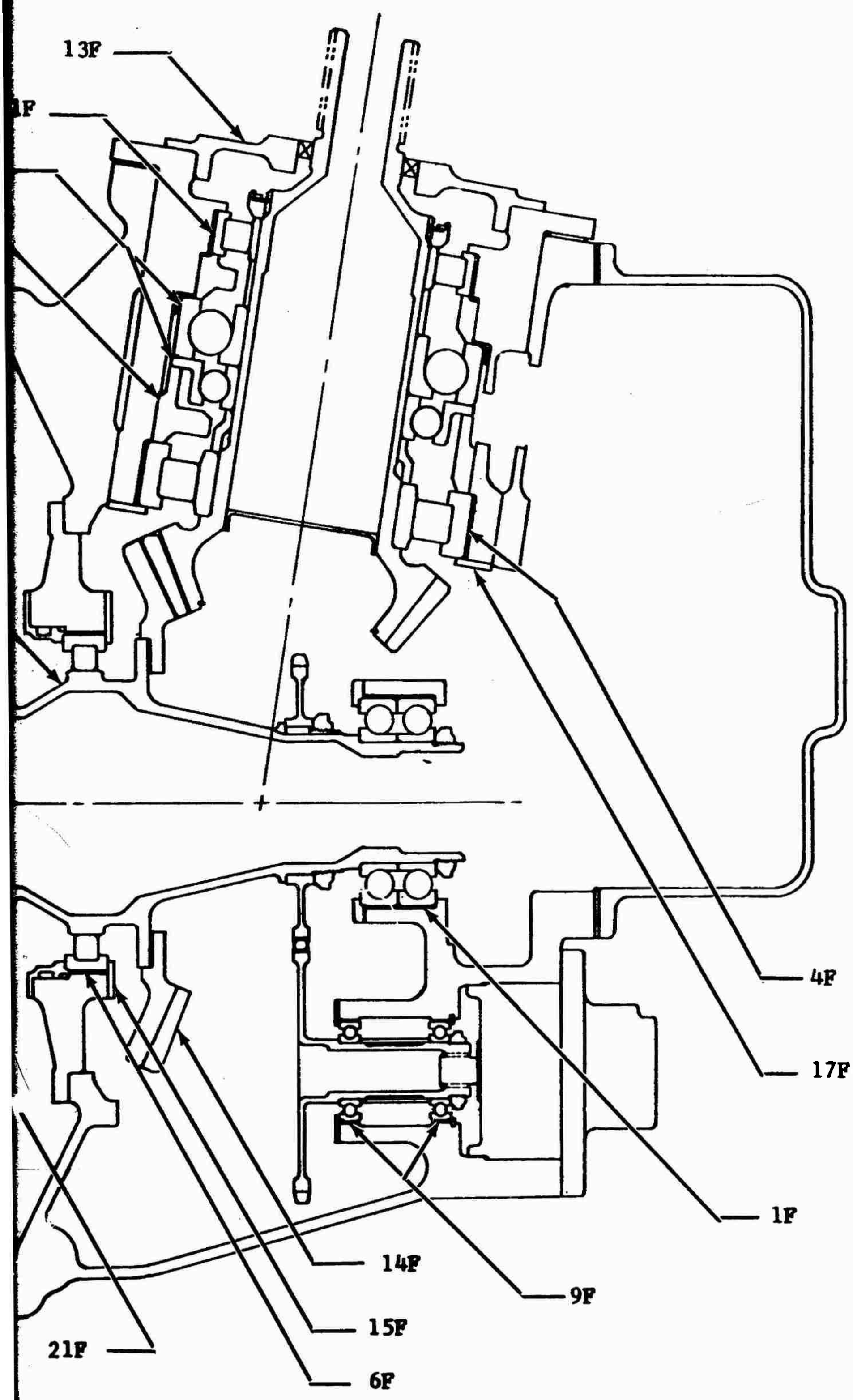

ITEM NO.	PART NUMBER	PART NAME
1F	114DS143	Bearing
2F	114DS144	Bearing
3F	114DS145	Bearing
4F	114DS240	Bearing
5F	114DS241	Bearing
6F	114DS243	Bearing
7F	114DS244	Bearing
8F	114DS250	Bearing
9F	114DS255	Bearing
10F	114DS258	Bearing
11F	114DS262	Bearing
12F	114D1043	Gear
13F	114D1050	Retainer
14F	114D1053	Gear
15F	114D1072	Retainer
16F	114D1074	Lubricator
17F	114D1079	Retainer
18F	114D1088	Support Assy
19F	114D2077	Gear
20F	114D2084	Gear
21F	114D2184	Retainer

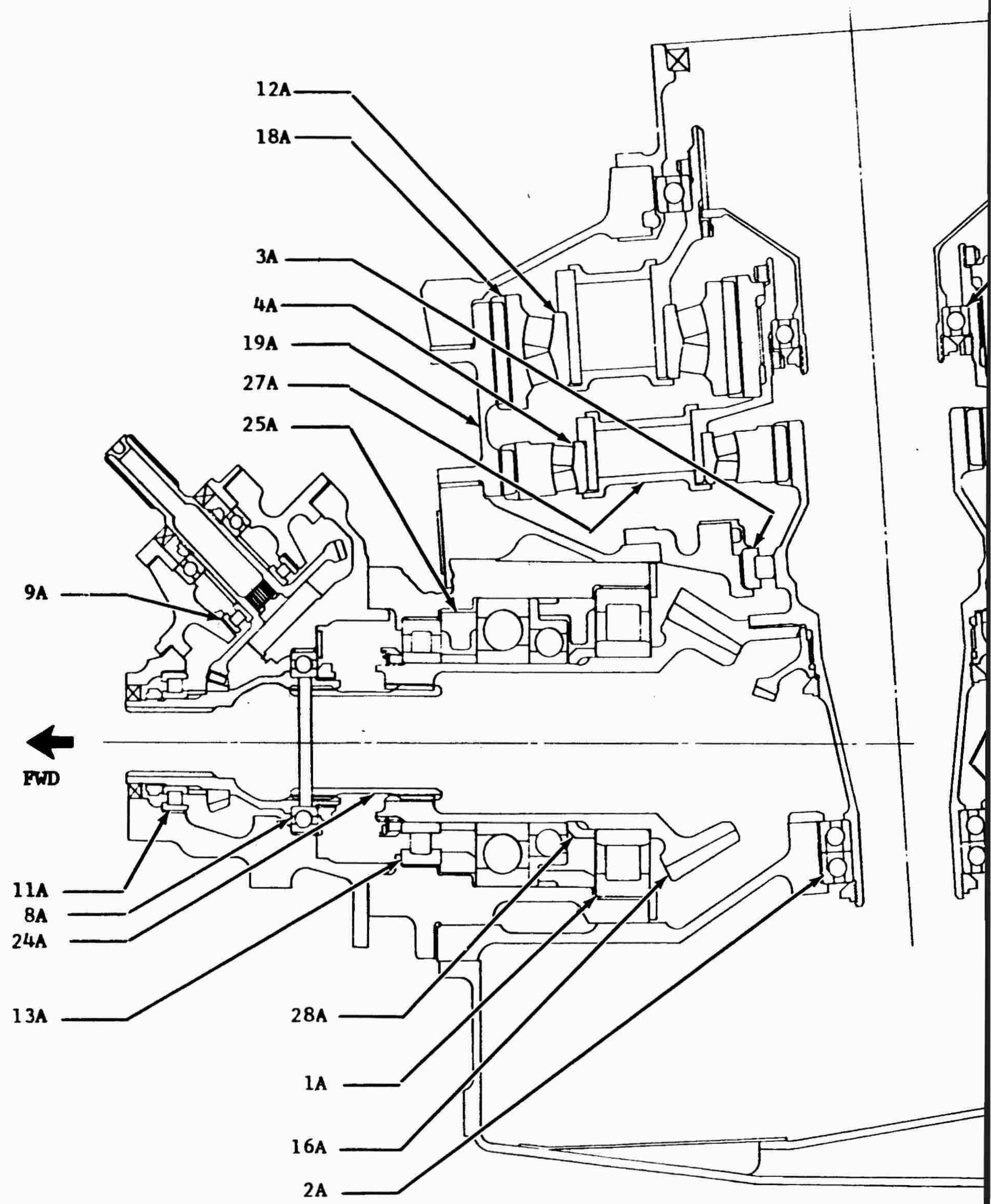

Figure 5. Vertol Aft Transmission.

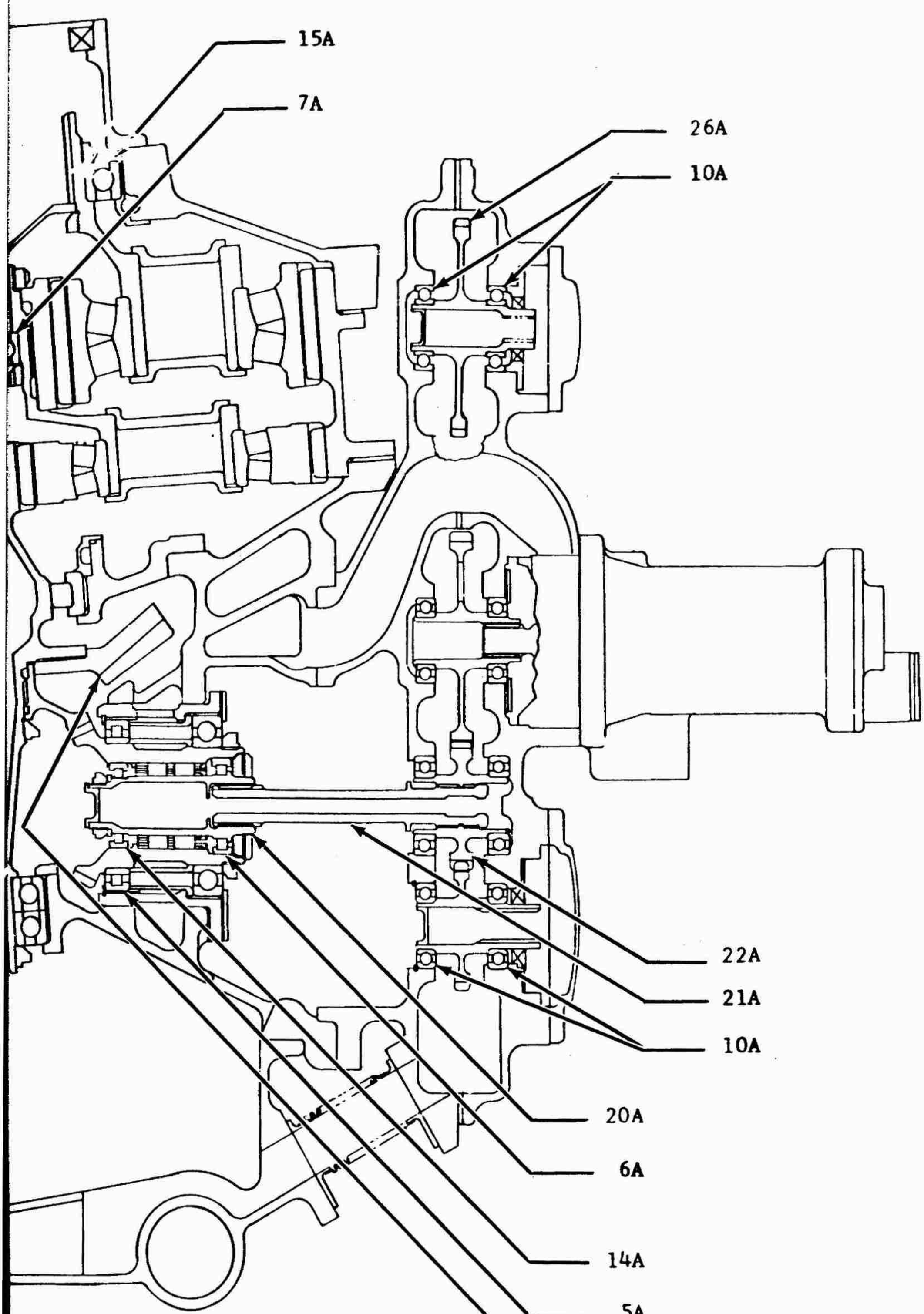

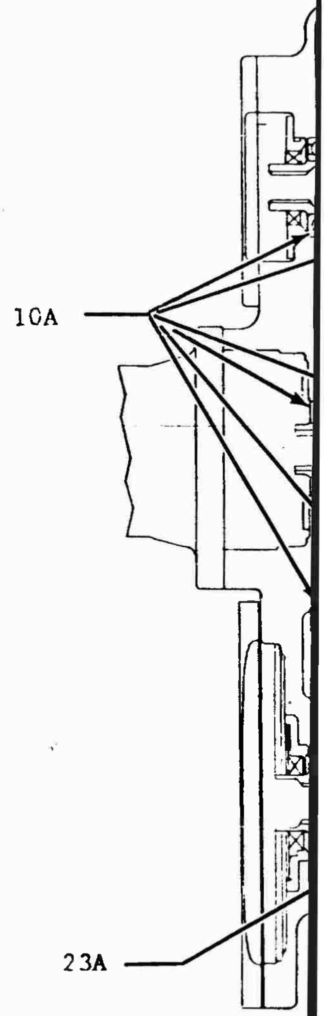

SECTION TH
DRIVE

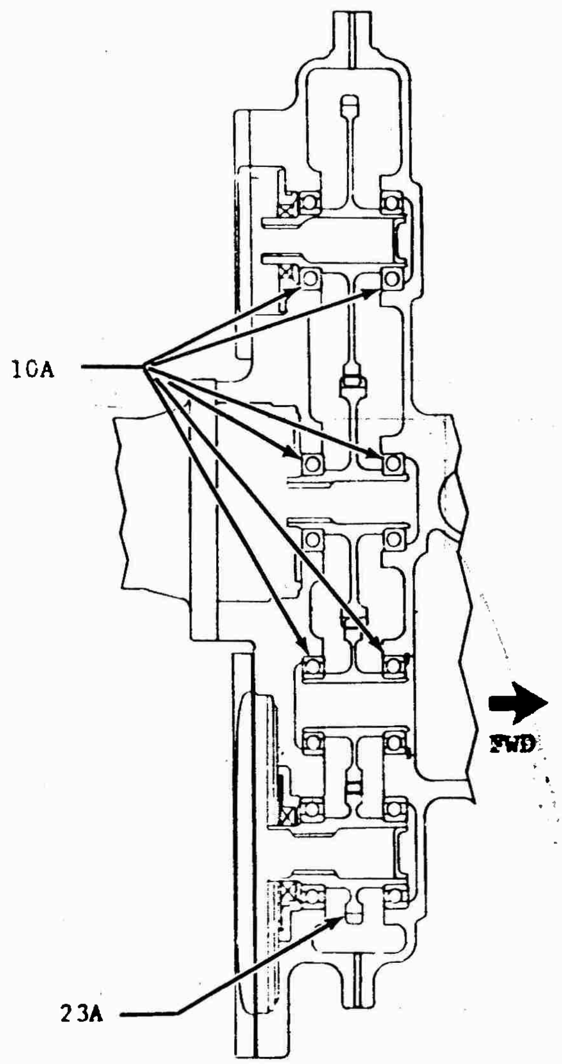

SECTION THRU ACCESSORY
DRIVE ASSEMBLY

ITEM NO.	PART NUMBER	PART NAME
1A	114DS240	Bearing
2A	114DS242	Bearing
3A	114DS243	Bearing
4A	114DS244	Bearing
5A	114DS247	Bearing
6A	114DS249	Bearing
7A	114DS250	Bearing
8A	114DS251	Bearing
9A	114DS253	Bearing
10A	114DS256	Bearing
11A	114DS257	Bearing
12A	114DS258	Bearing
13A	114DS262	Bearing
14A	114DS265	Bearing
15A	114DS274	Bearing
16A	114D2045	Pinion
17A	114D2062	Gear
18A	114D2084	Gear
19A	114D2086	Gear
20A	114D2093	Shaft
21A	114D2105	Shaft
22A	114D2106	Gear
23A	114D2107	Gear
24A	114D2116	Shaft
25A	114D2145	Lubricator
26A	114D2178	Gear
27A	114D2184	Retainer
28A	114D2191	Spacer

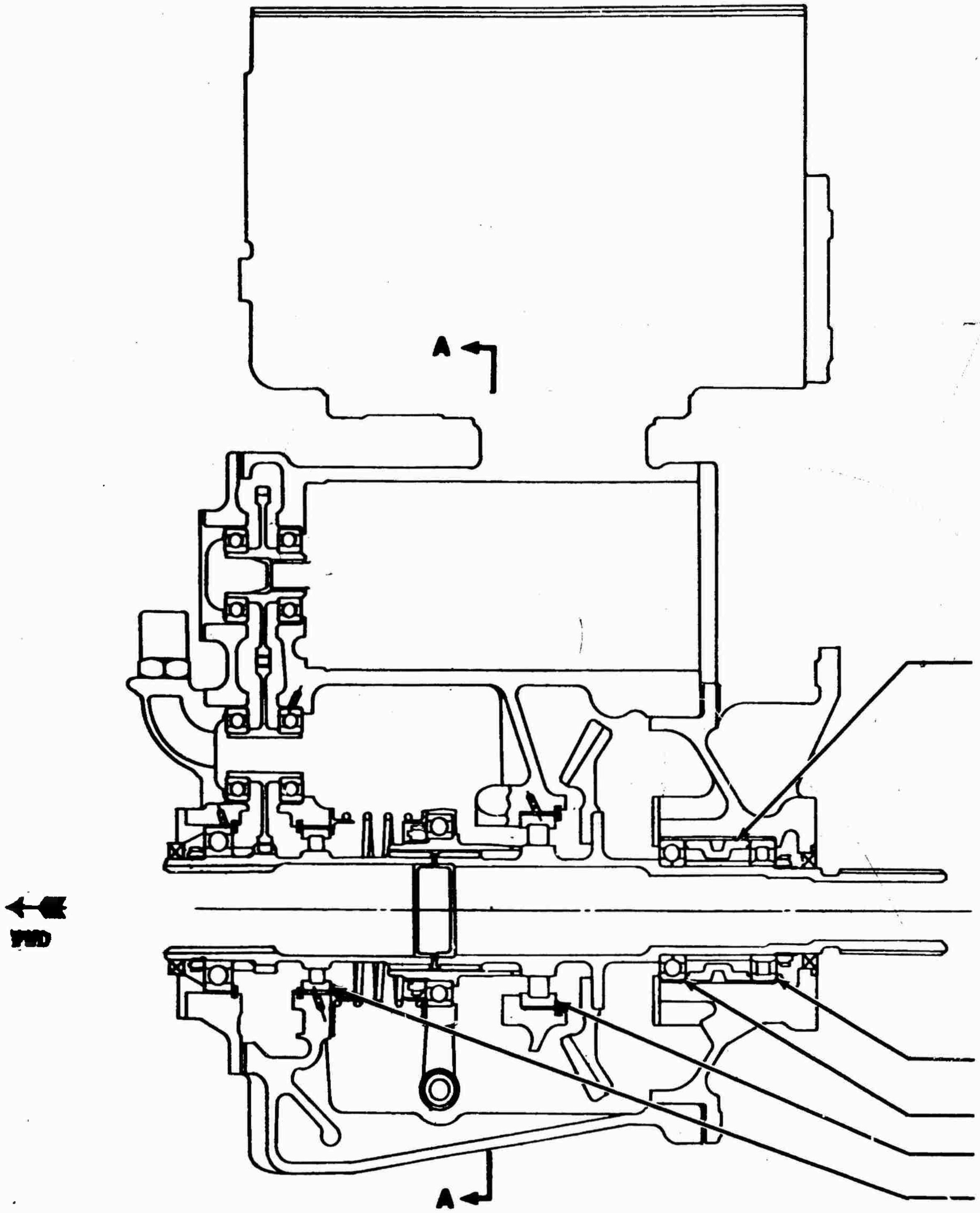

Figure 6. Vertol Combining Transmission.

ITEM NO.	PART NUMBER	PART NAME
1C	114DS541	Bearing
2C	114DS542	Bearing
3C	114DS543	Bearing
4C	114DS544	Bearing
5C	114DS545	Bearing
6C	114DS549	Bearing
7C	114D5045	Support
8C	114D5047	Gear
9C	114D5063	Lubricator
10C	114D5110	Baffle

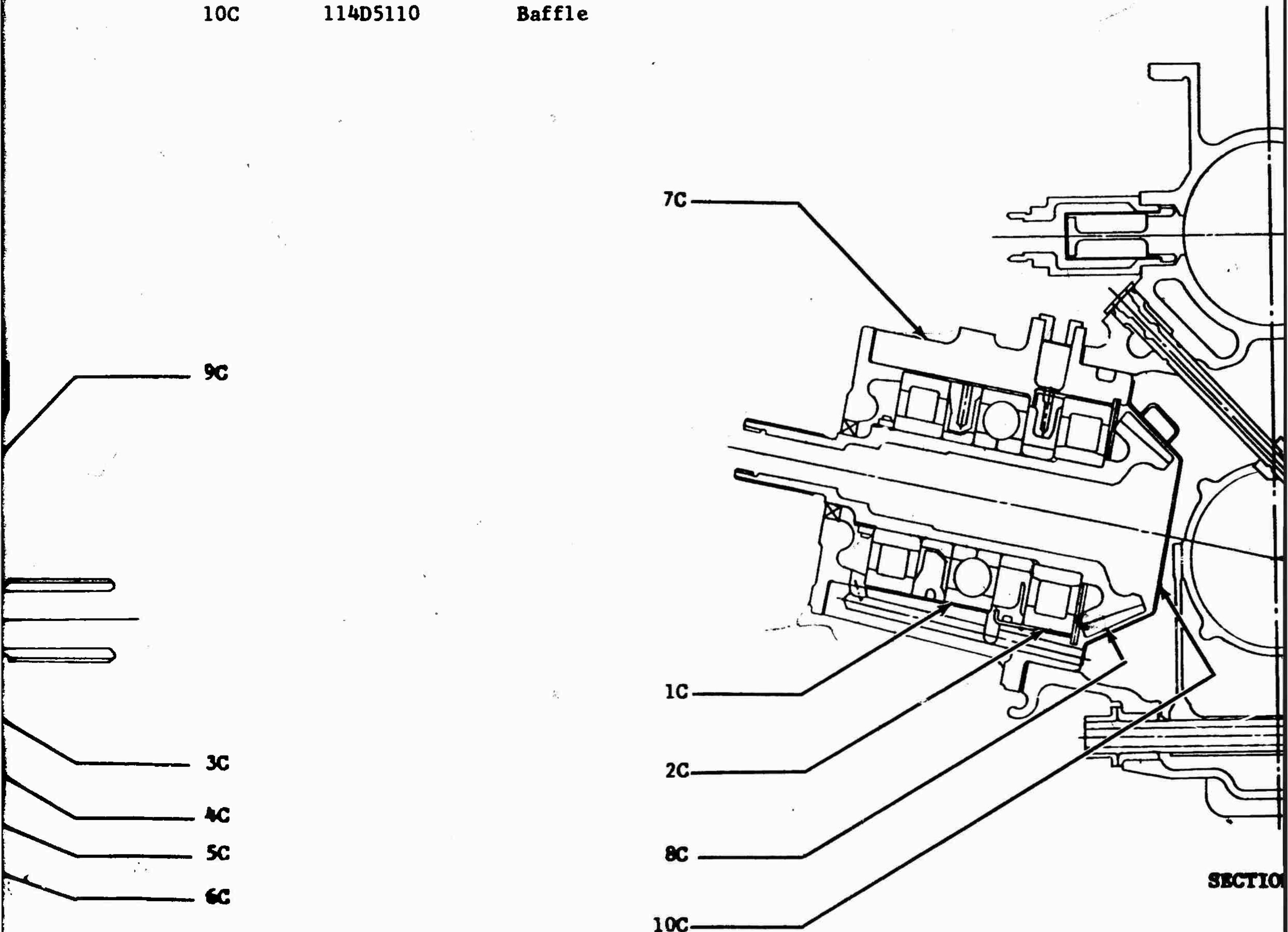

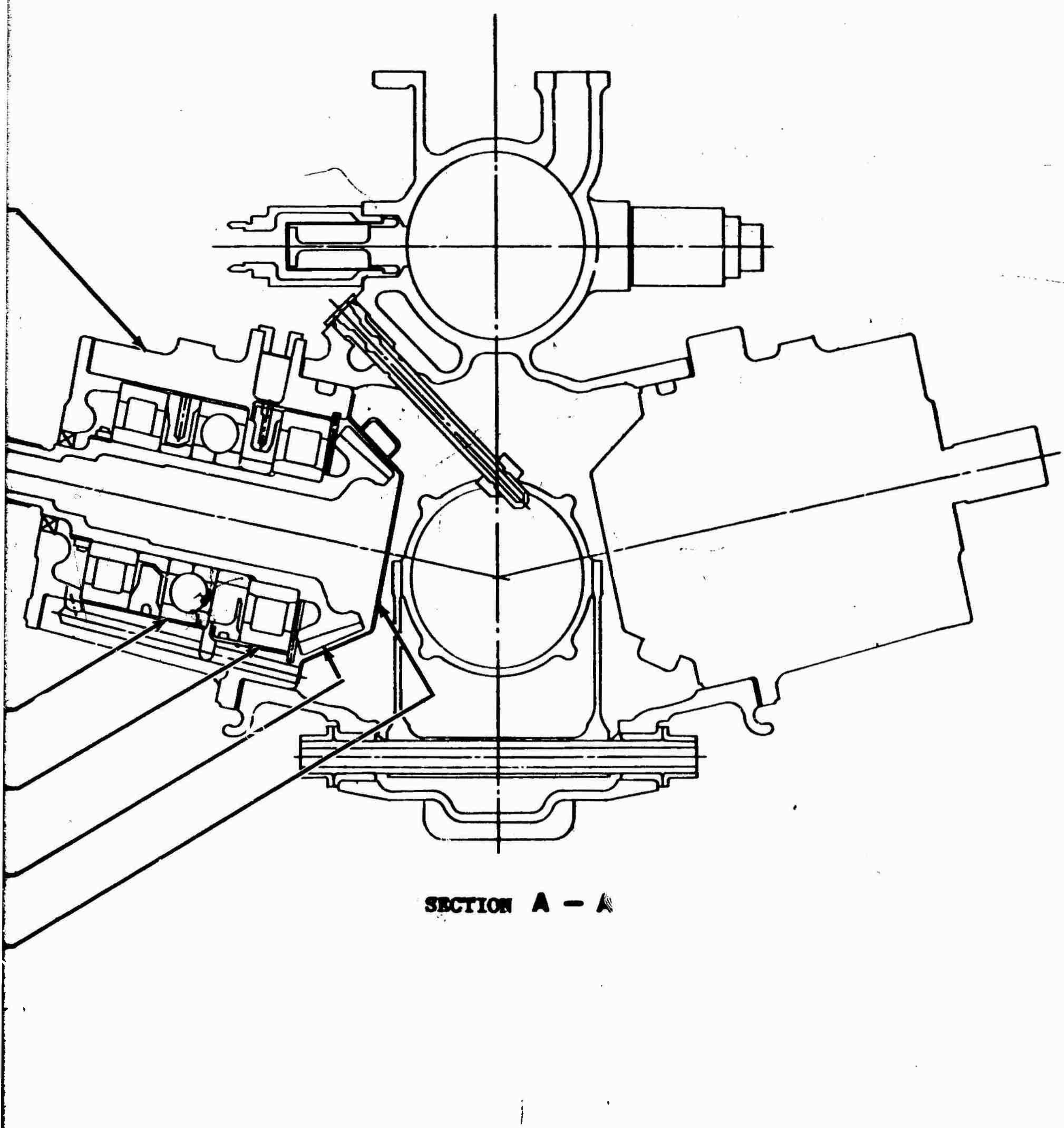

SECTION A — A

speed reduction of 56:33 is accomplished at the combining gearbox. The forward and aft transmissions each have the same overall reduction: 51:29 spiral bevel set driving into the lower sun gear of a 2-stage planetary reduction assembly. The lower sun drives the carrier through the planet idlers with a reduction of 4.78:1, and the lower carrier drives the upper sun gear. The upper sun gear drives the upper carrier through six planet idlers with a reduction of 3.65:1. The upper carrier drives the mast at 230 rpm at an engine output speed of 15,160 rpm.

METHODS EMPLOYED

All too often M & R programs yield statistical data which cannot be correlated to real-life cause and effect. Although the acquisition of numerous statistical signatures and generic failure rates does indeed provide useful information when viewed in a broad context, the identification of physical wear phenomena viewed from an interdisciplinary approach is prerequisite to establishing significant areas for needed research and development effort.

The principal method employed to achieve the program objectives was the detailed visual examination and meaningful reporting of the condition of parts replaced during overhaul of the Army's UH-1 and CH-47 transmissions at ARADMAC. This in turn required on-site monitoring of the disassembly of failed transmission units by skilled scientists well versed in the arts of failure analysis.

Past experience by the Contractor on in-house M & R programs has served to highlight the extreme importance of witnessing disassembly. The determination of primary and secondary failure modes and causes cannot be effectively made without this witness. Often, additional factors such as improper initial assembly, improper field maintenance methods, or improper disassembly techniques can materially distort functional failure statistics.

Consequently, the success of this study in producing useful information depended upon intelligent failure mode determinations and the exercise of sound judgment in definition of the roles of cause and effect.

ORGANIZATION OF PROGRAM

The program was initiated by the selection and training of an engineering team to collect data. Detail drawings were reviewed to familiarize this on-site review team with the design of each of the four transmissions. In-house component overhaul was witnessed to establish monitoring procedures and to gain familiarity with component records and failure types. A glossary (compatible with American Gear Manufacturers Association and Anti-Friction Bearing Manufacturers Association terminology) of common failure modes was compiled and associated with examples taken from overhaul components, to aid in achieving uniformity in reporting. This glossary appears as Appendix I to this report.

Work sheets for logging and reporting failure data were developed. Gearbox failure analysis sheets (GFAS) (Figure 7) were designed to record component historical data and component condition. It was also used to record other information noted during disassembly that might be helpful later in analyzing detail part failures. Detail failure analysis sheets (DFAS) (Figures 8, 9, and 10) were used to record failure data of a detail part. Because of the difference in failure modes of gears, bearings, and general parts such as cases, housings, or shafts, a different type of DFAS sheet was prepared for each. Both GFAS and DFAS sheets were designed to permit ease of transfer of collected data to computer storage files. Complete instructions for use and identification coding of these sheets are included in Appendix II.

The on-site team at ARADMAC spent five months monitoring transmission overhaul and inspecting failed components during the data-collection phase of this study. A total of two hundred and fifty-one transmissions were inspected, yielding over 1600 DFAS sheets.

DATA COLLECTION

Data collection methods were designed to minimize interference with normal overhaul component processing at ARADMAC. Figure 11 clearly shows the delineation between ARADMAC and BHC on-site inspection team functions. It should be emphasized that the on-site team did not participate in any way with the component replacement decisions made by ARADMAC personnel nor did they furnish any additional failure criteria. However, it must be conceded that due to the necessity of identification tagging the detail parts at disassembly, some intensification of inspection level may have followed. Although the individual failure rates may be slightly influenced by this factor, the validity of the failure mode observations and analytical conclusions were not compromised.

The evaluation of a transmission for suitability for use in this study began with the review of the 634 form historical records. Definitive records which were sufficiently complete to exclude the inclusion of battle or accident damaged components were the sole requirement. In the event that more transmissions became available than could be satisfactorily monitored at disassembly on any given day, preference was given to first-time overhaul units. First-time overhaul units were far more desirable since the total time on any component was, with great certainty, simply that of the transmission assembly; the additional variables of prior overhaul criteria, skills, and methods were eliminated from the study.

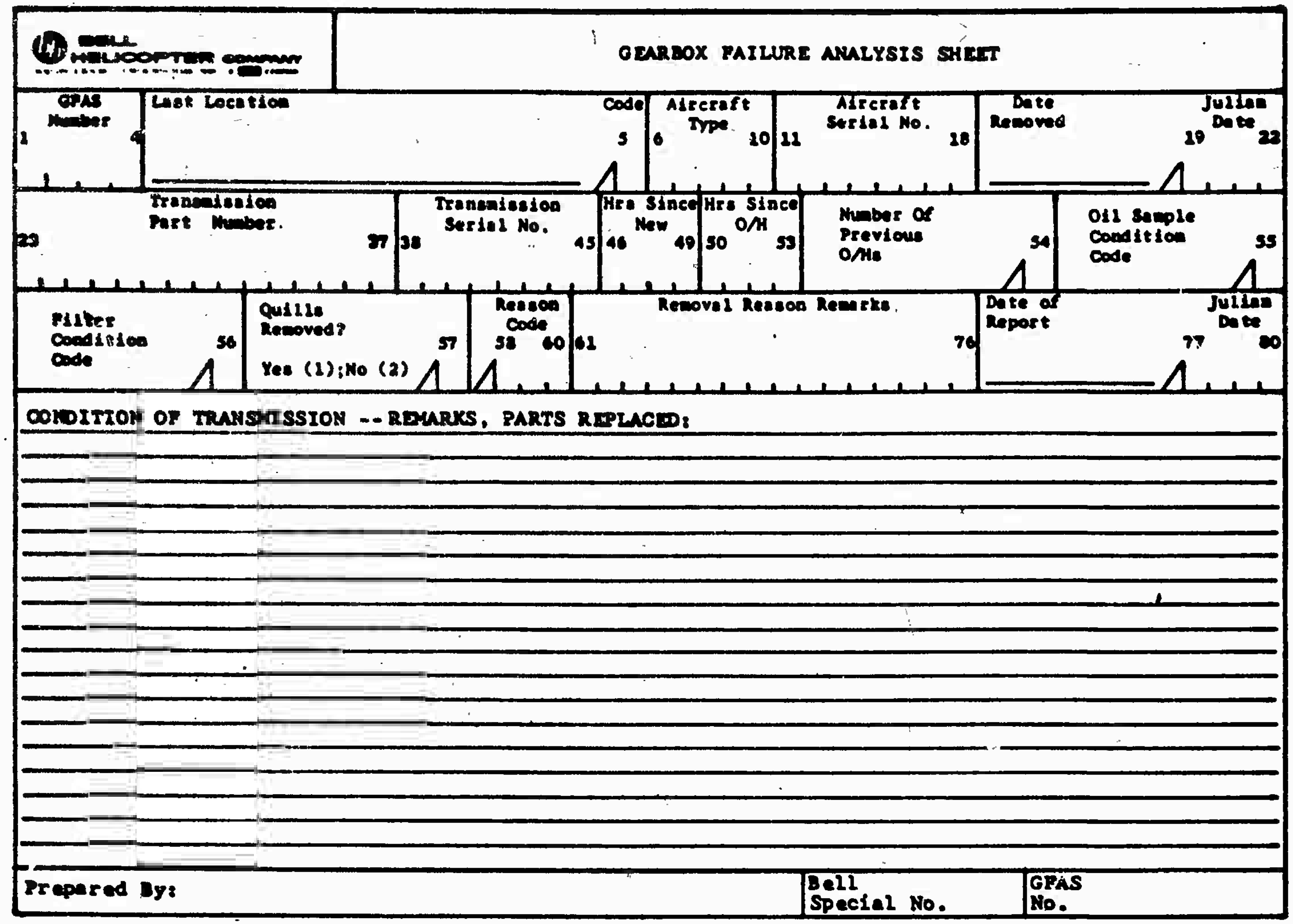

Figure 7. Gearbox Failure Analysis Log Sheet.

BELL HELICOPTER COMPANY

DETAIL FAILURE ANALYSIS SHEET (GEARS)

DFAS NUMBER 1–7	
A	

DATE DA MO YR 8–13	PART NUMBER 14–28	PART NAME 29–38	PART SERIAL NUMBER 39–46	REF. DATA 47–50

FAILURE TYPE:	FAILURE IDENTIFIED BY:	PROBABLE SHORT TERM EFFECT OF FAILURE:	CONTINUED CAPABILITY PROBABILITY:
(1) Primary (2) Secondary 51	1- Visual 2- Visual Optics 3- Magnaflux 4- Zyglo 5- Sonic 6- Other 52	1- No Apparent Effect 2- Noisy Operation 3- High Temp. Operation 4- Loss of Oil 5- High Vibration 6- Loss of Drive 7- Probable Seizure 53	(1) Over 100 Hours (2) Under 100 Hours (3) Failure Eminent 54

ENTER FAILURE MODE DESCRIPTION IF "OTHER" BLOCK BELOW IS CHECKED 55 ... 79 | 80: 1

8 ... 17
1- WEAR
-Destructive Wear
-Abrasive Wear
-Galling
-Scoring
-Frosting
-Corrosive Wear
-Interference Wear
-Burning
-Discoloration
-Misalignment
-Surface Treatment Worn Through

18 ... 20
-Oil Absent
-Corrosion - Other

21 ... 27
2- SURFACE CONTACT FATIGUE
-Destructive Pitting
-Spalling - Fan Shape
-Arrested Pitting
-Pitch Line
-Addendum Origin
-Dedendum Origin
-Case Crushing

40 ... 46
3- BREAKAGE
-Fatigue
-Wear
-Overload
-Misalignment
-Quench Cracks
-Grind Cracks
-Impact

59
4- DEBRIS IN MESH
-Moderate Damage
-Heavy Damage

78 | 80: 2
5- CORROSION IN STORAGE
6- OTHER

GEAR TOOTH OR SPLINE FAILURE MODE AND DEFINITION

DISPOSITION OF FAILED PART: Scrapped____; Forwarded For Inspection____

SUMMARY AND REMARKS:

Prepared By:	Analysis Complete:	Bell Special No.	DFAS No.

Figure 8. Detail Failure Analysis Log Sheet (Gears).

BELL HELICOPTER COMPANY

DETAIL FAILURE ANALYSIS SHEET (BEARINGS)

1 DFAS NUMBER 7 B

DATE DA MO YR 8–13	PART NUMBER 14–28	PART NAME 29–38	PART SERIAL NUMBER 39–46	REF. DATA 47–50

FAILURE TYPE: (1) Primary (2) Secondary — 51

FAILURE IDENTIFIED BY: 1- Visual 2- Visual Optics 3- Magnaflux 4- Zyglo 5- Sonic 6- Other — 52

PROBABLE SHORT TERM EFFECT OF FAILURE: 1- No Apparent Effect 2- Noisy Operation 3- High Temp. Operation 4- Loss of Oil 5- High Vibration 6- Loss of Drive 7- Probable Seizure — 53

CONTINUED CAPABILITY PROBABILITY: (1) Over 100 Hours (2) Under 100 Hours (3) Failure Eminent — 54

ENTER FAILURE MODE DESCRIPTION IF "OTHER" BLOCK BELOW IS CHECKED 55–79 80 1

8: 1- LIMITED LIFE 2- CAGE FAILURE

9–18: -Wear On Inner, -Wear On Outer, -Pocket Wear, -Cracked, -Rivets Failed, -Dented, -Incorrect Instal., -Spot Welds Failed, -Folded Tangs Failed, -Out Of Round

(3) OUTER RING 21–36 37 38 39

(4) INNER RING 40–55 56 57 58

(5) BALL OR ROLLER 59–74 75 76 77 78 80 2

-Spalling, -Pitting, -Corrosion, -Dented, -Ext. Debris, -Int. Debris, -Broken, -Cracked, -Smearing, -Glazing, -Wear, -Grooved, -Brinneled, -Fretting, -Creeping, -Spinning, -Incorrect Installation, -Disassembly Damage, -Discolored Due To Temp, 6- CORROSION IN STORAGE, 7- OTHER

BEARING FAILURE MODE AND DEFINITION

DISPOSITION OF FAILED PART: Scrapped ___ ; Forwarded For Inspection ___ .

SUMMARY AND REMARKS:

Prepared By:	Analysis Complete:	Bell Special No.	DFAS No.

Figure 9. Detail Failure Analysis Log Sheet (Bearings).

BELL HELICOPTER COMPANY

DETAIL FAILURE ANALYSIS SHEET (GENERAL PARTS)

1 DFAS NUMBER 7

C

DATE DA MO YR 8 13	PART NUMBER 14 28	PART NAME 29 38	PART SERIAL NUMBER 39 46	REF. DATA 47 50

FAILURE TYPE:	FAILURE IDENTIFIED BY:	PROBABLE SHORT TERM EFFECT OF FAILURE:	CONTINUED CAPABILITY PROBABILITY:
(1) Primary (2) Secondary 51	1- Visual 2- Visual Optics 3- Magnaflux 4- Zyglo 5- Sonic 6- Other 52	1- No Apparent Effect 2- Noisy Operation 3- High Temp. Operation 4- Loss of Oil 5- High Vibration 6- Loss of Drive 7- Probable Seizure 53	(1) Over 100 Hours (2) Under 100 Hours (3) Failure Eminent 54

ENTER FAILURE MODE DESCRIPTION IF "OTHER" BLOCK BELOW IS CHECKED 55 79 80 1

8 12 13 14 15 16 21 23 25 26 27 28 40 59 78 80 2

1- CASES -Fretting Corrosion -Cracked -Wear -Break -Fatigue -Corrosion In Use -Handling Damage -Corrosion In Storage -Corrosion Other

2- SHAFTS -Wear -Crack -Fretting Corrosion -Fatigue -Corrosion In Use -Threads Galled -Corrosion In Storage -Corrosion Other

3- OTHER

GENERAL PARTS FAILURE MODE AND DEFINITION

DISPOSITION OF FAILED PART: Scrapped___; Forwarded For Inspection___.

SUMMARY AND REMARKS:

Prepared By:	Analysis Complete:	Bell Special No.	DFAS No.

Figure 10. Detail Failure Analysis Log Sheet (General Parts).

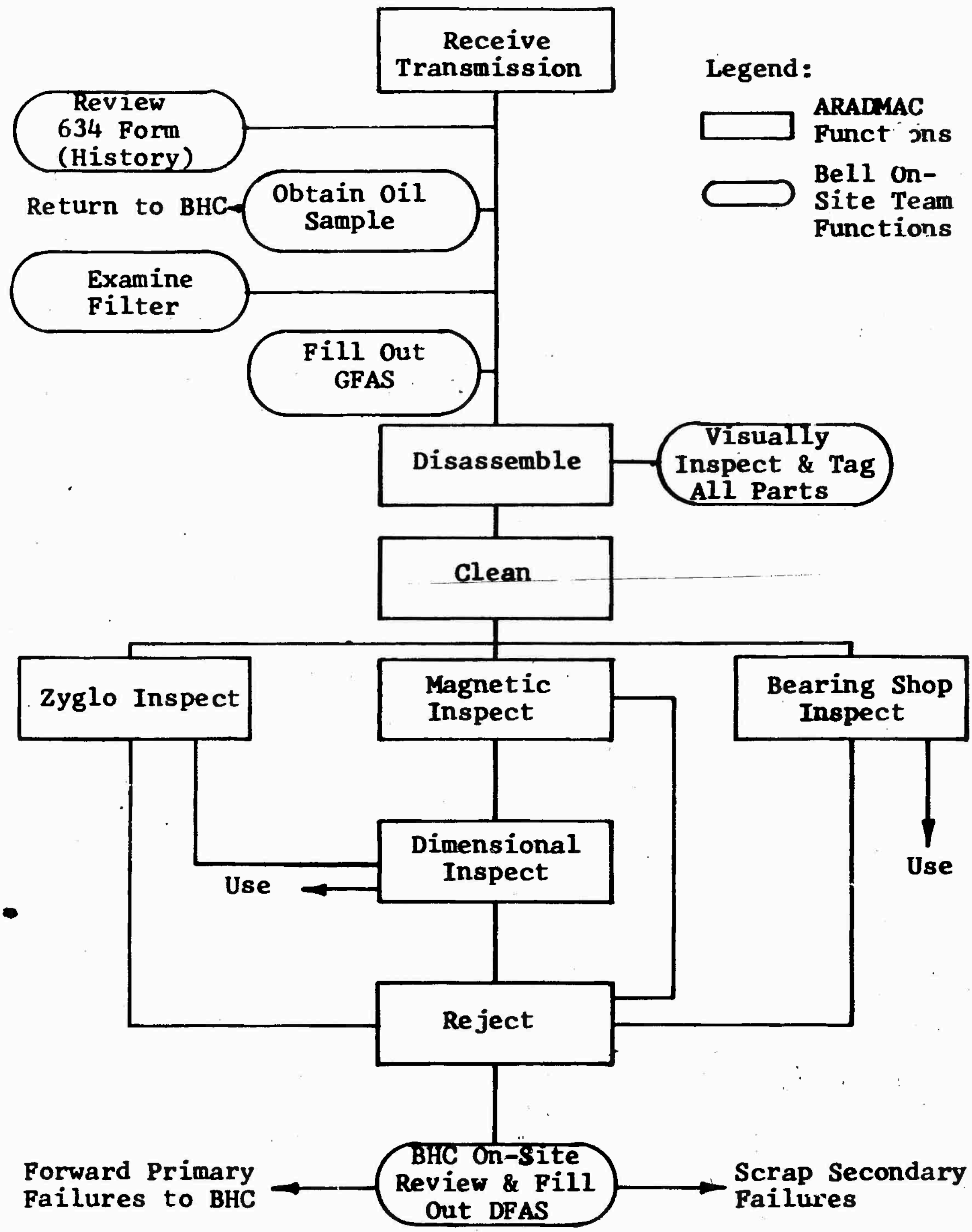

Figure 11. Review Program Processing Interface .

The chosen transmission was then assigned a GFAS number, and the appropriate historical data were transcribed. An immediate visual inspection was made for external evidence of failure, field damage, or field repair. An oil sample was collected and identified by GFAS number. The oil filter, pump inlet screen, and magnetic chip detector were inspected during disassembly, and the observed condition was noted and compared with the reason for removal stated on the historical records or failure reports. All parts were identified with wired-on embossed metal tags for subsequent traceability to the proper GFAS. Parts having multiple application in the transmission were identified by location codes to aid in failure identification relative to specific operating stresses, e.g., UH-1 upper and lower planet idler gears. Copies of the GFAS were forwarded to BHC for project review.

The subject transmission components were then processed through normal overhaul procedures. All parts rejected by ARADMAC Quality Control (except standard replacement items such as O-rings, seals, etc.) were held for final on-site team inspection and disposition. These parts were each assigned a DFAS number, and the failure information was recorded therein. The DFAS number coding assured traceability to the proper GFAS (see Appendix II, File Operating Instructions). Parts awarded a primary failure classification were forwarded to BHC for further analysis. Secondary failure parts were discarded. Copies of the DFAS were then forwarded to BHC for project review.

DATA PROCESSING

The failure analysis sheets, GFAS and DFAS, were forwarded to the BHC computer data processing center for keypunch transcription to computer cards. These were subsequently processed through the computer, and the data were stored in the computer file. A process flow chart may be seen as Figure 12.

Periodic file updating was accomplished as additional GFAS and DFAS were acquired and reviewed.

In a similar manner the engineering design data were transcribed from the gear and bearing design criteria sheets (discussed in the next section of this report) and stored in the computer file as the component designs were analyzed and the criteria sheets were completed.

COMPUTER PROGRAM

A computer program was developed to store and analyze collected data. The program was comprised of two storage files and an

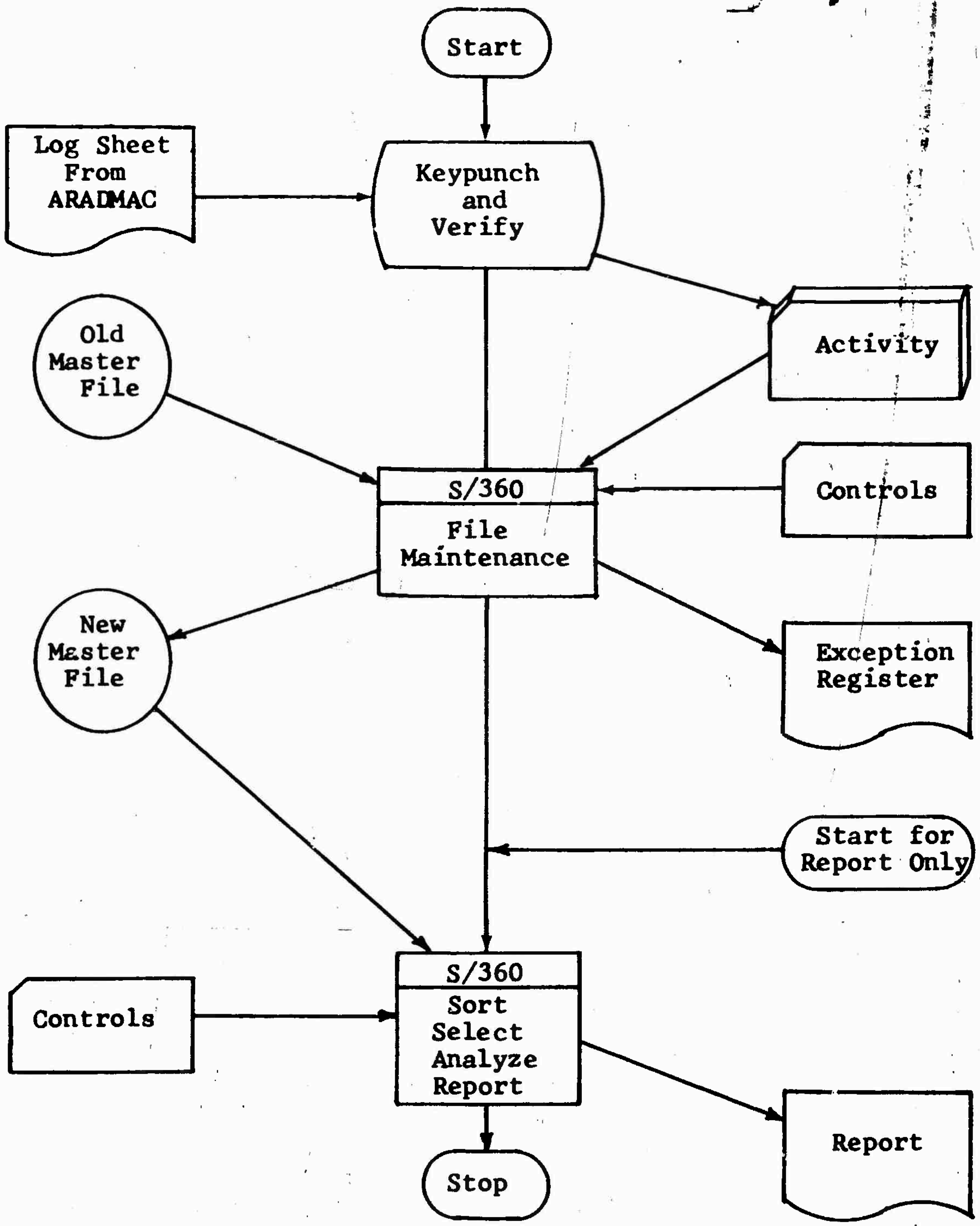

Figure 12. Computer Program Flow Chart.

analytical section. The storage files contain GFAS and DFAS data and design criteria data. The GFAS and DFAS files were constantly revised and updated as sheets were forwarded to keypunch and as final evaluation of primary failures necessitated revision of earlier diagnoses or added new information.

The design criteria file was created through engineering analysis of the gears and bearings in the four study transmissions. Design characteristics, materials, speeds, loads, and system functions were employed to produce operating stresses and life prognosis indices for all of the gear and bearing components. Data were taken from the detail engineering drawings and used to calculate subsequent data or were entered directly into the design criteria sheets, shown in Figure 13 for gears and in Figure 14 for bearings. When subsequent calculations were required, these were accomplished manually or by using computer design programs existing at BHC.

A brief explanation of the source of the symbolic data used on the Design Criteria sheets follows:

DESIGN CRITERIA, GEARS

Entry Order	Description
1-15	Part Number of Gear
16	Type or Family of Gear *
17-21	Diametral Pitch
22-24	Number of Teeth
25-29	Face Width - Inches
30-33	Normal Operating Pressure Angle
34-37	Mean Spiral or Helix Angle
38-41	Bevel Gear Axes Intersection Angle
42-46	Outside Diameter at Max. Tooth Top Land - Inches
47	Material *
48	Profile Modification *

DESIGN CRITERIA, GEARS

PART NUMBER	TYPE	DIAM. PITCH	NO. TEETH	FACE WIDTH	PRESSURE ANGLE	SPIRAL ANGLE	SHAFT ANGLE	O.D.	MAT'L.
1 15	16	17 21	22 24	25 29	30 33	34 37	38 41	42 46	47

PROFILE MOD.	SURFACE FINISH	PITCH LINE VEL.	COMPRESSIVE STRESS	TEMP. RISE °F	METHOD OF LUBRICATION	MINIMUM FILM	W_T	N_P	MESH
48	49 50	51 55	56 58	59 61	62	63 65	66 70	71 75	76

ENTRY CODE

16. TYPE: 1. - Spur, 2. - Helical, 3. - Spiral Bevel
47. MATERIAL: 1. - AMS6260 Carb., 2. - AMS6265 Carb., AMS6470 nitrided

48. PROFILE MODIFICATION: 0. - None (true involute), 2. - K-Chart, 3. - Tilted Pressure Angle,

62. METHOD OF LUBRICATION: 1. - Jet into Mesh, 2. - Jet out of Mesh, 3. - Both, 4. - Mist
76. MESH: 0. - Not Applicable, 1. - Lower Plenetary Pinion with Sun Gear, 2. - Lower Planetary Pinion with Ring Gear, 3. - Upper Planetary Pinion with Sun Gear, 4. - Upper Planetary Pinion with Ring Gear

Figure 13. Design Criteria Log Sheet - Gears.

DESIGN CRITERIA, BEARINGS

PART NUMBER	TYPE	O.D. (MM)	I.D. (MM)	WIDTH (MM)	NO. ROLLING ELEMENTS	BALL OR ROLLER DIA.	ROLLER LENGTH	TYPE OF RETAINER	RETAINER MATERIAL
1 15	16	17 20	21 24	25 28	29 30	31 34	35 38	39	40

RING MATERIAL	BALL OR ROLLER MAT'L	CONTACT ANGLE	INTERNAL CLEARANCE	INNER RACE CURVATURE %	OUTER RACE CURVATURE %	PRELOAD	METHOD OF LUB	N	C
41	42	43 46	47 50	51 52	53 54	55 58	59	60 64	65 68

O.D. FIT	I.D. FIT	F_X		PART NUMBER	F_Y	F_Z	M_Z	M_Y	BALL OR ROLLER MAX LOAD
69 72	73 76	77 80		1 15	16 20	21 25	26 30	31 35	36 39

CONTROLLING RACE	MAX HERTZ STRESS	C/P	SURF. FINISH INNER RACE	SURF. FINISH OUTER RACE	SURF. FINISH BALLS OR ROL	MINIMUM FILM THICKNESS
40	41 43	44 46	47 49	50 52	53 55	56 58

ENTRY CODE

16. Type: 1 - Cyl. Roller, 2 - Spherical Roller, 3 - Radial Ball, 4 - Angular Contact
5 - Duplex DB, 6 - Duplex DF, 7 - Duplex DT, 8 - Triplex

39. Type Retainer: 1 - One-Piece I.R. Riding, 2 - One-Piece O.R. Riding, 3 - Riveted I.R. Riding,
4 - Riveted O.R. Riding

40. Retainer Material: 1 - Micarta, 2 - Nylatron, 3 - Al. Bronze, 4 - Silver Plated Bronze,
5 - Steel

41 or 42. Material: 1 - 52100, 2 - M-50

59. Method of Lubrication: 1 - Pressure Feed, 2 - Gravity Feed, 3 - Jet, 4 - Mist

69 & 73. Ten thousandths.

40. Controlling Race: 1 - Inner Race, 0 - Outer Race

Figure 14. Design Criteria Log Sheet - Bearings.

Entry Order	Description
49-50	Surface Finish - AA
51-55	Pitch Line Velocity - Ft/Min
56-58	Pitch Line Compressive Stress - $Lb/In.^2 \times 10^3$
59-61	AGMA Scoring Temp. Index Rise - Ref. 2
62	Lubrication Method *
63-65	EHD Film Thickness - 10^{-6} In. - Ref. 9
66-70	Tangential Tooth Load - Max. Horsepower
71-75	Max. Normal RPM of Pinion
76	Mesh Location *

* See Entry Code on Figure 13

DESIGN CRITERIA, BEARINGS

Entry Order	Description
1-15 (Card I)	Part Number of Bearing
16	Type *
17-20	Outside Dia. - mm
21-24	Inside Dia. - mm
25-28	Width - mm
29-30	Number of Rolling Elements
31-34	Ball or Roller Diameter - Inches
35-38	Roller Length - Inches
39	Type of Retainer *

Entry Order	Description
40	Retainer Material *
41	Ring Material *
42	Ball or Roller Material *
43-46	Installed Contact Angle - Degrees
47-50	Internal Clearance in Ten Thousandths of an Inch
51-52	Inner Race Curvature Radius in % of Ball Dia.
53-54	Outer Race Curvature Radius in % of Ball Dia.
55-58	Operating Preload - Pounds
59	Lubrication Method *
60-64	Inner Ring RPM
65-68	AFBMA Basic Dynamic Capacity - 10^3 Pounds - Ref. 3
69-72	Outside Diameter Fitup - Ten Thousandths of an Inch
73-76	Inside Diameter Fitup - Ten Thousandths of an Inch
77-80	Radial Load Vector - Max. HP - Pounds
1-15 (Card II)	Part Number of Bearing
16-20	Orthogonal Radial Load Vector - Max. HP - Pounds
21-25	Thrust Load - Max. HP - Pounds
26-30	Moment Load - Max. HP - Inch-Pounds

Entry Order	Description
31-35	Orthogonal Moment Load - Max. HP - Inch Pounds
36-39	Max. Rolling Element Load - Pounds - Ref. 21
40	Race Controlling Ball Dynamics - Ref. 21 *
41-43	Max. Hertz Stress - $Lb/In.^2 \times 10^3$
44-46	Basic Dynamic Capacity/Load
47-49	Surface Finish Inner Race - AA
50-52	Surface Finish Outer Race - AA
53-55	Surface Finish Rolling Element - AA
56-58	EHD Oil Film Thickness - 10^{-6} In. - Ref. 10

* See Entry Code on Figure 14.

The analytical portion of the program was devised to interrogate the GFAS, DFAS, and design criteria files with respect to selected limits or test criteria. Simple statistical failure quantities and rates for particular part numbers, part types, or any precoded index could be readily listed. The listing of these data with respect to any specific stored design criteria (such as operating stress level band) was similarly produced. In addition, correlation studies could be conducted directly. Any test equation using the stored variable could be programmed, executed, and listed. In this manner, failure rate correlation examinations with respect to new parameters such as Dowson film thickness ratios (Reference 4) could be easily accomplished.

EXAMINATION OF FAILURES

Failed parts rejected by ARADMAC Quality Control were withheld for program study evaluation to determine the mode and cause of failure. This evaluation included a visual inspection along with a review of disassembly notes, component historical records, and noted results of ARADMAC Quality Control

inspections. If the mode and/or reason for failure was known, it was recorded on the analysis sheet for computer storage file acquisition. Failed parts on which the mode or reason for failure could not be determined, and all part-caused (primary) failures from first-time overhaul components, were forwarded to BHC for additional analysis.

Parts that were replaced were categorized according to the reason for removal. These categories generally are termed (1) standard replacement, (2) conditional replacement, and (3) mandatory replacement.

Standard replacement items are all parts that are necessarily damaged during removal, or that normally deteriorate from aging or wear during one TBO period so that they are not suitable for reuse and are disposed of at overhaul without consideration of condition. This includes such things as oil seals, gaskets, and packings.

Conditional replacement items are those parts that are suitable for reuse at overhaul provided they are judged to be in serviceable condition and capable of completion of another TBO period. This includes most gears, bearings, shafts, and cases.

Mandatory replacement items are those that have past service failure history or that have exhibited limited fatigue lives beyond the first TBO period and have had finite service lives established.

All parts that were replaced because of conditional or mandatory reasons were considered failed parts. Those from the conditional replacement and mandatory replacement categorics were classified as primary (part caused) or secondary (externally caused) failures. Primary failures are those that ostensibly occurred as the result of normal operating loads and speeds, in a normal operating environment, and become unserviceable because of some condition other than expected wear. Cracked, broken, pitted, or spalled parts are primary failures. Secondary (or externally caused) failures are those that result from loads, speeds, or conditions that are not expected during normal operation, or those parts that have worn during normal operation so that they no longer meet preestablished dimensional requirements. Failures that resulted from corrosion, debris damage, improper handling or installation, or operation without oil were considered secondary failures. Parts that are in serviceable condition but were replaced because of established limited lives were considered secondary failures.

ANALYSIS OF FAILURES

Failed parts forwarded to BHC for additional evaluation were inspected visually, dimensionally, chemically, and metallurgically for conformity to applicable engineering drawings, specifications, process methods, and quality control standards.

The extent of this examination depended upon the difficulty of failure mode and cause determination and the commonality with respect to other collected specimens. Approximately 75 detail parts were subjected to extensive evaluations which included:

A- and C-Type DFAS

1. Surface finish and waviness measurements
2. Tooth spacing
3. Profile and lead measurements
4. Concentricity and parallelism of important surfaces
5. Magnaflux or Zyglo inspection
6. Nital etch inspection for grinding, tempering or carbon depletion
7. Hardness testing
8. Preparation of metallurgical specimens
9. Macro- and microstructure examination
10. Superficial hardness gradient measurement
11. Retained austenite measurement by X-ray diffraction
12. Microcleanliness and inclusion rating
13. Spectrographic chemical analysis

B-Type DFAS

1. Bore, O.D., and width, measurement
2. Eccentricity, squareness, and runout measurements
3. Radial and axial play

4. Contact angle

5. Retainer land and pocket clearances

6. Surface finish and waviness

7. Magnaflux and Zyglo

8. Nital etch inspection for grinding, tempering or carbon depletion

9. Hardness testing

10. Preparation of metallurgical specimens

11. Macro- and microstructure examination

12. Superficial hardness gradient measurement

13. Retained austenite measurement by X-ray diffraction

14. Microcleanliness and inclusion rating

15. Spectrographic chemical analysis

In addition to the analyses performed at BHC, outside assistance was obtained. Eight selected failed bearings were evaluated by the Fafnir Bearing Company, New Britain, Connecticut, with respect to the identical variables listed under B Type DFAS part. Three sets of failed parts, each consisting of two failed bearings and one failed gear tooth were sent to Battelle Memorial Institute, Columbus, Ohio, for scanning electron microscope examination to determine fracture modes and failure origin locations to aid in identification of specific cause of failure. Failed oil pumps were returned to the manufacturer (W. H. Nichols Company) for evaluation. Freewheeling clutch sprags were inspected by the manufacturer (Borg Warner Corp.), and certain abnormally high drag bearings were returned to the manufacturer (Marlin Rockwell Corp.) for inspection. Twenty oil samples from selected components were analyzed by Wear Check, Toronto, Ontario, in an attempt to correlate wear phenomena and failure modes with lubricant condition and spectographic analysis of solid contaminants.

RESULTS

During the five-month period of on-site data collection, a total of 251 transmissions was evaluated, as shown in Table I. From these there was a total of 1671 failed parts, with 183 classed as primary failures. The major causes of failure were corrosion damage, limited life, and debris damage. There were 417 parts damaged by corrosion, 275 replaced because of established limited lives, and 161 damaged by debris.

The reasons for component removal for overhaul are shown in Table II. One hundred and ninety-six of the 251 transmissions successfully completed the scheduled time between overhaul (TBO) period. This was a 78% completion rate with 22%, or 55 units, removed prematurely. In spite of these early removals, the mean time between removal (MTBR) was 75% or more of the scheduled TBO period for all four types of transmissions included and more than 80% for all except Vertol CH-47B forward transmissions. It is significant to note that the MTBR of all 173 Bell transmissions was within 1% of that for the 132 first-time overhaul units alone.

A brief discussion of the more common failure modes and some additional explanation of the classification and discussion follows.

Corrosion damage in general is not considered the result of normal operation; it is considered to be a secondary failure. There are a few areas, however, where fretting and corrosion, partially as the result of galvanic action, are expected during normal operation. This is experienced on Bell transmissions on mating surfaces between the steel planetary ring gear case and the magnesium cases, and between the steel liner for the mast thrust bearing and the magnesium top case. This condition is usually not severe during normal operation when the calendar time between overhauls is not excessively long. Prolonged storage periods after removal for overhaul, or inadequate preservation after removal, usually result in extensive damage to these areas. The corrosion damage observed during review resulted primarily from inadequate corrosion protection and preservation during use or after component removal from the aircraft. Corrosion damage was classified with respect to cause, i.e., from operation or from storage. If buildup of corrosion products was evident on contacting bearing or gear surfaces, such that subsequent operation would wear it away, the damage was classified as corrosion in storage. There were 97 parts in this category. Buildup on noncontacting surfaces could not be classified.

TABLE I. STUDY COMPONENT BREAKDOWN

Component	Part Number	Qty	Total Qty	No. First Overhaul	Scheduled TBO (Hours)	Mean Time (Hours)	% of TBO Completed
Bell	204-040-009-29	1					
	204-040-009-31	9					
	204-040-009-53	4					
	204-040-009-57	27					
	204-040-009-59	2	173	132	1100	995.5	90.5
	204-040-009-65	3					
	204-040-016-1	46					
	205-040-001-11	8					
	205-040-001-17	73					
Vertol Fwd	114D1001-25	5					
	114D1001-26	20	40	23	(CH-47A 800	652.2	81.5)
	114D1001-27	2			(CH-47B 600	449.8	75.0)
	114D1001-532	13					
Vertol Aft	114D2001-24	4					
	114D2001-25	3					
	114D2001-26	7					
	114D2001-27	3	32	25	(CH-47A 1200	1078.4	89.9)
	114D2001-56	7			(CH-47B 600	522.6	87.1)
	114D2001-537	4					
	114D2001-560	4					
Vertol Combining	114D5001-18	6	6	6	1200	1189.2	99.1
TOTALS			251	196			

STUDY COMPONENT BREAKDOWN

TBO)	Mean Time (Hours)	% of TBO Completed	REASON FOR REMOVAL FOR OVERHAUL: Scheduled Maintenance or Time Change (Qty)	(%)	Internal Failure or Metal Contamination (Qty)	%.)	Other (Qty)	(%)
00	995.5	90.5	139	80.3	15	8.7	19	11.0
00 00	652.2 449.8	81.5) 75.0)	28	70.0	7	17.5	5	12.5
00 00	1078.4 522.6	89.9) 87.1)	25	78.1	6	18.8	1	3.1
00	1189.2	99.1	6	100.0	0	--	0	--
			198	78.9	28	11.2	25	9.9

TABLE II. REASON FOR REMOVAL OF INDIVIDUAL TRANSMISSIONS

Removal Code (Ref. 1)	Reason for Removal	Bell	VERTOL Fwd	VERTOL Aft	VERTOL Combining	Total	% Total
803	No defect - removed for time change	132	27	25	6	190	75.7
306	Contamination	8	1	2	-	11	4.4
374	Internal failure	6	4	-	-	10	3.9
372	Metal on magnetic plug	1	2	4	-	7	2.8
804	No defect - removed for scheduled maintenance	5	1	-	-	6	2.4
111	Burst	2	1	-	-	3	1.2
690	Vibration excessive	-	3	-	-	3	1.2
380	Scheduled maintenance	2	-	-	-	2	.8
464	Overspeed	2	-	-	-	2	.8
503	Sudden stop	2	-	-	-	2	.8
Unk.	Unknown	2	-	-	-	2	.8
020	Worn excessively	1	1	-	-	2	.8
008	Noisy	1	-	-	-	1	.4

TABLE II - Continued

Removal Code (Ref. 1)	Reason for Removal	Bell	VERTOL Fwd	VERTOL Aft	VERTOL Combining	Total	% Total
120	Chafed	1	-	-	-	1	.4
154	Overstressed	1	-	-	-	1	.4
190	Cracked	1	-	1	-	2	.8
268	Scarred	1	-	-	-	1	.4
370	Jammed	1	-	-	-	1	.4
381	Leaking	1	-	-	-	1	.4
251	Low oil pressure	1	-	-	-	1	.4
481	Overheats	1	-	-	-	1	.4
910	Chipped	1	-	-	-	1	.4
	TOTALS	173	40	32	6	251	100.0

Limited-life parts have had finite lives established by testing and by analysis of failure history. Some groups of limited-life parts experienced no primary failures in components included on this program. These, nonetheless, would still be considered as life-limiting parts, since the sample field considered here is small. All parts replaced because of limited life were inspected, and the actual condition of the part was coded. Primary failures were evaluated to determine cause of failure, and those that exhibited no discrepancy were considered secondary failures because of limited life.

Debris damage caused by ingestion of entrapped metal particles in gear meshes or in bearings constitutes secondary failure and is not the result of normal operation. The transmission lubrication systems use screens and filters and deliver filtered oil by forced flow or through oil jets to most gears and bearings. Debris damage usually results when metal particles from a primary failure are carried by runoff oil into another gear mesh or bearing. Debris damage is particularly high when the primary failure is a mast bearing or an upper planetary part because of its location in the top of the transmission. This exposes most of the gears and bearings to the particles carried in runoff oil on its path back to the sump.

Other secondary failures resulting from causes other than normal operation are not life-limiting and should not be considered in determining design criteria for longer lived components. Such things as handling or installation damage, arrested pitting, isolated cases of processing or manufacturing defects, or damage from operation without oil should be considered only if component design is such that this damage is probable.

Secondary failures caused by wear should be considered life-limiting even though none may have resulted in nonfunctional parts. Parts replaced because of wear are presumed not capable of completion of another TBO period and would, therefore, become primary failures with substantially lengthened overhaul periods. All primary failures must be considered as life-limiting although parts having relatively low primary failure rates, or those that are considered to be isolated failures, should receive further historical failure inquiry if they are from components represented by relatively small sample fields.

Specific discussions of the individual failed components are given in the following sections by classification of transmission type.

BELL UH-1 TRANSMISSIONS

One hundred seventy-three Bell UH-1 transmissions were included in this program, with 132 of them in for first-time overhaul. One hundred thirty-nine had completed the scheduled TBO (time between overhaul) period, 15 were removed because of internal failure or metal contamination, and 19 were removed for miscellaneous reasons. The mean operating time was 995.5 hours, or 91% of the scheduled TBO.

Failed parts are listed in Table III and are located diagrammatically in Figure 3. Quantities per transmission shown for Items No. 3, 4, 5, and 35 are not whole numbers since 22 of the transmissions were the 16-planetary pinion configuration, and 151 were the 12-pinion configuration, f a mean value of 12.5 parts per transmission.

The reasons for replacement of parts are discussed below:

Items No. 1, 2, 37, and 38 - Tail rotor drive train gears (P/N's 204-040-103-7, 204-040-104-13, 204-040-762-1, and 204-040-763-1). The maximum replacement rate for these four gears was 5.8%, which was exhibited by the 204-040-104-13 spiral bevel pinion (driven member). There were no primary failures in this group, and all except one pair of bevel gears (Items 1 and 2, P/N's 204-040-103-7 and 204-040-104-13) could have continued in operation. This set of gears was scored and spalled on the face of the teeth (Figure 15) as the result of running without oil. Examination of the microstructure disclosed rehardening at the surface in the scored area. Operation without oil was evident in this component at disassembly on the main input bevel gears as well as on this set. Items No. 37 and 38 spur gears were replaced because of scuffing at the tip of the pinion teeth (Figure 16) and in the flank of the gear teeth, and for corrosion damage. Scuffing to a lesser degree is not uncommon on this set and is somewhat self-correcting. Current overhaul documents permit this condition provided the maximum depth of material removed does not exceed 0.0004 inch. In normal overhaul procedure this condition is evaluated visually without setting up the gears in an involute test machine, since ARADMAC does not have gear inspection equipment. Involute traces run (at BHC) on the most severe sample parts show that the maximum depth of wear rarely exceeds this limit (Figure 17).

Item No. 3 - Planetary idler pinion (P/N 204-040-108-7) had a replacement rate of 12.2%, but there were no primary failures. These were replaced for corrosion or debris damage, or for pitting wear in the flank of the teeth (Figure 18). Applicable overhaul documents allow pitting wear in the flank of the

TABLE III. PARTS REPLACED - BELL TRANSMISSION

Item No.	Part Number	Part Name	Quantity Replaced
1	204-040-103-7	Gear, Spiral Bevel, Tail Rotor Drive	4
2	2[illegible]-040-104-13	Pinion, Spiral Bevel, Tail Rotor Drive	10
3	204-040-108-7	Pinion, Planetary	264
4	204-040-132-1	Race, Bearing, Planetary Pinion	147
5	204-040-133-1	Retainer, Bearing, Planetary Pinion	41
6	204-040-135-1	Bearing, Ball, Planetary Support and Accessory Drive	124
7	204-040-142-1	Bearing, Ball, Freewheeling	107
8	204-040-143-1	Bearing, Duplex, Ball, Tail Rotor Drive	52
9	204-040-190-7	Race, Inner, Freewheeling	9
10	204-040-191-7	Race, Outer, Freewheeling	6
11	204-040-250-9	Sleeve Assembly, Offset, Tail Rotor Drive	1
12	204-040-269-3	Bearing, Roller, Input Pinion	15
13	204-040-270-3	Bearing, Roller, Lower Mast	10
14	204-040-271-3	Bearing, Roller, Input Gear Shaft	10
15	204-040-305-1	Sleeve Assembly, Tail Rotor Drive	3
16	204-040-310-1	Bearing, Roller, Tail Rotor Drive	15
17	204-040-313-1	Spacer, Tail Rotor Drive	3
18	204-040-324-5	Shaft, Main Input Gear	5
19	204-040-329-1	Gear, Lower Sun	23
20	204-040-330-1, -3 **	Gear, Upper Sun	83
21	204-040-331-5	Ring Gear Assembly, Planetary	9

PARTS REPLACED - BELL TRANSMISSION

	Quantity Replaced	Quantity Per Trans.	% Replacement	Quantity Primary Failures	% Primary Failures
Rotor Drive	4	1	2.3	0	0
l Rotor Drive	10	1	5.8	0	0
	264	12.5 *	12.2	0	0
Pinion	147	12.5 *	6.8	2	0.09
ary Pinion	41	4.5	3.2	0	0
Support and	124	3	23.9	2	0.38
ng	107	2	30.9	0	0
il Rotor Drive	52	4	7.5	2	0.29
	9	1	5.2	5	2.89
	6	1	3.5	0	0
Tail Rotor Drive	1	1	0.6	0	0
ion	15	1	8.7	0	0
t	10	1	5.8	0	0
r Shaft	10	1	5.8	0	0
r Drive	3	2	0.9	0	0
r Drive	15	3	2.9	1	0.19
	3	1	1.7	0	0
	5	1	2.9	1	0.58
	23	1	13.3	0	0
	83	1	48.0	57	32.95
ary	9	1	5.2	3	1.74

TABLE III - Continued

Item No.	Part Number	Part Name	Quantity Replaced	Qua I Tr
22	204-040-339-5	Housing, Jet No. 2	1	
23	204-040-345-7	Bearing, Duplex Ball, Input Gear Shaft	38	
24	204-040-346-3	Bearing Triplex Ball, Input Pinion	59	
25	204-040-353-23	Case Assembly, Main, Bevel Gear	25	
26	204-040-354-9	Case Assembly, Support	4	
27	204-040-355-1, -3	Case Assembly, Accessory and Tail Rotor Drive	4	
28	204-040-356-1	Sleeve, Spiral Bevel, Input	1	
29	204-040-359-1	Case, Top	29	
30	204-040-360-3	Planetary Assembly, Upper	1	
31	204-040-379-3	Quill Assembly, Generator Drive	1	
32	204-040-386-1	Case, Support, Bevel Gear	10	
33	204-040-397-1	Spider, Planetary	2	
34	204-040-700-1	Pinion, Spiral Bevel, Input	7	
35	204-040-701-3	Gear, Spiral Bevel, Input	7	
36	204-040-725-1, -3	Roller, Pinion, Planetary	15	1
37	204-040-762-1	Pinion, Accessory and Tail Rotor Drive	5	
38	204-040-763-1	Gear, Accessory and Tail Rotor Drive	7	
39	204-040-789-1	Washer, Spacer, Planetary	2	
40	GG1669 (Nichols)	Oil Pump	28	
41	X-131720 (Borg-Warner)	Freewheeling Clutch	11	

* Twenty-two transmissions were the 16-pinion configuration, and 151 were the 12-pinion configuratio

** Six were -1

III - Continued

	Quantity Replaced	Quantity Per Trans.	% Replacement	Quantity Primary Failures	% Primary Failures
	1	1	0.6	0	0
Shaft	38	1	22.0	21	12.14
n	59	1	34.1	38	21.97
	25	1	1.7	1	0.58
	4	1	2.3	0	0
Rotor Drive	4	1	2.9	0	0
	1	1	0.6	0	0
	29	1	16.8	0	0
	1	1	0.6	0	0
	1	1	0.6	0	0
	10	1	5.8	0	0
	2	1	1.1	0	0
	7	1	4.0	1	0.58
	7	1	4.0	3	1.74
	15	12.5 *	0.6	0	0
Drive	5	1	2.9	0	0
ive	7	1	4.0	0	0
	2	4	0.3	2	0.33
	28	1	16.2	0	0
	11	1	6.4	4	2.31

were the 12-pinion configuration.

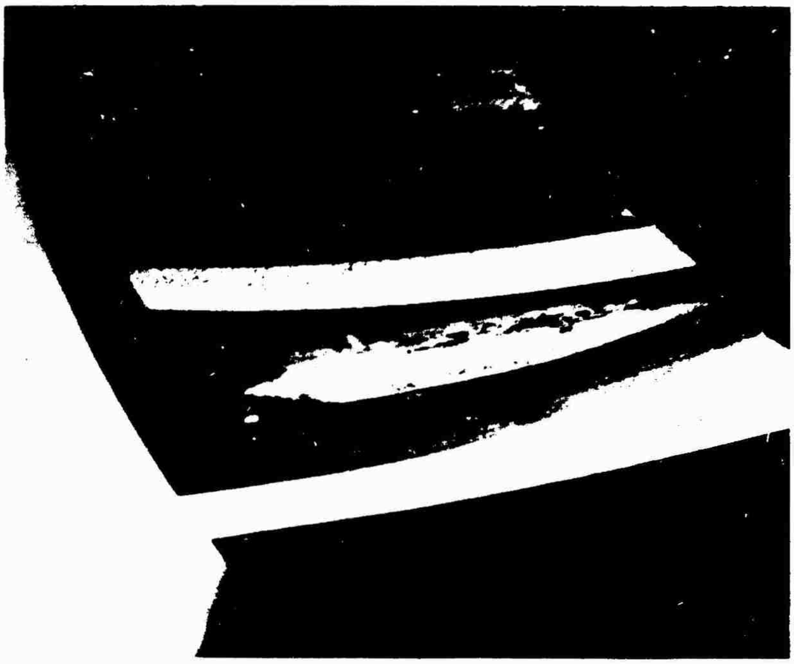

Figure 15. Scored and Spalled Bevel Gear (P/N 204-040-103-7).

Figure 16. Scoring at the Tip of Gear Tooth (Driven) P/N 204-040-762-1).

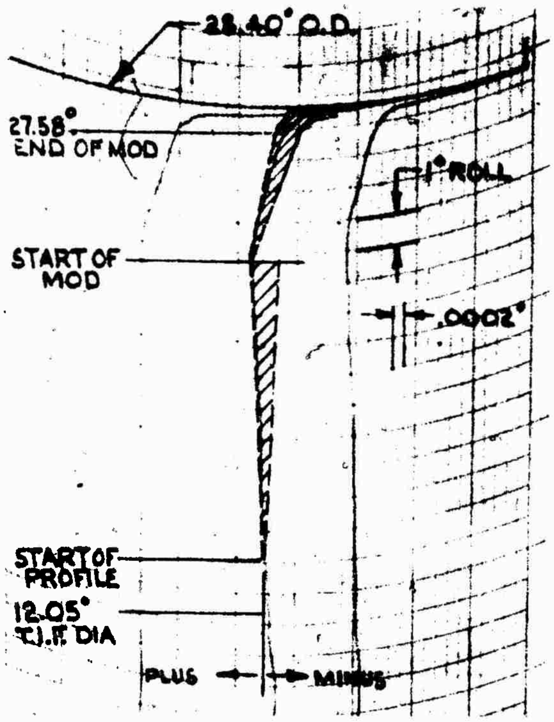

Figure 17. Involute Profile Trace of Tail Rotor Driven Pinion (P/N 204-040-762-1).

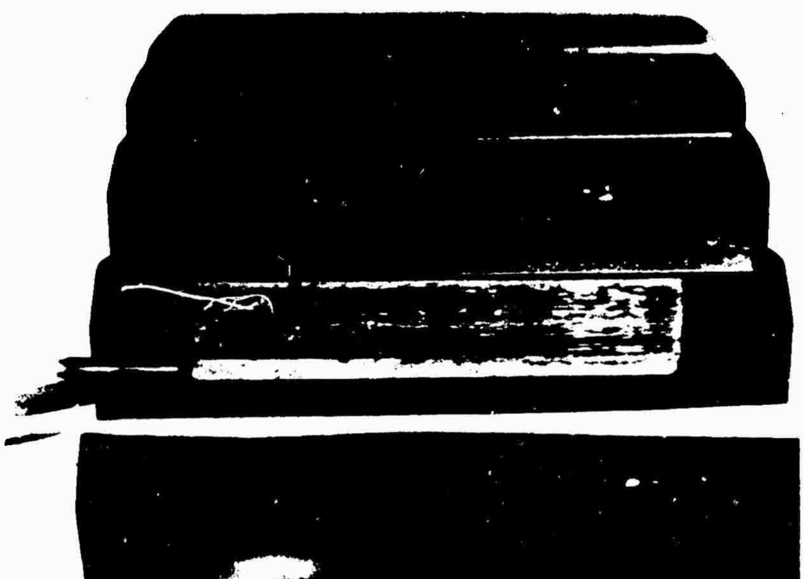

Figure 18. Pitting in Flank of Teeth of Planetary Idler Pinion (P/N 204-040-108-7).

teeth to a depth of 0.0004 inch. As with Items 37 and 38, it is normal overhaul procedure to evaluate this condition visually. Involute chart traces run on the most severe sample pinions from this group (at BHC) were found to be marginal in depth (Figure 18). Maximum depth of pitting wear on the involute trace measures 0.00043 inch (Figure 19). The load distribution condition resulting from the involute modification employed, which produced this wear pitting, is self-correcting, and only in rare instances progresses much farther than the allowable depth. This condition is not considered life limiting.

Item No. 4 - Planetary idler bearing race (P/N 204-040-132-1) normally has a relatively high rejection rate because of handling damage. The exterior or O.D. of this cylindrical component is the bearing raceway, and as such it is susceptible to damage if handled improperly. The majority of these were replaced because of nicks and dents. Thirty-six were replaced because of corrosion or debris damage. One had a nonmetallic inclusion, approximately 0.30 inch long (Figure 20). A longitudinal section taken at the inclusion contained a rehardened area on the surface 0.101 inch in length. The damage was limited to this area and is typical of a grinding burn.

Item No. 5 - Planetary pinion bearing retainers (P/N 204-040-133-1) were replaced because of minor flaking on the tangs (Figure 21). This flaking results when the edge break is inadequate. As may be seen in the photograph, the flaking is limited to the sharp edge of the tang, and it rarely progresses past that shown. This condition does not render the part unserviceable.

Item No. 6 - Bearings (P/N 204-040-135-1) had a replacement rate of 23.9%, primarily because of corrosion or debris damage. There were several replaced because of installation, disassembly, or handling damage. Two were replaced because of excessively high drag torque; they were returned to the manufacturer (Marlin Rockwell Corp.) for inspection. It was determined that the high drag torque was caused by the phenolic ball retainer being tight on the inner ring. The inner rings and retainers showed signs of overheating, and there was heavy wear in the ball pockets in the retainers. Two wide areas in the ball path in the outer rings, located 180° from each other suggest the possibility that the outer rings were squeezed into an out-of-round position during operation. Condition of the inner rings and retainers suggests that the bearings operated with insufficient lubrication, and the drag resulted when overheating caused the retainers to become dimensionally unstable. Neither historical records nor inspection at disassembly indicated operation without oil. Two other bearings were replaced because of fatigue failures in

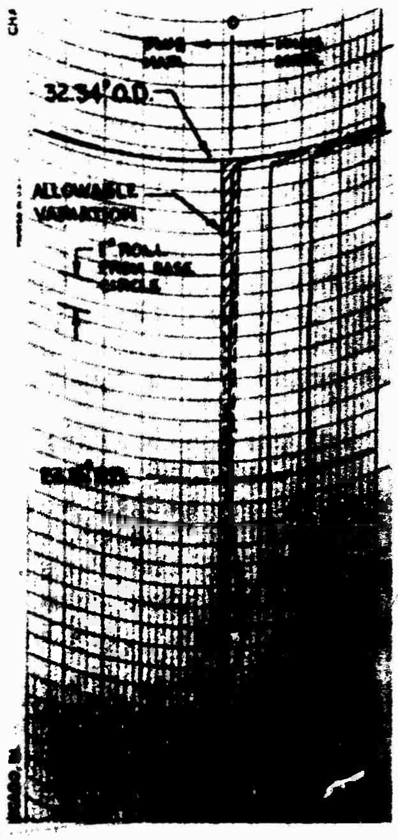

Figure 19. Involute Profile Trace of Planetary Pinion Showing Extent of Pitting Wear.

Figure 20. Inclusion in Planetary Bearing Race (P/N 204-040-132-1).

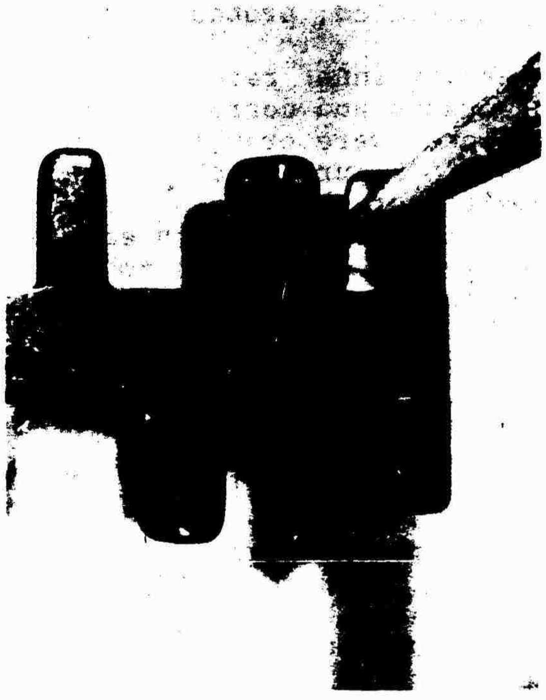

Figure 21. Flaking on Planetary Bearing Retainer (P/N 204-040-133-1).

the ball path in the outer rings (Figure 22). Both failures were subsurface initiated, one from a strong inclusion. No metallurgical defects were found in the other bearing.

Item No. 7 - Bearings (P/N 204-040-142-1) had a replacement rate of 30.9% with no primary failures. These were replaced mainly for corrosion or debris damage or for fretting and false brinelling caused by extensive operation without relative rotation of the inner and outer rings (Figure 23). These bearings are installed in the freewheeling clutch and in normal operation serve only as spacers between the clutch inner and outer races. Only during autorotation of the aircraft is there relative rotation of bearing inner and outer rings. During normal powered flight the bearing balls remain in contact with inner and outer rings in one location, and the fretting probably results from slight movement caused by oscillatory loads from the input drive shaft or main rotor vibration.

Item No. 8 - Bearings (P/N 204-040-143-1) had a replacement rate of 7.5%, with two of 52 having primary failures. Most were replaced because of corrosion or debris damage. There was partial decarburization in the failed raceway area of one of these that resulted in a low hardness value. The other failure was surface initiated, probably from debris damage.

Item No. 9 - Freewheeling inner races (P/N 204-040-190-7) were replaced because of cracks and corrosion and debris damage. Five of the nine replaced were cracked on the sprag clutch surface at an oil hole. Figure 24 shows that the edge break at the oil hole near the crack is less than .010 inch. The drawing requires a 0.015- to 0.025-inch edge break. The oil hole is drilled through at a 45° angle to the clutch surface, and the crack occurs in the thin section at the hole.

Item No. 10 - Freewheeling outer races (P/N 204-040-191-7) were replaced because of corrosion and debris damage only. The replacement rate was 3.5%. There were no primary failures.

Items No. 12, 13, 14, and 16 - Roller bearings (P/N's 204-040-269-3, 204-040-270-3, 204-040-271-3, and 204-040-310-1) were replaced because of assembly damage or corrosion and debris damage. Item No. 12 had the highest rejection rate - 8.7%, with five of the 15 replaced because of assembly damage (Figure 25). This occurs when the nose of the input pinion is not properly aligned when the input quill is installed. The input quill on three of these had been removed or changed in the field, so the damage could have been done either on initial buildup or in field repair.

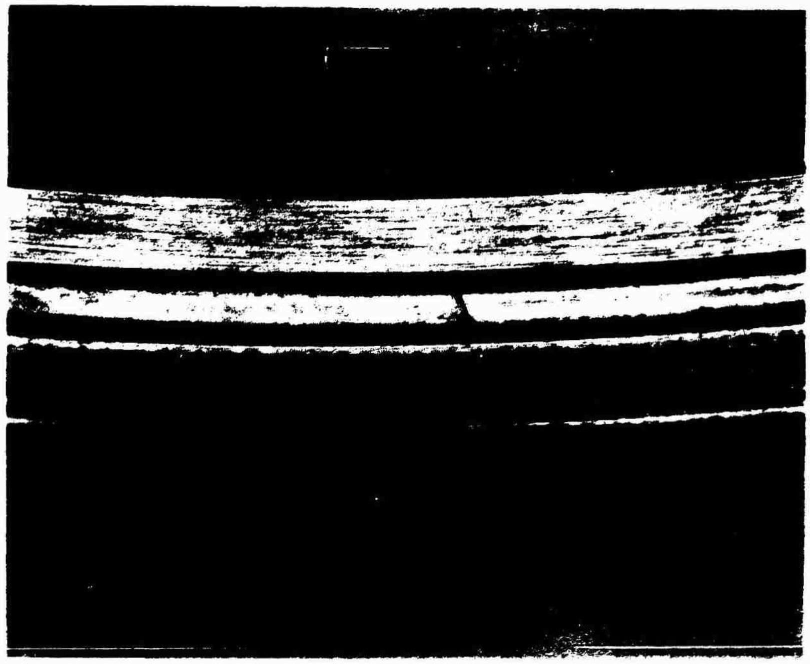

Figure 22. Spalled Bearing Outer Ring (P/N 204-040-135-1).

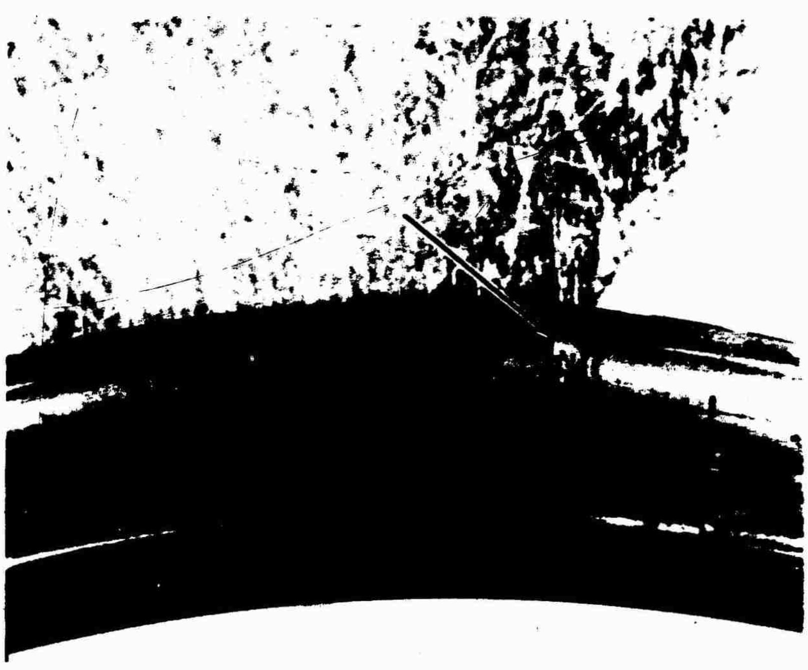

Figure 23. Fretting and Brinelling on Bearing Inner Race (P/N 204-040-142-1).

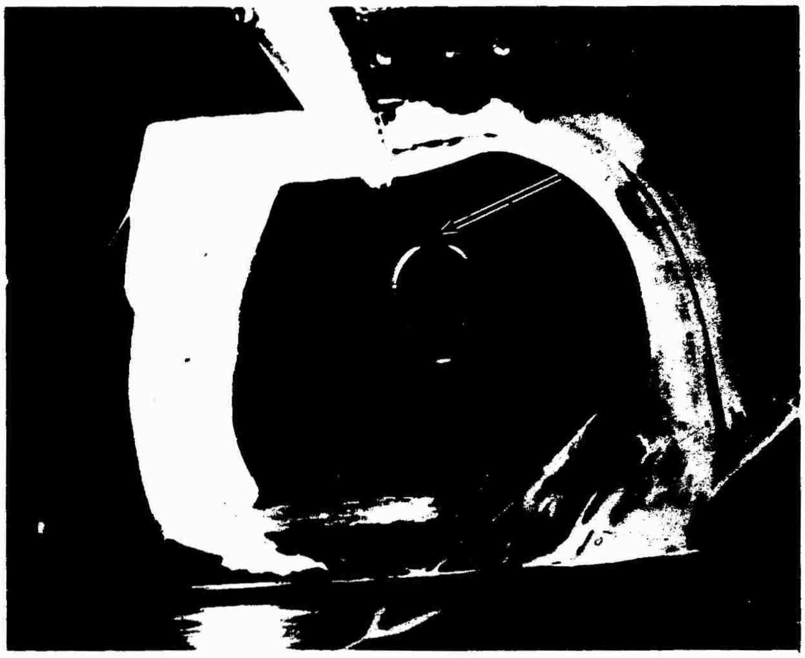

Figure 24. Crack on Freewheeling Clutch Inner Race (P/N 204-040-190-7).

Figure 25. Installation Damage on Bearing Roller (P/N 204-040-269-3).

Item No. 17 - Spacers, tail rotor drive (P/N 204-040-313-1), were replaced because of excessive wear. The maximum depth of wear found was 0.0008 inch. This wear, caused by the lip of the oil seal, is shown in Figure 26. The worn area is well polished and the part is within usable limits.

Item No. 18 - Shaft, bevel gear (P/N 204-040-324-5). One was spalled on the roller bearing surface, and the other four were damaged by corrosion. The spalled area was surface initiated and probably was caused by debris damage (Figure 27). Case surface hardness and core hardness were within drawing limits, and microstructure was good.

Item No. 19 - Sun gears, lower (P/N 204-040-329-1), were replaced for wear at the tips of the gear teeth. The replacement rate was 13.3% with no primary failures. Tip wear of the sun gear teeth corresponds to the flank pitting wear exhibited by Item 3 (P/N 204-040-108-7). Involute profile traces taken on sample gears (at BHC, selected visually as those, with the most severe tip wear) show the maximum depth of wear at the tips to be .00044 inch, Figure 28. All the replaced gears were inspected visually and discarded at overhaul. The applicable overhaul document allows 0.0004 inch depth of wear, but some that were measured at BHC were within usable limits. The gear wear shown in Figure 29 is more severe than generally seen at overhaul and is past acceptable limits. In addition to the wear, there was some corrosion and debris damage present in the replaced gears. This wear condition is generally self-correcting and rarely progresses past the allowable depth of wear.

Item No. 20 - Sun gears, upper (P/N 204-040-330-1 and -3), were replaced primarily for pitting and spalling on the face of the gear teeth (Figure 30). Eighty-three were replaced for a rate of 48.0%, with 57 of the 83 having primary failures. Involute profile and lead traces showed gear-tooth geometry to be within allowable manufacturing limits. Tooth spacing measurements and surface finish readings were all within drawing limits. Hardness checks were made of the case-hardened surface and of the core, and all were within allowable limits. No discrepancies were found in microstructure or retained austenite. An extensive discussion of this failure is presented in subsequent sections of this report.

Item No. 21 - Ring gears, planetary (P/N 204-040-331-5), were replaced primarily because of debris damage caused by ingestion of metal particles into gear mesh. Three had gear teeth chipped at the ends (Figure 31). This chipping or flaking occurs on the ends of teeth when the edge break is insufficient. Teeth with inadequate edge break have a sharp corner

Figure 26. Oil Seal Wear on Spacer (P/N 204-040-131-1).

Figure 27. Spalling on Roller Bearing Surface of Bevel Gear Shaft (P/N 204-040-324-5).

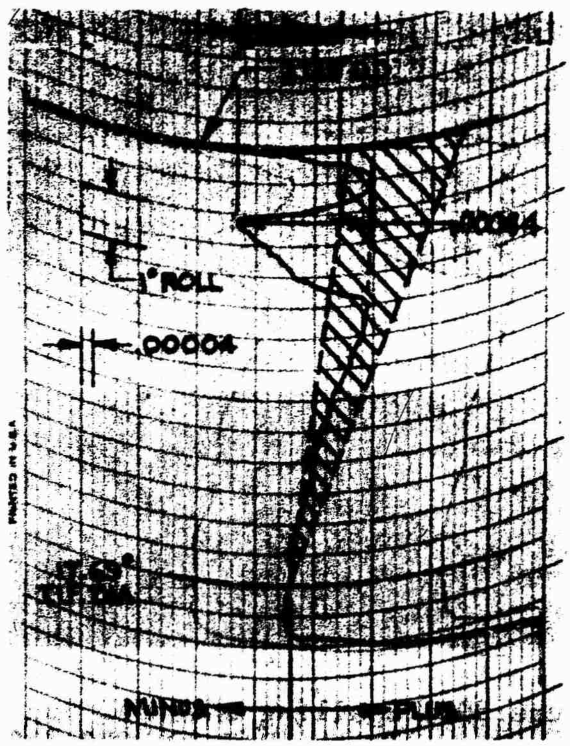

Figure 28. Involute Trace of Lower Sun Gear (P/N 204-040-329-1).

Figure 29. Gear Tooth Tip Wear on Lower Planetary Sun Gear (P/N 204-040-329-1).

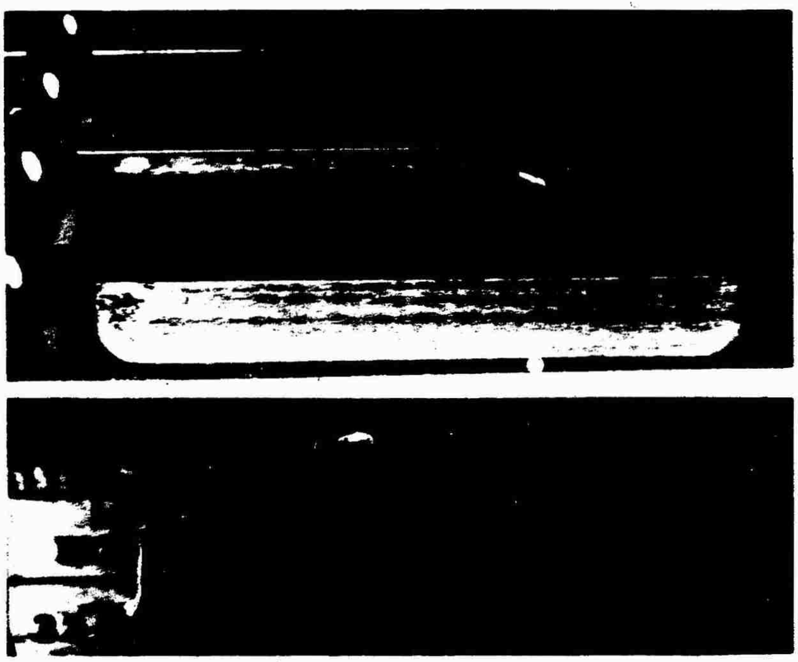

Figure 30. Spalling on Upper Sun Gear Tooth (P/N 204-040-330-3).

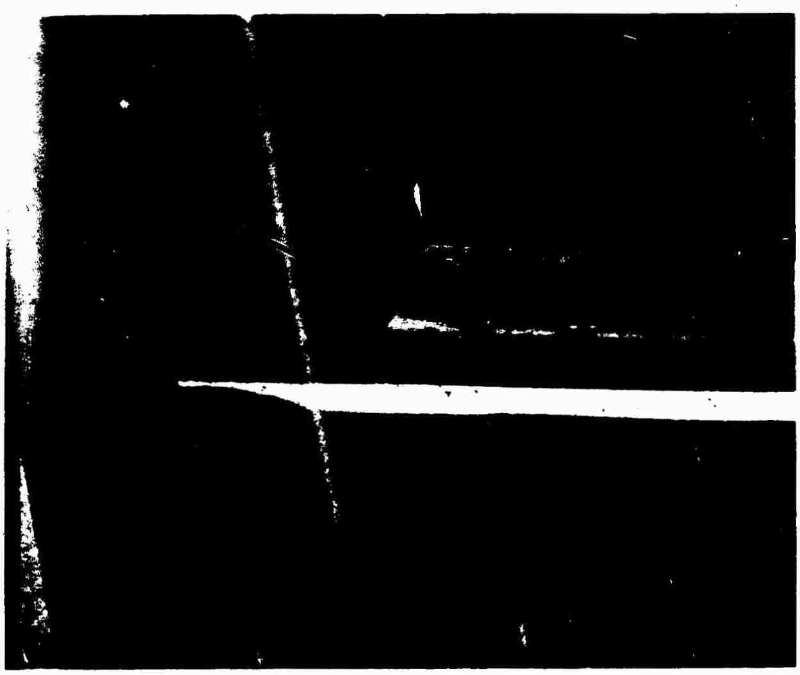

Figure 31. Flaking at the End of Planetary Ring Gear Teeth (P/N 204-040-331-5).

that is very brittle after nitriding. This gear, meshing with one with a greater tooth face width, is highly loaded at the end of the teeth, and the flaking results. Recently revised overhaul requirements permit reuse of this part after hand stoning the flaked area, provided the fractured area cleans up with the rework extending no more than 0.020 inch from the original end of the tooth. Figure 32 shows the edge break at the end of a tooth. It may be seen in the figure that the chamfer is only about 20° to the plane of the end of the tooth. The drawing requirement for edge break is 0.015 inch radius or 0.015 inch x 45° chamfer. This contributes to the fracture occurrences.

Item No. 23 - Bearings, duplex, gear shaft (P/N 204-040-345-7), had a replacement rate of 22%, with 21 of the 38 replaced parts having primary failures. Of these, 18 had fatigue failures in the outer ring and 1 on the inner ring. The others were damaged by corrosion and/or debris. Samples of failed bearings were examined by the BHC Lab and by the Fafnir Bearing Company. Results indicated subsurface initiated failures, with no deficiencies in material or heat treatment reported.

Item No. 24 - Bearings, triplex, input (P/N 204-040-346-3), had a replacement rate of 34.1%, with 38 of the 59 replaced having primary failures. Of these, 28 had fatigue failures in the outer ring, 7 on the inner ring, and 2 on the balls. See Figures 33, 34, and 35. These were examined by BHC Lab, with results indicating failures as surface or near surface initiated. Analysis of one of the failed balls (Figure 33) showed it to have uneven carbide distribution and to be extremely brittle, which is judged to be sufficient cause for failure. The outer ring shown in Figure 34 exhibits a banding or segregated alloy content in the zone of spalling failure. The inner ring shown in Figure 35 is typical of the shallow surface or near surface failure origins which existed.

Item No. 25 - Cases, main bevel gear (P/N 204-040-353-23). Two were replaced because of corrosion damage, and one was replaced because of a cracked web. The crack was in a web on the outer surface of the case, supporting the input quill mounting port. The damaged area had been ground down so that analysis of the failure was inconclusive. The fracture is typical of fatigue failure in magnesium, but there is no history of previous failures in this area.

Items No. 26, 27, and 28 - Cases, main support, sump assembly, and input sleeve (P/N 204-040-354-9, 204-040-355-1 and -3, and 204-040-356-1), were replaced because of handling damage, corrosion in storage, or damage caused by chafing from an improperly supported external oil hose.

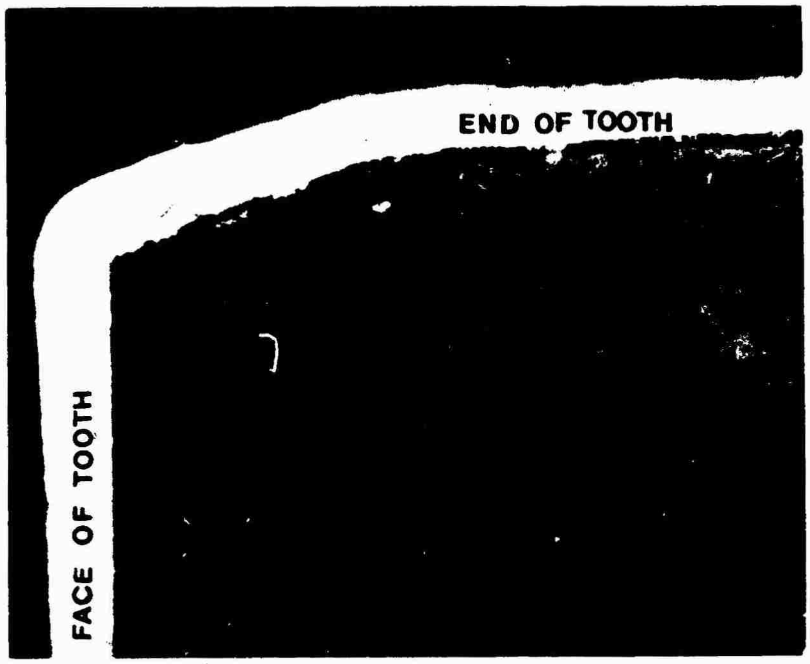

Figure 32. Profile Section Showing Chamfer at End of Ring Gear Tooth (P/N 204-040-331-5).

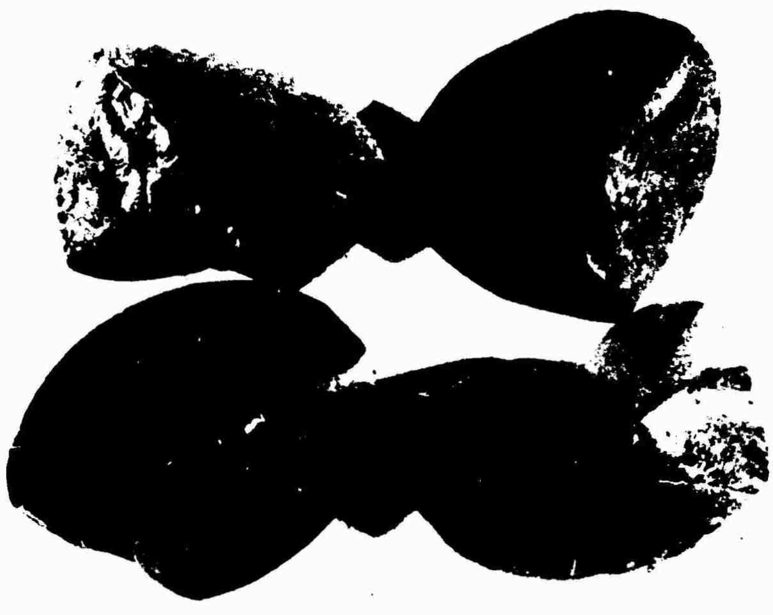

Figure 33. Fractured Bearing Balls (P/N 204-040-346-3).

Figure 34. Banded Microstructure in Area of Spalling (P/N 204-040-346-3).

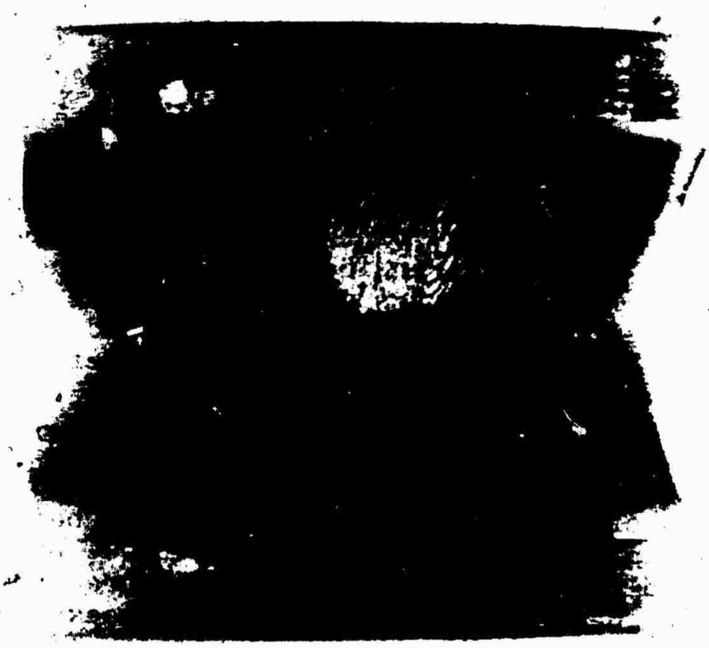

Figure 35. Spalled Inner Ring (P/N 204-040-346-3).

Item No. 29 - Cases, top (P/N 204-040-359-1), had a replacement rate of 16.8%, with all but one being for corrosion damage. One was replaced because of a manufacturing defect, i.e., failure to drill a bleed hole in a threaded hole for a stud and cracking resulted when the stud was installed.

Item No. 30 - Planetary assembly (P/N 204-040-360-3), Item No. 31 - Quill assembly (P/N 204-040-379-3), and Item No. 33 - Planetary spider (P/N 204-040-397-1) were replaced because of corrosion damage that occurred in storage, after the component was removed from service.

Item No. 32 - Case, bevel gear support (P/N 204-040-386-1), had a replacement rate of 17.3%, with 10 being replaced because of corrosion damage. The corrosion occurred on the mounting flange that is in contact with a segmented steel shim. The corrosion results when moisture accumulates in the gaps between the segmented shims.

Item No. 34 - Pinion, input bevel (P/N 204-040-700-1), had a replacement rate of 4.0%, with four of the seven being replaced because of corrosion in storage, one because of debris damage, one for scored gear teeth resulting from operation without oil (Figure 36), and one because of a fatigue failure on the roller bearing surface on the nose of the pinion (Figure 37). The failure was surface initiated. Material and heat treatment were within drawing requirements and microstructure was good. A line of heavy wear may be seen on the bearing roller surface (Figure 37) passing through the spalled area. This is located near the inner end of the roller path. Figure 25 shows typical damage near the end of a roller. This is frequently caused by not having the input quill properly aligned when it is installed in the transmission, and the nose of the pinion damages the end of the roller as the quill is forced in. There are slight indications on the end of the pinion of being jammed against something, but the indications are not conclusive. Surfaces of the rollers had indentations and damage from debris such that it could not definitely be determined if installation damage contributed to the failure of the bearing race.

Item No. 35 - Gears, input bevel (P/N 204-040-701-3), had a replacement rate of 4.0%, with two of the seven being replaced because of handling damage, two were run without oil and had scored teeth, and three had stress corrosion cracks on the back face of the gear (Figures 38 and 39). Cracks on this surface were encountered at BHC several years ago and were thoroughly investigated at that time. It was determined that the cracking resulted from stress corrosion, caused by residual tensile stresses from quenching and subsequent grinding, and

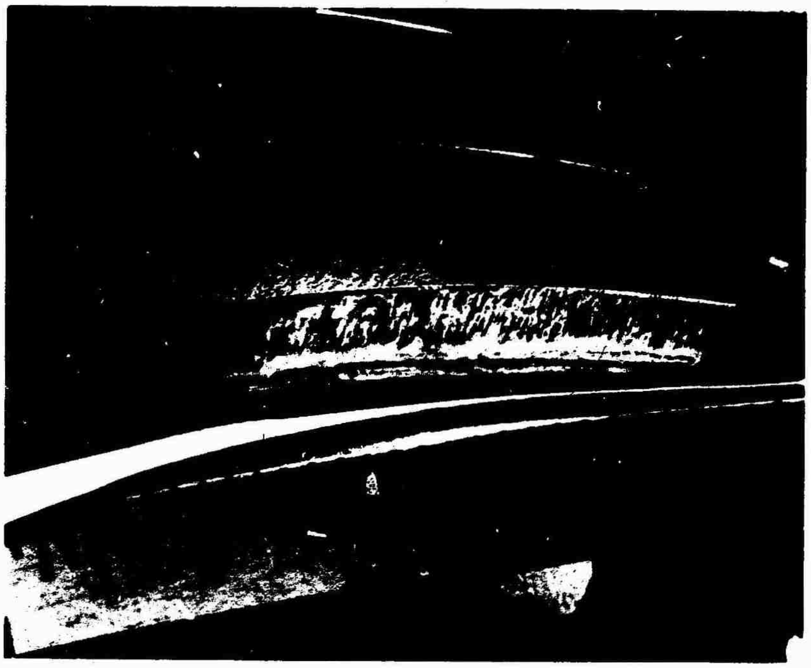

Figure 36. Scored Teeth on Input Pinion (P/N 204-040-700-1).

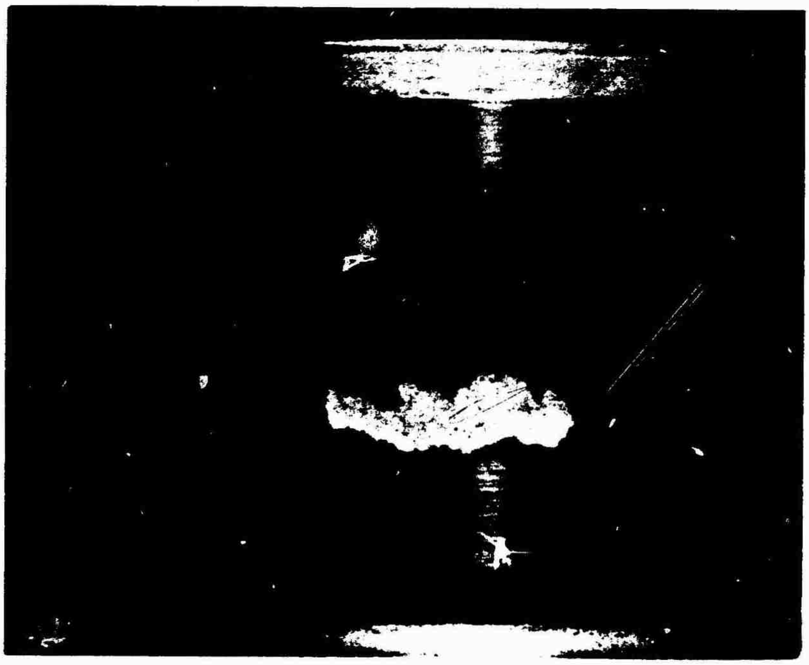

Figure 37. Spalled Roller Bearing Surface on Input Pinion (P/N 204-040-700-1).

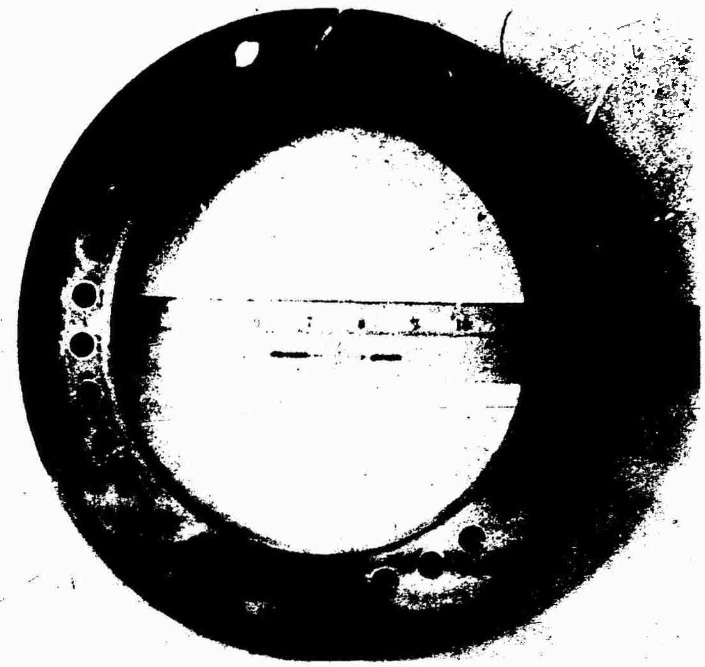

Figure 38. Cracks on the Back Face of Input Bevel Gear (P/N 204-040-701-3).

Figure 39. Close-Up of Crack on Input Bevel Gear (P/N 204-040-701-3).

then subjecting the part to a corrosive black oxide solution at elevated temperature. Changes were made in manufacturing procedures (quench-dies and grinding wheel down-feed control) to prevent this condition, and stock was purged to scrap cracked parts. Cracked gears were tested 100 hours under takeoff power conditions with no indication of propagation of the cracks.

Item No. 36 - Rollers, planetary pinion, were replaced because of corrosion or debris damage. The replacement rate was 0.6%.

Item No. 39 - Washers, planetary (P/N 204-040-789-1). Two were replaced because of cracks (Figure 40). This condition was encountered at BHC in 1968 and was thoroughly investigated then. It was determined that the probable cause of failure was hydrogen embrittlement caused by electrolytic etching prior to black oxide treatment. Cracking occurred only on parts made from alternate material (AlSl 4140 steel); AlSl 4340 steel is the primary material. Manufacturing changes were made to prevent recurrence of this condition, and stock was purged to scrap all suspected parts.

Item No. 40 - Oil pumps (P/N Nichols GC-1669). The replacement rate was 16.2%. Twenty-one were replaced because of debris damage, five were replaced for corrosion damage, and one was replaced for pitted gerotors (Figure 41). Pitting on the inner surface of the outer gerotor frequently results from ingestion of metal particles. There is some evidence of indentations and cuts on the pitted surface of most of these. Three representative sample pumps were returned to the manufacturer (W. H. Nichols Co.) for evaluation. Their findings substantiated indications of debris damage and suggested that possibly some pitting resulted from cavitation. The pumps were inspected and functionally tested by the manufacturer, and in their opinion the pumps are serviceable.

Item No. 41 - Clutch, freewheeling (P/N Borg Warner X-131720), had a replacement rate of 6.4%, with four replaced for drag spring wear, three for sprag wear, and four for broken sprags (Figure 42). Maximum depth of wear found on drag springs was 0.005 inch. Overhaul requirements permit wear to 50% of original spring thickness. These measured approximately 0.025 inch thick in unworn areas, leaving them still serviceable. Sprag wear is not measured at overhaul, but it is evaluated by visual inspection. Those retired had been judged marginal by visual inspection. Three of the four fractured sprags were evaluated by the BHC Metallurgical Lab. One of these indicated coarse martensite that was very brittle near the surface, but the other two showed uniform cross-sectional properties with very finely dispersed carbides.

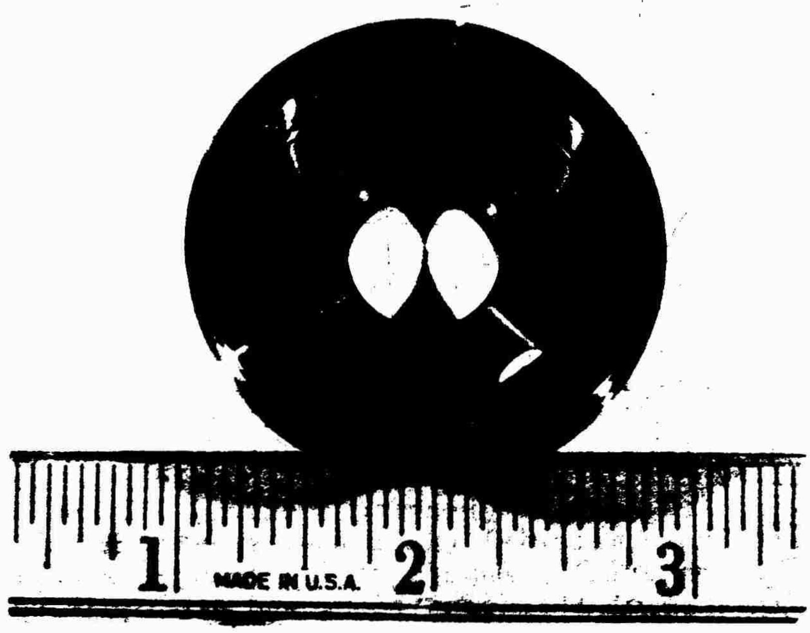

Figure 40. Cracked Planetary Washer (P/N 204-040-789-1).

Figure 41. Pitted Inner Surface of Oil Pump Gerotor (P/N GC1669).

Figure 42. Broken Sprag in Freewheeling Clutch (P/N X-131720).

VERTOL CH-47 FORWARD TRANSMISSIONS

Forty Vertol forward transmissions were included in this program, with 23 in for first-time overhaul. Twenty-eight had completed the scheduled TBO (time between overhaul) period, seven were removed prematurely because of internal failure or metal contamination, and five were removed prematurely for miscellaneous reasons. The mean operating time for the CH-47A models was 652.2 hours, or 81.52% of the scheduled TBO. Mean operating time for the CH-47B models was 449.8 hours, or 74.95% of the scheduled TBO.

Failed parts are listed in Table IV and are located diagrammatically in Figure 4. The reasons for replacement of the parts are given below.

Item No. 1F - Bearing (P/N 114DS143-1). Thirty-four were replaced because of limited life. Two of these had corrosion pitting on the races, and one had a fatigue failure in the outer ring (Figure 43). The failure was extensively examined, and a detailed discussion follows in Analysis of Failure Modes.

Item No. 2F - Bearing (P/N 114DS144-1). Thirty-nine were replaced because of limited life. Twelve of these had spalled races or balls: three were inner ring failures, three were outer ring failures, four were ball failures, and two were both inner ring and ball failures. Two failed balls from one bearing are shown in Figure 44. Both spalled areas have a distinctive straight line running through them. Metallurgical analysis revealed these lines to be large subsurface nonmetallic inclusions. All of the balls and the rings from the bearing were inspected by magnetic particle means. The inclusions were visible on the two failed balls (Figure 44) and on another ball that had not yet failed. Etching of the ball surfaces gave further evidence of defects in the steel (Figure 45). This identified the polar ends of the grain flow in the balls and showed that the inclusions were oriented longitudinally with the rolling direction of the forged bar. Hardness measurements were typical (Rc63) for hardened and tempered 52100 steel. The microstructure was normal, consisting of fine carbides in a matrix of tempered martensite.

Fracture origins of the failed balls and outer races were subsurface, with origins ranging from 0.006 inch to 0.025 inch below the surface. The inner ring fractures were surface initiated, possibly caused by debris damage or corrosion. Corrosion pitting was evident on one bearing that failed and on three others that had not (Figures 46 and 47). Wear patterns over the pitted areas of the bearing shown indicate that the pitting occurred prior to most or all of the bearing operation.

TABLE IV. PARTS REPLACED - VERTOL FORWARD TRANSMISSION

Item No.	Part Number	Part Name	Quantity Replaced	Quantity Per Trans.
1F	114DS143-1	Bearing, Ball, Sun Gear Shaft	34	1
2F	114DS144-1	Bearing, Ball, Rotor Shaft	39	1
3F	114DS145-1	Bearing, Roller, Rotor Shaft	6	1
4F	114DS240-2	Bearing, Roller, Spiral Bevel Gear Shaft	6	1
5F	114DS241-1	Bearing, Ball, Spiral Bevel Pinion Shaft	3	1
6F	114DS243-1	Bearing, Roller, Sun Gear	40	1
7F	114DS244-1	Bearing, Roller, 1st Stage Planetary Gear	67	4
8F	114DS250-1	Bearing, Ball, 2nd Stage Carrier Support	5	1
9F	114DS255-1	Bearing, Ball, Lube Pump Drive	3	2
10F	114DS258-4	Bearing, Roller, 2nd Stage Planetary Gear	8	6
11F	114DS262-1	Bearing, Roller, Spiral Bevel Pinion Gear	7	1
12F	114D1043-1	Pinion, Sun, 1st Stage Planetary	2	1
13F	114D1050-1	Retainer, Bearing, Pinion Gear	1	1
14F	114D1053-1	Gear, Spiral Bevel Ring	3	1
15F	114D1072-1	Retainer, Bearing, Sun Gear	3	1
16F	114D1074-1	Lubricator, Bearing, Pinion Gear	1	1
17F	114D1079-1	Retainer, Bearing, Pinion Gear	1	1
18F	114D1088-12,-14	Support Assembly, Ribbed	3	1
19F	114D2077-1	Gear, Sun, 2nd Stage Planetary	1	1
20F	114D2084-1	Gear, 2nd Stage Planetary	13	6
21F	114D2184-1	Retainer, Bearing, 1st Stage Planetary	12	4

H

ACED - VERTOL FORWARD TRANSMISSION

	Quantity Replaced	Quantity Per Trans.	% Replacement	Quantity Primary Failures	% Primary Failures
	34	1	85.0	1	2.50
	39	1	97.5	12	30.00
	6	1	15.0	0	0
aft	6	1	15.0	0	0
aft	3	1	7.5	0	0
	40	1	100.0	0	0
Gear	67	4	41.9	0	0
ort	5	1	12.5	0	0
	3	2	3.8	0	0
Gear	8	6	3.3	2	0.83
Gear	7	1	17.5	0	0
	2	1	5.0	0	0
	1	1	2.5	0	0
	3	1	7.5	0	0
	3	1	7.5	0	0
	1	1	2.5	0	0
	1	1	2.5	0	0
	3	1	7.5	3	7.50
	1	1	2.5	0	0
	13	6	5.4	0	0
ry	12	4	7.5	10	6.25

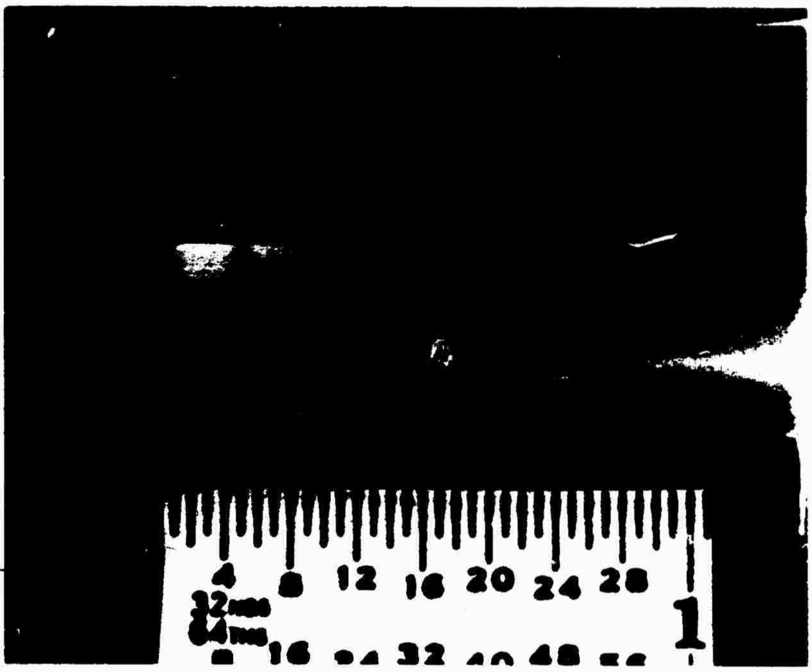

Figure 43: Spalled Bearing Outer Ring (P/N 114DS143-1).

(A) Photograph of Failed Ball at 3X

(B) Photograph of Ball - Failure Eminent at 3X

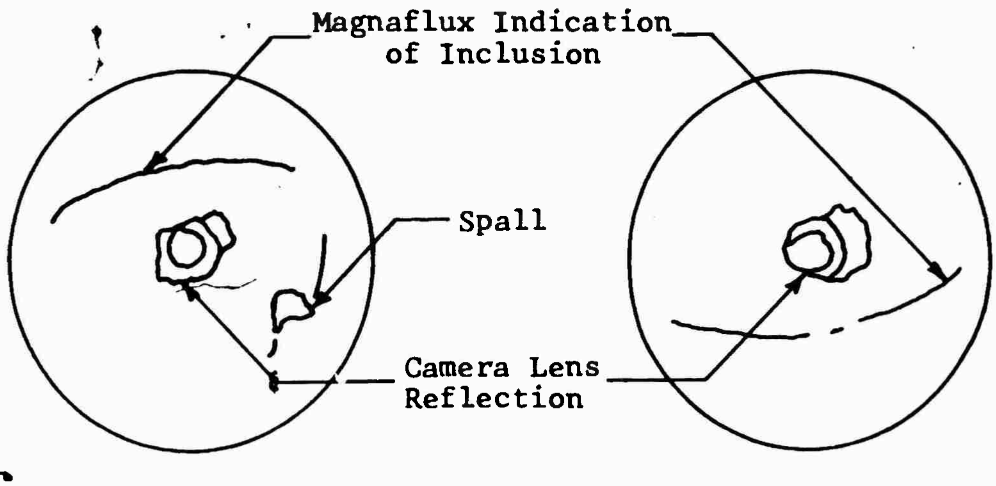

(C) Identification Sketches of Above Photographs

Figure 44. Nonmetallic Inclusions in Bearing Balls.

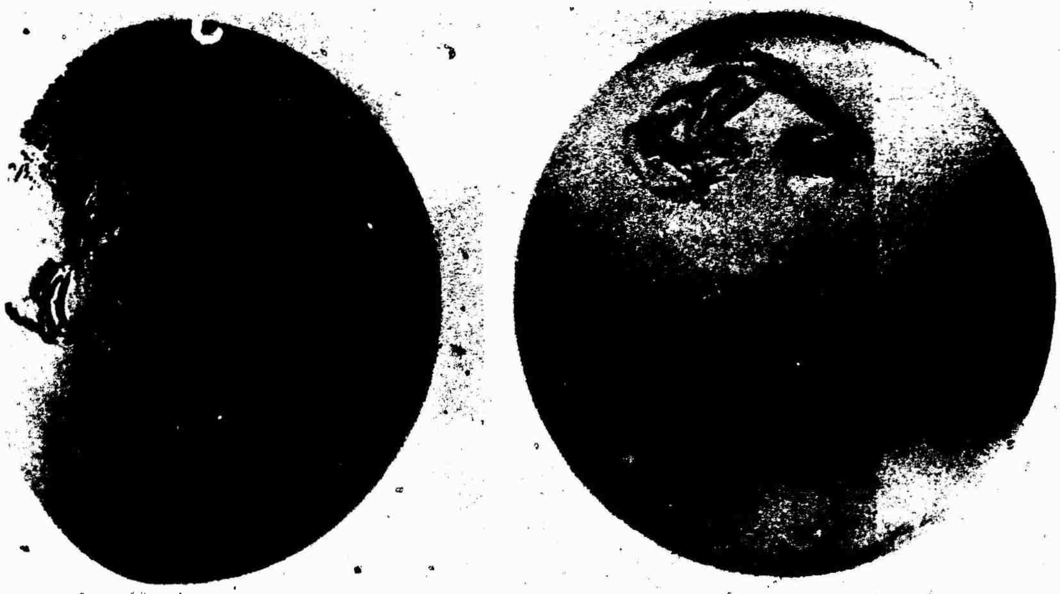

(A) Photographs of Deep Etched Bearing Balls at 1.5X

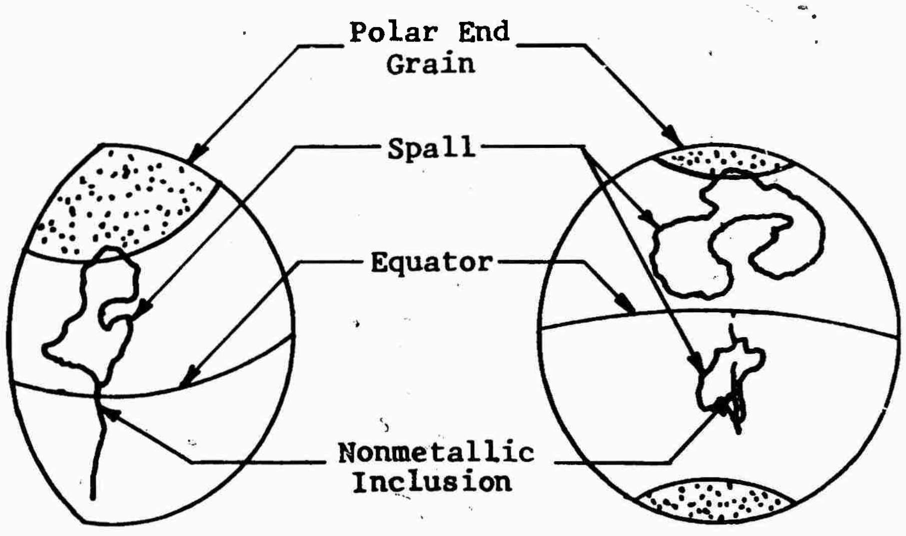

(B) Identification Sketches of Above Photographs

Figure 45. Deep Etching of Bearing Balls.

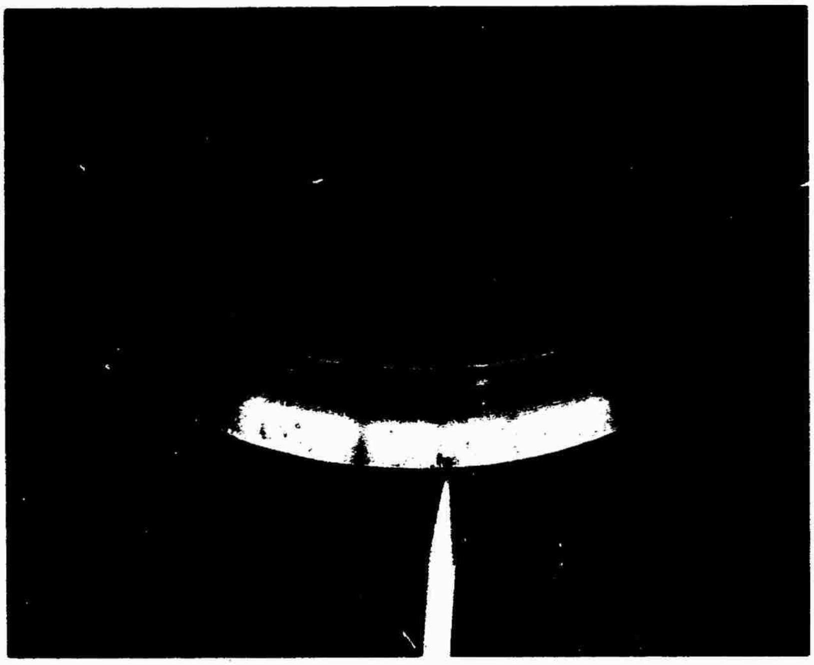

Figure 46. Corrosion Pitting on Bearing Race (P/N 114DS144-1).

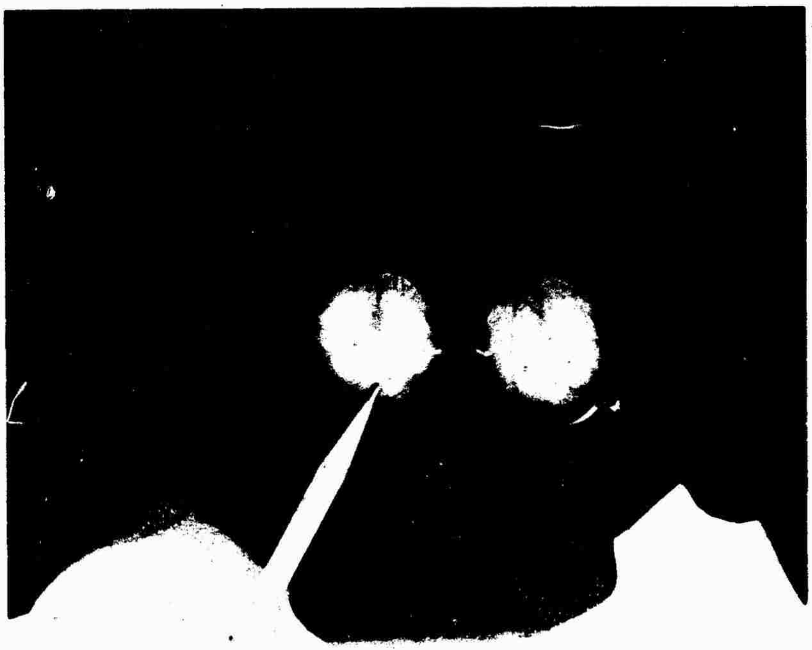

Figure 47. Corrosion Pitting on Bearing Balls (P/N 114DS144-1).

Hardness values appeared to be normal for 52100 steel; however, the spectrochemical analysis indicated that material for the balls was below AMS6444B or AMS6445A (52100) limits on carbon and chromium, and the races were below AMS6445A limits for chromium. The microstructure appeared to be normal for low alloy high carbon steel that was heat treated properly to this hardness level. No material defects were found that were identified as fracture causes.

Item No. 3F - Bearing (P/N 114DS145-1). Six were replaced because of corrosion and/or debris damage. There were no primary failures.

Items No. 4F, 5F, and 11F - Bearings (P/N 114DS240-2, 114DS241-1, and 114DS262-1). These input pinion bearings were replaced because of debris or corrosion damage. Item 4F was replaced because of fretting on the inner diameter.

Item No. 6F - Bearing (P/N 114DS243-1). Forty were replaced because of limited life. The only defects found in these were debris damage to one and corrosion damage to six. There were no primary failures.

Item No. 7F - Bearing (P/N 114DS244-1. Sixty-seven were replaced because of limited life. The only defect found among these was corrosion damage to three, which had occurred since removal from service. There were no primary failures.

Items No. 8F and 9F - Bearings (P/N 114DS250-1 and 114DS255-1). Eight were replaced because of debris damage and corrosion. There were no primary failures.

Item No. 10F - Bearing (P/N 114DS258-4). Two had fatigue failures on the inner race, and six were replaced because of corrosion damage. This part is also used in the aft transmission where the failure modes were essentially identical. Figures that are representative of these failures appear in the section Vertol CH-47 Aft Transmission.

Item No. 12F - Sun pinion (P/N 114D1043-1). Two were replaced, one because of corrosion pitting on the roller bearing surface, and the other for spalling on the face of one gear tooth (Figure 48). The spalling failure was surface initiated. Case and core structure were found to be within drawing requirements, and microstructure was typical of AMS6260 carburized steel. The lack of indications of distress around the failed area on the tooth, and in this area on the other teeth, indicates the probability that this failure resulted from a foreign particle going through gear mesh. There were marks on the back face of this tooth but on no other teeth of the

Figure 48. Spalled Tooth on First-Stage Planetary Sun Gear (P/N 114D1043-1).

gear. Corresponding marks were found on the driven face and opposing coast side faces of two teeth on a mating planetary idler gear. These marks might indicate that some foreign particle had gone through gear mesh, wedging the back face of the sun pinion tooth against the mating planet gear tooth, and causing surface damage to the tooth that failed. The source of the foreign particle could not be determined.

Item No. 13F - Retainer assembly (P/N 114D1050-1). One was replaced for corrosion pitting in the bore for the oil seal.

Item No. 14F - Gear (P/N 114D1053-1). Three were replaced for corrosion damage on the teeth.

Item No. 15F - Retainer (P/N 114D1072-1). Three were replaced because of wear caused by spinning of the outer ring of the 114DS243 bearing (Item No. 6F).

Item No. 16F - Lubricator (P/N 114D1074-1). One was replaced because of wear caused by spinning of the outer ring of the 114DS241-1 bearing.

Item No. 17F - Retainer (P/N 114D1079-1). One was replaced because of wear caused by the outer ring of the 114DS241-1 bearing spinning in the support assembly.

Item No. 18F - Support assembly (P/N 114D1088-12 and -14). Three were replaced because of a crack at the flange in the bore for the upper mast bearing (Figure 49). Location and orientation of the crack was essentially the same for all three parts. Origin of the fracture was on the inner diameter of the shoulder or flange for the bearing (Figure 50). Bare metal from wear was exposed on the surface at the origin (Figure 51). A fracture profile through the origin showed fairly flat transgranular cracking typical of fatigue in aluminum alloys. Spectrochemical analysis conformed to specification QQ-A 367 for 2014 material. Hardness and electrical conductivity indicated that the material was heat treated to the T6 condition. Microstructure was typical of 2014-T6 material. No material defects were found that might have initiated the fracture.

Item No. 19F - Gear (P/N 114D2077-1). One was replaced because of corrosion pitting.

Item No. 20F - Gear (P/N 114D2084-1). Thirteen were replaced, 12 for corrosion damage and one for handling damage.

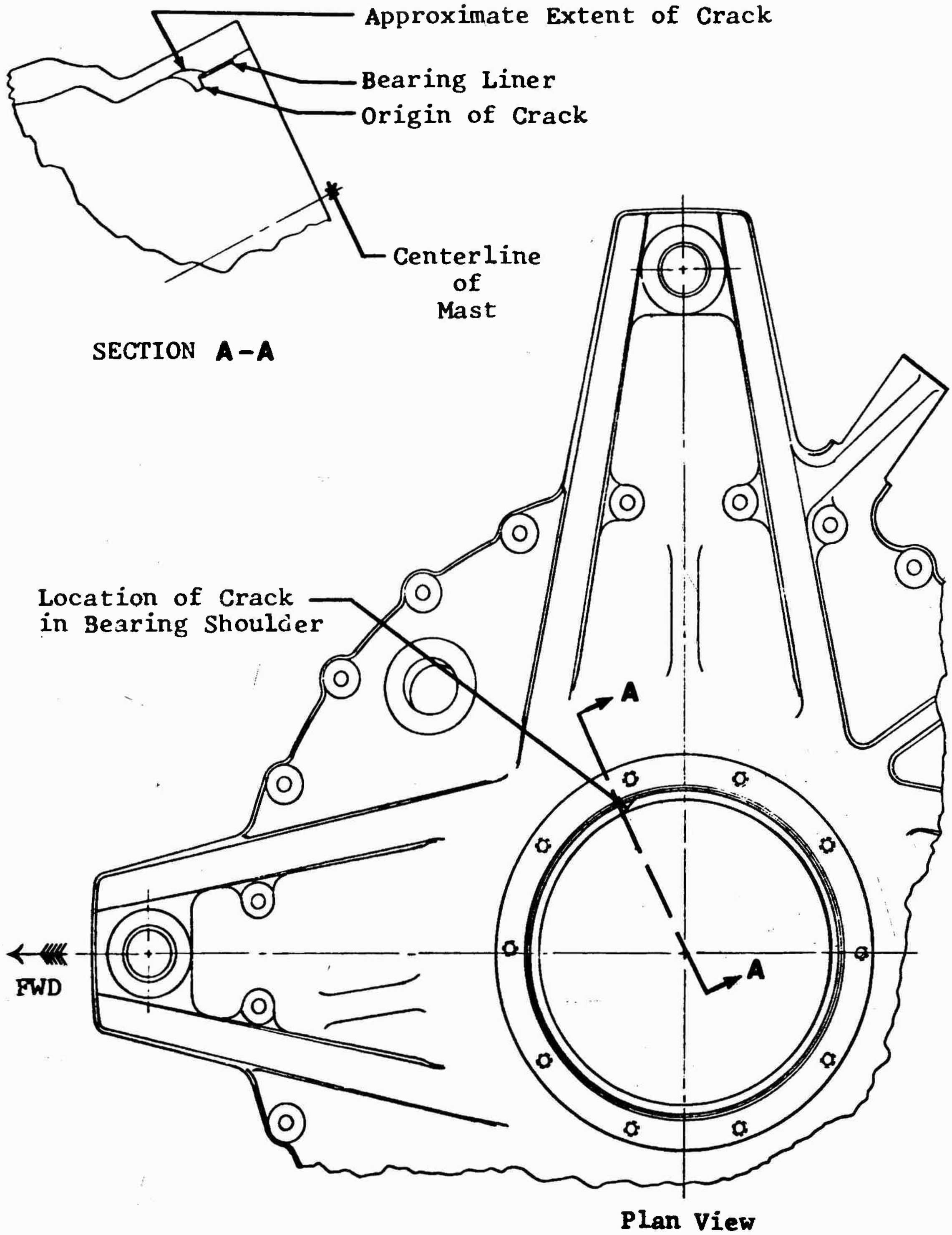

Figure 49. Support Assembly, Vertol Forward Transmission (P/N 114D1088).

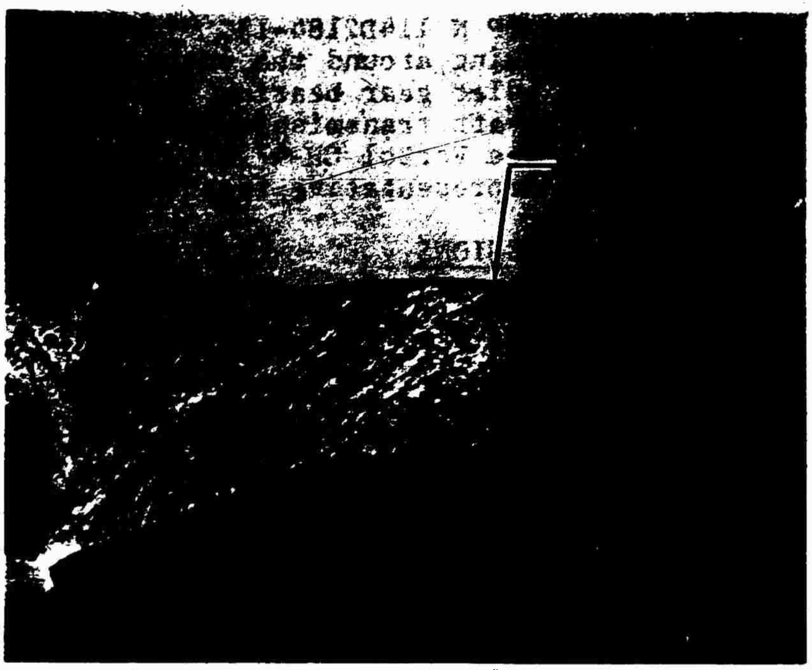

Figure 50. Fracture Face of Cracked Support Assembly (P/N 114D1088-14).

Figure 51. Cracked Support Assembly (P/N 114D1088-14).

Item No. 21F - Retainer (P/N 114D2184-1). Twelve were replaced because of wear and cracking around the outer edge where it contacts the planetary idler gear bearing inner ring. This part is also used in the aft transmission and the failure modes were identical. See Vertol CH-47 Aft Transmissions section of Results for representative figures.

VERTOL CH-47 AFT TRANSMISSIONS

Thirty-two Vertol aft transmissions were included in this program; of these, 25 were in for first-time overhaul. Twenty-five had completed the scheduled TBO period, and seven had been removed prematurely (six for internal failure or metal contamination, and one because of a cracked case). The mean operating time since new or overhaul for the CH-47A models was 1078.4 hours, or 89.9% of the scheduled TBO. Mean operating time for the CH-47B models was 522.6 hours, or 87.1% of the scheduled TBO.

Failed parts are listed in Table V and are located diagrammatically in Figure 5. The reasons for replacement of parts are given below.

Item No. 1A - Roller bearing (P/N 114DS240-2), a total quantity of eight was replaced, for a rejection rate of 25.0%. Six parts had corrosion or debris damage and four had rollers that were spalled (Figure 52). One failure had progressed sufficiently that the outer race was also spalled. Laboratory analyses were performed on the failed parts by the Fafnir Bearing Co. and by BHC. The roller failure appears as a longitudinal crack with flaking along the edges. The crack is located near the midpoint of the roller and does not extend into either end radius. A section profile (Figure 53) shows the fracture extending relatively deep into the roller (0.025 inch) with flaking of the bearing surface at the crack. This spalling appears to be secondary to the crack. Hardness measurements ranged from Rc64 to 65. The microstructure is not considered typical for properly heat treated M-50 steel in that it contains areas of coarse acicular martensite. These coarse needles were found throughout the roller. This coarse martensite, along with the high hardness (greater than Rc63) suggests that at least some of the martensite within the material had not been sufficiently tempered. Retained austenite was checked by X-ray diffraction and found to be negligible.

Item No. 2A - Ball bearing (P/N 114DS242-1) had one primary failure, with a total of 27 parts replaced due to limited life. The replacement rate was 42.2%. Both outer rings of this duplex bearing had spalled. The component was sent to Fafnir

TABLE V. PARTS REPLACED - VERTOL /

Item No.	Part Number	Part Name	Q R
1A	114DS240-2	Bearing, Roller, Spiral Bevel Gear Shaft	
2A	114DS242-1	Bearing, Ball, Sun Gear	
3A	114DS243-1	Bearing, Roller, Sun Gear	
4A	114DS244-12	Bearing, Roller, 1st Stage Planetary	
5A	114DS247-1	Bearing, Roller, Clutch Shaft	
6A	114DS249-1	Bearing, Roller, Clutch Shaft	
7A	114DS250-1	Bearing, Ball, Carrier Support	
8A	114DS251-1	Bearing, Ball, Input Shaft	
9A	114DS253-1	Bearing, Roller, Fan Drive	
10A	114DS256-1	Bearing, Ball, Hydraulic Pump Drive	
11A	114DS257-1	Bearing, Roller, Input Shaft	
12A	114DS258-4	Bearing, Roller, 2nd Stage Planetary Gear	
13A	114DS262-1,-2	Bearing, Roller, Spiral Bevel Pinion Gear	
14A	114DS265-1	Bearing, Roller, Clutch Shaft	
15A	114DS274-1	Bearing, Ball, Carrier Support	
16A	114D2045-5	Gear, Spiral Bevel Pinion	
17A	114D2062-1	Gear, Spiral Bevel	
18A	114D2084-1	Gear, Planetary Pinion, 2nd Stage	
19A	114D2086-3	Gear, Ring, Planetary	
20A	114D2093-3	Shaft, Clutch, Accessory Drive	

TABLE V. PARTS REPLACED - VERTOL AFT TRANSMISSION

	Quantity Replaced	Quantity Per Trans.	% Replacement	Quantity Primary Failures	% Primary Failures
Roller, Spiral Bevel Gear Shaft	8	1	25.0	4	12.50
Ball, Sun Gear	27	2	42.2	1	1.56
Roller, Sun Gear	26	1	81.3	0	0
Roller, 1st Stage Planetary	41	4	32.0	1	0.78
Roller, Clutch Shaft	4	1	12.5	0	0
Roller, Clutch Shaft	13	1	40.6	0	0
Ball, Carrier Support	2	1	6.3	0	0
Ball, Input Shaft	1	1	3.1	0	0
Roller, Fan Drive	1	1	3.1	0	0
Ball, Hydraulic Pump Drive	6	10	1.9	0	0
Roller, Input Shaft	5	1	15.6	0	0
Roller, 2nd Stage Planetary Gear	4	6	2.1	3	1.56
Roller, Spiral Bevel Pinion Gear	5	1	15.6	0	0
Roller, Clutch Shaft	14	1	43.8	0	0
Ball, Carrier Support	1	1	3.1	0	0
iral Bevel Pinion	2	1	6.3	0	0
iral Bevel	3	1	9.4	0	0
anetary Pinion, 2nd Stage	1	1	0.5	0	0
ng, Planetary	2	1	6.3	0	0
lutch, Accessory Drive	5	1	15.6	0	0

TABLE V - Continued

Item No.	Part Number	Part Name	Quantity Replaced	Quantity Per Trans.
21A	114D2105-1	Shaft, Quill Accessory Drive	3	1
22A	114D2106-1	Gear, Spur, Accessory Drive	2	1
23A	114D2107-1	Gear, Alternator Drive	4	2
24A	114D2116-3	Shaft, Quill, Blower Drive	1	1
25A	114D2145-1	Lubricator, Bearing, Pinion Gear	1	1
26A	114D2178-1	Gear, Spur, Hydraulic Pump Drive	1	1
27A	114D2184-1	Retainer, Bearing, 1st Stage Planetary	13	4
28A	114D2191-2	Spacer, Bearing, Pinion Gear	2	1

A

TABLE V - Continued					
	Quantity Replaced	Quantity Per Trans.	% Replacement	Quantity Primary Failures	% Primary Failures
Accessory Drive	3	1	9.4	0	0
Accessory Drive	2	1	6.3	0	0
ator Drive	4	2	6.3	0	0
, Blower Drive	1	1	3.1	0	0
Bearing, Pinion Gear	1	1	3.1	0	0
Hydraulic Pump Drive	1	1	3.1	0	0
aring, 1st Stage Planetary	13	4	10.2	11	8.59
ing, Pinion Gear	2	1	6.3	0	0

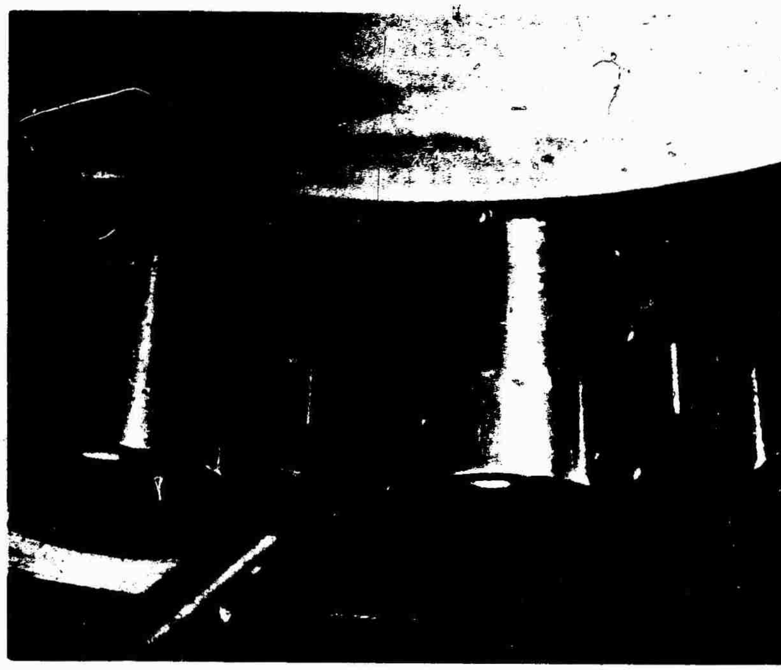

Figure 52. Spalled Bearing Roller (P/N 114DS240-2).

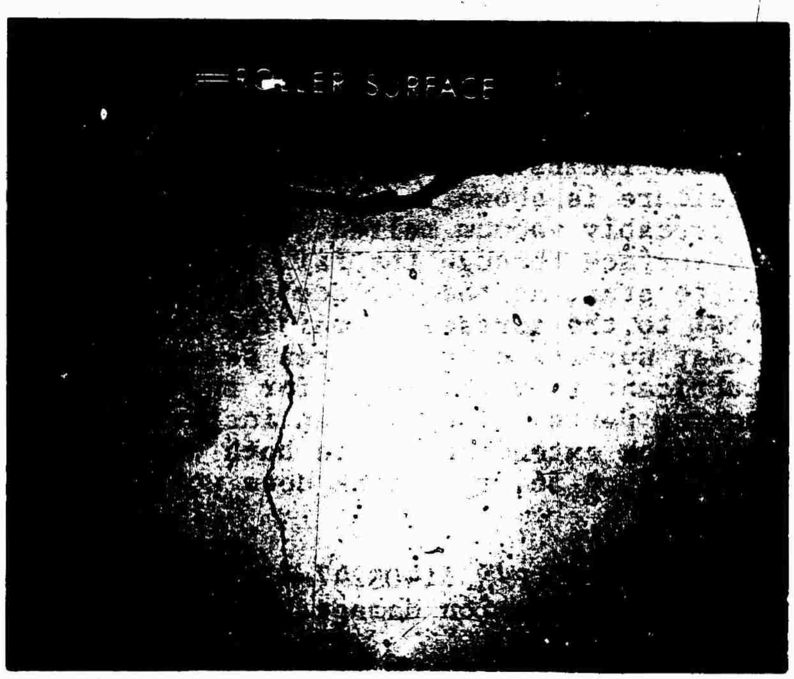

Figure 53. Spalled Roller (P/N 114DS242-1).

Bearing Company for analysis. There were no obvious metallurgical or dimensional defects which were likely to result in premature failure. However, both rings exhibited retained austenite levels of approximately 11%, which is considered to be high for good aircraft bearing quality. The dimensional stability of a bearing with this austenite level is unsatisfactory. Subsequent in-service growth can adversely influence installed preload.

Item No. 3A - Roller bearing (P/N 114DS243-1) had no failures. Twenty-six parts, replaced because of limited life, were inspected. All were serviceable with only corrosion or debris damage noted.

Item No. 4A - Bearing, lower planetary (P/N 114DS244-12), had one primary failure. An additional 40 parts were replaced because of limited life. All except one of these were adjudged to be serviceable. The failed bearing had an incipient spall in the inner race (Figure 54). No metal had yet been lost from the spalled area, and the failure appeared as a crack. Magnetic particle inspection of the ring revealed no indications other than those visible to the naked eye. The ring was inspected after surface temper etch, a technique used to reveal localized hard or soft areas resulting from overheating (usually due to grinding) or work hardening. There were very faint lines oriented circumferentially around the race that may have been caused by grinding damage, or they may be the result of bearing operation. Hardness, Shepherd Fracture grain size, and retained austenite were all satisfactory. Microstructure was good and the steel was very clean. The micro-nonmetallic inclusion content of a cross section through the failure is shown in Table VI and indicates that the steel is probably vacuum melted. A metallographic examination of the surface through the failed area revealed a crack that appeared to start at the surface (Figure 55) and propagate almost parallel to the surface, remaining very shallow. This suggests a point surface origin, often associated with insufficient lubricant film thickness for the relative roughness of the contacting parts. There is an inclusion in the failed area with the crack extending out in both directions, but as may be seen in Figure 56, the crack does not extend through the inclusion.

Item No. 5A - Bearings (P/N 114DS247-1). A total of four were replaced, three for corrosion damage, and one for disassembly or handling damage.

Items No. 6A and 14A - Bearings (P/N 114DS249-1 and 114DS265-1) had a 40.6% and a 43.8% replacement rate, respectively, because of wear on the ends of the rollers (Figures 57 and 58). Wear on

Figure 54. Incipient Spall on Bearing Inner Race (P/N 114DS244-13) (Magnification 4X).

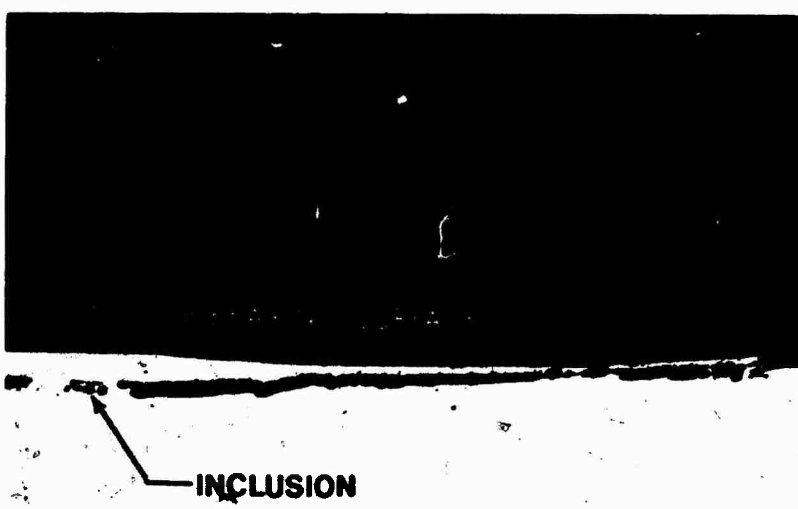

Figure 55. Section Through Crack in Bearing Race (P/N 114DS244-13) (Magnification 100X).

TABLE VI. MICRO-NONMETALLIC INCLUSION CONTENT IN BEARINGS

Part Number of Failed Part	J-K Rating			
	A	B	C	D
114DS244-13	0 - 0	0 - 0	0 - 0	0 - 1/2
114DS258-3 (Inner Race)	0 - 0	0 - 0	0 - 0	0 - 1/2
114DS258-3 (Roller)	0 - 0	0 - 0	0 - 0	0 - 0

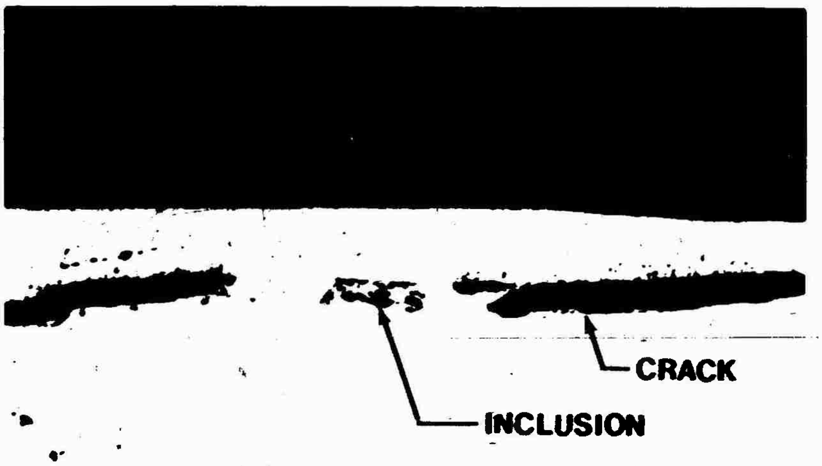

Figure 56. Enlarged Section Through Crack in Bearing Inner Ring (P/N 114DS244-13) (Magnification 200X).

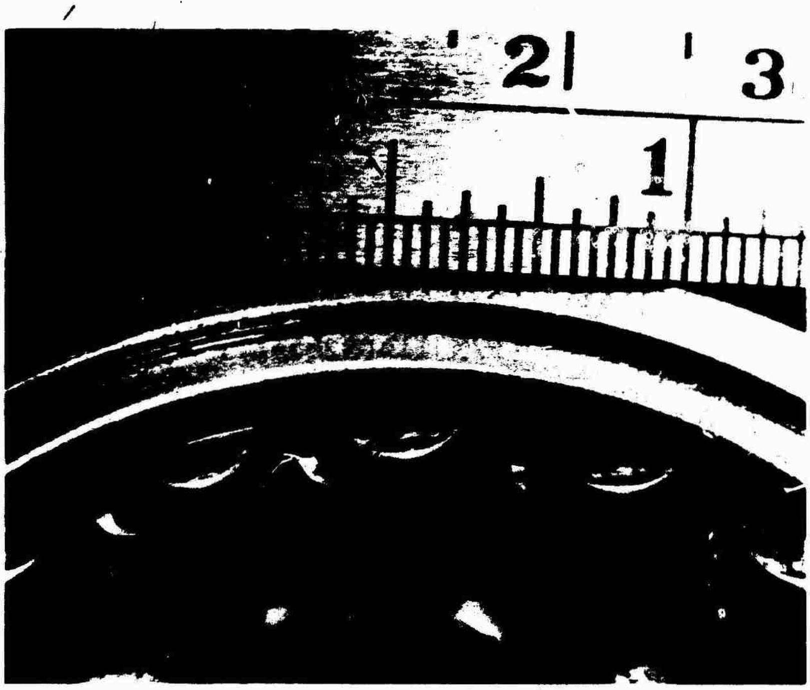

Figure 57. Roller Bearing End Wear (P/N 114DS249-1).

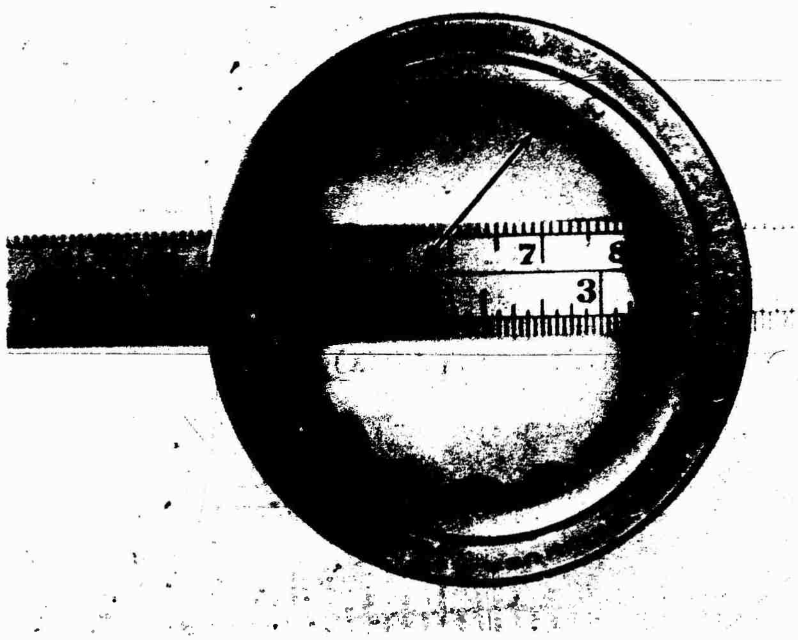

Figure 58. Roller Bearing End Wear (P/N 114DS265-1).

the mating surface to the bearings is shown in Figures 59 and 60. This clutch shaft, Item 20A (P/N 114D2093-3), is fretted and worn both on the shoulder and on the bearing diameter where the rollers contacted and remained for long periods of operation with insufficient relative rotation of clutch inner and outer races. There were no primary failures, and hardness of rollers and shafts met drawing requirements.

Items No. 7A, 8A, 9A, 10A, and 11A - Bearings (P/N's 114DS250-1, 114DS251-1, 114DS256-1, and 114DS257-1) were replaced because of corrosion, debris damage, or handling damage. There were no primary failures.

Item No. 12A - Bearing (P/N 114DS258-4), there was a total of four replaced, one for corrosion damage, one for spalling on a roller, and two for spalling on the inner races (Figures 61 and 62). Magnetic particle inspection of the inner rings revealed no indications other than cracks associated with the spalls. There were several straight line indications on the roller in addition to those visible to the naked eye. These extended in the longitudinal direction. It could not be determined if these indications were due to cracks resulting from the failure or to seams or inclusions that might have caused the failure. Surface temper etch inspection revealed no discrepancies except a very faint indication (white band) approximately 1/16 inch to 1/8 inch wide and about 2 inches long on a nonfailed race. There were indications on the failed roller of alternate light and dark bands (Figure 63). These may be due to grinding burns but are more likely the result of debris damage work hardening the surface. The hardness, grain size, and retained austenite were all satisfactory. Microstructure of each part was satisfactory, and the steel was very clean. The micro-nonmetallic inclusion content of a cross section through each part is shown in Table VI and indicates that the steel was probably vacuum melted. No deficiencies were found that could definitely be labeled as failure cause. It is possible that the failed roller may have had seams or inclusions that initiated the failure, or it is possible that grinding burns may have contributed to the failure. The investigation was inconclusive in that possible failure mode causes still include grinding damage, surface imperfections, surface inclusions, and inadequate lubrication conditions.

Items No. 13A and 15A - Bearings (P/N's 114DS262-1 and 114DS274-1) were replaced because of corrosion, debris damage, or handling damage. There were no primary failures.

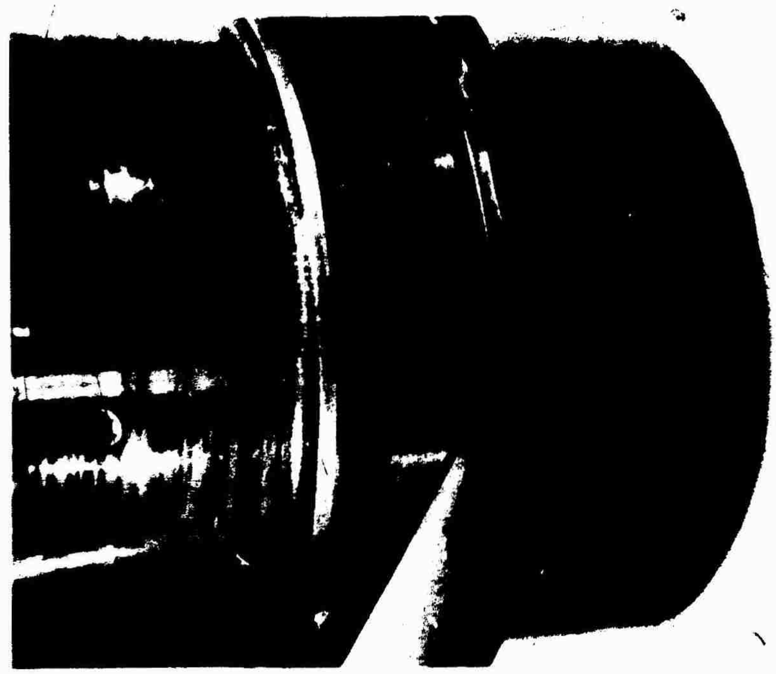

Figure 59. Bearing Roller End Wear on Freewheeling Inner Race (P/N 114D2093-3).

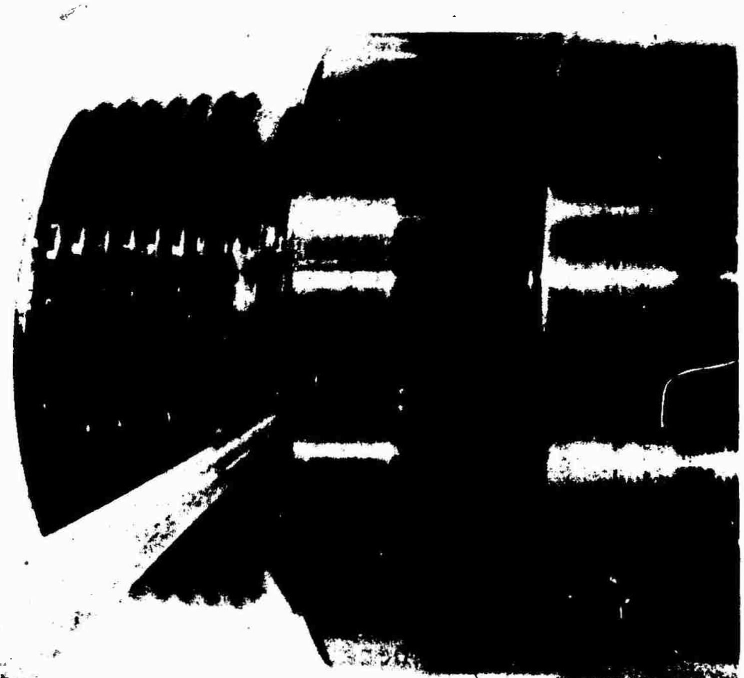

Figure 60. Roller Wear on Freewheeling Clutch Inner Race (P/N 114D2093-3).

Figure 61. Spalled Planetary Pinion Bearing Roller (P/N 114DS258-3) (Magnification 3X).

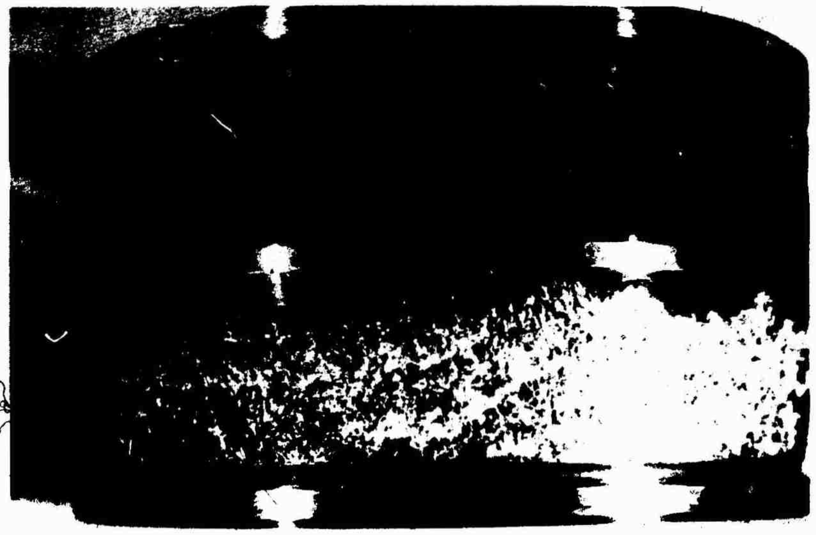

Figure 62. Spalled Planetary Pinion Bearing Inner Race (P/N 114DS258-3) (Magnification 3X).

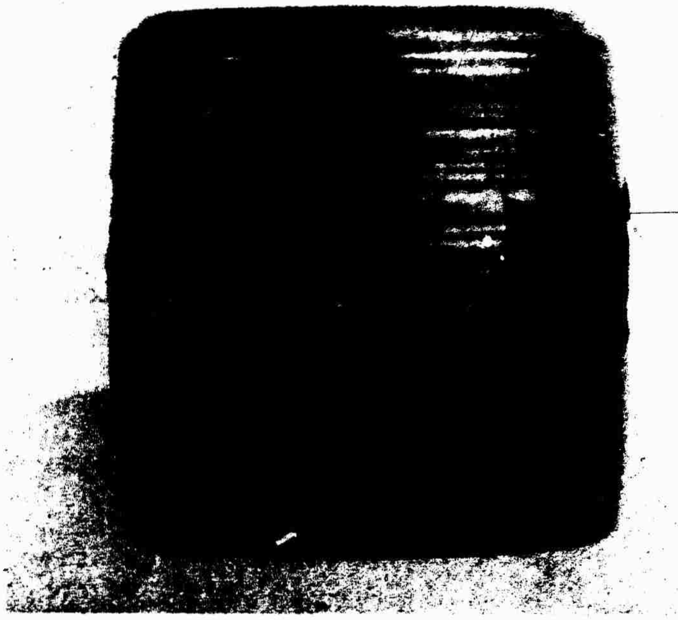

Figure 63. Failed Bearing Roller (P/N 114DS258-3) (Magnification 4X).

Item No. 16A - Pinion, and 17A - Gear (P/N's 114DS2045-5 and 114D2062-1). Two pinions and three gears were replaced because of pitting on the gear teeth (Figures 64 and 65). The heavy wear in the flank of the pinion tooth and along the addendum of the gear tooth resulted from the pinion moving out of mesh. The normal gear pattern may be seen as the lightly worn area above the pitting in Figure 64. Figures 66 and 67 show wear on the bearing journals of the pinion caused by bearings spinning. Figure 68 shows fretting and wear on the outer diameter of the input roller bearing, and Figures 69 and 70 show wear on the bearing inner ring and outer ring spacers, Items 28A and 25A (P/N's 114D2191-2 and 114D2145-1). This wear on pinion, bearings, and spacers permitted the pinion to move out of mesh, resulting in inferior tooth bearing contact, which produced contact stresses sufficiently high to induce pitting of the gear teeth. One gear had spots on the faces of several teeth that appeared to be frosting or scuffing (Figure 71). The outline of these areas was faintly visible on teeth of the mating pinion. Wear on the teeth outside of these areas appears to be normal, except that there is evidence of improper pinion location or shimming, i.e., the high and back pattern location shown in Figure 71. Surface finish on the pinion teeth and in nonfrosted areas of the gear teeth is satisfactory. A cross section through a frosted area showed the depth of affected material to be less than .0002 inch (Figure 72). Surface hardness was Rc62.8 and core hardness was Rc41.0 (drawing requirements are Rc60-64 and Rc36-40, respectively). No abnormalities in microstructure were found. There was evidence of debris damage to other gear meshes and bearings in the transmission by ingestion of entrapped particles. One bearing in this transmission was found to have a spalled roller, but the failure was in early stages with only small particles missing. It is considered improbable that the spots of surface distress on the teeth of the gear were caused by debris particles going through gear mesh. Since the distress occurs near a possible zone of single tooth contact, as evidenced by the short face contact, and bears distinct family resemblance to scuffing, it is concluded that this isolated failure mode is that of a lubrication failure. Since the improper pinion location may have been partially due to the customary bearing and spacer wear, which would have occurred during the 596 hours this part operated, this failure has been classified as secondary.

Item No. 18A - Planetary idler pinion (P/N 114D2084-1) and Item No. 19A - Ring gear (P/N 114D2086-3) were replaced because of handling damage and debris damage.

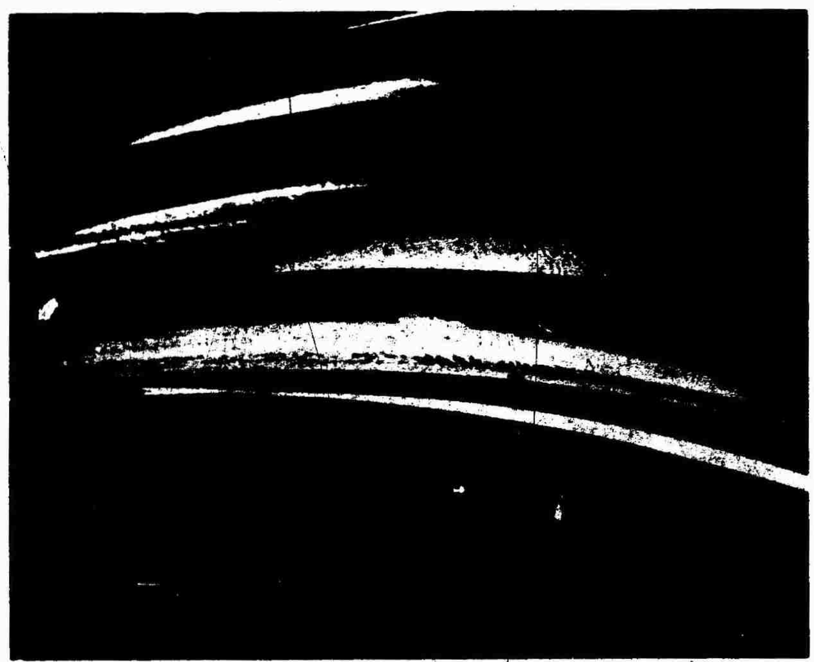

Figure 64. Pitting in Flank of Input Pinion (P/N 114D2045-5).

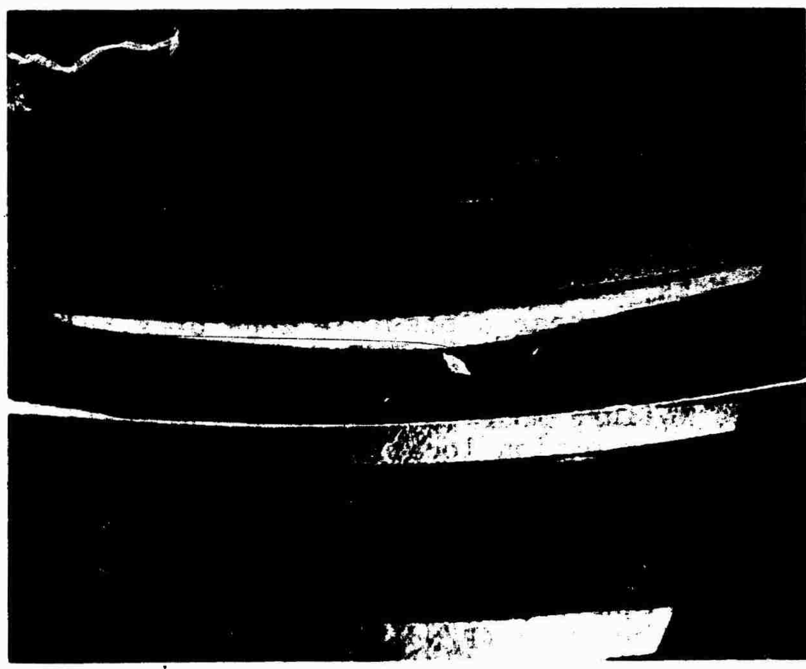

Figure 65. Pitting in Addendum of Spiral Bevel Gear Teeth (P/N 114D2062-1).

Figure 66. Wear on Bearing Journal of Input Pinion (P/N 114D2045-5).

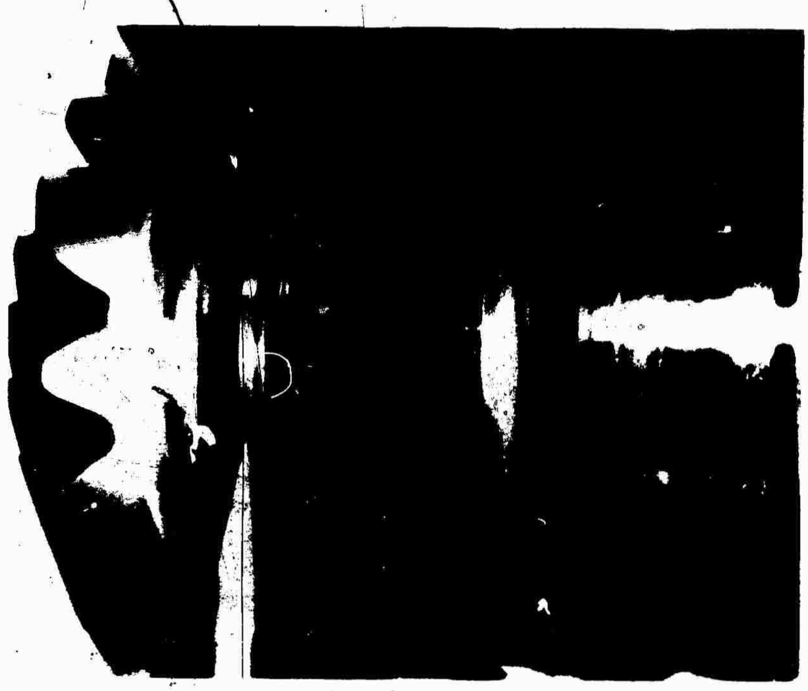

Figure 67. Wear on Bearing Journal Shoulder of Input Pinion (P/N 114D2045-5).

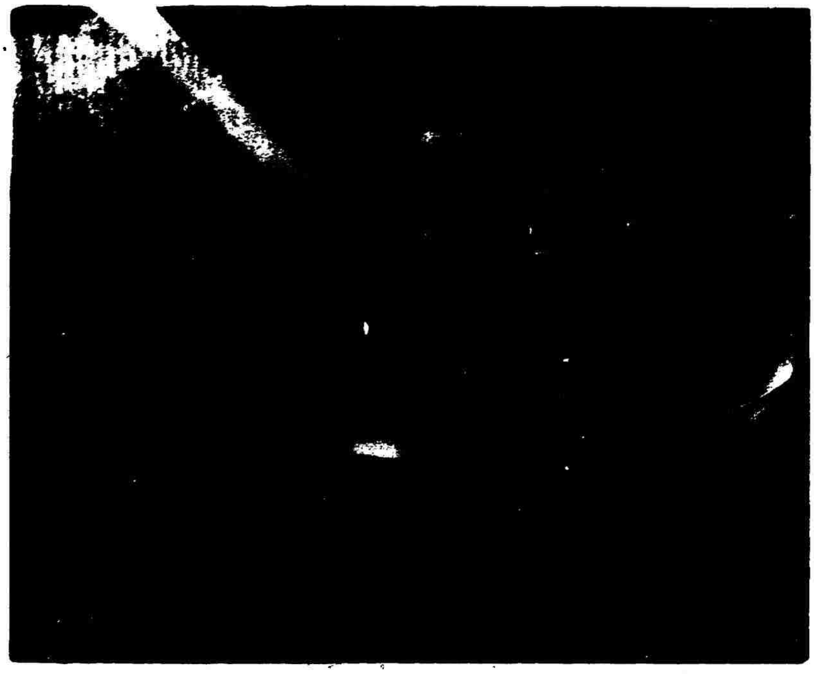

Figure 68. Fretting on Outer Ring of Input Roller Bearing (P/N 114DS240-2).

Figure 69. Wear on Face of Bearing Inner Ring Spacer (P/N 114D2191-2).

Figure 70. Wear on Face of Lubricator (Bearing Outer Ring Spacer) (P/N 114D2145-1).

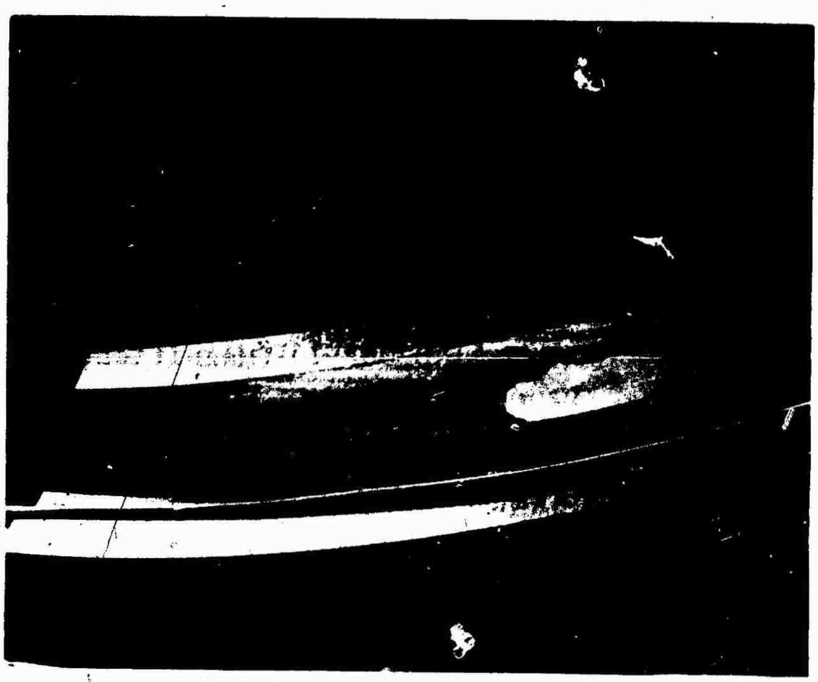

Figure 71. Frosted Spiral Bevel Gear Tooth Face (P/N 114D2C62-1).

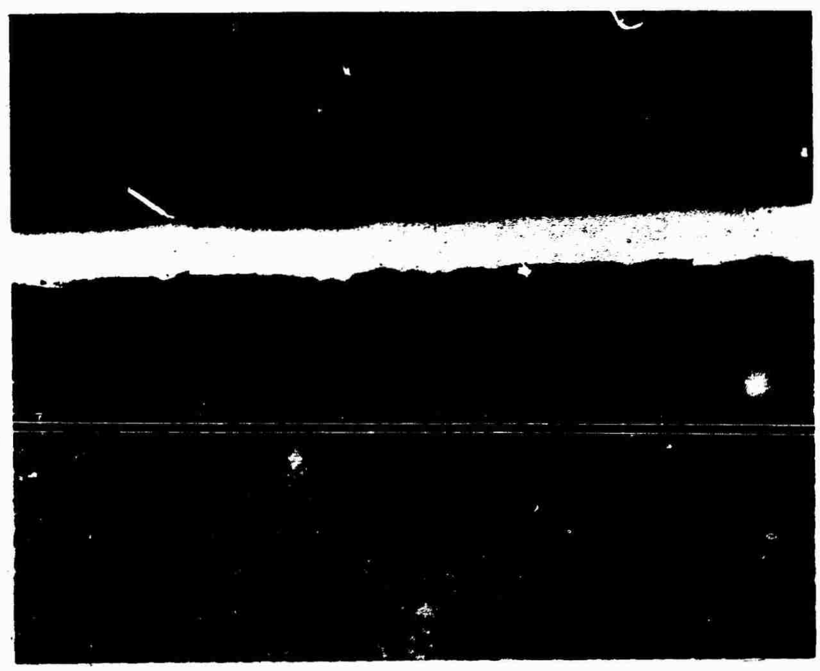

Figure 72. Section View Through Frosted Spiral Bevel Gear Tooth (P/N 114D2062-1) (Magnification 300X).

Item No. 21A - Shaft (P/N 114D2105-1) was replaced because of fretting corrosion and excessive wear on the spline teeth (Figure 73). Hardness on the teeth checked within drawing requirements. The wear pattern shown in this figure is typical for a misaligned condition.

Item No. 22A - Gear (P/N 114D2106-1) was replaced because of one chipped tooth (Figure 74). The fracture was surface initiated and was highly irregular, suggesting static overload. Microstructure of case and core was good. The fracture was on only one tooth and was located outside of the load contact pattern of the tooth, indicating the probable cause to be handling damage.

Items No. 23A and 26A - Accessory drive gears (P/N's 114D2107-1 and 114D2178-1) and Item No. 24A - Shaft (P/N 114D2116-3) were replaced because of corrosion and debris damage and excessive spline teeth wear. Hardness of spline teeth checked within drawing requirements. Advanced state of wear may be seen in Figures 75 and 76.

Item No. 27A - Retainers (P/N 114D2184-1) were replaced because of excessive wear and cracking around the outer edge where the retainer contacts the planetary pinion bearing inner race (Figures 77 and 78). A total of 13 were replaced for a replacement rate of 10.2%. Eleven of the 13 were cracked, giving a primary failure rate of 8.59%. Fracturing in the wear area was mainly transgranular with some flaking near the edge, caused by corrosion products expanding the cracks. Corrosion appears to be an after effect, not the cause of fracturing. Chemical composition and hardness were both within drawing limits.

VERTOL CH-47 COMBINING TRANSMISSIONS

Six Vertol combining transmissions were included in this program, all of which were first-time overhauls. All had completed the scheduled TBO (time between overhaul) period of 1200 hours, with the actual mean time 1189.2 hours.

Failed parts are listed in Table VII and are located diagrammatically in Figure 6. Reasons for replacement of the parts are given below.

Item No. 1C - Bearing (P/N 114DS541-2). Two were replaced because of corrosion and debris damage. The debris damage was very minor indentations on the rollers. Analysis of the oil indicated a high ferrous count, and the magnetic plug had a substantial quantity of fine magnetic particles on it. Wear on the lubricator (P/N 114D5063-1) on the aft output shaft

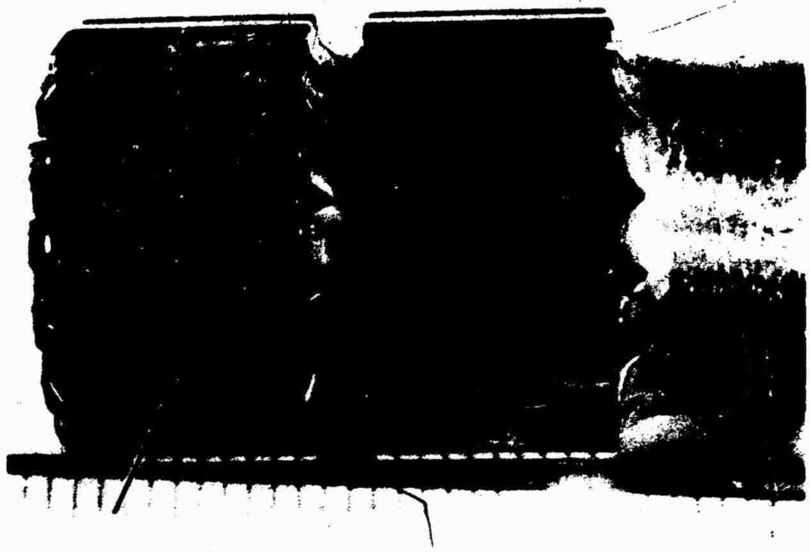

Figure 73. Spline Wear on Shaft (P/N 114D2105-1).

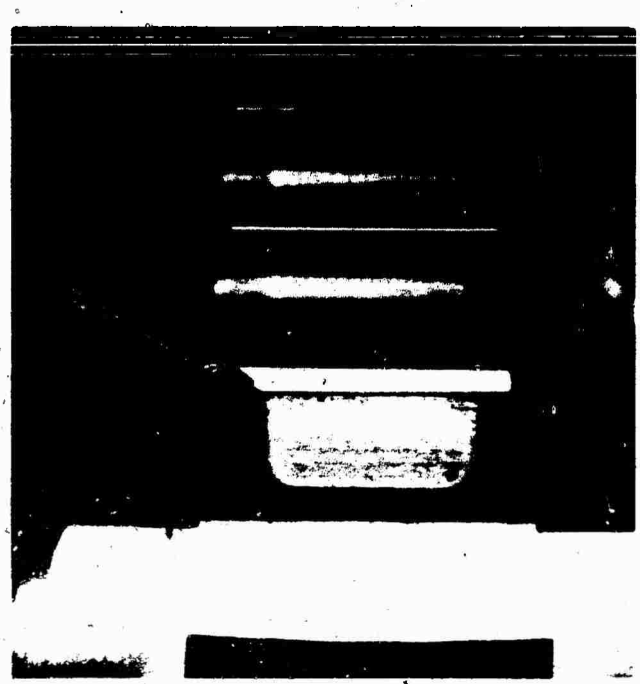

Figure 74. Broken Gear Tooth (P/N 114D2106-1).

Figure 75. Spline Wear (P/N 114D2107-1).

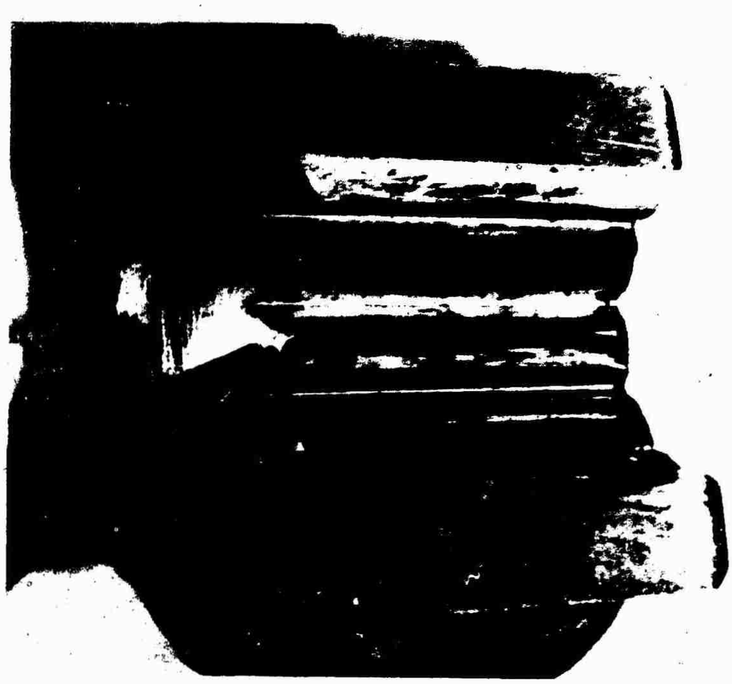

Figure 76. Spline Wear (P/N 114D2178-1).

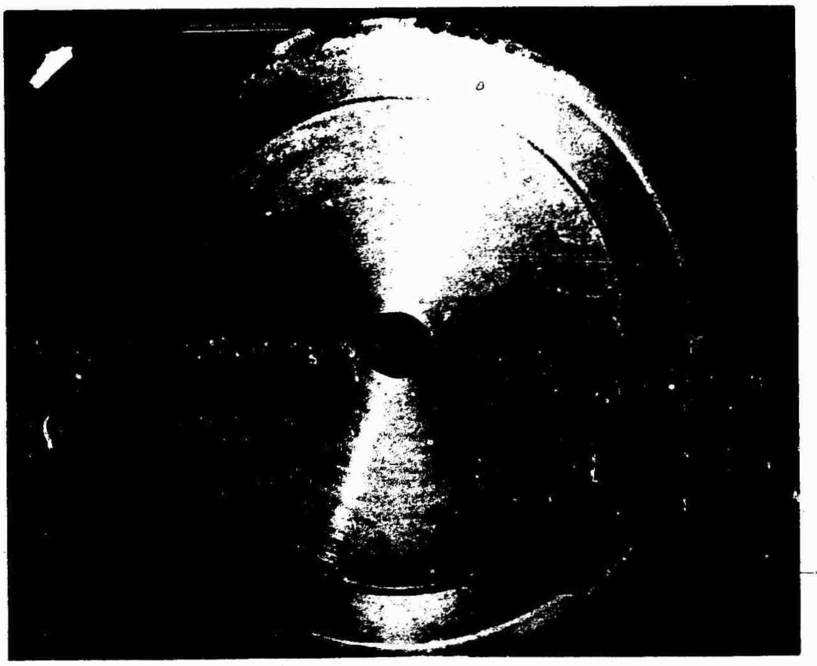

Figure 77. Wear and Cracking on Retainer (P/N 114D2184-1).

Figure 78. Close-Up of Wear and Cracking on Retainer (P/N 114D2184).

TABLE VII. PARTS REPLACED - VERTOL

Item No.	Part Number	Part Name
1C	114DS541-2	Bearing, Ball, Input Gear
2C	114DS542-4	Bearing, Roller, Input Gear
3C	114DS543-1	Bearing, Roller, Aft Output Shaft
4C	114DS544-1	Bearing, Ball, Aft Output Shaft
5C	114DS545-1	Bearing, Roller, Spiral Bevel Gear Shaft
6C	114DS549-1	Bearing, Roller, Forward Output Shaft
7C	114D5045-7	Support, Assembly, Input Pinion
8C	114D5047-1	Gear, Spiral Bevel Pinion
9C	114D5063-1	Lubricator, Output, Aft

TABLE VII. PARTS REPLACED - VERTOL COMBINING TRANSMISSION

e	Quantity Replaced	Quantity Per Trans.	% Replacement	Quantity Primary Failures	% Primary Failures
Ball, Input Gear	2	2	16.7	0	0
Roller, Input Gear	4	2	33.3	1	8.33
Roller, Aft Output Shaft	2	1	33.3	0	0
Ball, Aft Output Shaft	2	1	33.3	0	0
Roller, Spiral Bevel Gear Shaft	1	1	16.7	0	0
Roller, Forward Output Shaft	1	1	16.7	0	0
Assembly, Input Pinion	1	2	8.3	0	0
iral Bevel Pinion	1	1	16.7	0	0
or, Output, Aft	3	1	50.0	0	0

indicated that the bearings had spun in the housing. This wear possibly accounted for the metal particles in the oil and the debris damage.

Item No. 2C - Bearing (P/N 114DS542-1). Four were replaced because of limited life. One of these had no defects, two had corrosion pitting, and one had one spalled roller (Figure 79). There were multiple debris indentations on the roller surface and race. A section was taken through the fractured area of the roller which revealed a network of cracks with spalling and flaking at the surface (Figure 80). Microstructure appeared to be normal for M-50 material. Chemical analysis showed the material to be within limits for AMS6490 (M-50) steel. Hardness values ranged from Rc64.5 to 65.5. This is considered to be maximum hardness for this alloy. The fracture on the roller was most probably surface or near surface initiated, and there was secondary debris damage to the rollers and races. There was very little material flaked out of the failed roller. This bearing was from the same transmission as the debris-damaged bearing above (Item 1C). The metal particles on the magnetic plug and the high ferrous count in the oil indicate the possibility that debris might have contributed to bearing failure.

Item No. 3C - Bearing (P/N 114DS543-1). Two were replaced because of corrosion pitting and grooved rollers. The grooving was light and was worn by the retainer tang that is bent down to hold the rollers in place. Analysis of the oil indicated a high ferrous count. Bearing outer rings have spun in the input supports (P/N 114D5045), and gear teeth of one input spiral bevel pinion has rubbed against the oil baffle (P/N 114D5110) that is installed around the gear teeth. This possibly accounts for the metal particles in the oil. It is likely that the grooved rollers in the bearing resulted from operation with this abrasive oil.

Item No. 4C - Bearing (P/N 114DS544-1). One was replaced because of limited life and another replaced because of grooved and corroded balls.

Item No. 5C - Bearing (P/N 114DS545-1). One was replaced because of very small indentations and grooves in the rollers. The magnetic plug was loaded with minute metal particles. Bearing outer rings at both input gears have spun in the support assemblies (P/N 114D5045), and the gear teeth of one input pinion has rubbed against the metal baffle (P/N 114D5110). This possibly accounts for the metal particles in the oil. It is likely that the small indentations and grooves in the bearing rollers were caused by these metal particles in the oil.

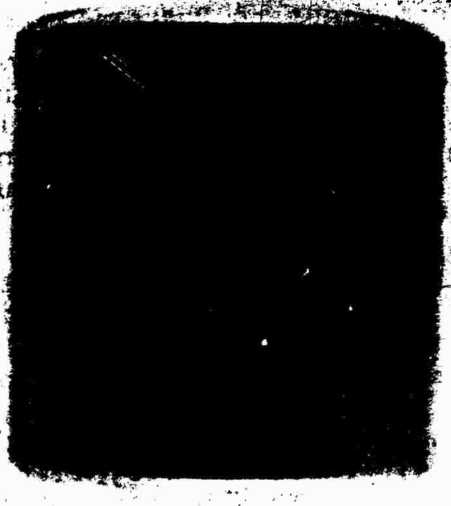

Figure 79. Spalled Bearing Roller (P/N 114DS542-4) Magnification 3X.

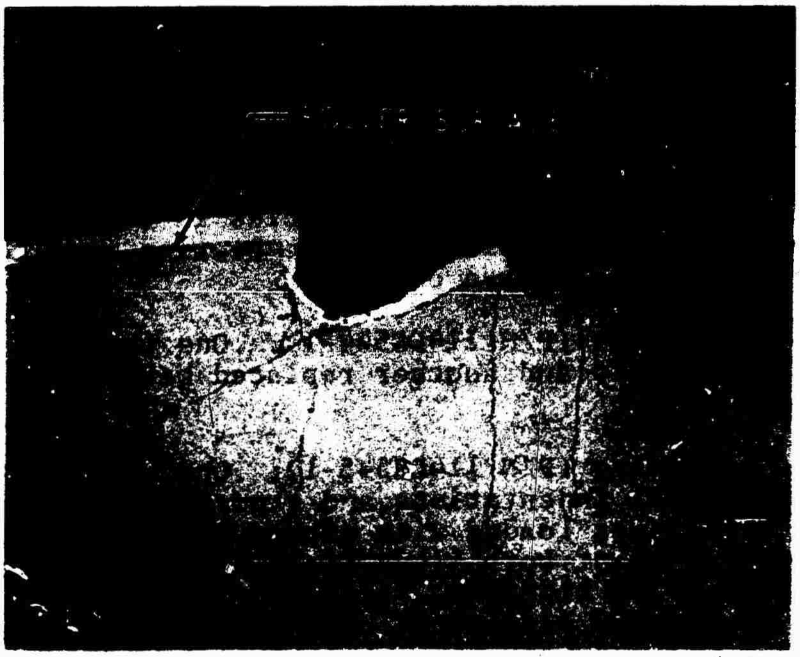

Figure 80. Section Through Fractured Roller (P/N 114DS542-4) Magnification 40X.

Item No. 6C - Bearing (P/N 114DS549-1). One was replaced because of corrosion pitting and grooved rollers. This bearing is from the same component as the one with grooved rollers in Item 3C above. The damage to this bearing likely resulted from the same conditions.

Item No. 7C - Support, input pinion (P/N 114D5045-7). One was replaced because of assembly damage. The mounting flange was cracked by tightening the mounting bolts while a washer was caught between the mating faces of the support and the shim on the main case.

Item No. 8C - Gear (P/N 114D5047-1). One was replaced because of a chipped tooth. The damage was outside of the gear tooth wear pattern and resulted from assembly or handling damage.

Item No. 9C - Lubricator (P/N 114D5063-1). Three were replaced because of wear (Figure 81). This part acts as a spacer and is clamped axially between two bearings (P/N's 114DS543-1 and 114DS544-1) on the aft output shaft. The wear results from the outer rings of the bearings spinning in the support assembly (P/N 114D5043-1). Length of the part shown is 0.020 inch below minimum drawing dimension, and length of the three parts ranged from 0.008 inch to 0.056 inch below drawing minimum.

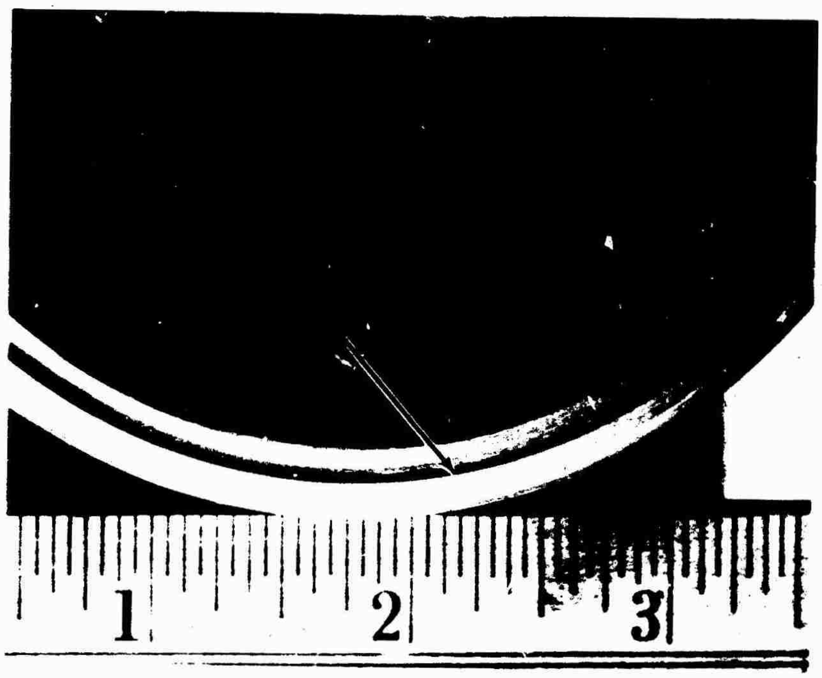

Figure 81. Wear on Face of Retainer (P/N 114D5063-1).

ANALYSIS OF FAILURE MODES

Statistical data must never be employed in engineering work without a thorough understanding of the assumptions, limitations, and exclusions used in its generation or accumulation. With respect to the data furnished in this section, the following five observations are directed toward this objective.

1. The population sampled was selected from transmissions with relatively complete historical records as they arrived at ARADMAC. While this ensures higher confidence in the accuracy of the study results, little is known concerning the probability of the indicated failure rates representing the entire population. However, the observed failure modes should remain representative.

2. Not all failed components were reviewed after ARADMAC rejection. Since the monitoring tags had to be removed in process at various inspection operations, the possibility exists that not all tags were reinstalled. In this event, such parts would go to rework or direct scrap. The number of monitoring tags consumed was more than parts returned for evaluation. However, some tagged parts could have been judged usable by ARADMAC and the tag legitimately discarded. It is estimated that approximately 15% of the parts tagged were subsequently lost to review. As a result, the stated failure rates may be slightly lower than actual, but the mode of failure and the relative percentage of the failed components from a given mode classification remain typical.

3. The sample field for CH-47 transmissions is appreciably smaller than for UH-1 transmissions. Hence, there is less confidence in CH-47 data than in UH-1 data.

4. The data presented herein represent a period in time on the evolutionary cycle of both the UH-1 and CH-47 transmission systems. They should not be used to conclude the relative design merits of either vehicle drive system or to assess the capability of either in today's or future configuration or environment. For instance, in the case of the UH-1, the two ball thrust bearings which account for the majority of bearing failures have been redesigned

and furnished in M-50 material for approximately two years. The UH-1 upper sun gear pitting phenomenon has been drastically altered by the advent of reduced surface roughness - dissimilar hardness - sun-planet combinations. Similar product improvement evolutionary changes are probably in effect on the CH-47 also. Due to the vast number of transmissions involved, the extent of the modification, and the availability of new components, the incorporation of such improvements may require many years to effect.

5. The applicability of the data resulting from this study is limited to and representative of helicopter transmissions in the 600- to 1200-hour TBO level. This may be clearly visualized by considering the simultaneous existence of numerous competing failure modes. Some of the competing failure modes have very slow progression rates while others have relatively fast rates. It is entirely likely that certain modes which are now purely secondary might attain significant primary rates in an extended transmission life environment. A good case in point may be that of corrosion, i.e., significant increases in TBO could conceivably elevate corrosion from a secondary to a primary failure category.

With these restrictions clearly in focus, the following six topics are presented.

DISTRIBUTION OF FAILURE MODES

The 1000-hour generic failure rates in percent of total monitored quantity for the broad families of gears, bearings, and all other details are given in Table VIII.

TABLE VIII. GENERIC FAILURE RATES

	Failure Rate = %/1000 Hours Primary Only	 Total (Replacement)
Gears	.68	5.69
Bearings	1.37	17.7
Other	.35	1.14

Bearings, as shown, are twice as likely to exhibit primary failure as gears and four times as likely to do so than other components, such as cases, studs, oil jets, shafts, oil pumps, etc. The secondary failures, often caused by debris from primary failures or corrosion, exhibit a similar tendency with respect to relative failure rates. However, the total rate of replacements increases 8-fold to 5.7% for gears, 12-fold to 17.7% for bearings and only 3-fold to 1.14% for other components. Consideration of geometrical relationships existent in bearings, as compared to gears, reveals the nature of increased secondary failure rate for bearings. The high geometrical osculation of the bearings encourages a greater degree of debris entrapment, while that of gears generally expels or sheds most debris. High secondary failure rates then would naturally favor bearings.

The high bearing replacement rate is worthy of further examination with regard to general classification or type of bearing. If we drop the replacement time signatures of the individual components, as required in determining generic failure rates, and simply consider the entire lot of reviewed bearings with respect to their relative frequency of failure, we find the further comparison shown in Table IX.

TABLE IX. BEARING FAILURE RATES

	Primary Failures		Secondary Failures	
	Balls	Rollers	Balls	Rollers
Total Replaced	76	12	429	305
% of Replacement	15.05	3.79	84.95	96.21
% of Total Observed	2.868	.2866	15.1640	7.2844

	Balls	Rollers
Total Bearings Inspected	2829	4187
Failure Rate, $\frac{\text{No. Failures}}{\text{100 Bearings}}$	17.850	7.415

All bearings have been classified as either ball (point contact) or roller (line or mixed point-line contact) for this comparison. The replacement rate for ball bearings is over twice that for rollers - probably demonstrating their increased tendency toward debris entrapment and greater fragility with respect to denting initiated fatigue. However, the primary failure rate ratio is significant in that the ball failure rate is over ten times greater than the roller.

As will be shown later in the bearing section, the calculated life ratios are inadequate to substantiate this disparity.

The generic failure rates exhibited by the individual gearboxes are shown in Table X.

TABLE X. GENERIC FAILURE RATES BY INDIVIDUAL TRANSMISSION

	Failure Rate = %/1000 Hours							
	Primary Only				Total (Replacement)			
	B	F	A	C	B	F	A	C
Gears	1.0	-	-	-	6.9	3.1	2.5	4.6
Bearings	1.2	3.1	.10	1.8	11.9	44.3	16.8	9.5
Other	.08	1.3	.72	-	.79	2.2	1.5	1.8

A brief discussion of the primary failure modes as found in the subject transmissions follows:

UH-1 (B)

In this transmission there were three parts with relatively high primary failure rates and three additional parts with rates greater than 0.5%/1000 hours. These were:

Item	Part Number	Nomenclature	Failure Rate (%/1000 Hrs)
20	204-040-330-3	Sun Gear, Upper Planetary	32.95
24	204-040-346-3	Bearing, Triplex Input Pinion	21.97
23	204-040-345-7	Bearing, Duplex Bevel Gear	12.14

Item	Part Number	Nomenclature	Failure Rate (%/1000 Hrs)
9	204-040-190-7	Race, Over-Running Clutch	2.89
41	X-131720	Over-Running Clutch	2.31
35	204-040-701-3	Bevel Gear	1.73

As may be recalled from the Results section, Items 9 and 35 above were concerned with manufacturing process problems which were subsequently corrected. Item 41 replacement is primarily a drag spring wear problem. However, 67% of all primary failures (primary failures represent 12% of the total number of failures) are comprised of Items 20, 23, and 24. The mode of failure for all three is rolling-sliding contact fatigue resulting in spalling or pitting of the loaded wear surface. These failure modes will be discussed in detail in subsequent sections. Although the reliability of this transmission at achieving TBO is excellent, as indicated by an MTBR of 90.5% TBO, any increase in scheduled TBO would seem to be severely limited by the high failure rate of Item 20.

CH-47 (F)

There were six components in this transmission which exhibited primary failure tendencies. All six were above 0.5%/1000 hours. They were:

Item	Part Number	Nomenclature	Failure Rate (%/1000 Hrs)
2F	114DS144-1	Bearing, Ball, Rotor Shaft	51.2
18F	114D1088-12 & -14	Support Assembly, Ribbed	12.8
21F	114D2184-1	Retainer, Bearing, First-Stage Planetary	10.7
1F	114DS143-1	Bearing, Ball, Sun Gear Shaft	4.29
10F	114DS258-4	Bearing, Roller, Second-Stage Planetary Gear	1.42

Failures of rolling contact fatigue on item 2F occurred on both inner and outer races of the bearing, as well as on the rolling elements. Inner race failures were predominantly

surface originated, while ball and outer race failures were subsurface. While large nonmetallic inclusions were found in some balls, and some ring material was found to be low on alloy content, many of the failures could not be attributed to these causes. The failure mode is predominantly thin lubricant film in characteristic and is discussed in greater detail, subsequently.

Failure modes for Item 10F and Item 1F are also rolling contact fatigue.

The failure mode for Item 18F was bending fatigue and no material deficiencies were found. Crack location in Item 18F was identical in all failed parts.

Item 21F experienced cracking or flaking of metal around the outer edge where it clamped against the planet idler bearing inner ring. None of the failures had approached the point of the washer becoming nonfunctional, but a substantial quantity of aluminum alloy particles that might be expected to cause debris damage to other parts of the transmission were produced.

Items 6A, 14A, and 20A, clutch bearings and shaft, had relatively high replacement rates, but there were no primary failures. The parts were still functional, but a substantial quantity of metal particles was released into the transmission by the bearing fretting and spinning.

All other failed parts were still functional, but were replaced because of limited life, corrosion, debris damage, handling damage, or some other secondary damage that does not limit the life of the component.

CH-47 (A)

Primary failures in the aft transmission were limited to four bearings and the first-stage planetary bearing retainer. The occurrence rates are:

Item	Part Number	Nomenclature	Failure Rate (%/1000 Hrs)
1A	114DS240-2	Bearing, Roller, Spiral Bevel Gear Shaft	17.5
27A	114DS184-1	Retainer, Bearing, First-Stage Planetary	12.0
2A	114DS242-1	Bearing, Ball, Sun Gear	2.18

Item	Part Number	Nomenclature	Failure Rate (%/1000 Hrs)
12A	114DS258-4	Bearing, Roller, Second-Stage Planetary	2.18
4A	114DS244-12	Bearing, Roller First-Stage Planetary	1.1

The failure mode for Item 1A was rolling contact fatigue of the rollers with secondary damage to the races and other rollers. No deficiencies were found in chemical composition, grain structure, or heat treatment of the failed rollers. Surface finish on the bearing inner rings varied from 7AA to [illegible] AA. This condition will be discussed in a subsequent section. There was evidence on the inner and outer diameters of all eight of the bearings of rotation or spinning of inner rings on pinion shafts, and of outer rings fretting in housings (Figures 66, 67, 68, and 69). This resulted in wear that permitted the pinion to move axially out of gear mesh, causing the gear tooth contact pattern to shift from the desired position. Scuffing then occured in the flank of the pinion teeth and along the top of the gear tooth (Figure 64 and 65). The bearing spinning was evident on all of these bearings. Two spiral bevel pinions and gears were replaced because of this scuffing, for a secondary failure of 8.8%. Both sets were still functional, but the scuffing resulted in metal particles in the oil that might have been expected to cause bearing or gear tooth damage.

The fatigue failure on bearing 2A was approximately 0.040 inch in diameter and located in the ball path in the outer ring. The failure was surface initiated. No deficiency was found in material composition, grain structure, or heat treatment.

Item 4A had a fatigue failure in the roller path of the inner ring. The failure appeared to be subsurface in origin and there was very little evidence of secondary debris damage. No deficiency was found in material composition, grain structure, or heat treatment.

Three second-stage planet gear bearings, Item 12A, had primary failures. One had a spalled roller, one had a spalled inner ring, and the other had spalling on both the inner ring and roller. There was evidence of overheating on one failed inner ring. The tempering in this area was typical of that produced by grinding burns. No deficiency was found on the other two in material composition, grain structure, or heat treatment.

Eleven bearing retainers, Item 27A, were cracking or flaking around the outer edge. This part is identical to Item 21F discussed earlier in the Forward Transmission section, which exhibited a slightly lower rate of 10.7%.

CH-47 (C)

Only six combining transmissions were included in this program. From these there was only one primary failure, a roller bearing (P/N 114DS542-4) supporting the input pinion. Most of the other bearing spalling failures resulted from metal particles in the oil, and were adjudged to be secondary. There was evidence of bearing outer rings spinning in the input support and in the aft support assembly.

The items then that should be considered as life-limiting are the failed bearing above (P/N 114DS542-1), the thrust bearing on the aft output shaft that has an established limited life (P/N 114DS544-1), and the fits and other controlling factors concerned with the fretting, creeping, and spinning bearings.

All of these six boxes achieved their scheduled overhaul time of 1200 hours. However, the wear characteristics of the lubricator (Item 9C), gear shaft (Item 8C), and adjacent inner rings are such as to restrict further increases in TBO to very modest levels.

EFFECTS OF FAILURE MODES

This section is directed toward consideration of the effects of observed failures upon the operational capability of the transmission or assessment of the risks involved in continued operation in the presence of the various competing failure modes. Such topics are speculative since statistical evidence to support mathmatical proof cannot be obtained. The entire subject of failure progression rates is involved in a very complex inter-relationship (as well as far beyond the scope of this study) in making any intelligent prognosis. However, without recourse to any but superficial explanations, useful information can be produced by usage of estimated capabilities as given by the experienced engineer who examined the failed components as they became available. It is believed by the authors that capability judgments made by the on-site team at ARADMAC tended toward the conservative in all instances.

Every DFAS (Reference Figures 8, 9, 10, and 11) completed required the investigator to select the probable short-term effects on the transmission (if the failed component had been left in service) from an included list of seven probable effects. Items 1 through 7 were arranged in likely order of

increasing severity. The results of the investigator's judgments are presented in Figure 82. This distribution reveals that approximately 90% of the failed parts would have had no apparent effect on continued short-term (100 hours) operation. This further underscores the extreme difficulty in improving diagnostics capability - a virtual prerequisite to conditional overhaul.

In addition to these effects on short-term operation, each DFAS included a three choice prognosis on the remaining life that the failed part would exhibit at a wholly satisfactory operational and functional level. The three evaluation levels were: (1) capable of operating for more than 100 additional hours, (2) capable of operating less than an additional 100 hours, and (3) failure is eminent. In this instance, "failure" carried the connotation of catastropic. Of the 1671 failed parts, 1537 were classified as level (1), 120 as level (2), and 14 as level (3). The 14 components at level (3) were removed from 12 transmissions. Five of these twelve were early component removals and nine were time change components in for normal overhaul. Six of the fourteen discrepant parts were contained in four of these nine transmissions and rated as failure eminent due to severe corrosion that would certainly have lead to functional failure. One part was improperly coded in that extensive secondary debris damage existed, but catastropic failure was not eminent. One part was failed as a result of field maintenance or improper disassembly.

There then remained six level (3) components which were true primary failures; two were from time change transmissions and four were from early overhaul transmissions removed from service because of field diagnostics.

The first of these six was a CH-47 114DS258-3 planet bearing with an extensively spalled inner race, as seen in Figure 83. Total time on the transmission was 625 hours with only 63 hours since overhaul. Reason for component removal was magnetic chip detection. However, it is very improbable that catastropic failure is eminent, as this type of failure is progression rate limited. This represents but one location in six planet idler load paths of the final planetary drive. As this bearing spalls extensively, its idler gear is permitted to move out of full or equal load sharing position, and the other five planet gears become slightly overloaded. In this event the planet gear with the spalled raceway assumes a diminishing percentage of the transmitted load and further failure progression is arrested. However, the other five planet gears suffer the adverse effects of overload, and the likelihood of additional idler bearing failures is increased.

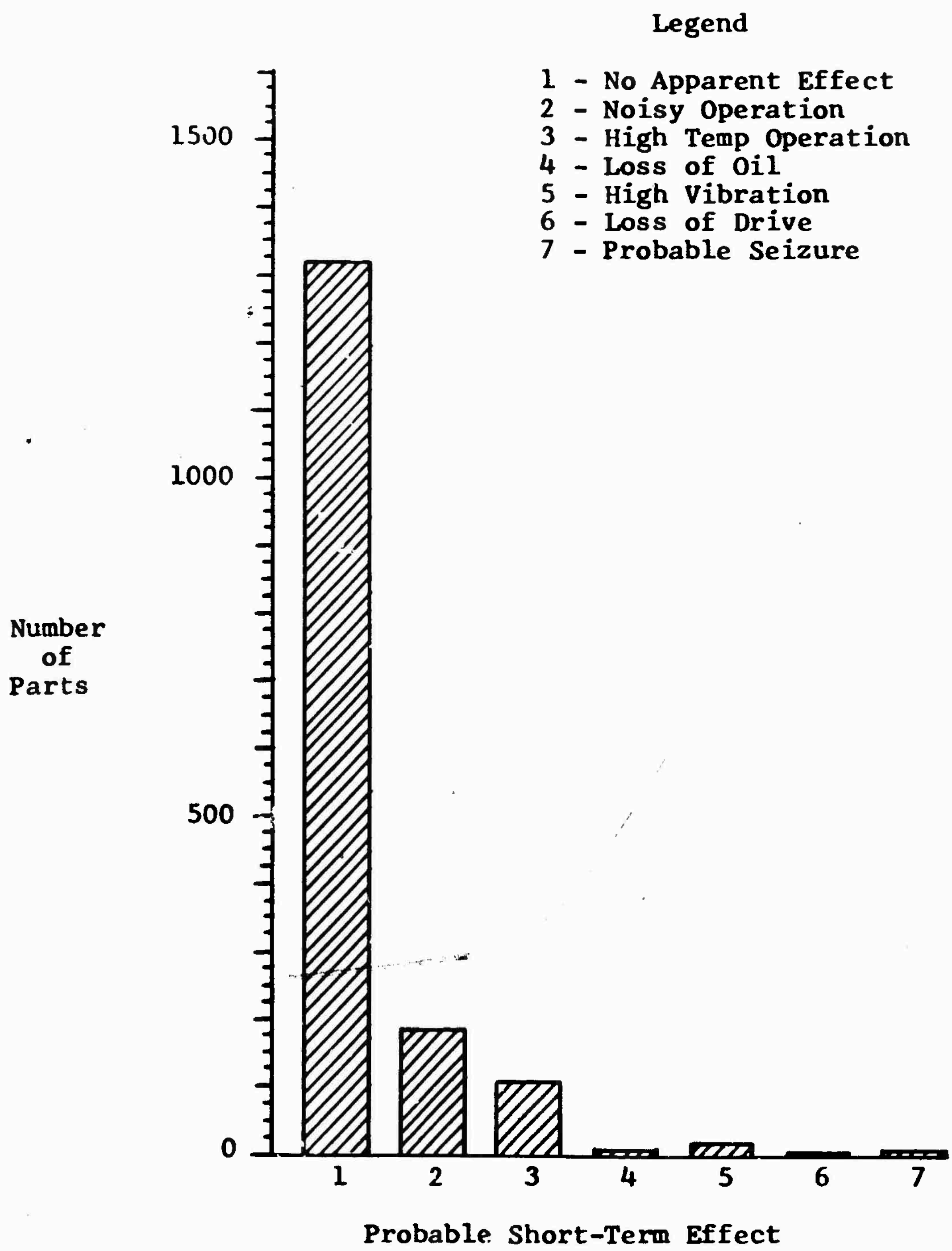

Figure 82. Short-Term Effect on Continued Operation.

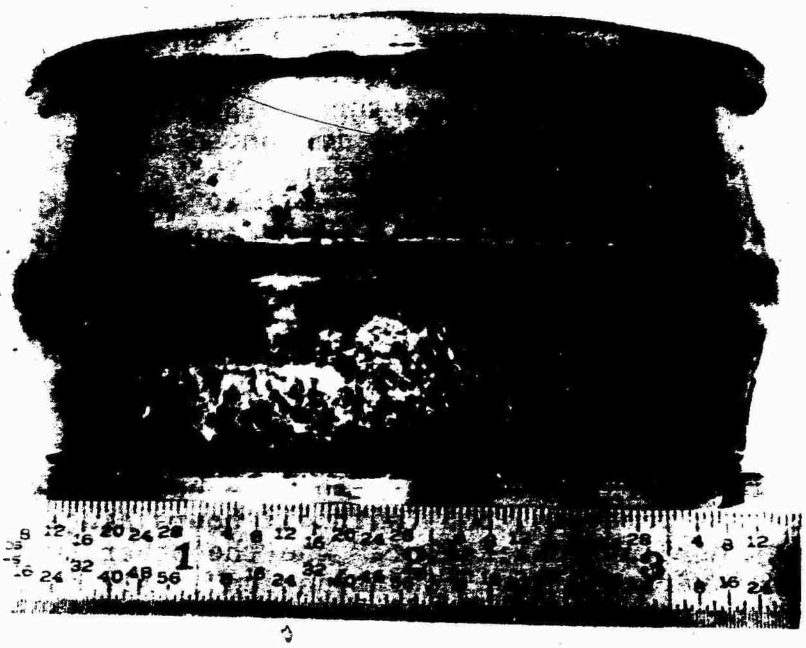

Figure 83. Spalled Planet Pinion Bearing Race (P/N 114DS258-3).

This description of the probable sequence of events is not general for all planetaries or all self-aligning type idler bearings. For example, if this bearing were in a higher speed application wherein the barrel-shaped rollers were under considerable gyroscopic acceleration such as to cause them to turn edgewise since the guiding surfaces were destroyed, then jamming of the planet gear could result. The resultant fractures would very probably release larger debris fragments, which could in turn lead to complete component failure.

The second of the six primary level (3) parts was a UH-1 204-040-330-3 upper planetary sun gear and may be seen in Figure 84. This part had 1114 hours time since new with no overhaul, and it was in a transmission removed for time change. Again, it must be assessed as improbable that catastropic failure is eminent, primarily due to the redundant load paths. This planetary features eight planet idler pinions. When the spalled tooth is in contact, seven other load paths are in contact on the sun gear. These also act to retard the failure progression rate as they assume the partial overload due to the eighth position becoming unloaded. Since this planetary features a hunting ratio, it is unlikely that any of the meshing idler pinion teeth were significantly damaged.

There remains four primary failures which are judged to be potentially catastropic. These were all in the UH-1 204-040-346-3 input bevel pinion triplex thrust bearing. One was in a component in for time change with 1084 hours operation. Two were premature removals, one (with 317 hours since overhaul) for reasons of "internal failure" and the other (with 966 hours since overhaul) for "contamination". All failures were in one of the two tandem thrust rows of the triple-row bearing. Although some load path redundancy exists here, the likelihood of the second row failing very soon was high. All four bearing sets had spalled races and balls. Some of the balls were fractured (Figure 85) into several wedge-shaped segments. One bearing had a multiple retainer fracture as shown in Figure 86. The ball segments of Figure 85 had skidded in the outer ring, wearing flats on the ball segments. A similar mode existed on the retainer of Figure 86. Catastropic failure could result most likely from a large segment of ball being released from the bearing and ricocheting into the main bevel mesh or a wedge-shaped member acting to jamb the rotating inner ring while wedging into a spall or fracture in the outer ring.

It is evident from the foregoing that diagnostic systems as used at the field maintenance level are inadequate to consider conditional overhaul of transmission components with

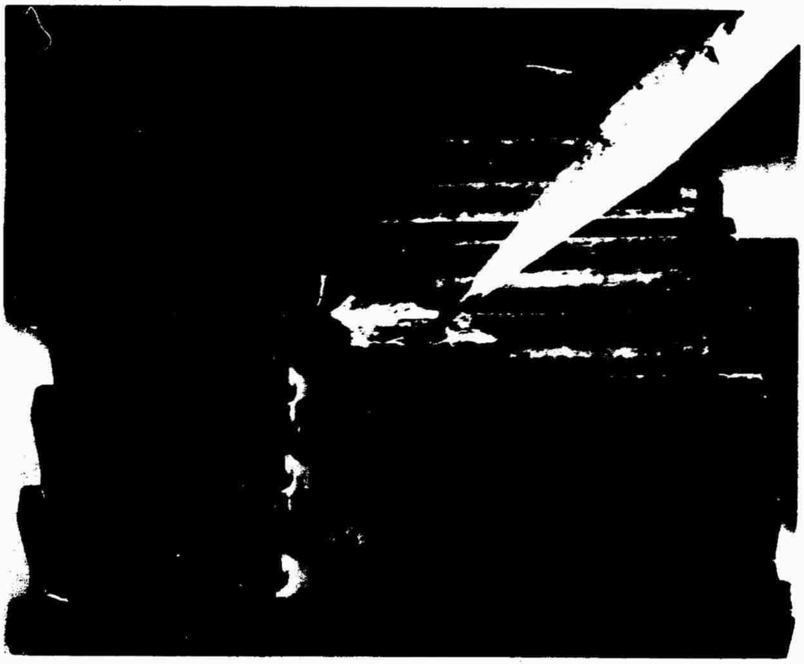

Figure 84. Chipped Tooth on Upper Sun Gear (P/N 204-040-330-3).

Figure 85. Fractured Bearing Ball (P/N 204-040-346-3).

Figure 86. Failed Bearing Retainer (P/N 204-040-346-3).

adequate safety. However, this does not preclude the safe employment of conditional overhaul operational methods with transmission components which have been specifically designed to facilitate adaptation of improved diagnostic techniques.

The relative cost effectiveness of conditional overhaul versus the preventative maintenance philosophy embodied in the scheduled overhaul approach cannot be addressed within the scope of this study. However, it is made clear that if conditional methods are employed, the diagnostics must be sufficiently sensitive to differentiate between the need for immediate component removal or permissible continued operation until a more convenient time is achieved.

OIL SAMPLE ANALYSIS CORRELATION

As previously noted, oil samples were collected from all 251 transmissions reviewed at ARADMAC and identified by corresponding GFAS numbers. Twenty of these were selected on a random basis and sent to Wear Check International, Toronto, Ontario, Canada, for chemical analysis of the contained wear particles, viscosity, sludge, and acid number determinations. Identification of one sample was lost, but the significant information from the other 19 analyses is presented in Table XI. This table lists the GFAS number; operating time; quantity of aluminum, iron, nickel, lead, and silicon in parts per million; dynamic viscosity of the oil in centistokes at 210°F; acidity of the oil; sludge content in percent; number of failed parts; and general comments on component condition.

Attempts at correlation proved interesting in that none were established. An increased nickel (Ni) content in the oil would be normally interpreted as indicative of a bearing failure since bearing steels contain nickel while most gear materials employed do not. All transmissions showed the same level of 1.5 except the three CH-47 combining boxes and one CH-47 forward and one CH-47 aft transmission. Of these, only C-005 contained a spalled bearing. All were very high time units. The cause of the slight increase in nickel was wear on faces of bearing rings due to creep and spinning. It should be noted that these three high time CH-47 combining transmissions also showed abnormally high iron (Fe) content, which was again indicative of shaft wear due to spinning bearing rings.

Correlation charts for number of parts failed are presented versus iron (Fe) in Figure 87, acidity of oil in Figure 88, viscosity of the oil in Figure 89, and silicon (Si) content in Figure 90.

TABLE XI. OIL ANALYSIS AND FAILURE

Trans. GFAS	Time Hours	Al	Fe	Ni	Pb	Si	C.S. 210°F	Nuet. No.	Sludge Content	No. of Failures	Comment On Condition
A016	240	3	32	1.5	10	3	4.10	.78	.10	10	Rust
A018	1196	3	15	1.5	13	2.5	3.24	.18	.02	3	Spline Wear
A019	1197	4	23	2.5	15	8	3.07	.31	.02	2	Corrosion
A020	1211	13	19	1.5	22	3	3.21	.43	.05	5	Wear & Spalling
A024	534	2.5	25	1.5	11	5	3.24	.3	.10	9	Corrosion
B077	1138	1.5	11	1.5	11	2.5	5.01	.34	.10	9	Corrosion
B103	1030	45	19	1.5	15	100	4.89	.36	.02	9	Spalling
B110	1098	5	19	1.5	13	25	3.31	.27	.02	5	--
B136	1108	1.5	10	1.5	10	2.5	5.51	.29	.10	5	--
B138	1103	2	12	1.5	12	5	4.99	.62	.1	7	Wear
B147	1104	1.8	13	1.5	20	3.5	5.55	.56	.01	6	Corrosion
B181	1132	1.5	15	1.5	14	3	4.97	.16	.02	3	Spalling
C001	1175	7	90	.3	13	7	3.89	.32	.05	5	Corrosion
C003	1237	6	74	2.5	20	13	4.15	.14	.05	2	--

TABLE XI - Continued

Trans. GFAS	Time Hours	Al	Fe	Ni	Pb	Si	C.S. 210°F	Nuet. No.	Sludge Content	No. of Failures	Comment On Condition
C005	1194	3	65	.3	18	4	3.8	.34	.02	5	Spalling
F004	790	13	17	1.5	11	5	3.21	.23	.05	8	Rust
F011	63	2.5	15	1.5	60	3	4.5	.10	.01	12	Spalling & Corrosion
F020	798	3	15	2.5	15	2	3.49	.16	.01	3	Retirement Life
F026	512	28	18	1.5	15	25	5.42	.23	.02	10	6 Retirement Life

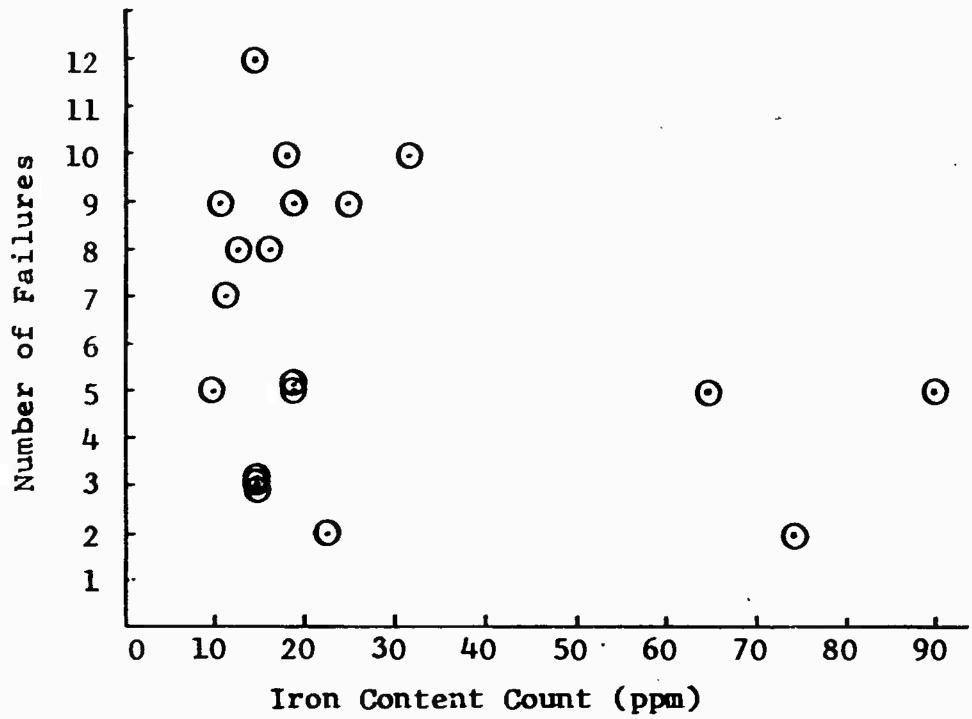

Figure 87. Oil Sample Iron Dispersion.

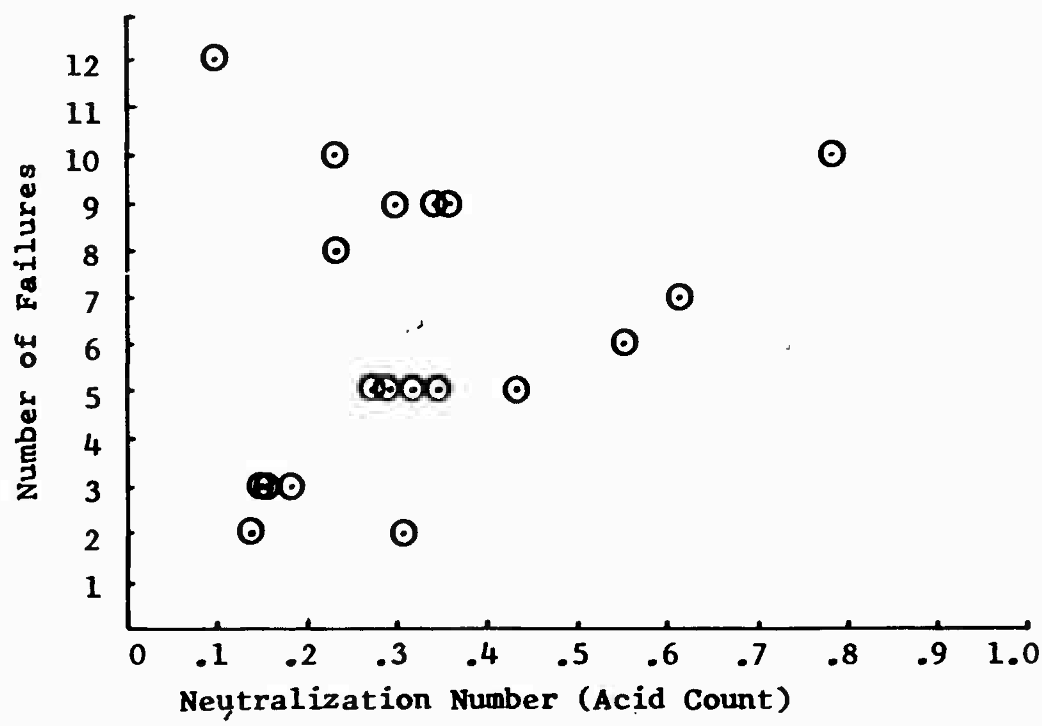

Figure 88. Oil Sample Neutralization Dispersion.

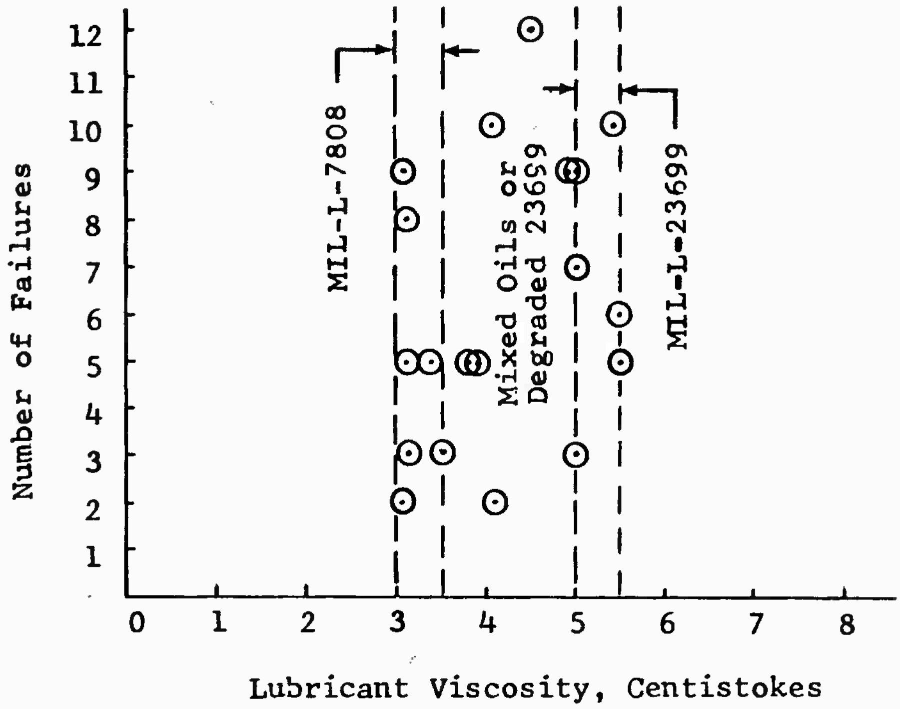

Figure 89. Oil Sample Viscosity Dispersion.

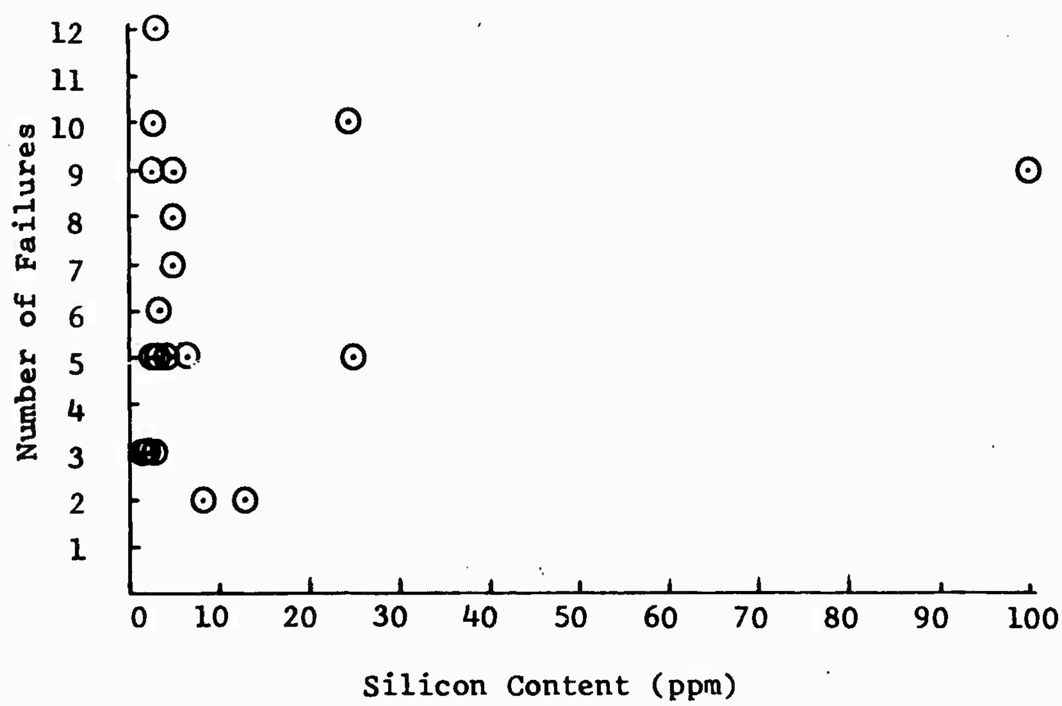

Figure 90. Oil Sample Silicon Dispersion.

The iron content is random by this index. Some slight correlation exists with respect to acidity in that high Neut. numbers indicate high replacement rate, but the converse is not true. The viscosity chart primarily reveals that six components were operating on MIL-L-7808, six components were operating on MIL-L-23699, and probably seven components were operating on mixed MIL-L-7808 and MIL-L-23699. Finally, the silicon content correlation is again insignificant. High silicon content suggests the ingestion of considerable amounts of sand, which in turn leads one to suspect high wear rates. Such was not the case.

It would appear that spectrographic, chemical, and physical analysis of transmission oil as currently employed is wholly ineffectual as a means of predicting the need for overhaul in helicopter transmissions in U. S. Army use.

GEAR DESIGN CORRELATIONS

The three generally accepted competing modes of failure for aircraft applications employing case hardened and ground high-accuracy gears are tooth breakage due to material fatigue in the root fillet section of the tooth form, pitting or spalling failures of the working face of the tooth, and scoring or scuffing of the active tooth profiles in the flank or addenda regions.

The engineering design practice used to define the risk of occurrence of these failure modes has been a simple statistical treatment of the calculated fillet bending stress, the tooth surface Hertzian or compressive stress, and the AGMA-Kelley-Blok temperature rise or flash temperature index, respectively.

Widely accepted allowable operating levels of these indices are in existence in AGMA (American Gear Manufacturers Association) and USAAVLABS publications. Evolution of the AGMA standards has been fostered through the need for strength and durability rating systems with accompanying allowable operating levels. Contributions from all phases of gear industry, from farm implement drive systems to rocket motor gearing, have been instrumental in the establishment of the present AGMA standards. Selected study areas funded by USAAVLABS have established other levels. However, the application of the above indices to a particular gear design, with the accepted allowables, can lead to widely varying operational characteristics and functional anomalies.

Table XII presents these and other indices as calculated for all the power transmission gears investigated in this study. All indices were calculated for full power (takeoff equivalent) at normal rated rpm. The table includes part number, name, location (L.S. = lower planetary sun, U.S. = upper planetary sun, U.R. = upper planetary ring, etc.), Pd (diametral pitch), pressure angle of the gear at the operating pitch diameter, pitch line velocity in feet per minute, compressive stress at the pitch line, two values for scuffing temperature rise, two values for elastohydrodynamic film thickness, Wt (tangential tooth load), pinion rpm, calculated bending stress, entrainment velocity of the mesh in feet per minute, and unit load index (pounds per inch of face times the diametral pitch). The reasons for inclusion of lubricant film thickness values will be discussed later in this report.

In general, it will be shown that pitting and wear are more strongly influenced by film thickness than calculated surface stresses. The three conventional failure modes are discussed separately below.

Bending Fatigue Failure

A chart showing the distribution of employed bending stresses may be seen as Figure 91. These values were calculated for uniform load distribution without recourse to misalignment or other load sharing factors. The AGMA method as outlined in Reference 23 was used on the spur analyses, and Gleason Computer Program No. A101 was employed for the spiral bevel gears. In the 7945 gears reviewed in the 251 transmissions monitored, no tooth breakage failures were observed. Even though no failures were observed, they do occur but only to a very slight level. (The authors can remember three in bevel gears from their experiences with over 15,000 UH-1 transmissions over the past 15 years.) However, the statistical reliability implied is very encouraging in that it exceeds 99.975% for an average of 913 hours operation.

This failure mode has been essentially eliminated by the use of "clean" steel produced through vacuum arc remelting processes, excellent heat treating controls and practices, accurate tooth spacing, and the use of root fillet forms with a minimum notch concentration factor. These measures have placed the strength in bending above that to which gear optimized for bending stress can be safely loaded in consideration of other failure modes. The generally accepted allowable bending stress for aircraft quality gearing is 55,000 to 65,000 psi, as defined in AGMA Specification 225.01 (Reference 2). Upon use of proper modifying factors for misalignment, load sharing, and dynamic overload at high speeds, this

TABLE XII. GEA

Part Number	Name	Location	P_d	Pressure Angle	Velocity P.L. (Ft/Min)	Compressive Stress (PSI)	T
Bell							AGMA
204-040-108	Planet	L.S.	8.5	22.0	3554	156000	10
204-040-108	Planet	L.R.	8.5	22.0	3554	156000	4
204-040-108	Planet	U.S.	8.5	22.0	1151	162000	6
204-040-108	Planet	U.R.	8.5	22.0	1151	161000	2
204-040-102	Pinion	Gen. Drive	6.292	20.0	7544	83000	10
204-040-104	Pinion	T.R. Drive	7.714	20.0	3152	213000	9
204-040-103	Gear	T.R. Drive	7.714	20.0	3152	28000	9
204-040-762	Gear	Spur, T.R.	10.0	20.0	3152	156000	5
204-040-763	Pinion	Spur, T.R.	10.0	20.0	4309	156000	5
204-040-329	Gear	Lower Sun	8.5	22.0	3554	156000	10
204-040-331	Gear	Lower Ring	8.5	22.0	0	156000	4
204-040-331	Gear	Upper Ring	8.5	22.0	0	161000	2
204-040-330	Gear	Upper Sun	8.5	22.0	1151	162000	6
204-040-700	Pinion	Input	5.391	20.0	7944	189000	23
204-040-701	Gear	Input	5.391	20.0	7944	189000	23
Forward							
114D1044-008	Pinion	Fwd Input	3.841	22.5	11839	214000	29
114D1053-001	Gear	Fwd Input	3.841	22.5	11839	214000	29
114D1043-001	Gear	L.S. Fwd	5.000	25.0	4660	164000	10
114D2076-001	Planet	L.R. Fwd	5.000	25.0	4660	140000	1
1142076-001	Planet	L.S. Fwd	5.000	25.0	4660	164000	10
114D2084-001	Planet	U.S. Fwd	5.000	25.0	1265	161000	5
114D2084-001	Planet	U.R. Fwd	5.000	25.0	1265	149000	1
114D2077-001	Gear	U.S. Fwd	5.000	25.0	1265	161000	5
114D2086-003	Gear	U.R. Fwd	5.000	25.0	0	149000	1
114D2086-003	Gear	L.R. Fwd	5.000	25.0	0	140000	1
Combining							
114D5047-007	Pinion	Combining	5.546	20.0	15687	212000	26
114D5056-001	Gear	Combining	5.546	20.0	15687	212000	26

/-/

PRECEDING PAGE BLANK

GEAR CALCULATIONS

Temperature Rise (°F)		EHD Film (In. x 10^{-6})		W_t (Lb)	Pinion (RPM)	Bending Stress (PSI)	Entrainment Vel. (Ft/Min)	(Lbs x Pd/In.) Unit Load
AGMA	BHC	CROOK. (BHC)	DOWSON					
102	(148)	11.3		1731	2024	29663	1450	11038
42	(58)	14.5		1731	3740	31915	1670	11038
62	(141)	6.6		2675	656	41210	400	11038
24	(65)	7.0		2675	970	26600	538.5	11038
108		8.0		66	2994		3925	1695
95		8.0		1099	4016	30650	1575	12198
95		8.0		1099	4016	30650	1575	12198
58	(88)	14.9	(6.3)	805	2994	44017	1552	17889
58	(88)	14.9	(6.3)	805	2994	28086	1552	11500
102	(148)	11.3	(6.3)	1731	2024	34637	1450	15686
42	(58)	14.5	(8.4)	1731	3740	39194	1670	18392
24	(65)	7.0	(3.7)	2675	970	42100	538.5	19772
62	(141)	6.6	(2.8)	2675	656	33327	400	14765
230		8.0	(12.0)	4580	6400	32200	3925	16461
230		8.0	(12.0)	4580	6400	32200	3925	16461
295		20.0		9359	7064	31700	5920	16430
295		20.0		9359	7064	31700	5920	16430
107	(88)	27.4	(9.4)	4695	3178	32434	2066	13609
19.5	(16.5)	33.3	(16.2)	4695	2281	28143	2317	22209
107	(88)	27.0	(9.4)	4695	3178	27143	2066	22209
53	(85)	14.0	(3.9)	10495	609	30231	553	17177
14.9	(25.2)	17.6	(5.9)	10495	738	31520	645	17177
53	(85)	14.0	(3.9)	10495	609	35889	553	16023
14.9		17.6	(5.9)	10495	738	43345	645	19061
19.5		33.3	(16.2)	4695	2281	44113	2317	19664
263		20.0		5889	11987	0	7844	17419
263		20.0		5889	11987	0	7844	17419

TABLE XII - Cont

Part Number	Name	Location	P_d	Pressure Angle	Velocity P.L. (Ft/Min)	Compressive Stress (PSI)	Temperatu Rise (^oF)	
<u>Aft</u>							AGMA	
114D2045-005	Pinion	Aft Input	4.0	22.5	11384	230000	296	
114D2062-001	Gear	Aft Input	4.0	22.5	11384	230000	296	
114D2066-001	Gear	L.S. Aft	5.0	25.0	4660	164000	107	(
114D2076-001	Planet	L.S. Aft	5.0	25.0	4660	164000	107	(
114D2076-001	Planet	L.R. Aft	5.0	25.0	4660	140000	19.5	(
114D2084-001	Planet	U.S. Aft	5.0	25.0	1265	161000	53	(
114D2084-001	Planet	U.R. Aft	5.0	25.0	1265	149000	14.9	(
114D2077-001	Gear	U.S. Aft	5.0	25.0	1265	161000	53	(
114D2086-003	Gear	U.R. Aft	5.0	25.0	0	149000	14.9	
114D2086-003	Gear	L.R. Aft	5.0	25.0	0	140000	19.5	

ABLE XII - Continued

ive	Temperature Rise (°F)		EHD Film (In. x 10^{-6})		W_t (Lb)	Pinion (RPM)	Bending Stress (PSI)	Entrainment Vel.(Ft/Min)	(Lbs x Pd/In.) Unit Load
	AGMA	BHC	CROOK (BHC)	DOWSON					
	296		20		9751	7064	32900	5692	17100
	296		20		9751	7064	32900	5692	17100
	107	(88)	27	(9.4)	4695	3178	32434	2066	13609
	107	(88)	27	(9.4)	4695	3178	27143	2066	22209
	19.5	(16.5)	33.3	(16.2)	4696	2281	28143	2317	22209
	53	(85)	14	(3.9)	10495	609	30231	553	17177
	14.9	(25.2)	17.6	(5.9)	10495	738	31520	645	17177
	53	(85)	14	(3.9)	10495	609	35889	553	16023
	14.9		17.6	(5.9)	10495	738	43345	645	19061
	19.5		33.3	(16.2)	4695	2281	44113	2317	19664

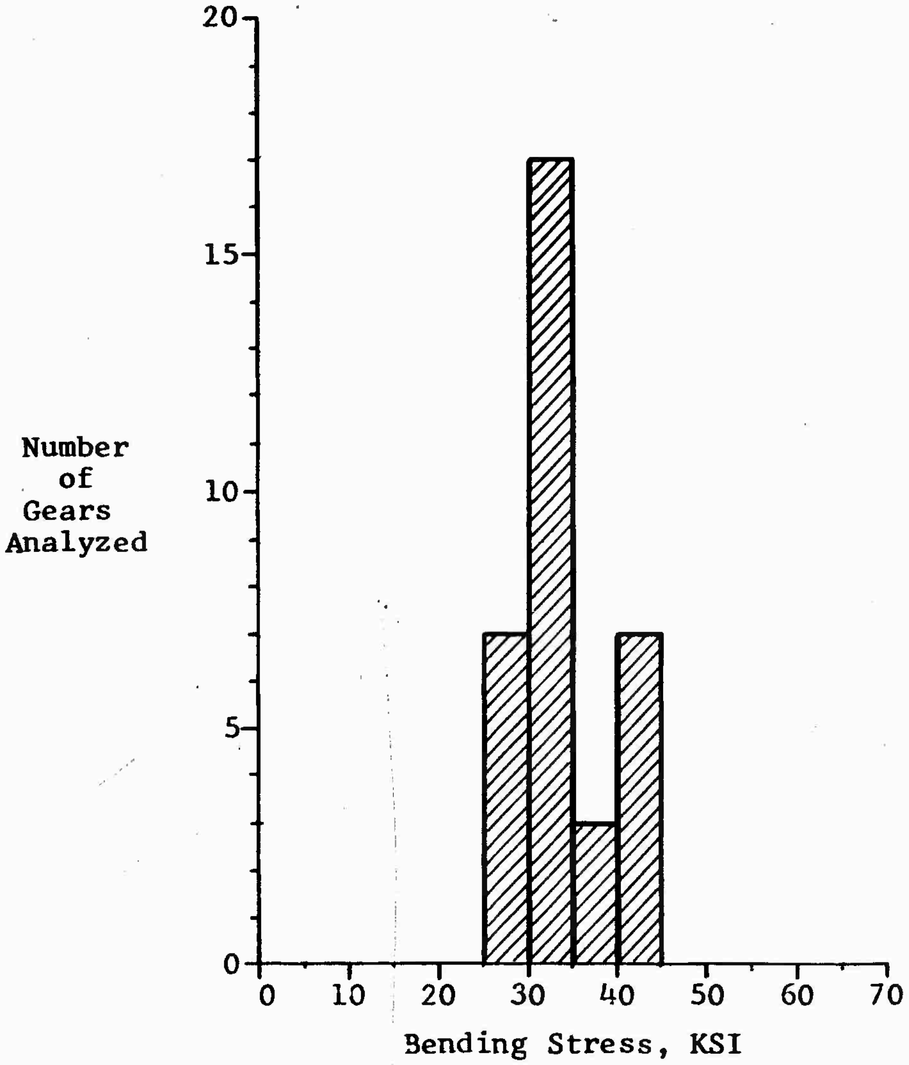

Figure 91. Gear Tooth Bending Stress Distribution.

allowable can be expressed in numbers as high as 100,000 psi, as shown in USAAVLABS Technical Report 66-85 (Reference 23). In general, properly designed and manufactured aircraft gears are now load capacity limited by pitting or spalling and scuffing failure modes.

Surface Compressive Failure (Pitting)

The classical relationship of pitting life as a function of Hertzian pitch line stress is presented in AGMA specifications as an inverse ninth or tenth power stress-life relationship. Figure 92 has been abstracted from the AGMA Specification 411.02. Note the allowable stress limit for grade 2 gears. Note also the location of the UH-1 upper sun gear at MTBR (995 hours) and full takeoff power of 1100 hp.

A corrected value for the UH-1 sun gear which assigns a combined misalignment and load distribution factor of 1.21 is also shown. Both points lie well within the suggested boundary. The 30% observed failure rate in pitting for this gear seems quite incongruous, and serves to illustrate the inadequacy of this index alone to predict the occurrence of pitting failures. This chart does not take into account the gear surface topography, the lubricant film thickness, chemical activity nor influence upon rate of failure progression after the first surface fissure occurs.

The particular failure modes have been described in Reference 22 as surface initiated , probably from tensile cracking of harsh asperity contacts through the thin oil film followed by rapid hydraulic propagation. More detailed definition of the lubricant condition, surface topography, and metallurgical states of the UH-1 upper sun gear will appear subsequently.

The distribution of unfactored calculated Hertzian or compressive stresses for all power gears in this program is shown in Figure 93. Spiral bevel gears stand alone to the right partially due to the increased ratio of peak to mean stress for point versus line contacts. Bevel gears are treated analytically as point contacts while spur gears are treated as line contacts. Neither assumption is purely justified in practice.

As noted above, the 204-040-330-3 upper sun gear in the UH-1 transmission was the sole observed primary pitting mode failure gear. Its contribution to the entire spectrum is graphically portrayed in Figure 94. The final section of Analysis of Failure Modes describes the observed failure mode, surface topography, and lubricant film condition in detail.

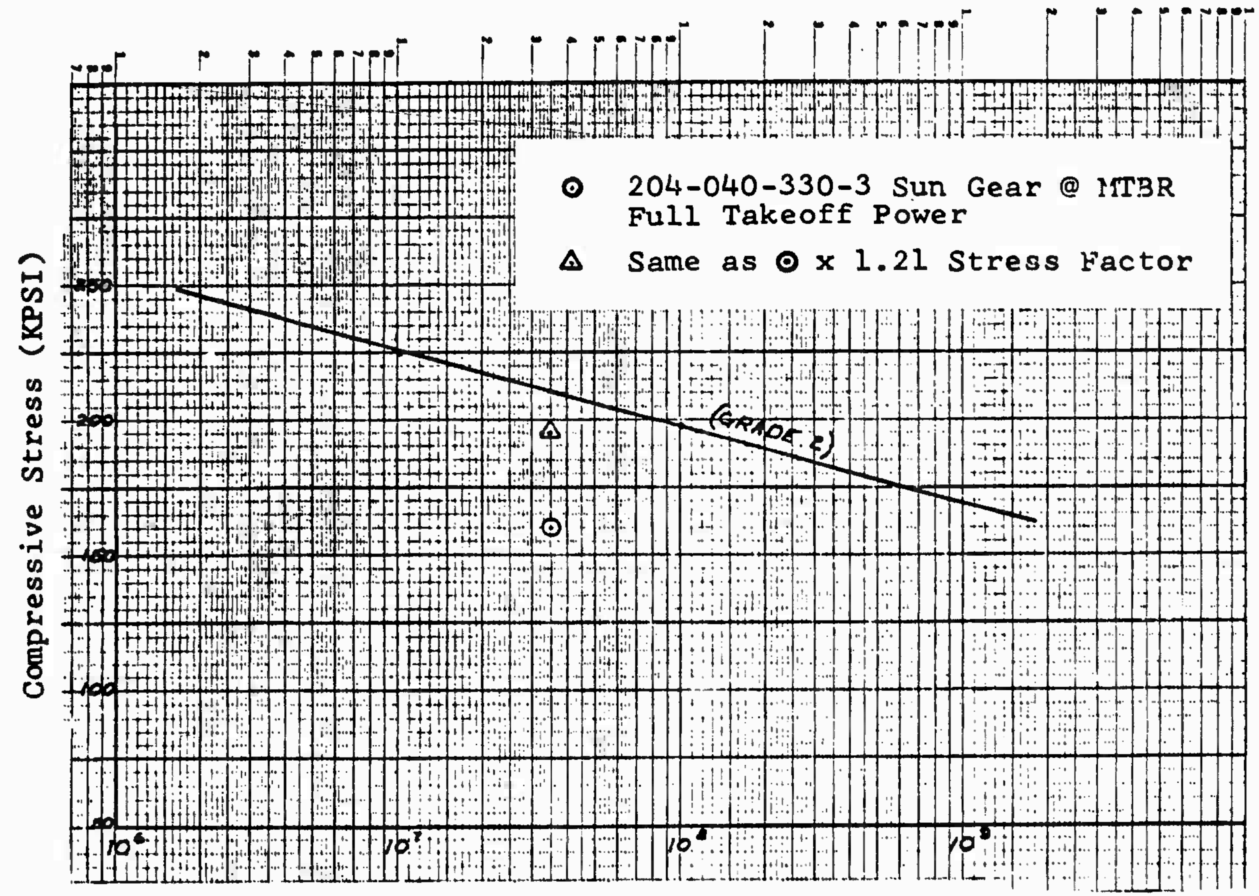

Figure 92. AGMA Contact Design Stress Limits (411.02 - September 1966).

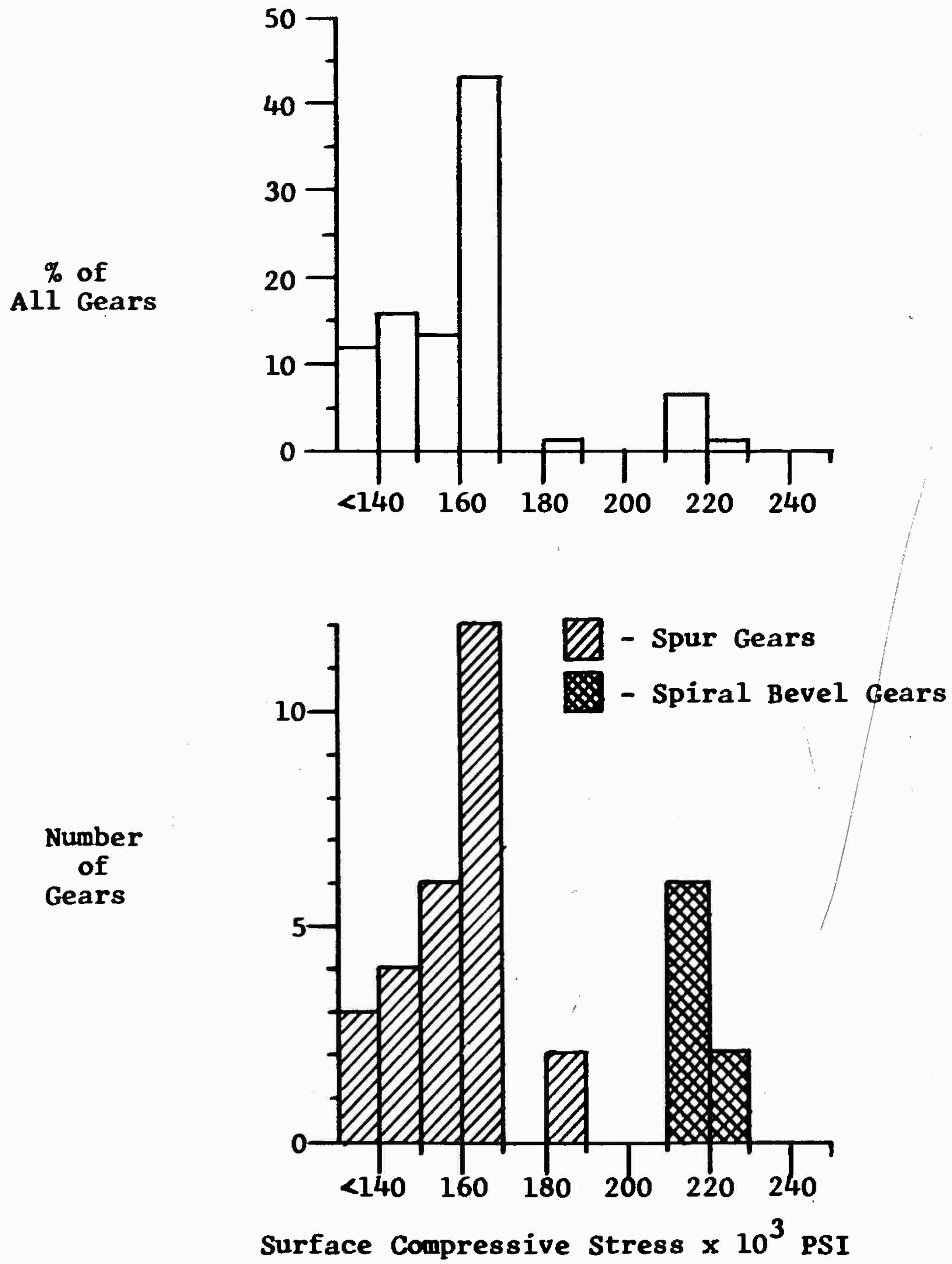

Note: Each planet idler counted as two gears.

Figure 93. Design Stress Distribution of Power Gears.

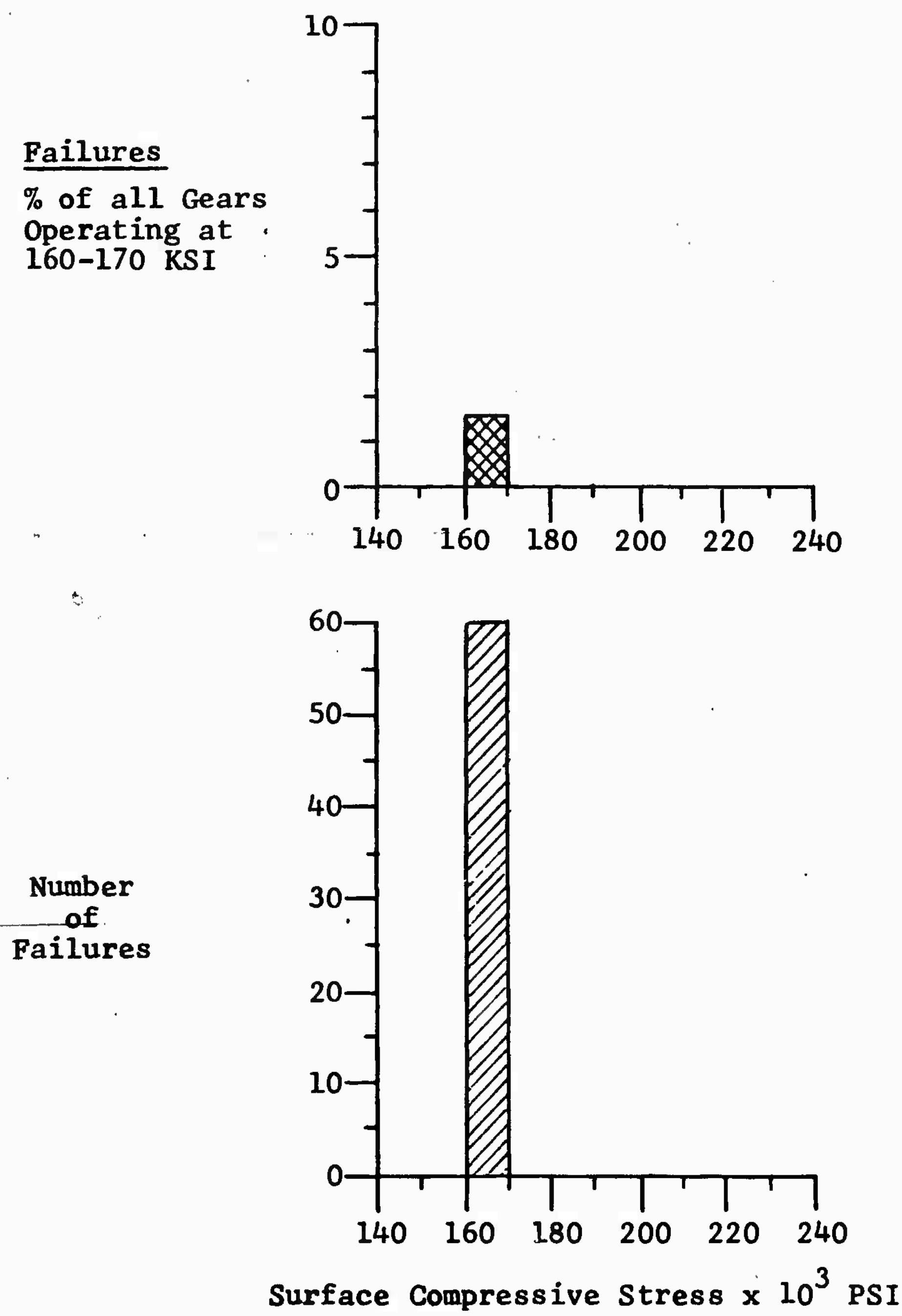

Figure 94. Failure Distribution of Power Gears.

Gear Scuffing Failures

The distribution of calculated scuffing or scoring index for gear tooth surface temperatures is given in Figure 95. There were no observed occurrences of primary failures due to scuffing. What did occur was judged to be secondary, due to contact misalignment resulting from wear of spacer or bearing parts and simple excessive power overloads.

Sample calculations for temperature rise may be found in Appendix III. The basis of this calculation is the simple hypothesis that a critical temperature exists at which the oil in the conjunction between two loaded-moving gear teeth will cease to lubricate and severe metal contact will follow and result in scuffing - the melting of a thin layer of tooth surface material. The stabilized steady state temperature of the gear blank is subtracted from this critical temperature to find the allowable temperature rise as defined in Figure 95. The temperature rise is that which occurs in the tooth pair conjunction as one tooth transmits power through the other. These stated values are representative of very safe design limits as evidenced by the absence of any primary failures. For comparative purposes, a line representing 10% probability of scoring (assuming a blank temperature of 210°F) is included in Figure 95. This value is taken from AGMA information sheet 217.01, which represented the results of field experience wherein data concerning case histories of large numbers of gear types operating in MIL-L-7808 were accumulated and analyzed.

The calculated temperature rise is a variable dependent upon load, surface finish, radii of curvature, speed, and coefficient of friction. One inflexibility of the scoring formula arises from the assumption of a constant coefficient of friction. All lubricant types are assumed to provide the same lubrication and hence exhibit a constant friction coefficient. This assumption is too restrictive to allow analytical generality. Lubricant properties, as affected by conjunction pressure and temperature variation, must be considered in determining lubrication regime. The coefficient of friction, in fact, is a variable from one gear mesh to another and also within any single gear mesh. The load varies from the first point of contact to the last point of contact, depending upon profile modification, contact ratio, and gear tooth deflection.

Intimately associated with the variation of load is the lubricant viscosity, film thickness, and related lubrication regime. Where full hydrodynamic lubrication exists with Newtonian fluids, the coefficient of friction is purely a function of lubricant viscosity (viscous shear) at the load-pressure

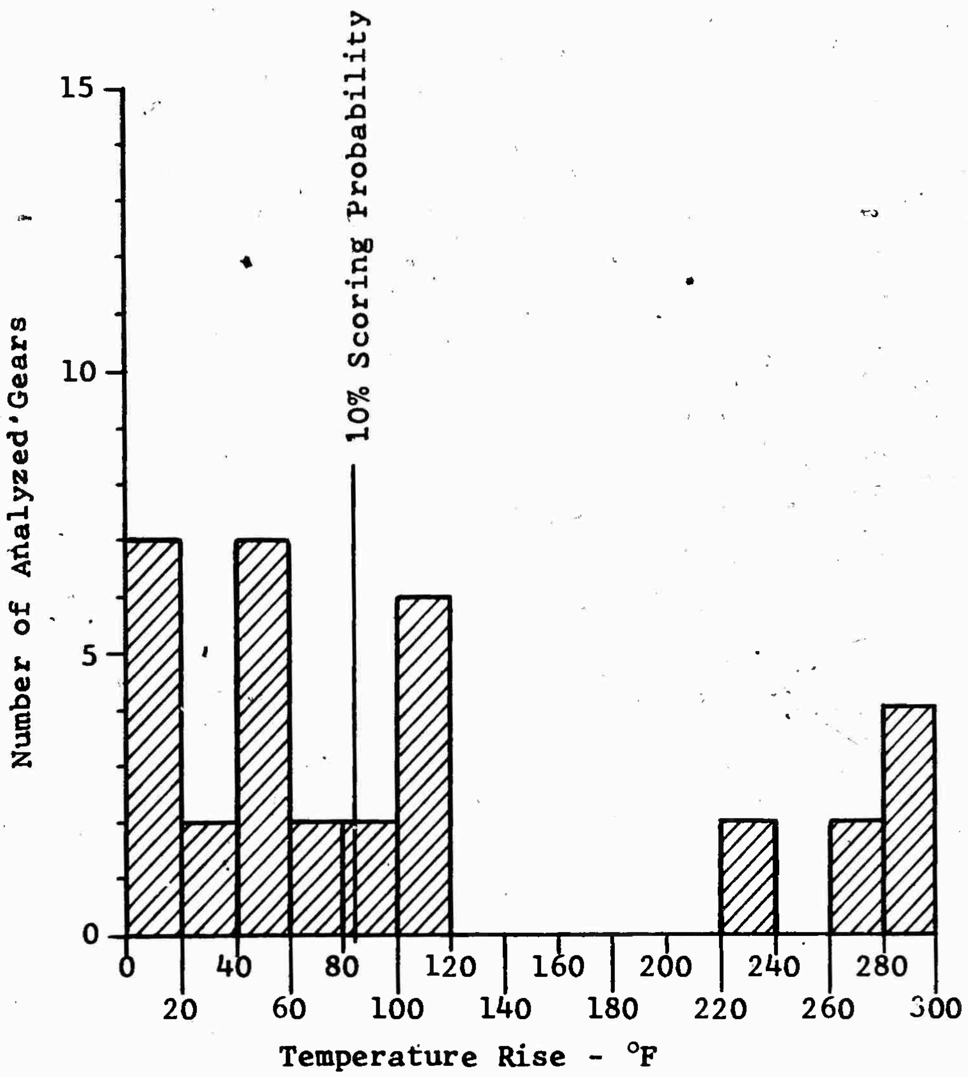

Figure 95. Distribution Scoring Index, Temperature Range.

conditions of the conjunction. As the lubricant film becomes smaller and the lubrication regime approaches boundary conditions, the coefficient of friction increases and is affected by surface finish in the guise of random asperity contacts. If conjunction stability is attained in the boundary lubrication regime, the result is wear at a constant rate (unless run-in occurs and surface refinement is accomplished). However, with increasing asperity contacts the friction increases with resultant temperature increases and conjunction instability. Once this condition is satisfied, the critical temperature concept seems to offer adequate predictability for operation in relatively nonreactive oils such as MIL-L-7808 and MIL-L-23699.

BEARING DESIGN CORRELATIONS

All bearings used in the primary power paths in the four transmissions in this study were analyzed with respect to conventional methods, and their predicted B_{10} lives at takeoff power and normal rated rpm are given in Table XIII. Other data presented in this table are: ring and element material, C/P (basic dynamic capacity over equivalent load), maximum load on single rolling element, maximum Hertz stress (PSI), EHD film thickness (SKF method, after Grubin), rpm, retainer material, B_{10} in revolutions, %/1000 hour failure rate, and retirement life.

Present bearing design technology evolved primarily from the work accomplished by Lundberg and Palmgren (References 13 and 14). The Anti-Friction Bearing Manufacturers Association (AFBMA) (Reference 3) has adopted the basic premises established by Lundberg and Palmgren in the form of the bearing rating standard. The AFBMA Standard, at present, is the only document available to provide a measure for bearing fatigue life or performance.

Fatigue life as determined by the statistical treatment devised by Lundberg and Palmgren is predicated on subsurface initiation of fatigue cracks in a through-hardened air-melt bearing material. The effect of lubrication on contact fatigue has been ignored entirely in the AFBMA Standards and quantitatively by Lundberg and Palmgren.

The mathematical model used in describing this failure mode (primarily subsurface fatigue initiation at or near oxide and nonmetallic inclusions) is a very general thing. In fact, it has been shown that Weibull statistics, the basis for meaningful presentation of test data, give a good fit not only on bearing failure distributions, but also on human mortality, vacuum tube lives, and many other systems both complex and simple.

TABLE

Part Number	Name	Matl	B_{10} Hours	C/P (Lb/Lb)	Max Roll Load (Lb)	Max Hertz St (PSI)
Bell						
204-040-132	Roller (Race) Lower		855		639	22200
204-040-135	Ball					
204-040-142	Ball					
204-040-143	Ball (206 Quill)		336	4.7	467	28800
204-040-143	Ball (207 Quill)		888	6.8	356	24600
204-040-143	Ball (213 Quill)		754	5.9	393	27400
204-040-269	Roller		5090	11.0	653	17400
204-040-270	Roller		11327			
204-040-271	Roller		33421	16.0	269	12200
204-040-310	Roller (206 Quill)		10322	13	357	16700
204-040-310	Roller (207 Quill)		456	5.3	771	24600
204-040-345	Ball		641	4.5	421	22900
204-040-346	Ball		372	4.5	787	24000
204-040-424	Ball		2073	25.0	62	19000
204-040-725	Roller (Lower)		855		639	22200
204-040-725	Roller (Upper)		531		936	26900
Aft						
114DS240	Roller	M-50	188	4.5	4274	22300
114DS241	Ball	M-50	391	5.1	1016	23300
114DS242	Ball		384	4.4	335	28200
114DS243	Roller		176	4.0	1492	21400
114DS244	Roller		2095	3.7	1232	20200
114DS247	Roller					
114DS248	Ball					
114DS249	Roller					
114DS250	Ball					
114DS251	Ball					
114DS252	Ball					
114DS253	Roller					
114DS255	Ball					
114DS256	Ball					
114DS257	Roller					
114DS258	Roller		3500	2.6	3280	23600
114DS262	Roller		1953	4.6	1269	16600
114DS265	Roller					

4

II. BEARING CALCULATIONS

…s	EHD* Film Thickness (In. x 10^{-6})	RPM	Basic Dyn. Cap. (Lb)	Retainer Material	B_{10} Number of Cycles (10^{-6})	Failure Rate (%/1000 Hours)	Retirement Life Hours
	11	3722		Al. Bronze	118.6	.28	
		2024	3870	Micarta		.38	
	12	4016	5030	Al. Bronze	80.96	.57	
	12	4171	5030	Al. Bronze	222.3	.57	
	12	4016	5030	Al. Bronze	181.7		
	20	6400	15500	Al. Bronze	1955	.57	
	22	2994	21900	Al. Bronze	5995.7		
	13	4016	10800	Al. Bronze	2487	.57	
	12	4171	10800	Al. Bronze	114.1		
	23	2994	21600	Micarta	115.1	12.14	
	33	6400	35200	Al. Bronze	142.8	21.97	
	16	6400	3220	Nylatron	796		
	11	3722		Al. Bronze	118.6		
	5	1206		Nylon	61.9		
	58	7064	60000	Al. Bronze	79.7	17.5	4000
	82	7064	31300	Al. Bronze	165.7		4000
	33	4017	13500	Al. Bronze	92.6	2.18	
	50	4017	35500	Al. Bronze	42.4		1200
	24	2281	34700	Ag. Pl. Bronze	286.7	1.1	1200
							1200
	10	738	55000	Ag. Pl. Bronze	155	2.18	3600 on -3 (400 on -7)
	67	7064	20300	Al. Bronze	827.8		

B

TABLE XIII - Contin

Part Number	Name	Matl	B_{10} Hours	C/P (Lb/Lb)	Max Roll Load (Lb)	Max Hertz Stress (PSI)	EHD* Film Thickness (In. x 10^{-6})	RP
Combining								
114DS252	Ball							
114DS541	Ball	M-50	846	6.0	810	224000	90	119
114DS542	Roller	M-50	168	5.1	3678	228000	83	119
114DS543	Roller		9051	9.3	190	146000	37	70
114DS544	Ball		346	5.3	141	242000	39	70
114DS545	Roller		5908	9.3	674	148000	51	70
114DS548	Ball							
114DS549	Roller							
114DS550	Ball							
114DS642	Roller	M-50	4081	10.0	1492	142000	83	119
Forward								
114DS143	Ball		489	4.6	654	292000	35	40
114DS240	Roller	M-50	229	4.7	4066	218000	58	70
114DS241	Ball	M-50	421	5.2	1053	236000	82	70
114DS243	Roller		219	3.9	1421	209000	50	40
114DS244	Roller			3.7	1232	202000	24	22
114DS258	Roller			2.6	3280	236000	10	7
114DS262	Roller		2355	4.8	1215	162000	67	70
114DS250	Ball							
114DS144	Ball		2317	3.7	3969	299000	4	2

* SKF Method (Reference 12)

H

II - Continued

EHD* Film ickness . x 10^{-6})	RPM	Basic Dyn. Cap (Lb)	Retainer Material	B_{10} Number of Cycles (10^{-6})	Failure Rate (%/1000 Hours)	Retirement Life Hours
90	11987	17300	Al. Bronze	608.5		5000
83	11987	41500	Al. Bronze	120.8	7.5	1200
37	7064	5800	Al. Bronze	3836		10000
39	7064	5410	Al. Bronze	146.6		1200
51	7064	21000	Al. Bronze	2504		10000
83	11987	28000	Al. Bronze	2935		10000
35	4017	19800	Al. Bronze		4.29	1200
58	7064	60000	Al. Bronze			
82	7064	31200	Al. Bronze			
50	4017	35500	Al. Bronze			
24	2281	34700	Ag. Pl. Bronze			
10	738	55000	Ag. Pl. Bronze		1.42	3600 on -3 (400 on -7)
67	7064	20300	Al. Bronze			10000
4	230	46300	Al. Bronze		51.2	500 (1200)

B

Observations made in this study show very conclusively that the type of failure treated in the classic bearing life determination occurs in but a very small segment of the total failure population. A review of the optical and metallurgical study reports performed on failed bearings (Reference 24) shows that Items 8, 18, 34, 2F, and 4A (item to part number correspondence is given in Figures 3, 4, 5, and 6) all exhibited surface initiated failures. Just as in human mortality, there exists many competing failure modes. In recent years, the advent of cleaner materials (vacuum arc remelt and degassing processes) has markedly reduced the probability of failure of the classic nature. To some extent, this cleanliness has also reduced the occurrence of surface-initiated failure modes by reducing the total number of surface stress risers. The vast majority of failures observed in this study were surface initiated and hydraulically propagated.

As shown earlier in Table IX, the Distribution of Failure Mode, the primary failure rate of ball bearings was 2.868%, while the primary failure rate of roller bearings was .2866%. This 10:1 ratio of failure occurrences leads one to inquire about the calculated life ratio. For all bearings included in this study, the average calculated full power B_{10} for ball bearings was 829 hours and that for roller bearings was 2881 hours for a ratio of 3.5:1. However, it should be noted that the range for ball bearings was 336 to 2317 hours, and the range for roller bearings was 176 to 33,421 hours. Since there was one abnormally high life roller bearing, some consideration should be given to removing it from the mean tabulation. If this is done, the B_{10} range for rollers is 176 to 11,327 hours and the new average is 1867 hours. The more representative ratio would then be 2.25:1 on mean B_{10} lives. Whichever case is considered, the disparity between calculated life and real life performance ranges from 3 to 5, i.e., experience indicates higher confidence in roller bearing performance than ball bearing performance.

The effects of sliding in Hertzian contacts as treated by Crook is shown in the following section where a comparison of isothermal and frictional EHD oil film thicknesses is shown for a spur gear mesh. A similar phenomenon has been shown to exist in ball bearings where sliding is present virtually throughout the contact area. The EHD lubricant film thickness, and consequently the subsurface stress distribution, is affected by surface compressive stress, lubricant pressure coefficient of viscosity, rolling speed, and relative sliding. Ball bearings, with inherently high osculation between balls and races, are subjected to appreciable periferal sliding in the contact ellipse as well as sliding at the center of the contact ellipse. The associated EHD film degradation at high

loads and moderate speeds results in sliding asperity contact and near-Hertzian compressive stress distribution. A reduced fatigue life for the bearing apparently exists under those conditions.

The condition of sliding in the contact zones of roller bearings does not exist except where rolling instability occurs on the rollers and skidding or skewing results. Under conditions of proper alignment and load maintenance, the rollers are well behaved, and relatively pure rolling is obtained between rollers and raceways. This leads to excellent (line) contact, and good EHD lubricant film is built and maintained. The net effect of proper lubrication, which is more easily attained with rollers than with ball bearings, appears to be a much superior surface endurance limit to similarly stressed ball bearings.

Another factor not actually covered in AFBMA is the introduction of new materials with properties that markedly enhance fatigue resistance in rolling loaded contact. The use of higher alloy content through-hardening tool steels, case carburized steels, and stainless steel as well as vacuum melt processing is not covered in AFBMA literature. However, the development of the statistical analysis of bearing fatigue is predicated on certain empirically determined material factors which are provided for in the AFBMA treatment. As a first step in including new material factors, it is suggested that sufficient endurance test data be accumulated for each prospective bearing material and subsequently incorporated into the existing AFBMA standard. In reality, the task becomes enormously ambitious, since any given material may demonstrate different life ratios for the various competing failure modes.

The distribution of maximum calculated compressive stress for all bearing applications studied is presented in Figure 96. Here the total bar height indicates the number of applications observed in the indicated stress range. Figure 97 reveals the failure distribution relative to the same stress ranges. Definite trend correlation of number of failures with compressive stress is shown. However, the picture is considerably less clear as presented in Figures 98 and 99. Figure 98 presents the usage and failure dispersion of ball bearings with respect to calculated B_{10} life. Figure 99 presents similar data for roller bearings. The correlation is not too good. Simple maximum compressive stress appears to offer better correlation than AFBMA calculated B_{10} life.

During the course of examination of failed bearings, it became apparent that a higher primary failure rate was being observed from one manufacturer. After collection and evaluation of all

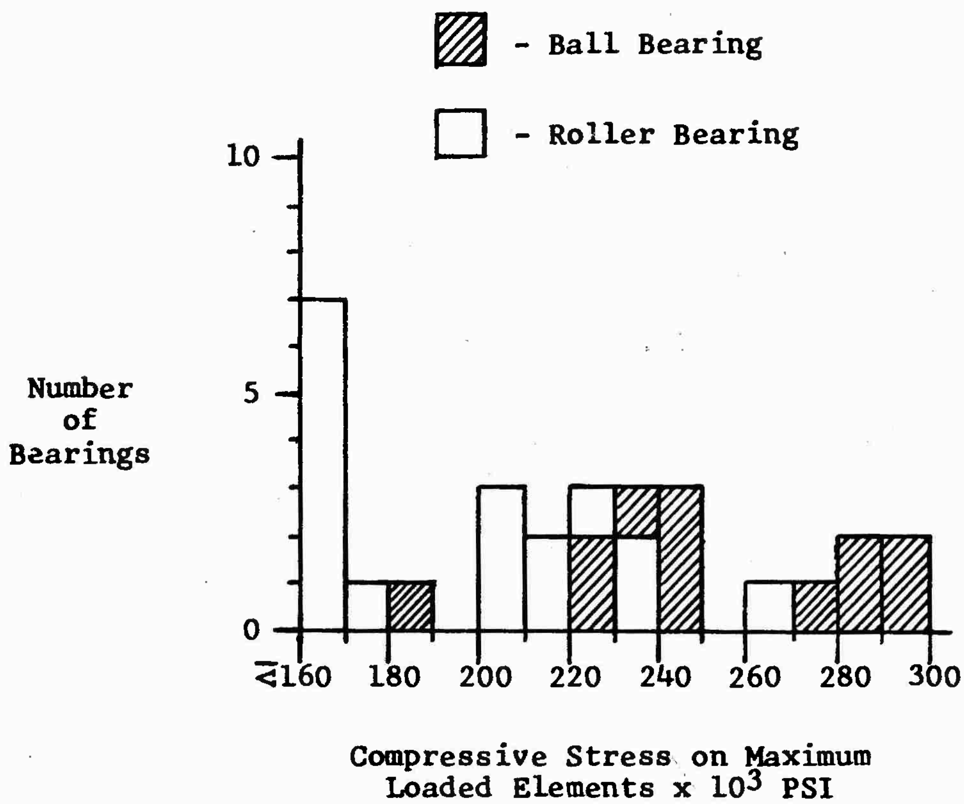

Figure 96. Design Stress Distribution of Ball and Roller Bearings.

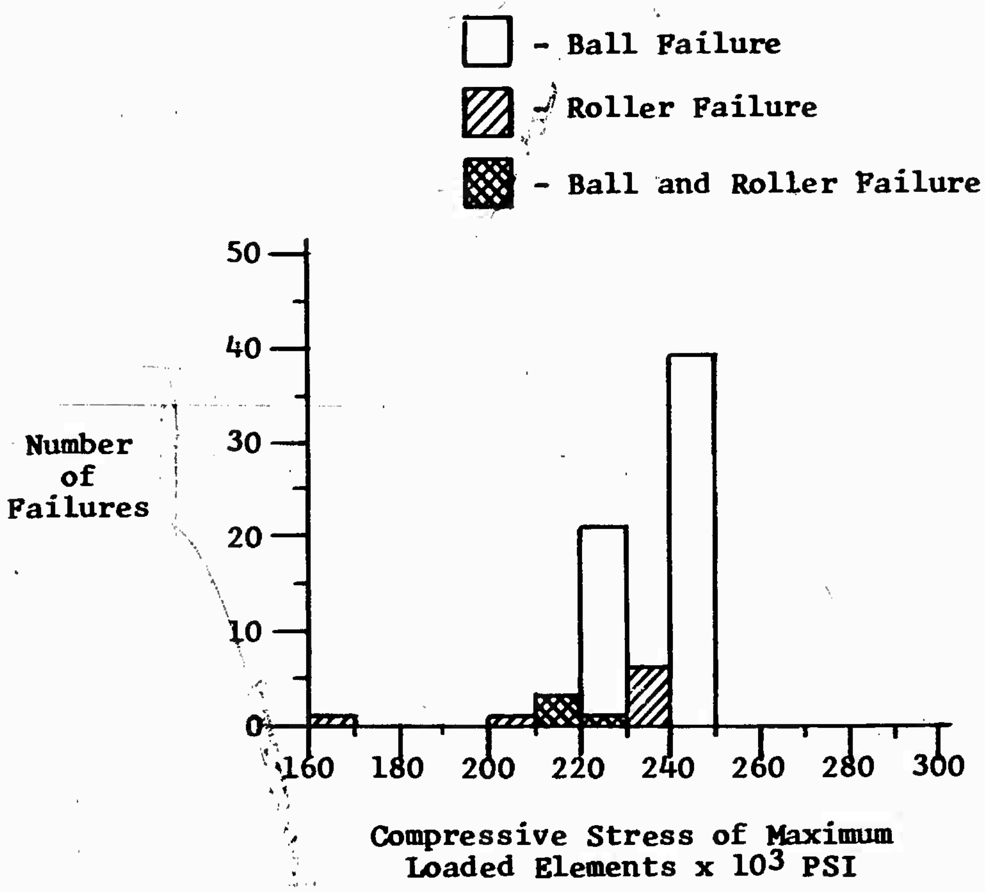

Figure 97. Failure Distribution of Ball and Roller Bearings.

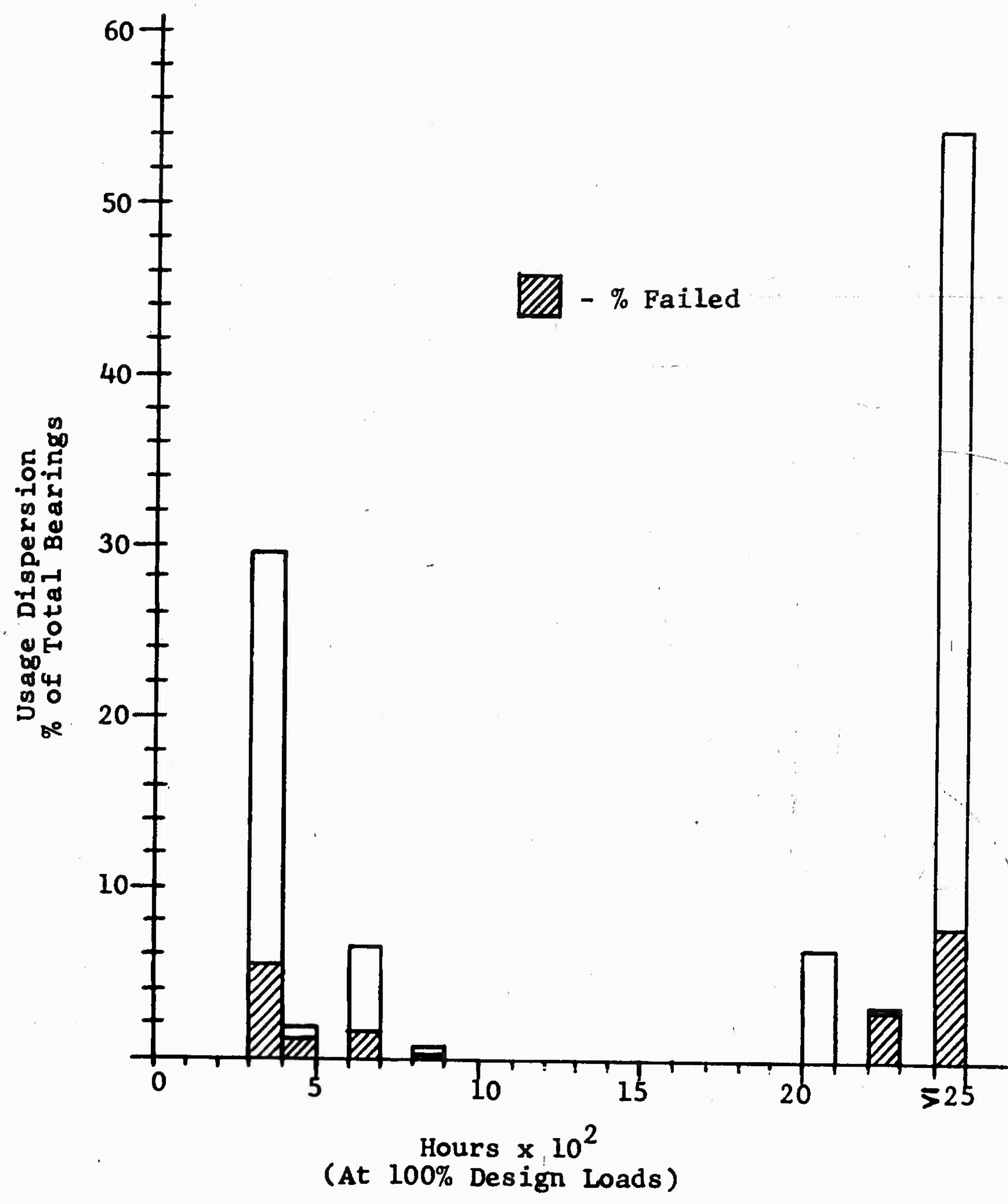

Figure 98. Ball Bearing B_{10} Life, Hours x 10^2 (At 100% Design Loads).

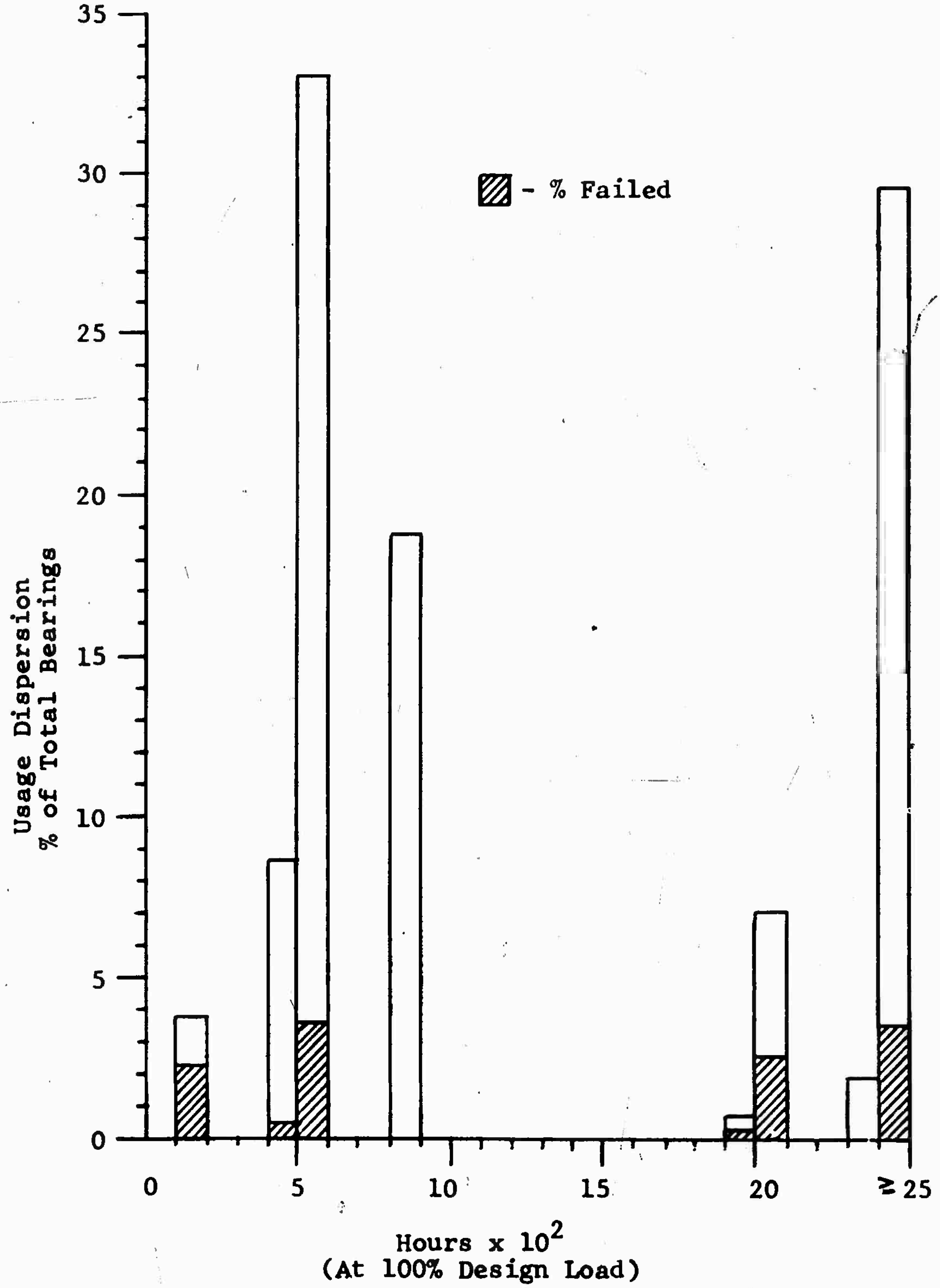

Figure 99. Roller Bearing B_{10} Life, Hours x 10^2 (At 100% Design Loads).

data where positive identification could be made, the tabulation shown in Table XIV resulted. While the primary failure rates of Manufacturers I and II were virtually identical, Manufacturer III indicated a doubled failure rate. Since the possibility existed that Manufacturer III had all the "tough" applications, a brief review of the minimum calculated B_{10} in each manufacturers group, the number of bearings replaced in the minimum life location, and the average calculated B_{10} of all the applications of each manufacturer's bearings was conducted. The results listed in Table XIV show that Manufacturer III had the singular lowest life application, had the least failures in the lowest life location, and was in between the other two in average calculated life. It would appear from these statistics that on the average, Manufacturer III produced an inferior bearing. In the following section on elastohydrodynamics, some interesting measurements on inner race surface finishes from this source are presented.

An attempt was made to plot the overhaul experience for two particular bearings on Weibull paper to check the order of predicted life to real life ratio. Weibull plots for the CH-47 114DS240-2 roller bearing (M-50) and the UH-1 204-040-345-7 ball duplex bearing are presented in Figures 100 and 101, respectively.

The predicted service B_{10} life from Figure 100 is approximately 10^9 inner ring revolutions. The calculated B_{10} at 100% power is 17.5×10^6 revolutions. Applying the often used life improvement factor for M-50 material (5) gives 87.5×10^6, close to 10^8 revolutions. If a cubic or quartic mean spectrum sufficient to obtain an equivalent life increase of 10 were employed, an average power setting requirement of 50% takeoff would result. This appears a bit low. One is left to conclude that in this instance the experienced life exceeds the accepted calculated life.

In the instance of Figure 101, the predicted service B_{10} life is approximately 2.5×10^8 inner ring revolutions. The calculated B_{10} is 1.15×10^8 at 100% power. Using a life factor of 2 for clean vacuum degassed 52100 gives a corrected B_{10} of 2.3×10^8. This value is essentially identical to that experienced. However, it is doubtful that the UH-1 is operated at 100% power for 100% of the time. A reasonable cubic mean level would be 70% power. The calculated correction would be $\left(\frac{1}{.7}\right)^3 = (1.4)^3 = 2.74$ for a new B_{10} of 6.2×10^8 revolutions.

TABLE XIV. BEARING LIFE BY MANUFACTURER				
MFR		Min B_{10}	No. Replaced at Min B_{10}	Avg. B_{10}
I	$\frac{\text{Primary Failures}}{\text{Total Monitored}} = \frac{13}{149} = .087$	336	19	472
II	$\frac{\text{Primary Failures}}{\text{Total Monitored}} = \frac{33}{402} = .082$	176	64	2051
III	$\frac{\text{Primary Failures}}{\text{Total Monitored}} = \frac{33}{208} = .159$	168	4	1180

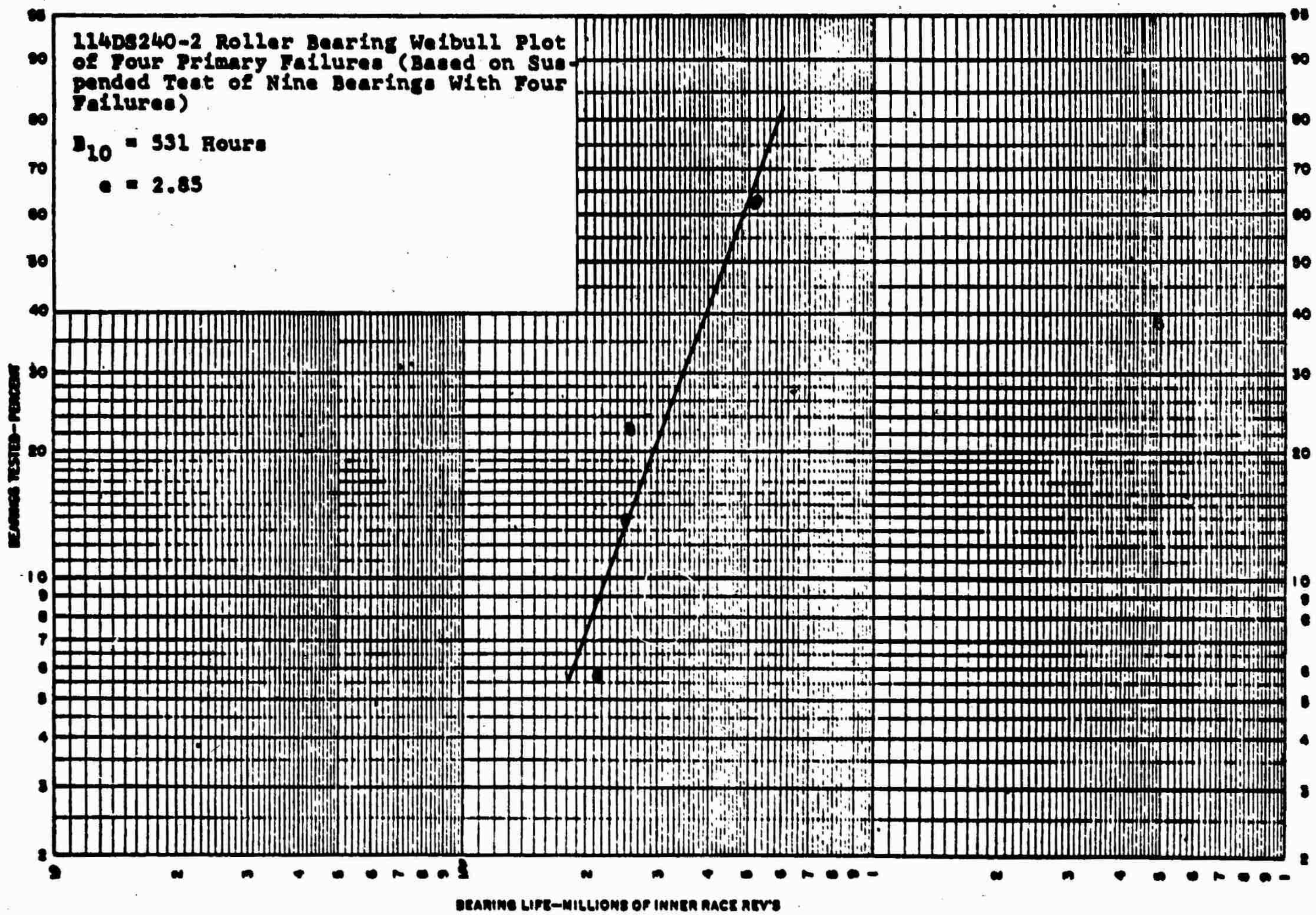

Figure 100. Failure Distribution of 114DS240 Bearing by Suspended Test Analysis.

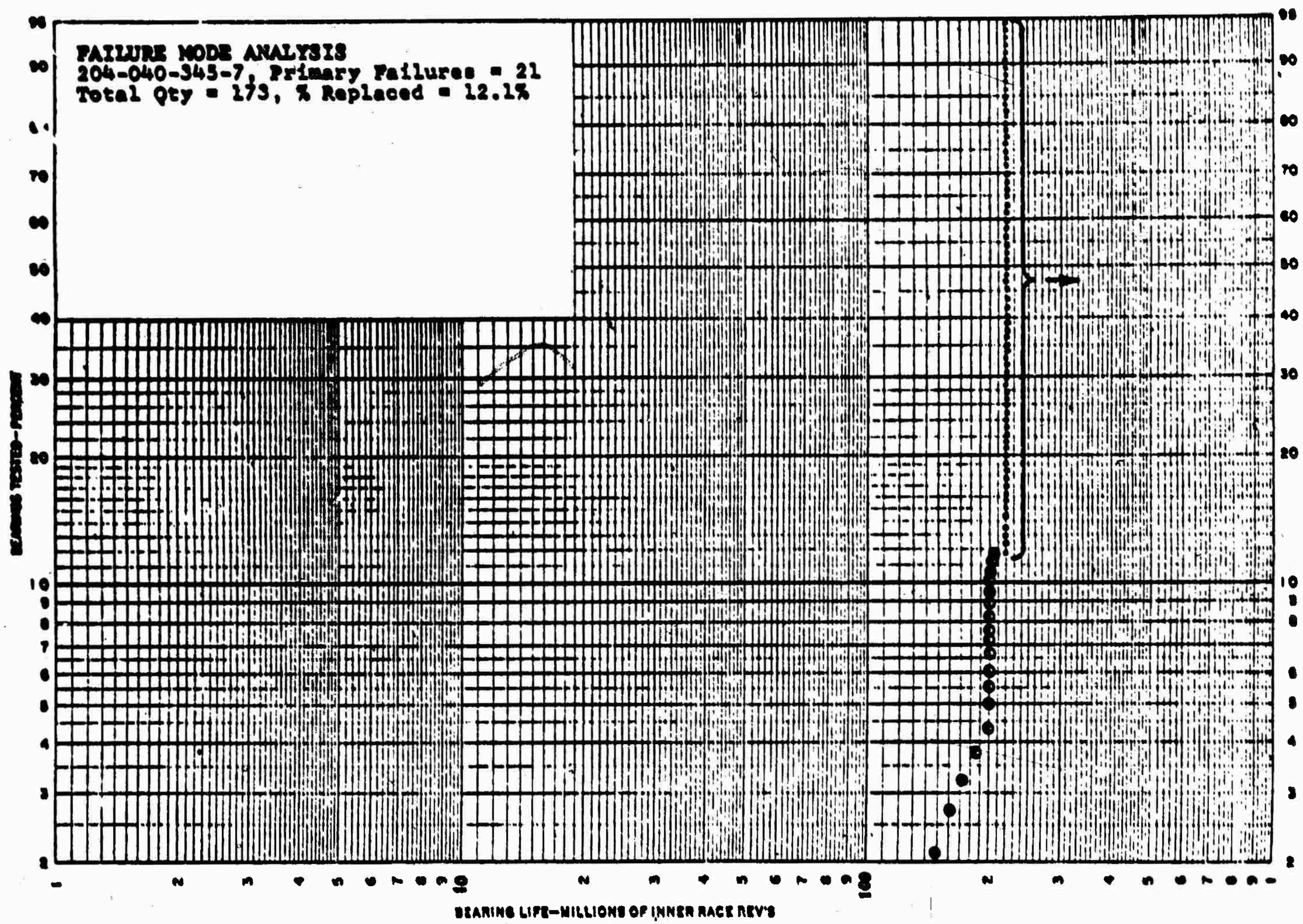

Figure 101. Failure Distribution of 204-040-345 Bearing.

In this instance the experienced life is less than that calculated. In general, these results add to our earlier findings concerning the disparity in roller over ball bearing calculated experienced life ratios.

An investigation was conducted at Battelle Memorial Institute using scanning electron beam microscopy techniques to attempt confirmation of failure origin locations in two selected bearing spalls. These were chosen based upon macroscopic evaluation of failure mode and classification into surface initiated and subsurface initiated. The first specimen chosen may be seen in Figure 102. It is a section of outer ring from a failed CH-47 114DS143-1 bearing. The spalled area was tentatively identified as surface initiated by the "upstream arrowhead" characteristic and the shallow sides of the pitted area. A 50x enlarged view of the spall is shown as Figure 103.

Location of the origin of the failure could not be positively determined. The central portion of the spalled region appeared to be severely beaten or abraded; this was most likely from the action of the balls running over entrapped debris. Surface cracking immediately adjacent to the spalled area is more severe toward the axially loaded shoulder and into the direction of ball movement, i.e., toward the top and right-hand side of Figure 103, indicating that the spalled region was probably propagating preferentially along both of these directions. The area labeled "C" in Figure 103 appeared to have been formed by some form of impact or abrasive action. Its origin and significance could not be determined, but it definitely did not appear to be a massive inclusion. The abrasion could have resulted from an initial chip formation which propagated at a slight angle from the surface.

The entire spalled area was carefully examined, and those areas labeled "A" and "B" in Figure 103 were considered representative of the basic spalling propagation mechanism that was observed. Area "A" is shown at higher magnification in Figures 104 and 105, and shows the propagation of the spalling by the formation of a small flat chip at the edge of the spalled region. The chips evidently were formed by the propagation of a subsurface crack and then fractured away from the parent material by the formation of secondary cracks between the subsurface crack and the surface of the bearing race. The subsurface crack could have been hydraulically propagated. Fine striations may be seen in Figures 104 and 105, running approximately parallel to the rolling direction of the race. Although the origin of the striations can only be speculated upon, they are most likely formed by the relative movement between the chips and the substrate. It should have been possible to determine the origin by finding the converging point of the

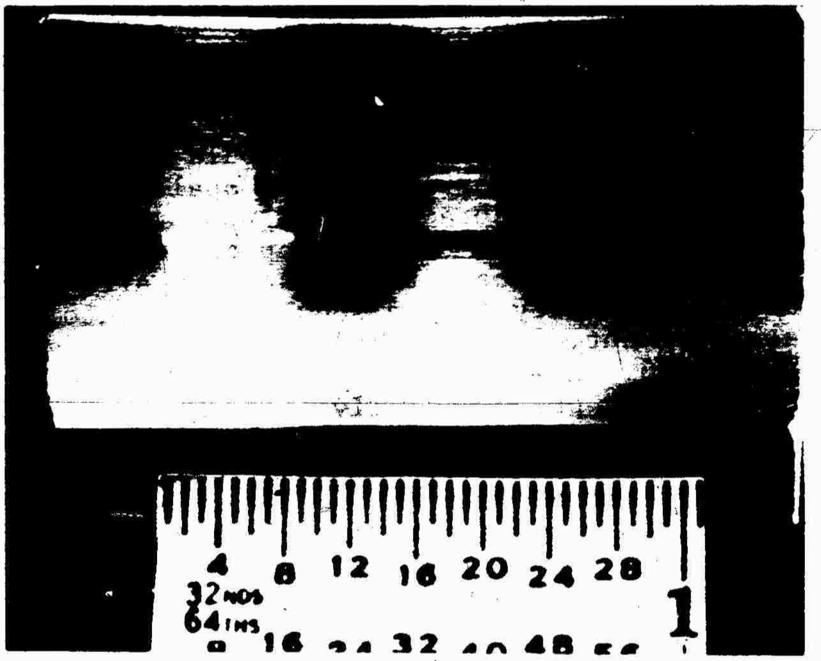

Figure 102. Section From Bearing Outer Ring Showing Surface Initiated Failure (P/N 114DS143-1).

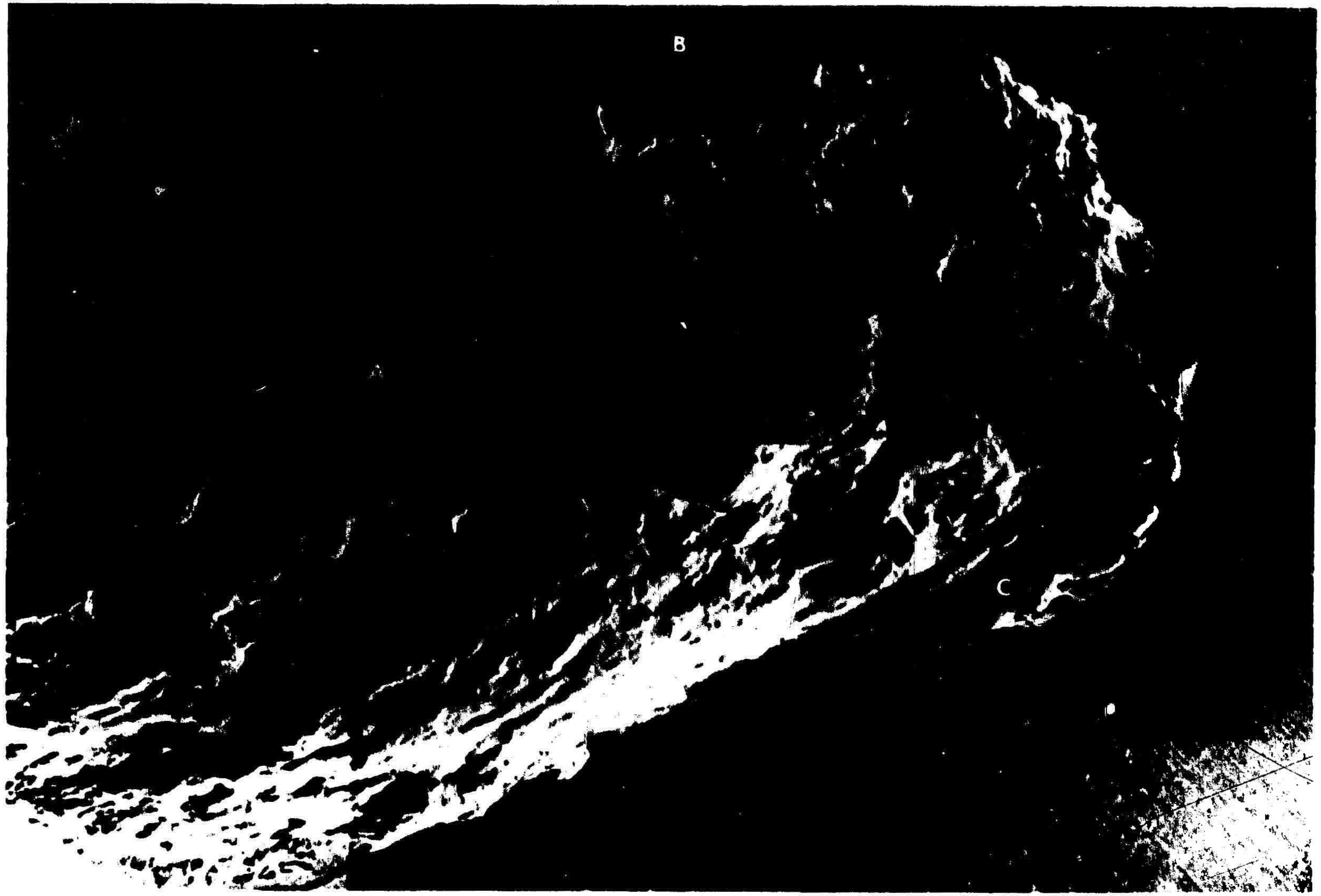

Figure 103. Enlarged View of Spalled Bearing Outer Race (P/N 114DS143-1) Magnification 50X.

Figure 104. Enlarged View of Area A (P/N 114DS143-1). Magnification 200X

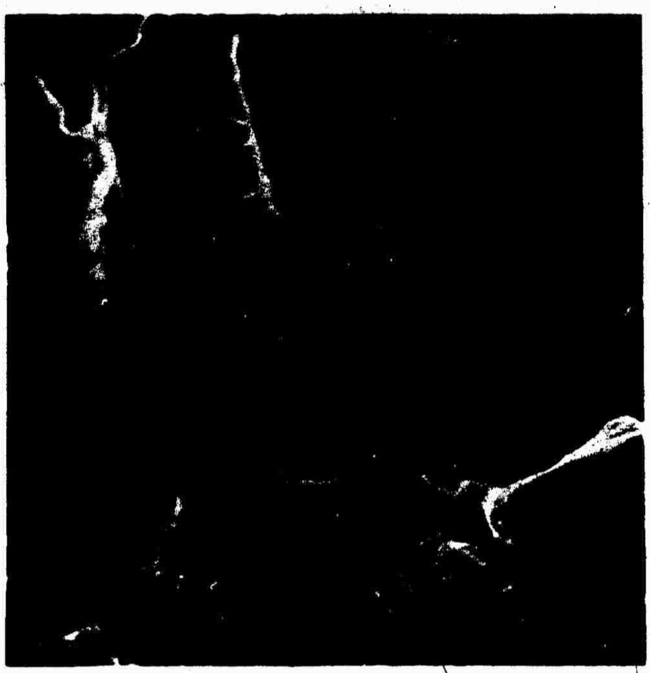

Figure 105. Enlarged View of Area A (P/N 114DS143-1). Magnification 2000X

striations, but the debris damage to the central portion of the spalled area, from balls rolling over entrapped particles, makes this impossible. Figures 106 and 107 show a subsurface crack in area "A" located nearly parallel to the surface of the race. The spalling failure is suspected to have been the result of surface damage of undetermined origin.

The second specimen selected may be seen in Figure 108. This fatigue spall bears the macroscopic characteristics of a classical subsurface initiated failure. The lateral propagation and steep sided fractures of the pit are characteristic of this failure type. Figure 109 is a 50x S.E.M. stereoptican view of the fatigue spall. Use of a suitable stereoptican viewer will enable the reader to gain excellent perspective of the relative steepness of the pit walls. Figure 110 is a photo montage of the entire spall area.

The striking difference between the spalled regions in Figures 103 and 110 can be easily seen. The spalled region in Figure 103 appeared to be fairly characteristic of fatigue spalling, with the major spalling action being approximately parallel to the surface of the bearing race. However, the spalled region in Figure 110 was associated with an exceptionally deep and severe crack that appeared to have propagated normal to the surface of the race. The crack also extended along the axis of the race, i.e., normal to the rolling direction of the race. The crack definitely appears to be related to material defect in the race such as a forging lap, a stringer inclusion, or a pocket of inclusions.

The segment of the crack labeled area "a" in Figure 110 is shown at higher magnifications in Figure 111. Figure 111 indicates that local crevices are formed at the intersection of branching cracks. This may have been the mechanism by which the spalled region was initiated. The surface of the crack is shown more clearly on the right. It appears to have a crystalline appearance similar to that of the vertical secondary cracks in the first bearing specimen. No evidence of massive inclusions was found along this crack; however, evidence of a cluster of inclusions was found in area "b" of Figure 110 and this is shown in Figure 112. These inclusions apparently provided a preferential fracture path in this area. Inclusions of this nature could be associated with either a lap or an inclusion pocket, and this could have been the primary contributing factor to the initiation of the spalling failure.

Area "c" in Figure 110, shown at a higher magnification in Figure 113, had an appearance similar to that of the crevice shown in Figure 111. This area also somewhat resembled an

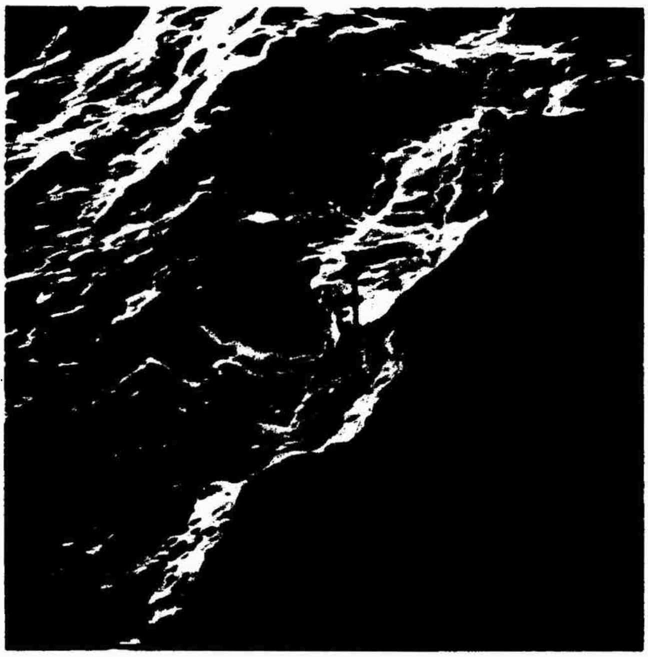

Figure 106. Enlarged View of Area B (P/N 114DS143-1). Magnification 500X

Figure 107. Enlarged View of Area B (P/N 114DS143-1). Magnification 2000X

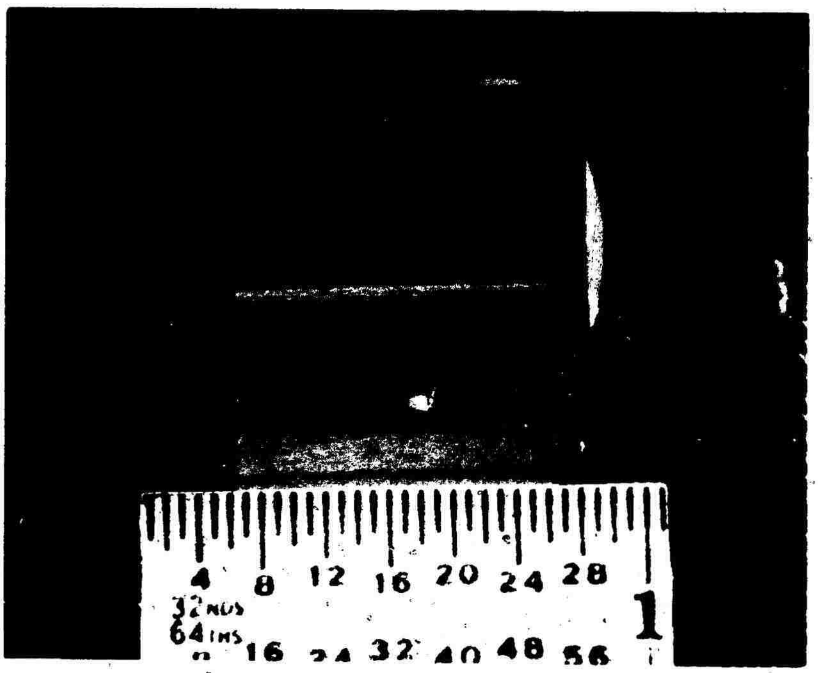

Figure 108. Section From Bearing Outer Ring Showing Fatigue Failure (P/N 114DS242-1).

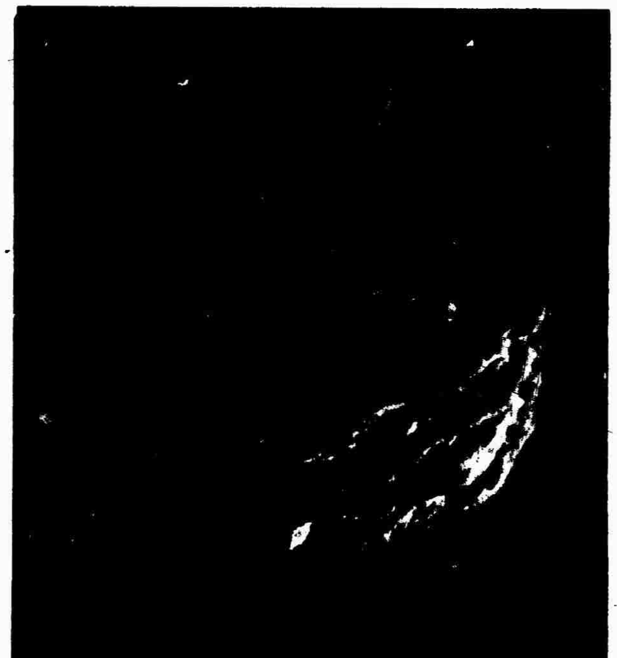

Magnification 50X

(Left)

Magnification 50X

(Right)

Figure 109. Stereoptican View of Fatigue Spall
(P/N 114DS242-1).

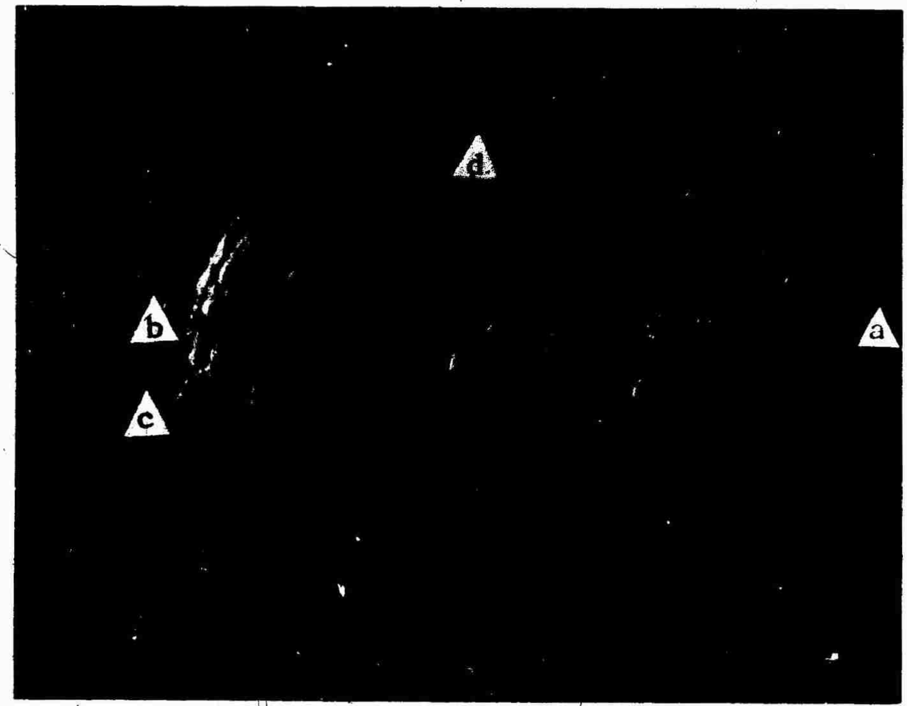

Figure 110. Montage of Fatigue Failure in Bearing Outer Ring (P/N 114DS242-1).
Magnification 50X

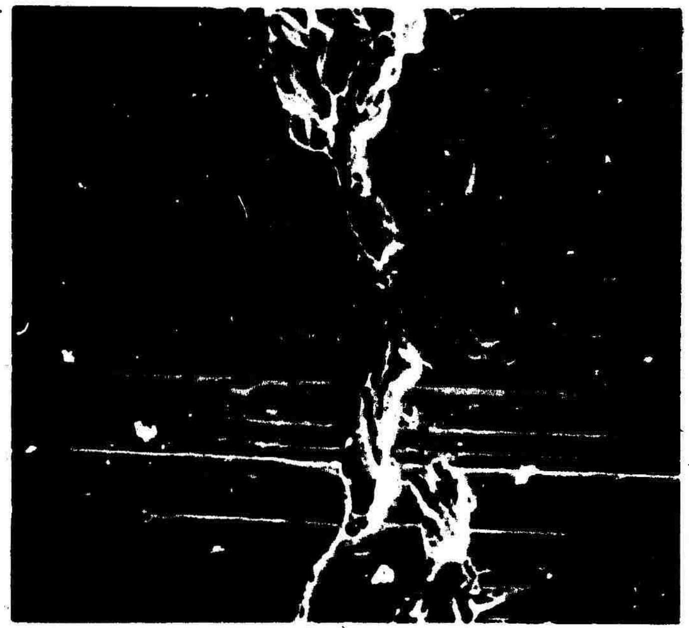

Magnification 500X

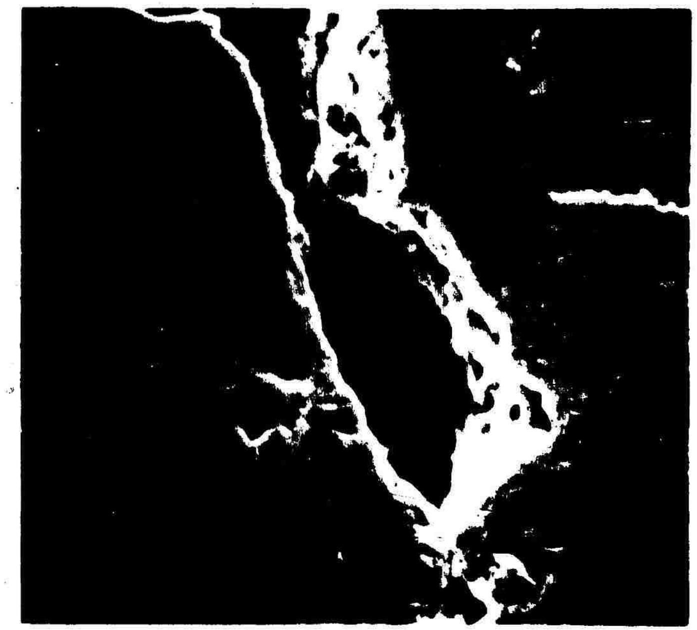

Magnification 2000X

Figure 111. Enlarged View of Area A
(P/N 114DS242-1).

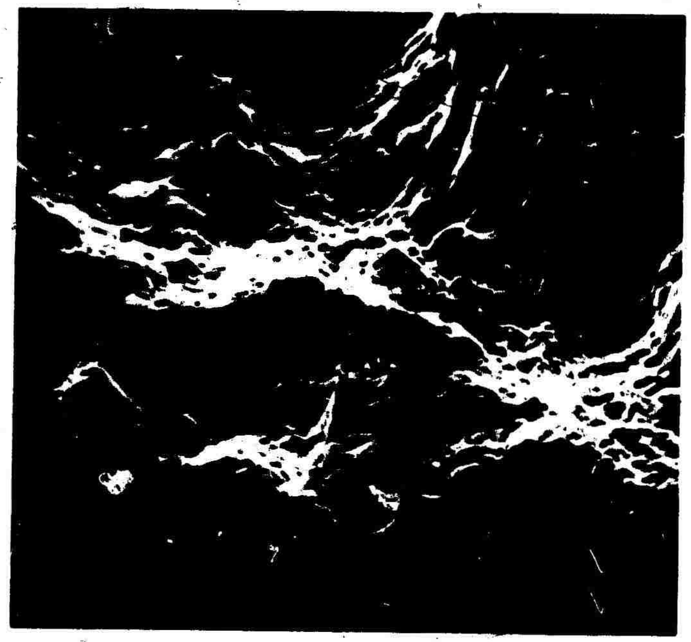

Magnification 500X

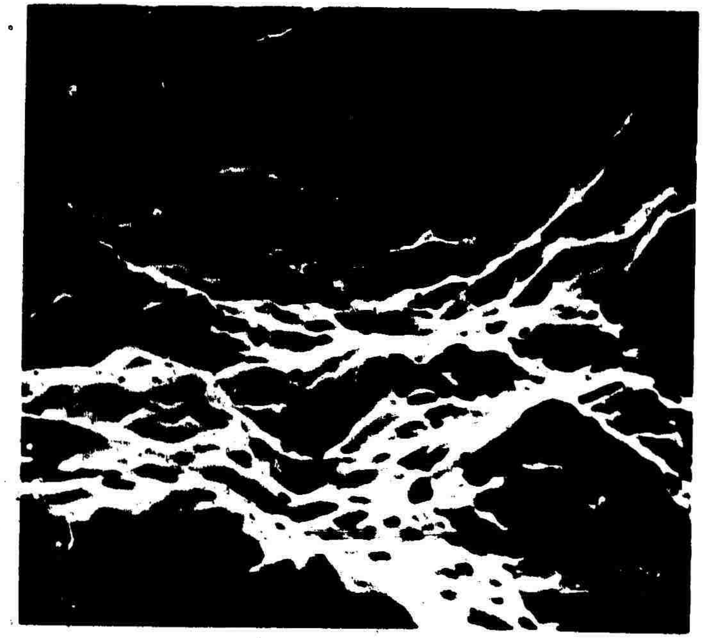

Magnification 2000X

Figure 112. Enlarged View of Area B (P/N 114DS242-1).

Magnification 500X

Figure 113. Enlarged View of Area C
(P/N 114DS242-1).

intergranular fracture. The general absence of the characteristic striations in both Figures 112 and 113 suggests that this particular portion of the spalled region was formed by a different mechanism than the one responsible for the spalling failure in the first specimen. The existence of a subsurface defect, as speculated above, appears to be the most logical explanation for this difference.

The shallow portion of the spalled region of this specimen between the areas "b" and "d" in Figure 110 appeared to be similar to the spalled region in the first specimen. This is seen more clearly in Figure 114, which is from area "d" in Figure 110. Striations approximately parallel to the rolling direction of the race are visible in both figures. The general appearance of the striations suggests that chip movement was toward the severe crack and that the spalled region was propagating away from the crack. This indicates that the spalling failure was initiated either by or at the severe crack.

The general condition of the surface of the race adjacent to the spalled region can be seen in Figures 111 and 114. Figure 115 is from an area adjacent to the spalled region where the most severe surface damage was detected. There was surprisingly little evidence of crack formation in the damaged area as compared with the earlier specimen; this could indicate that this specimen may have been more resistant to crack formation than the earlier specimen.

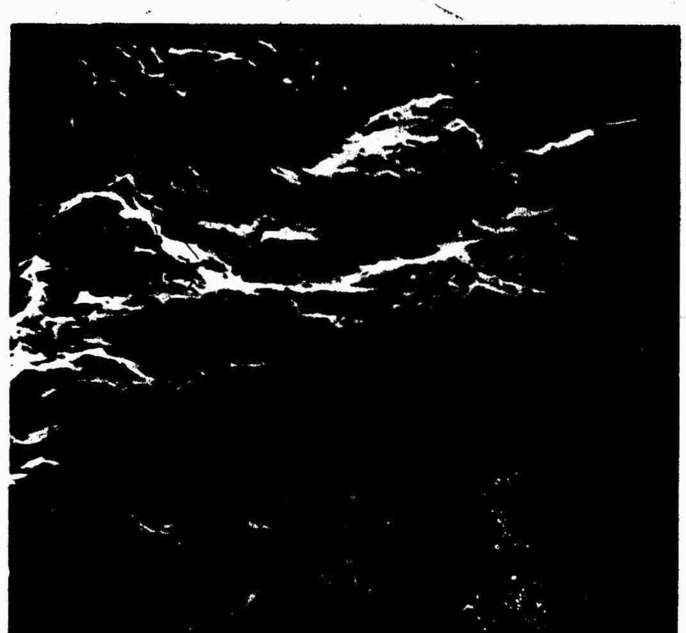

Magnification 500X

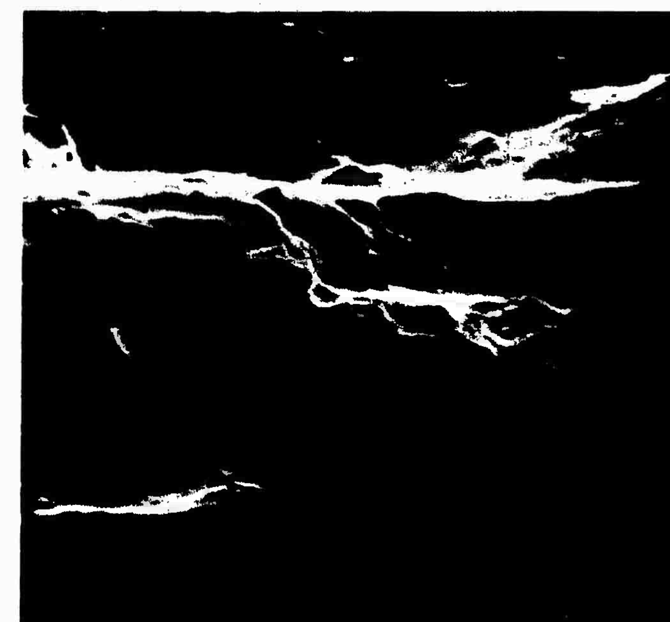

Magnification 2000X

Figure 114. Enlarged View of Area D (P/N 114DS242-1).

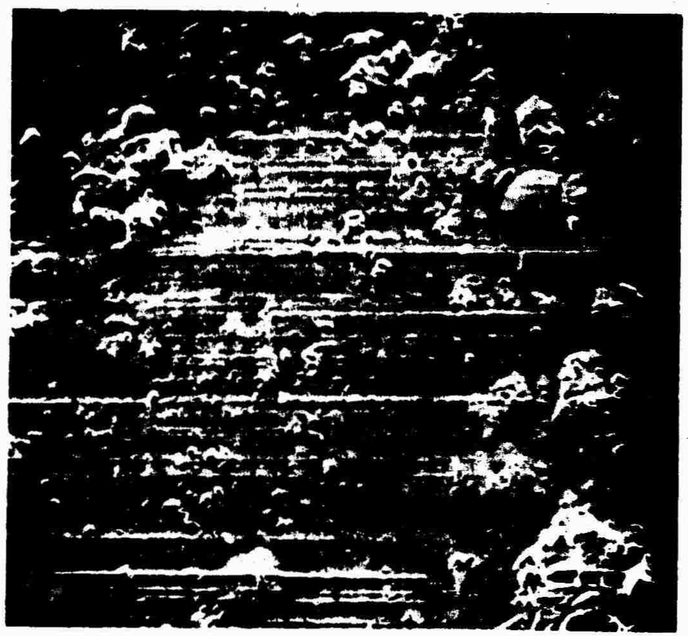

Magnification 500X

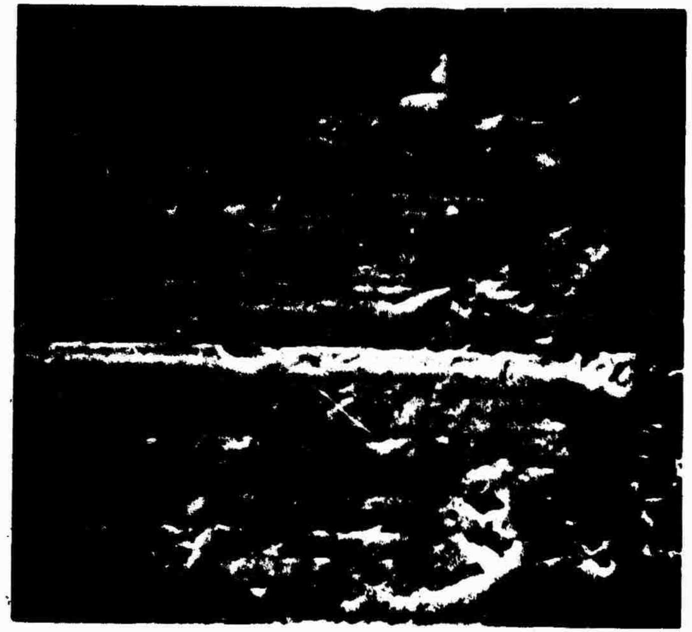

Magnification 2000X

Figure 115. Surface Damage Near the Spalled Region (P/N 114DS242-1).

LUBRICATION REGIME CORRELATION

The lubrication state in the conjunction between two load transmitting elements has been the subject of intensive research in the past decade. It has been thoroughly demonstrated that a state exists between boundary lubrication (where only the adsorbed and monolayer lubricant molecules exist in the conjunction) and full hydrodynamic lubrication (complete separation of the two loaded bodies by a film of lubricant) which has been relatively well understood for many years. This lubricant state has been mathematically defined through the additional consideration of the elastic properties of the metals and lubricant to the formerly treated lubricant viscosity and velocity considerations. Modifications were further made to consider the viscosity of the fluid under very high pressure fields such as exist in Hertzian contacts or conjunctions. The name quite naturally becomes elastohydrodynamics (EHD).

In this section, an attempt will be made to portray the influences of surface finish and topography and lubrication states upon the failure mode of surface contact or compressive loading fatigue.

The hypothesis has been advanced by numerous researchers that the relative frequency and harshness of surface asperity contacts in the loaded conjunction has a pronounced effect upon pitting or spalling endurance of the loaded elements. Tallian, Chiu, and McCool (Reference 10) have presented a method based upon Grubin's equation for EHD film thickness for estimating the lubrication regimes for ball and roller bearings. Their assessment places the effects of lubricant regime into three categories. When the EHD film is 3 to 4 times greater than the composite surface roughness, bearing life greater than AFBMA calculated is predicted. When it is transitional, i.e., on the order of 1 to 2, an area of possible surface distress tantamount to failure exists. Below a ratio of 1, definite surface distress, and life below that calculated, is predicted. Table XIII presents the complete tabulation of film thicknesses for all bearings in this study as calculated by the methods of Reference 10. The values range from 4×10^{-6} to 90×10^{-6} inches. An average value for surface roughness in ball bearings was found to be 4AA for the balls and 6AA for the inner races. The combined roughness number is then $(4^2 + 6^2)^{.5}$ or 7.2. Clearly by these predictions calculated life should be exceeded by actual life for all such bearings above a predicted film thickness of 22×10^{-6} inches. However, the two high failure rate UH-1 bearings have predicted films of 23×10^{-6} inches and 33×10^{-6} inches, and the two high failure rate CH-47 bearings have values of 4×10^{-6} and 58×10^{-6} inches. It is

strongly suspected that this equation may not adequately predict minimum films, since the effects of temperature rise in sliding contact are ignored and the coefficients of friction used seem not in line with recent findings concerning horseshoe constrictions at the rear of the contact in circular or elliptical contacts. In the case of the 114DS240 roller bearing (film thickness of 58 x 10^{-6} inches) with its 17.5 failure rate, it was found that surface finish of the inner rings varied enormously. Figure 116 clearly shows the magnitude of the variance on three rings removed from service. Proficorder charts were made of these three races and are presented in Figure 117. On the left may be seen the as-furnished finish and on the right can be seen the finish refinement due to run-in as found in the roller wear track. This figure clearly shows peak to valley distances on the order of 100 x 10^{-6} inches. An equivalent profilometer AA value would be at least 18 and perhaps 25 x 10^{-6} inches. A reduced finish number for this bearing with rollers at 5AA would be $(25^2+5^2)^{.5}$ or 25.5, which is into the transition lubrication range.

The CH-47 bearing with the 4 x 10^{-6}-inch film thickness had the highest failure rate. However, it is known that for identical applications, where essentially boundary lubrication exists, B_{10} life increases on the order of 40 times (relative to AFBMA predictions) have been experienced through type of material and cleanliness changes alone.

One last case in point is worthy of examination. The 204-040-725 roller bearings used in the upper and lower planetary assemblies of the Bell transmission are further examples of inadequately predicted B_{10} life. The life calculated for the upper planet bearings is 531 hours under conditions of 100% power and equal load sharing among the 8-planet idler pinions. At a mean spectrum load of 75%, the B_{10} life is 1260 hours. The operating conditions are: marginal lubrication, high load, and low speed. The predicted film thickness is but 5 x 10^{-6} inches. The inner ring and rollers are made of vacuum melt 52100 steel, and the outer ring is made of case carburized AMS6265 steel. No fatigue failures were experienced on any of the planet bearings in the 173 Bell transmissions reviewed at overhaul. A possible explanation would be an unreasonable assessment of mean spectrum load; however, regenerative testing of this planetary assembly at BHC verifies the high life exhibited through field experience. The load conditions in the BHC regenerative test stand were very closely controlled and monitored.

The answer again lies in the area of surface finish control. The very accurate inner races are ground, honed, and lap

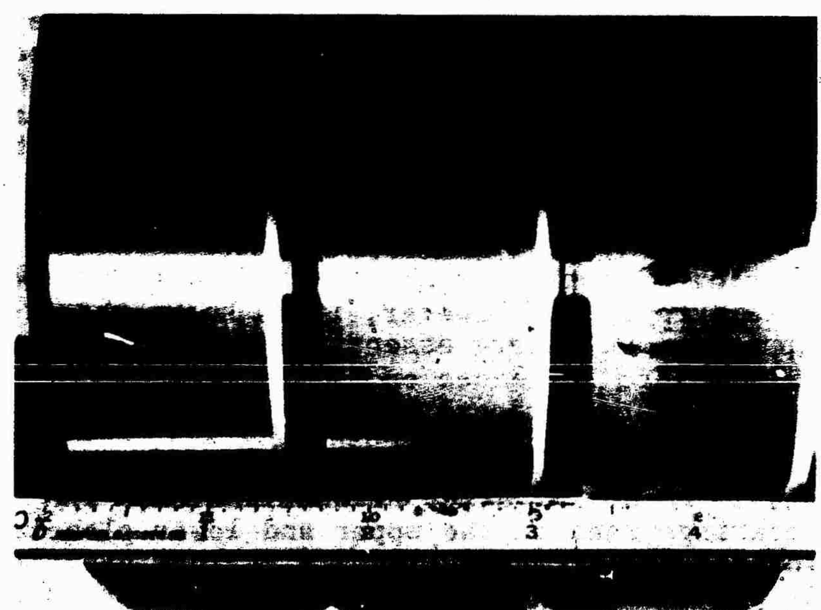

Figure 116. Variation in Surface Finish on Roller Bearing Inner Rings (P/N 114D3240-2).

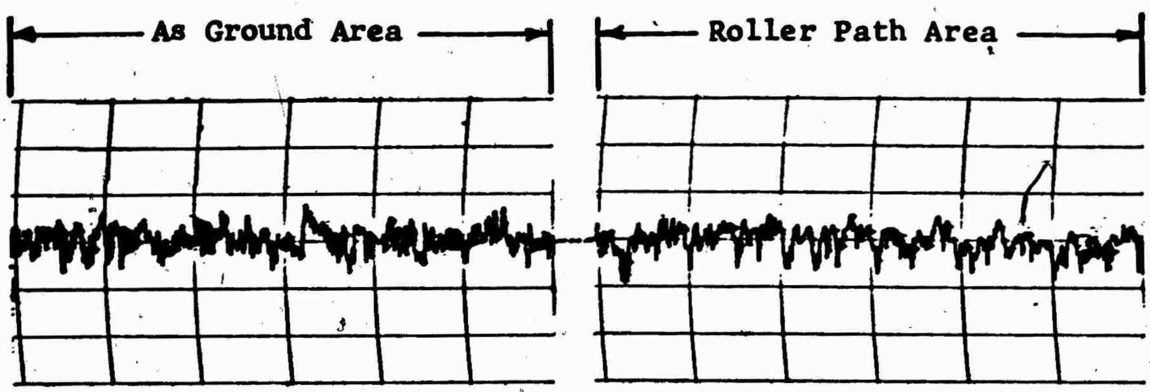

(A) A003B01

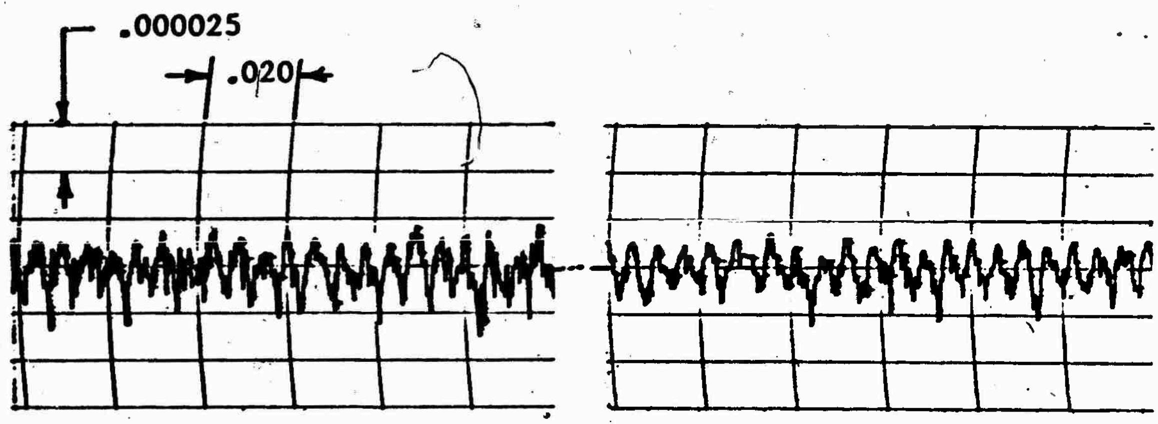

(B) A025B01

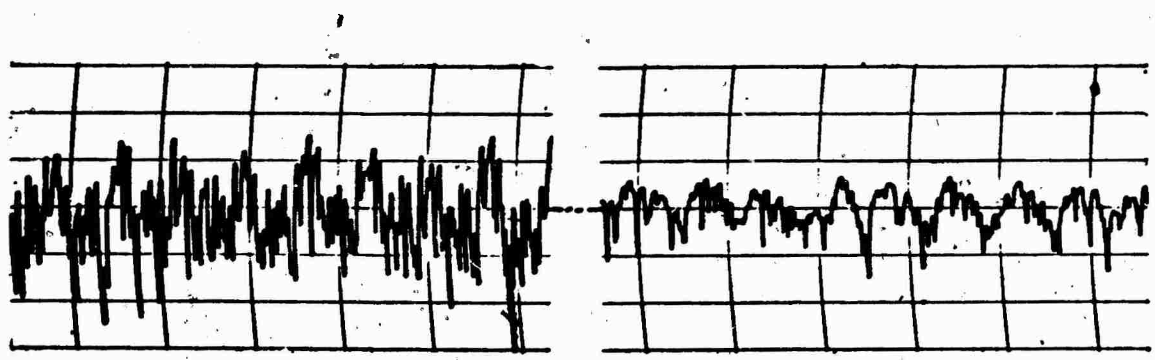

(C) A023B03

Figure 117. Raceway Surface Finish
(P/N 114DS240 Bearing).

polished to a 2 to 3AA finish level and black oxide coated. The rollers are also polished to a 3AA level. The combined roughness number is about 4. Although the critical ratio is in the 1 to 2 transitional zone (as defined on page 172), the excellent results seem to suggest that surface roughness may play a role of more significance than the linear proportionality suggested. This part was failure prone in its initial development testing a decade ago. The vacuum melted materials, refined surface finishes, and black oxide treatment were curative measures instigated at that time. They were extremely successful. Hence, it appears reasonable to conclude that film thickness calculations are a valuable design aid in the sense of warning of increased risk and the need for corrective action. It also seems that much work is needed in the area of elliptical contact film thickness predictions with higher sliding velocities such as found in angular contact ball thrust bearings.

A similar condition appears to exist in gear applications. The tabulation of design data for the gears considered in this study given in Table XII includes EHD film thickness predictions. The ninth column lists, first, a value obtained by a method employed at BHC based upon basic work attributable to Crook (Reference 20), Christensen (Reference 9), and Dyson (Reference 8), and secondly, a film thickness value as calculated using the isothermal Dowson equation (Reference 4). Figure 118 shows the relative values predicted by these methods. The higher values shown agree more closely with visual observations on ground gears of 16AA roughness in that no black oxide removal can be observed when the predicted film thickness reaches a value of 18 x 10^{-6} inches. The corresponding number by Dowson is 12 x 10^{-6} inches.

A further comparison of the two methods is shown in Figure 119. This depicts the predicted values of film thickness from first point to last point of contact for a gear pair in mesh. The upper curve takes into account the effect of friction value at the various points as influenced by sliding velocity in the mesh and its secondary effect upon the temperature and hence viscosity of the lubricant.

The Dowson equation (represented by the lower curve) is widely accepted and has the additional appeal of relative simplicity. The apparent disparity in estimated film thickness and real life observations may not be too serious. One of the most important variables in all EHD equations is the pressure viscosity coefficient (α). See Appendix III for its usage. This quantity is known with little precision and is generally estimated based upon measurements made in 1952 on fluids which were ancestral with regard to today's synthetic lubricants. The range of predictions seems believable with the use of scaling factors.

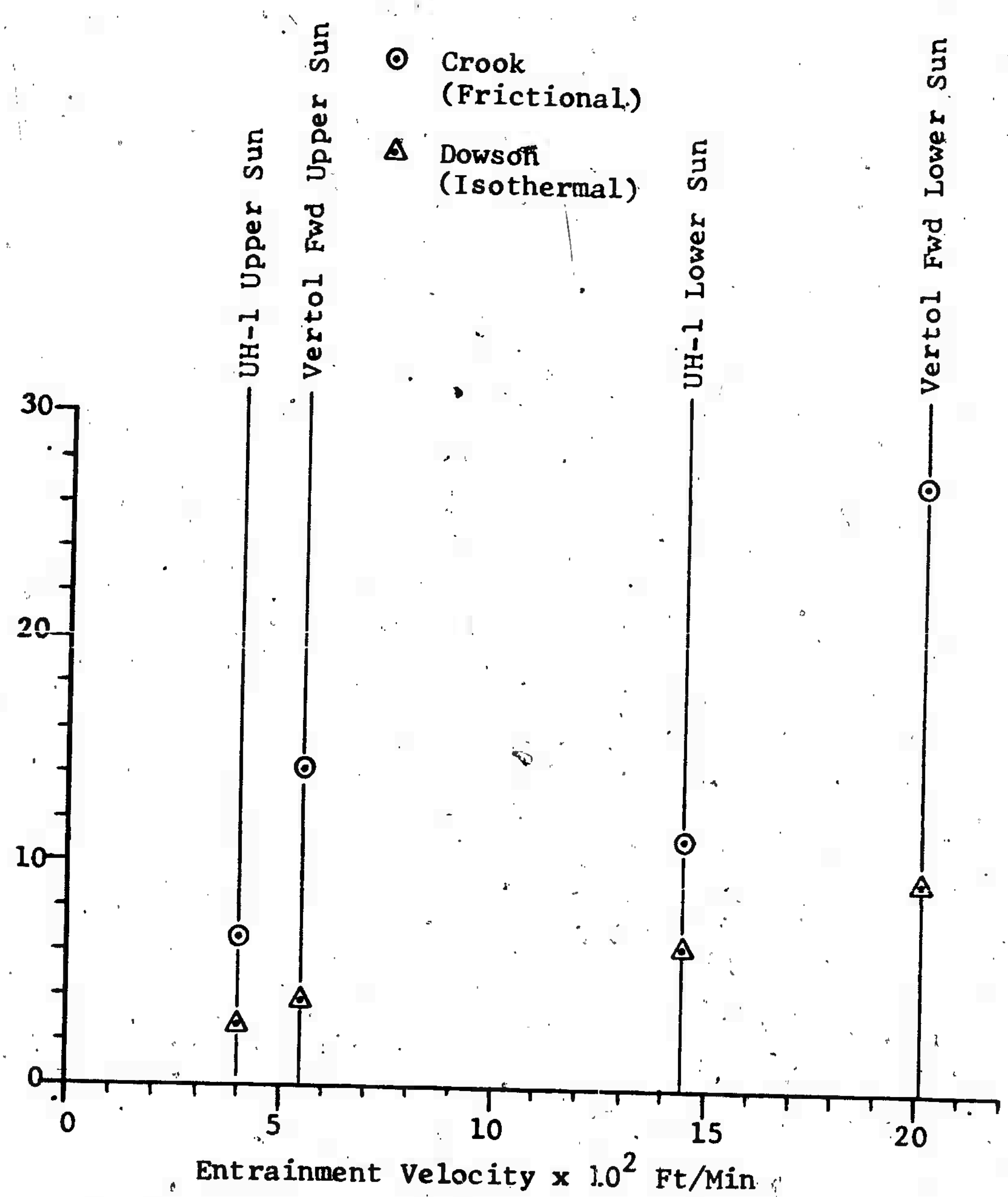

Figure 118. Comparative Film Thickness Predictions, Frictional and Isothermal.

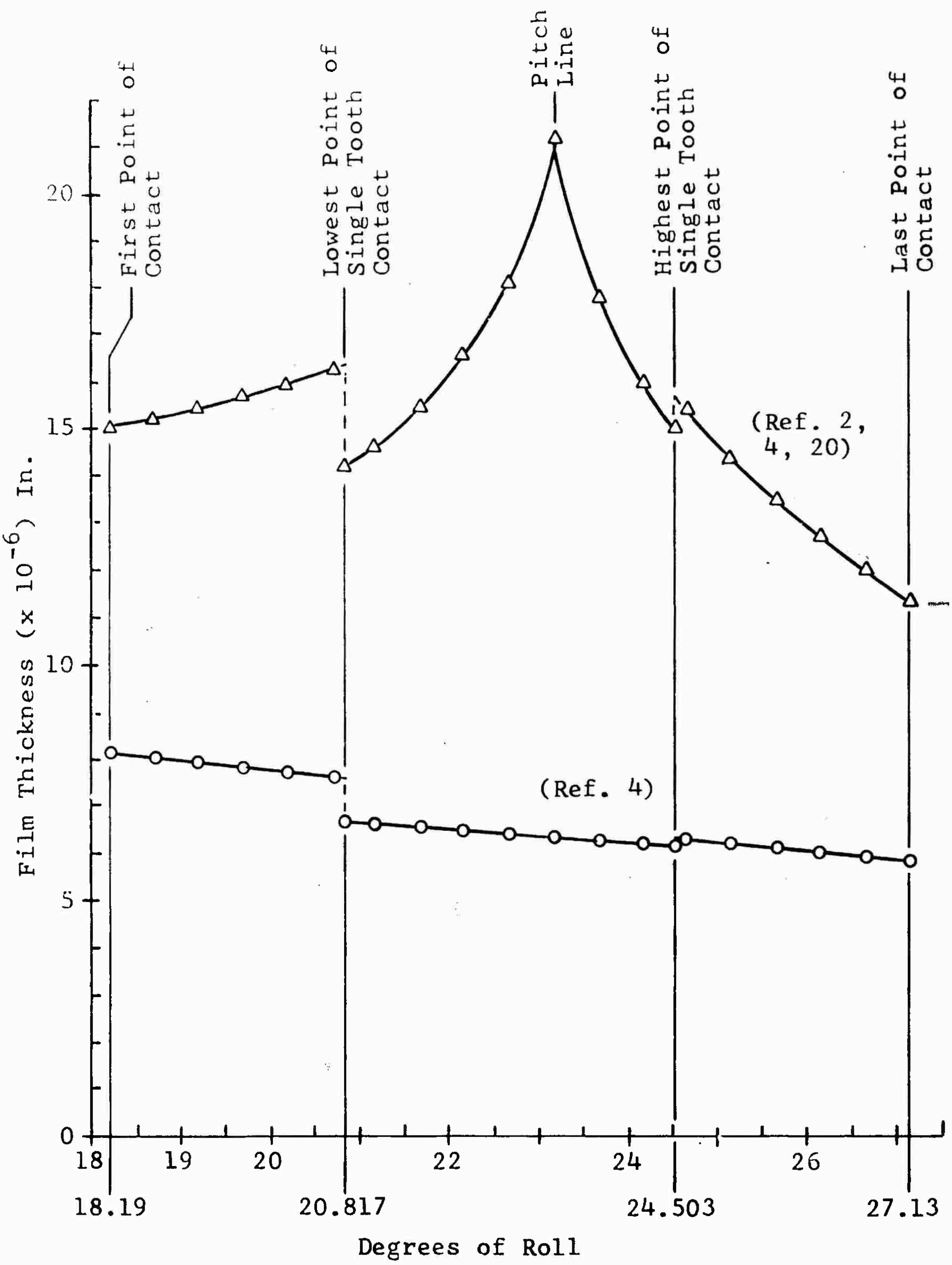

Figure 119. Variation in EHD Film Thickness vs Roll Angle 204-040-329 Driving 204-040-108 (MIL-L-7808).

For whichever method attempted, it is observed that the 204-040-330-3 sun gear (whose failure mode could not be predicted by conventional analyses) exhibits the lowest EHD film thickness. The next lowest (CH-47 upper sun gear) has a 40% thicker film by Dowson and a 100% increase by BHC. Since the surface initiated pitting mode was observed only on the UH-1 upper sun, it follows that a critical difference in lubricant states existed.

Since the 204-040-330-3 upper sun gear exhibited such a high failure rate and in view of the intimate association of lubrication to surface spalling or pitting, comprehensive examination of this surface-initiated pitting or spalling failure mode is made to assist in its understanding. A 204-040-330-3 sun gear with a typical surface failure may be seen in Figure 120.

The pitting failure is evident in the left-hand portion of the tooth. Immediately above the pit is an area of extreme wear. The shape of the wear area reveals a misalignment condition. Tests indicate this misalignment to be .001 inch/inch. In thicker film lubrication states, it is questionable whether its presence could be observed. Note also the asperity contacts as indicated by the black oxide removal from the ground surface prominances. Figure 121 is a 50x enlargement of this pit. Reference to the lettered areas of this pit are made for purposes of proper orientation in studying the surface topography mappings presented in Figure 122. Charts (A) and (B) of Figure 122 were made in the profile or sliding direction on the ground gear. The curvature of the gear tooth was removed from these charts by use of the specially constructed apparatus shown diagramatically in Figure 123. Chart (A) records the as-ground texture of the gear since it was taken out of the wear area on the left of Figure 120. Chart (B) records the wear area texture from a zone immediately to the right of the pit shown in Figure 120. Note here the smoothing or wear in the zone above the T.I.F. diameter, the virtually unchanged area at the rolling contact zone at the pitch line, and the destructive wear and surface rippling which has occurred near the O.D. in the zone of heavy visual wear in Figure 120.

Further enlightenment is offered in Chart (C), taken in the lead direction directly through the pit. The suggested topography is then a series of long but thin mounds oriented with their long axis in the lead or grinding direction. (Chart (D) is a short segment of a bearing inner race included to show the similarity of texture.) Figure 124 is a stereoptican view of the pit area. Use of a suitable stereoptican viewer will reveal, with full depth perception, the nature of these grinding lines or furrows.

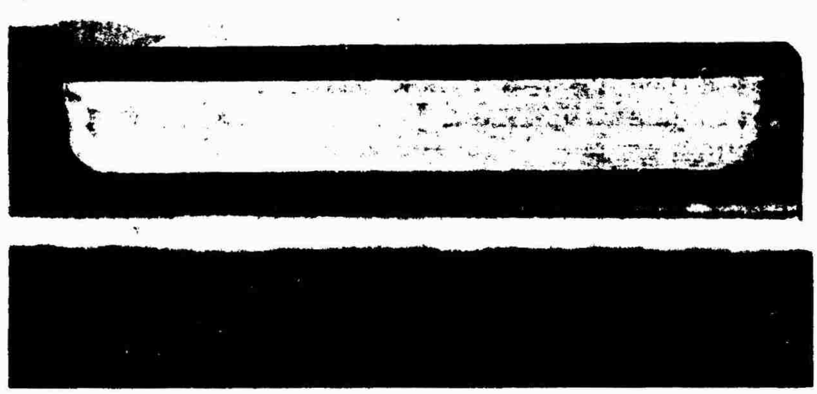

Figure 120. Surface Initiated Spalling Failure on Gear Tooth (P/N 204-040-330-3) Magnification 3X.

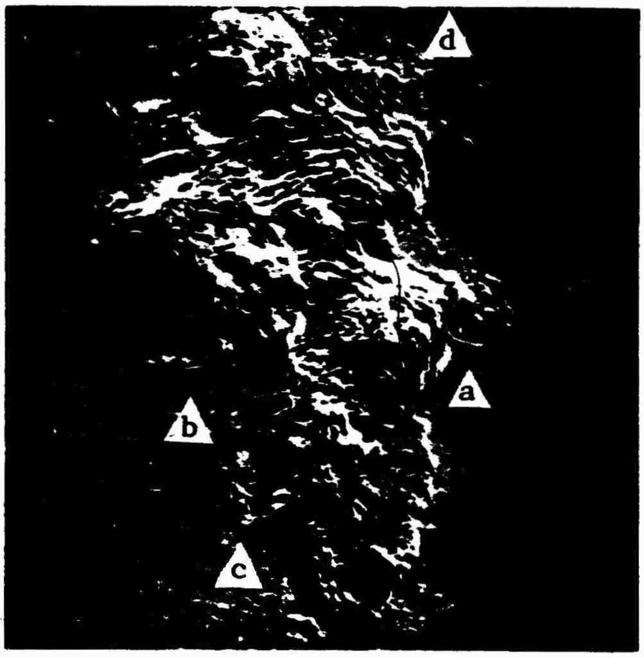

Figure 121. Enlarged View of Spalled Area
(P/N 204-040-330-3) Magnification 50X.

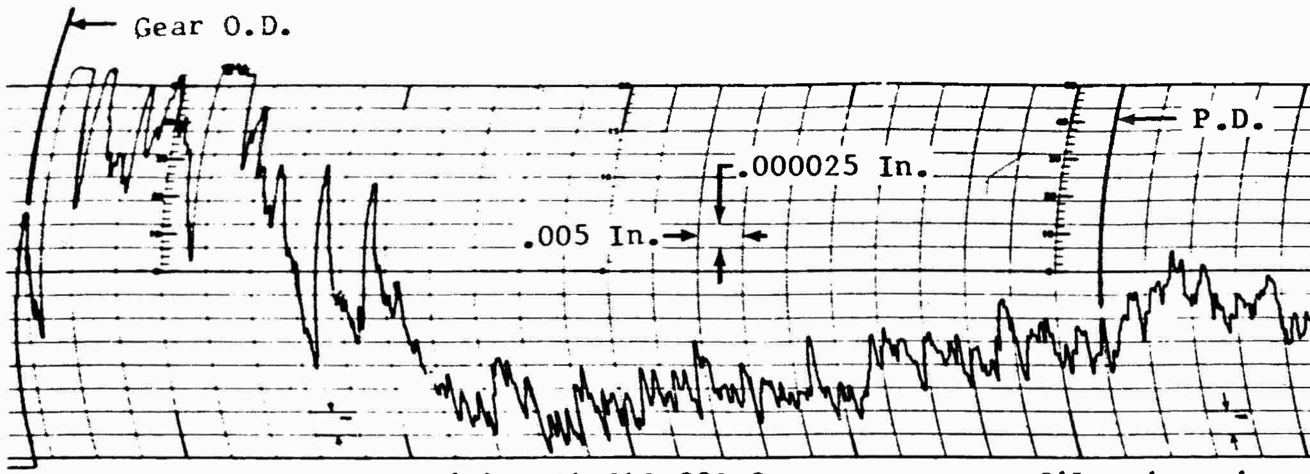

(A) 204-040-330-3 Sun Gear - Profile Direction -

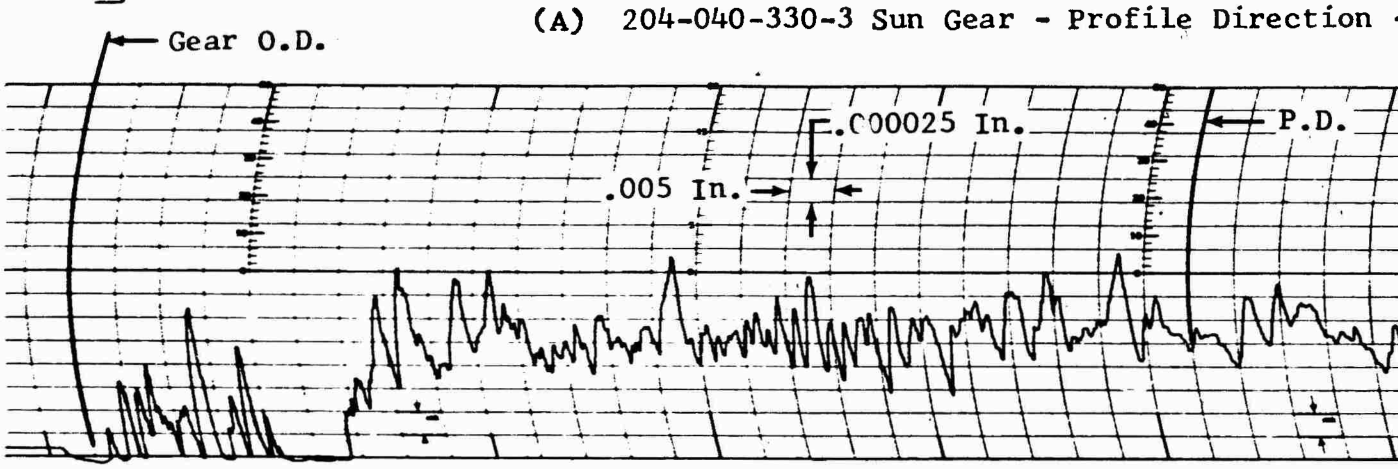

(B) 204-040-330-3 Sun Gear - Profile Direction -

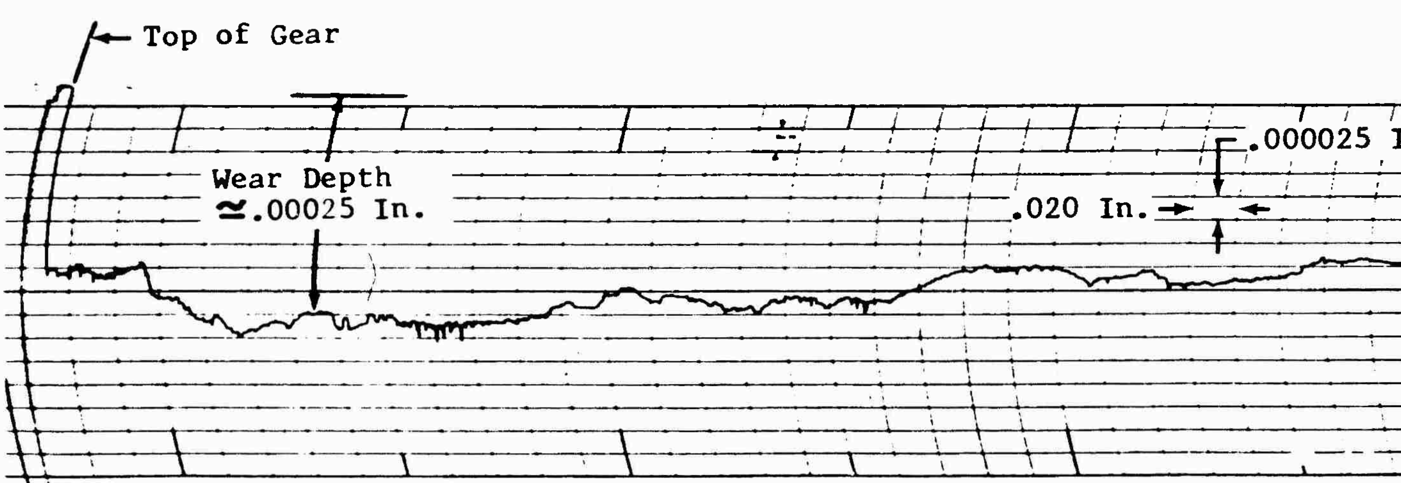

(C)

Figure 122. Surface Topography - Ground Gears and Bearings.

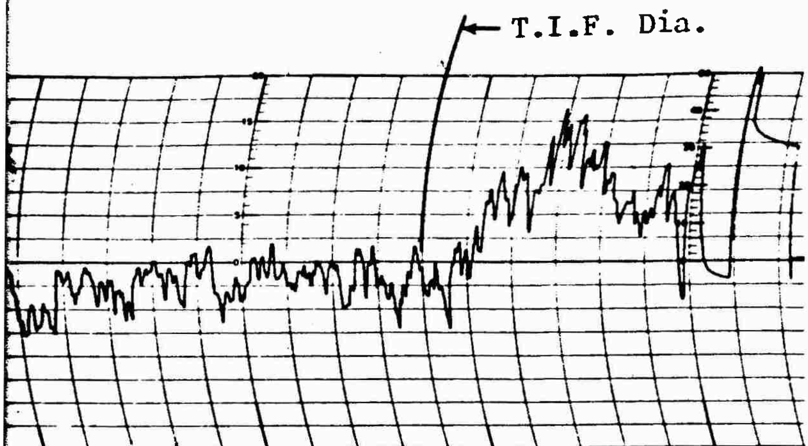

n - As Ground Area G

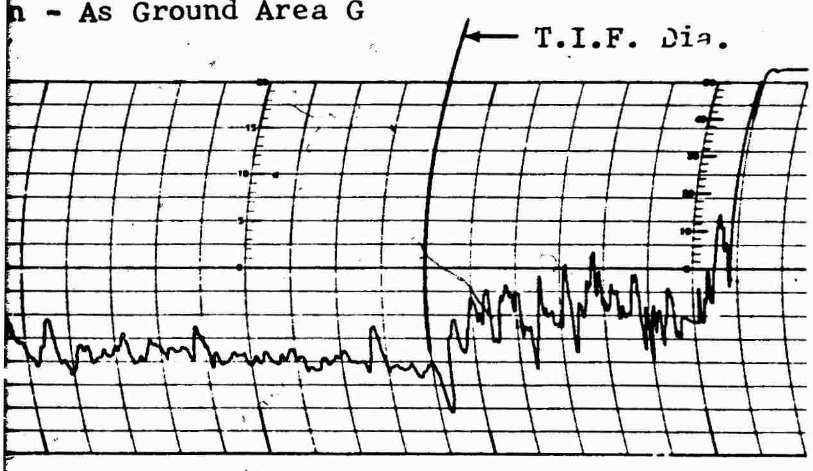

n - Wear Area W

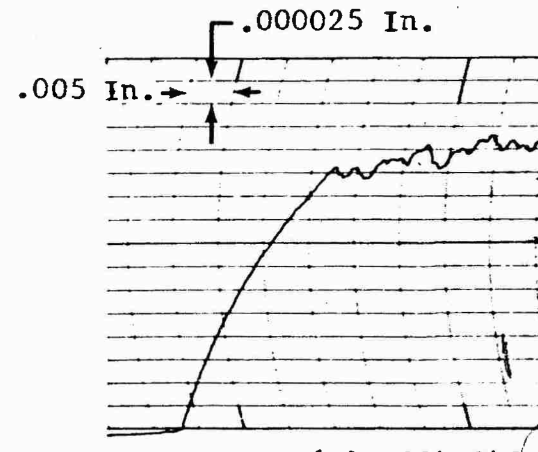

(D) 204-040-

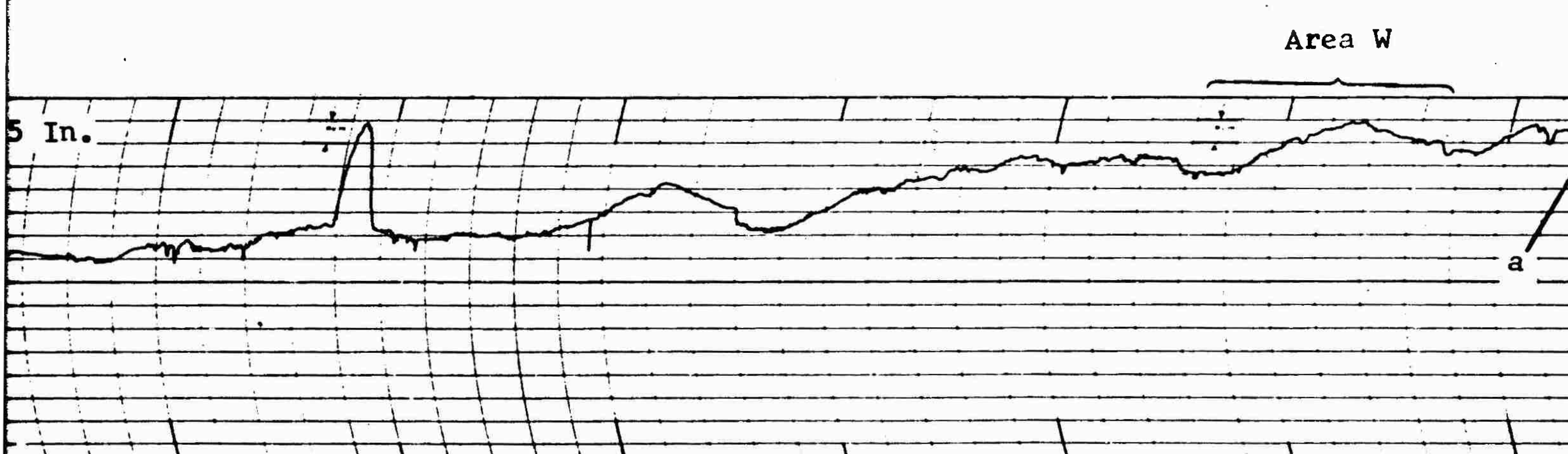

(C) 204-040-330-3 Sun Gear - Lead Direction

Dia.

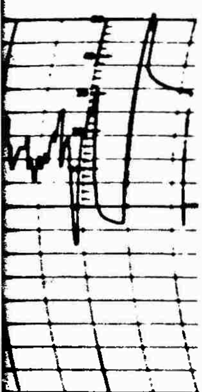

. Dia.

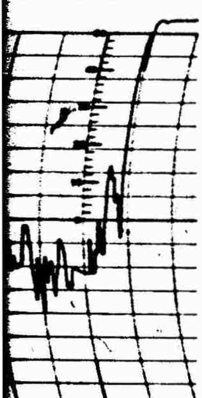

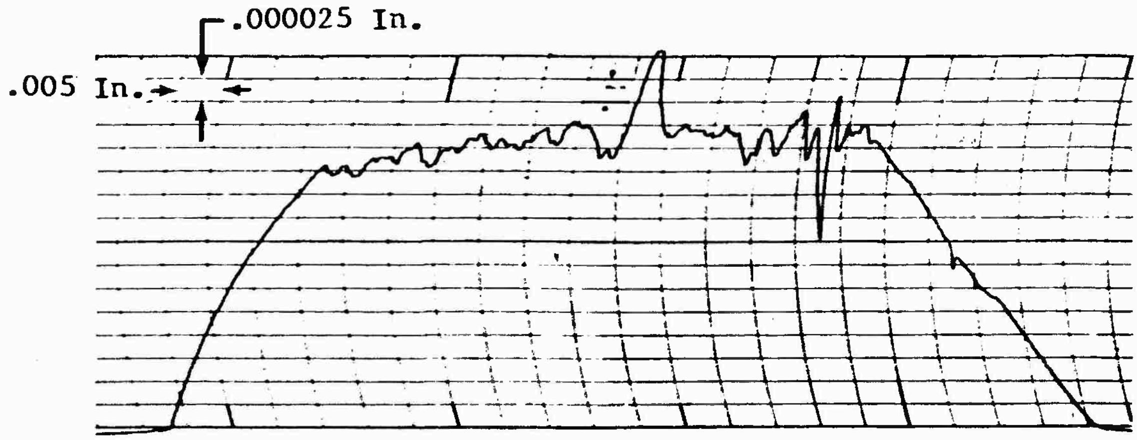

(D) 204-040-345-7 Bearing Inner Race

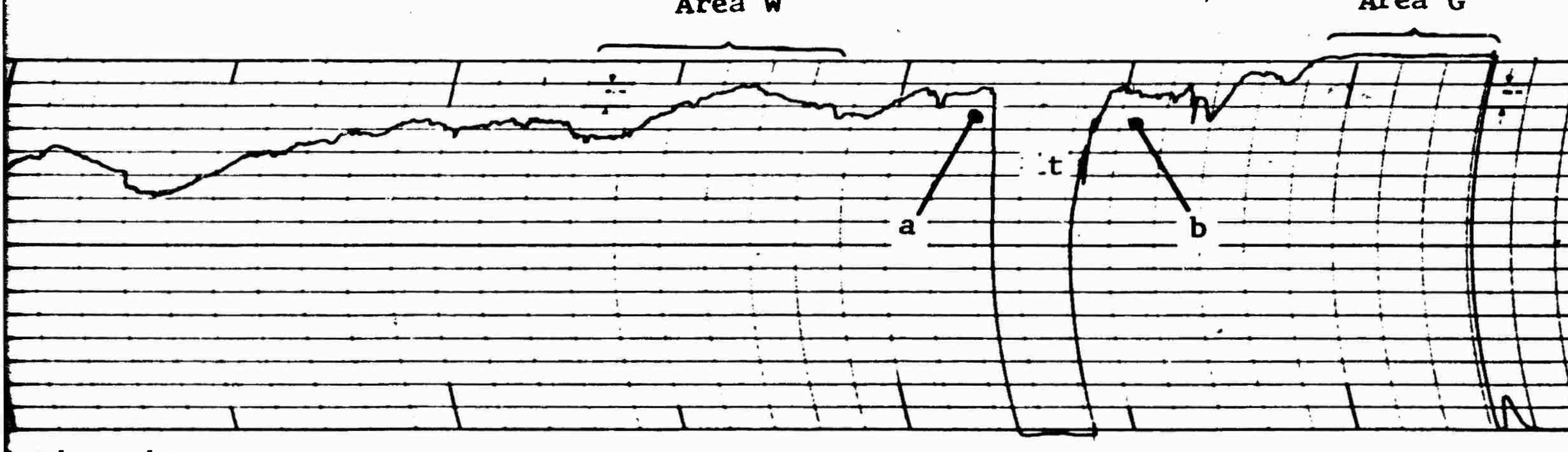

Direction

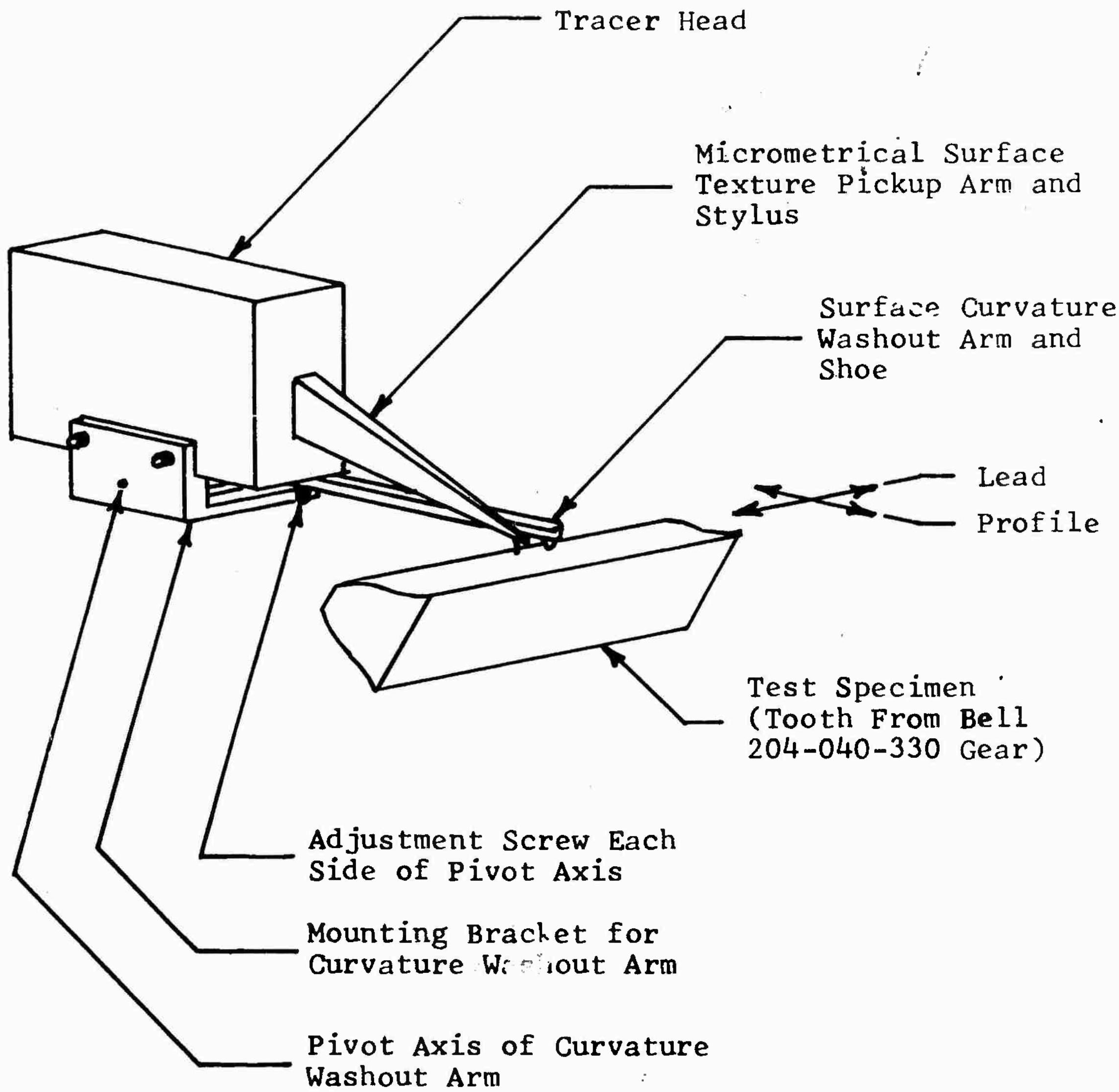

Figure 123. Surface Topography Measurement Technique.

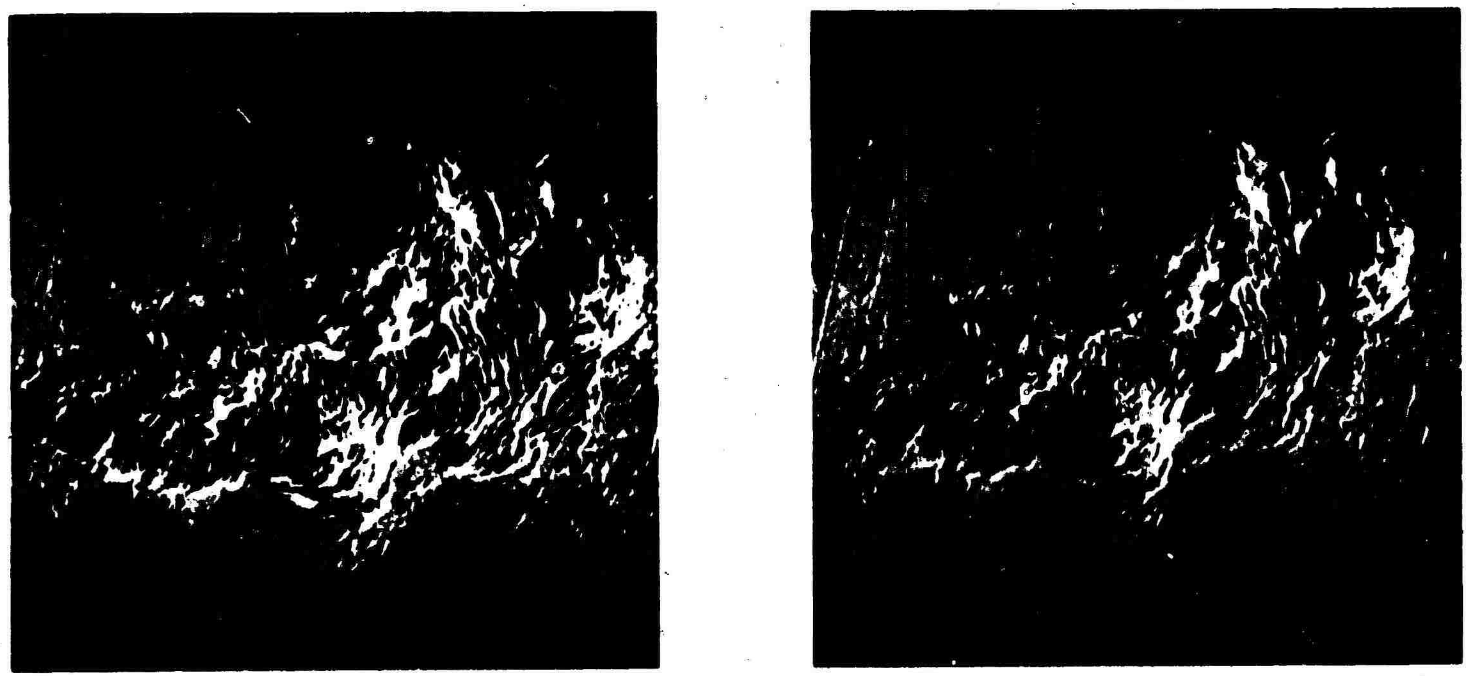

Magnification 50X

(Left)

Magnification 50X

(Right)

Figure 124. Stereoptican View of Surface Initiated Spalling (P/N 204-040-330-3).

Further examination of the nature of the pit and surrounding surfaces was done with the aid of a scanning electron microscope at Battelle Memorial Institute (Reference 24).

The spalled region shown in Figure 121 is shown enlarged in Figure 125; it shows nearly parallel facets that are oriented approximately normal to the rolling or rubbing direction of the mating gears. The facets are sloped toward the top of the gear tooth.

Chip formation at the edge of the spalled region in Area A is shown at higher magnification on the right. Striations were found on the edges of the chips where the secondary cracks had propagated, and some of these striations can be seen. The appearance of the striations indicates that the preceding chip moved upward as it separated from the edge of the spalled region as if it had adhered to the mating gear tooth. A relatively high density of subsurface cracks is shown at the edge of the spalled region.

The faceted nature of the spalled region in Area B is shown at higher magnifications in Figure 126. This figure shows the characteristic striations on the surfaces of the individual facets. The striations are approximately parallel to the rolling or rubbing direction of the gear teeth. The appearance of the striae, particularly on the right, suggests that the relative motion of the chips was from right to left in the figures or from the tip toward the pitch line of the gear tooth. This, plus the inclination of all of the facets toward the top of the gear tooth is believed to indicate that the spalled region initiated in the vicinity of the pitch line and propagated toward the tip of the tooth. It also shows small secondary cracks on the surfaces of the facets. These cracks were usually normal to the striations.

Small individual spalled areas that appeared to be in the process of linking up with the main spalled region in Area C of Figure 121 are shown in Figure 127. The surfaces of these small spalled areas appeared to be inclined at approximately the same angle as the facets, but the characteristic striations were not visible in these areas. This is believed to indicate that the mechanism of lateral propagation of the spalled region may not have been by the same mechanism that formed the facets. The facets were generally not well developed at the edges of the spalled region, as can be seen in Figure 125. The same condition can be seen to persist on the right of Figure 127, which is also from Area C. The facets appear to extend up to, and perhaps slightly under, the chip that is about to become separated, but they clearly do not extend to the edge of the spalled region in the upper portion. This again

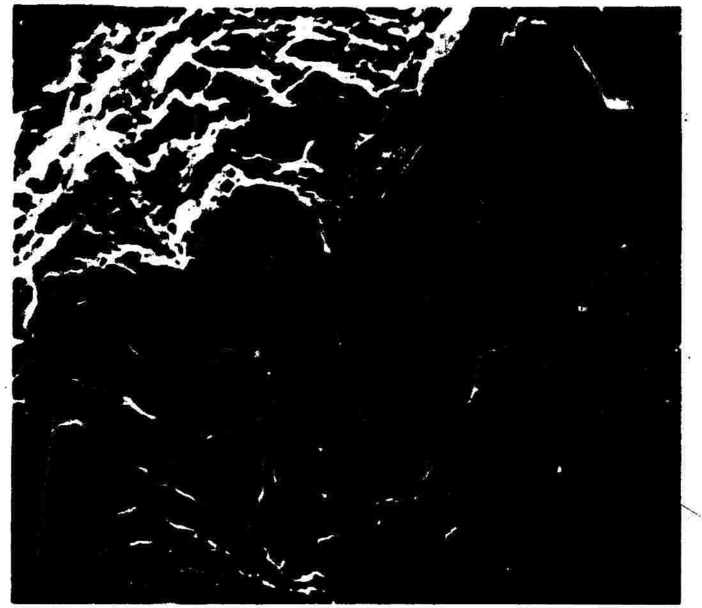

Magnification 200X

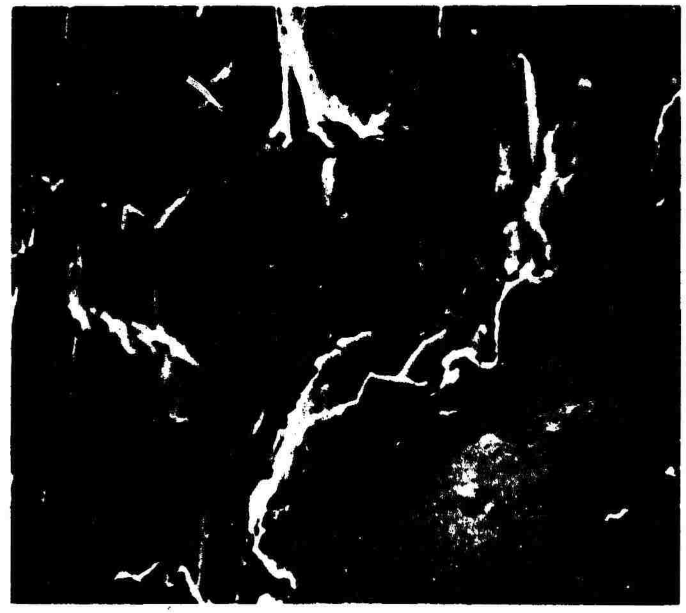

Magnification 1000X

Figure 125. Enlarged Views of Area A (P/N 204-040-330-3).

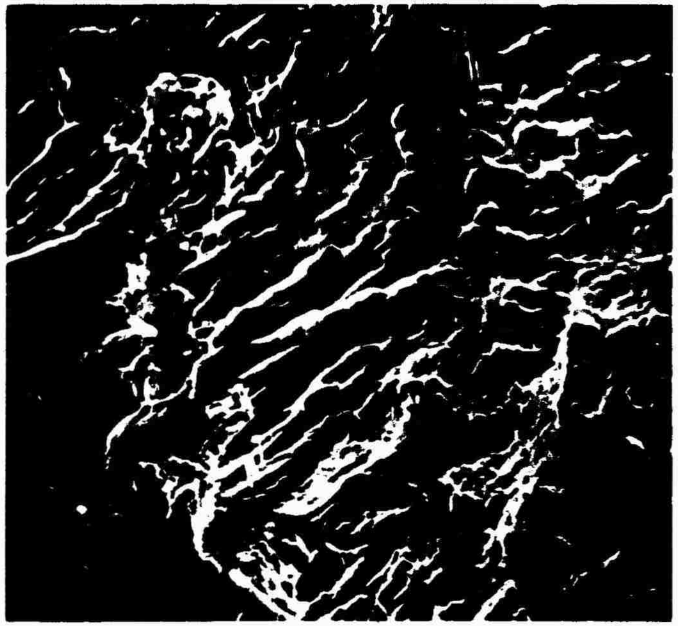

Magnification 200X.

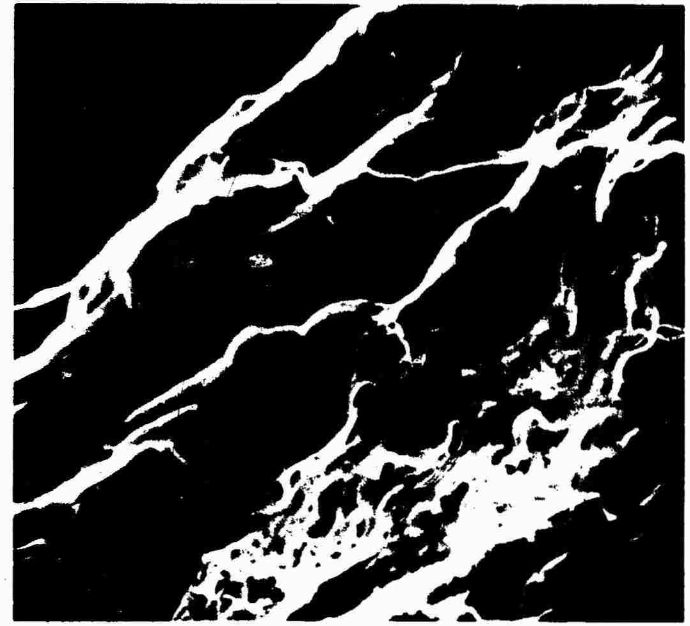

Magnification 1000X

Figure 126. Enlarged Views of Area B (P/N 204-040-330-3).

Magnification 1000X

Magnification 1000X

Figure 127. Enlarged Views of Area C (P/N 204-040-330-3).

suggests that two slightly different mechanisms are operating to cause the spalling. Therefore, formation of facets does not appear to be associated with lateral growth, but it does appear to be associated with an increase in the depth of the spalled region.

Striations on the facets in Area C of Figure 121 are shown more clearly in Figure 128. As before, the appearance of the striae in this area is believed to indicate that the relative movement of the chips was downward toward the pitch line (to the left in Figure 128), and that the spalled region propagated from an undetermined origin near the pitch line. The area shown in Figure 128 left was rotated approximately 120° counter-clockwise in Figure 128 right to obtain a better view of the sides of the facets. A small contamination particle is indicated by arrows in both figures to indicate the relative orientations of both figures. The facets were at an angle of approximately 45° to the surface of the gear tooth. The absence of striations on the vertical faces of the facets can be seen on the right, and these faces have a somewhat crystalline appearance. This suggests that the separation of chips was by formation of a small flat chip by propagation of a subsurface crack that then fractured away from the parent material by the formation of secondary cracks between the subsurface crack and the surface of the gear tooth. Although this mechanism is obviously a fracture process, the appearance of the resulting surfaces does not correspond with any of the common fracture morphologies, and the mode of fracture cannot be identified. It appears to be unique to rolling-sliding fatigue fractures. The tip of the gear teeth showed considerable evidence of abrasion. This abrasion can be seen in Area D of Figure 121 and is shown at higher magnification in Figure 129. Extensive cracks can also be seen in this area. The cracks were nearly parallel to the tip of the gear tooth; this suggests that the tensile component induced by the dragging force was a significant factor in the formation of these cracks.

A serious pitting condition was found to be associated with grinding marks across the gear tooth, and examples of the pitting are shown in Figure 130. The small angular pits occurred in relatively high densities along the grinding marks. Cracking was frequently found to be associated with the pits in areas adjacent to the spalled region, and several of the cracks radiating from the spalled region appeared to follow the grinding marks as can be seen in Figure 120. Harsh dragging contacts of these grinding asperities are suggested as initiating these fissures through tensile rupture. Hydraulic propagation of these pits when they occur near the pitch line seems plausible.

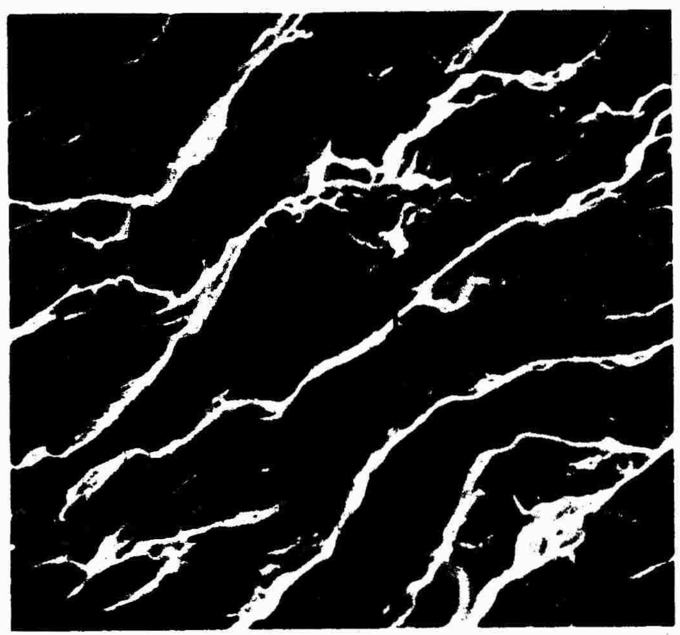

Magnification 1000X

Magnification 1000X

Figure 128. Enlarged Views of Area C (P/N 204-040-330-3).

Magnification 200X

Figure 129. Enlarged View of Area D
(P/N 204-040-330-3).

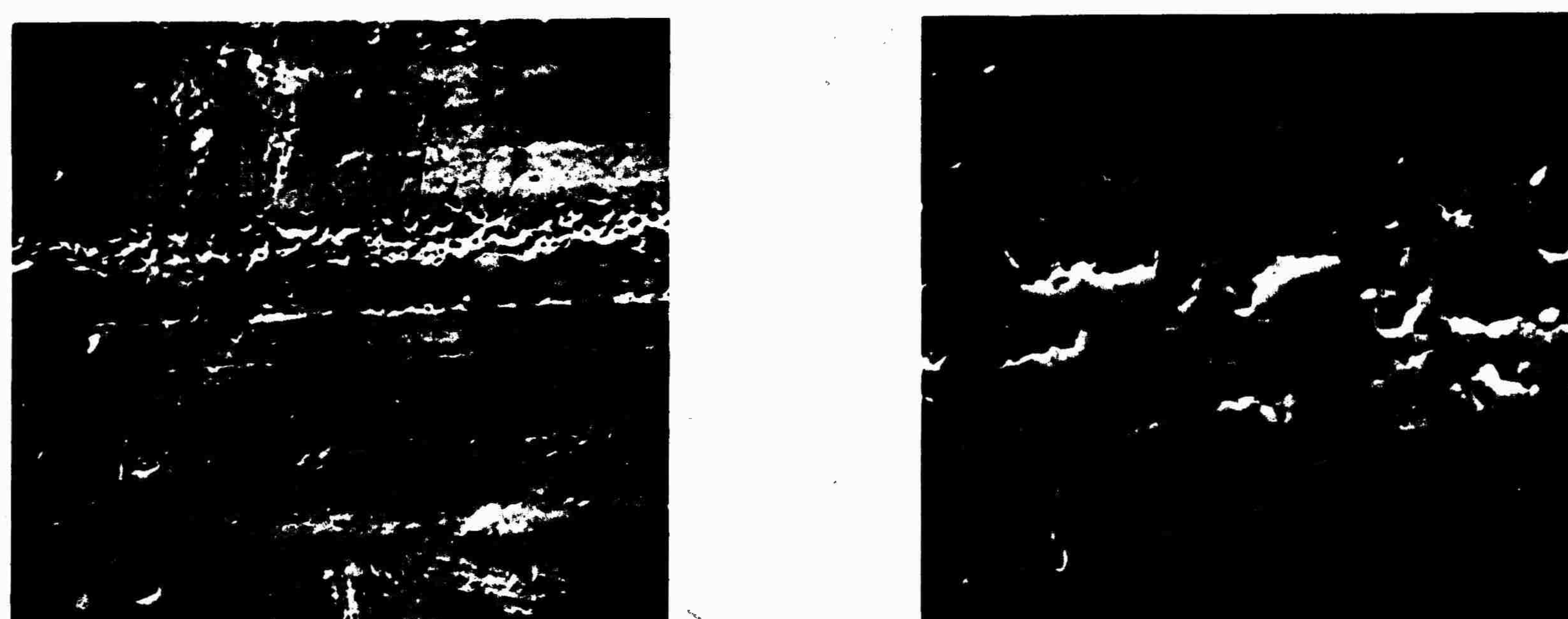

Magnification 500X

Magnification 2000X

Figure 130. Surface Pitting Near Spalled Area (P/N 204-040-330-3).

In the case of gear design as well as bearings, it would appear fruitful to investigate the predicted EHD film and compare it with known histories. Corrective measures in the form of surface finish refinement, entrainment velocity increases, and where possible, viscosity increases should be attempted when troublesome boundary lubricant regimes are predicted.

CONCLUSIONS

From this study of 251 UH-1 and CH-47 transmissions in overhaul at ARADMAC, it is concluded that:

1. Consideration should be given to reducing the extent of secondary damage by initial design arrangements since secondary failures caused by debris from the primary failures are extensive and costly. Compartmentalization is one possibility.

2. Changes should be made in the current overhaul criteria since a substantial part of the observed secondary failures resulted from assembly/disassembly or field maintenance action. Many parts were replaced for initial run-in wear, although the wear was self-correcting and occurred on parts with no primary failure history. Increased emphasis should be placed upon ease of field maintenance and overhaul in initial design.

3. Corrosion will become the dominant failure mode if the lives of the primary fatigue failure components are significantly improved, since a high percentage of parts were replaced at overhaul due to corrosion. Therefore, additional research should be directed toward preventing corrosion or improving both internal and external corrosion protection. Improvements in packaging and preservation of components for pre- and post-overhaul storage must be employed.

4. While the MTBR of the study components proved to be very near the TBO, the high replacement level of certain components (i.e., upper planetary sun gear, bevel gear and pinion support bearings, overrunning clutch components, rotor shaft bearings, support cases, bearing retainers, and planet gear bearings) prevent significant increases in TBO levels. Very few of the components in each transmission dominate the primary failure group and effectively control the TBO.

5. Conventional engineering methods are inadequate to predict the order of observed life or the failure modes. In many cases, gears having the same calculated stress values were observed to vary widely in life and failure mode. Bearing lives showed very little correlation with the standard B10 calculation. On the other hand, examination of the lubrication state of these various gear and bearing contacts proved to be helpful with respect to predicting the

failure mode, since in some cases relationship between predicted EHD film thickness and observed life was shown to exist.

6. Bearing metallurgical and manufacturing quality and consistency were found to be below those of gears, and the observed generic failure rates were considerably higher for bearings than gears.

7. Many of the primary failure modes observed have been drastically altered in later models of the transmissions studied due to product improvement and evolutionary changes. This illustrates the significance of the need for reevaluation of new helicopter transmission testing techniques to place emphasis upon finding the weak points early in the development cycle.

LITERATURE CITED

1. Army Equipment Record Procedures, U. S. Army TM-38-750, May 1967.

2. American Gear Manufacturers Association Technical Publications, AGMA Standards.

3. Standards for Ball and Roller Bearings and Steel Balls, Anti-Friction Bearing Manufacturers Association, Inc., 1960.

4. Dowson, D., Higginson, G. R., and Whitaker, A. V., Stress Distribution in Lubricated Rolling Contacts, Journal of Mechanical Engineering Sciences, 1962, No. 4, 121.

5. Johnson, L. G., The Statistical Treatment of Fatigue Experiments, General Motors Laboratories, GMR-202.

6. Coleman, W., A Scoring Formula for Bevel and Hypoid Gear Teeth, ASLE Transaction, October 1965, No. 65-LUBS.

7. Pressure-Viscosity Report, Volumes I and II, ASME Research Publication, 1953.

8. Dyson, A., Naylor, H., and Wilson, A. R., The Measurement of Oil Film Thickness in Elastohydrodynamic Contacts, Institution of Mechanical Engineers, Symposium in Leeds, Paper 10, September 1965.

9. Christensen, H., Nature of Metallic Contact in Mixed Lubrication, Institution of Mechanical Engineers, Symposium in Leeds, Paper 12, September 1965.

10. Chiu, Y. P., and McCool, J. I., Calculation of Minimum Lubricant Film Thickness in Rolling Bearings, SKF Research Laboratory Report No. AL64L006, 1964.

11. Bowen, C. W., Pitting Endurance of Carburized Spur Gears in Synthetic Lubricants, presented at the AGMA Technical Meeting, Chicago, Illinois, November 1967.

12. Weibull, W., A Statistical Theory of the Strength of Materials, Royal Swedish Academy of Engineering Sciences (Stockholm), 1939.

13. Lundberg, G., and Palmgren, A., Dynamic Capacity of Rolling Bearings, ACTA POLYTECHNICA, Royal Swedish Academy of Engineering Sciences, 1947.

14. Lundberg, G., and Palmgren, A., Dynamic Capacity of Roller Bearings, ACTA POLYTECHNICA, Royal Swedish Academy of Engineering Sciences, 1952.

15. 1400 Horsepower UH-1 Planetary Test on Regenerative Planetary Test Machine, Bell Helicopter Company Report No. 204-099-783, 1966.

16. Dudley, Darle W., Gear Handbook, The Design, Manufacture and Application of Gears, McGraw-Hill Book Co., 1962.

17. Aerospace Structural Materials Handbook, Vol. 1, Ferrous Alloys, Syracuse Univ. Press, Rev. 3, March 1966.

18. Palmgren, Arvid, Ball and Roller Bearing Engineering, S. H. Burbank & Company, Philadelphia, Pa., Copyright 1945, 1946, 1959, SKF Industries, Philadelphia, Pa.

19. Bowen, C. W., Low Speed Bearing Fatigue Problems and Their Possible Relation to Gear Problems, Presented at Aerospace Gearing Committee Meeting, Orlando, Florida, February 1964.

20. O'Donoghue, J. P., and Cameron, A., Friction and Temperature in Rolling Sliding Contacts.

21. Jones, A. B., Ball Motion and Sliding Friction in Ball Bearings, ASME-ARS Paper 58-AV-14, 1958.

22. Interdisciplinsry Approach to the Lubrication of Concentrated Contacts, A NASA Symposium, Proceedings Preprint Volume I and II, July 1969.

23. McIntire, W. L., and Malott, R. C., Advancement of Spur Gear Design Technology, Allison Division, General Motors, USAAVLABS Technical Report 66-85, U. S. Army Aviation Materiel Laboratories, Fort Eustis, Virginia, December 1966, AD 646648.

24. Metallurgical Analyses

Bell Helicopter Company

Met. Exam. Report Number 0068M-36	5 February 1968
Met. Exam. Report Number 0068M-70	25 March 1968
Met. Exam. Report Number TPL70-048	12 February 1970
Met. Exam. Report Number TPL70-49	13 February 1970
Met. Exam. Report Number TPL70-50	16 February 1970
Met. Exam. Report Number TPL70-0340	31 March 1970
Met. Exam. Report Number TPL70-341	20 March 1970
Met. Exam. Report Number TPL70-342	10 April 1970
Met. Exam. Report Number TPL70-348	23 March 1970
Met. Exam. Report Number TPL70-373	9 April 1970
Met. Exam. Report Number TPL70-394	9 April 1970
Met. Exam. Report Number TPL70-452	30 March 1970
Met. Exam. Report Number TPL70-467	24 March 1970
Met. Exam. Report Number TPL70-507	24 March 1970
Met. Exam. Report Number TPL70-573	9 April 1970
Met. Exam. Report Number TPL70-586	9 April 1970
Met. Exam. Report Number TPL70-610	25 March 1970
Met. Exam. Report Number TPL70-1128	4 June 1970

Battelle Memorial Institute

Stress Corrosion Cracking on 204-040-701 Gear	30 September 1966
Scanning Electron Microscopic Examinations of Spalling Failures	26 May 1970

Fafnir Bearing Company

Met. Lab. Report No. M-2270	8 June 1970
Met. Lab. Report Number M2276	23 June 1970

APPENDIX I

GLOSSARY OF DETAIL FAILURE ANALYSIS SHEET

GEAR ~~TOOTH~~ OR SPLINE

Wear

1. Destructive Wear

   Destructive wear is wear which has resulted in a corrosive change in the involute shape of the gear tooth. Destructive wear would be accompanied by extremely rough operations, nonuniform motion and shock overloads which would probably result in tooth breakage.

2. Abrasive Wear

   Under normal circumstances of lubrication, the occurrence of abrasive wear would be extremely infrequent. If the inclusion of sand and water in appreciable quantities should occur, abrasive wear may be observed. Fully case-hardened gears are not likely to exhibit any significant abrasive wear. Medium hard and soft gears will frequently exhibit this type of wear.

3. Galling

   Galling is a form of contact welding which results in the transfer of material from one gear member to another. It is also quite infrequent in moderate to high-speed gearing, but is often seen in low speed and stop-start type operations. An excellent example of spline galling occurs on the Model 206 sun gear spline.

4. Scoring

   This type of wear is often referred to as "scuffing" and is evidenced by radial wear lines superimposed on a roughened thin layer of melted material. Bright shiny wear on black oxided gear teeth must not be confused with true scoring. This condition though considered normal for many applications represents a lubrication state intermediate between thick film asperity separation and film failure conditions associated with scoring.

5. Frosting

The term frosting will be limited in usage to fully hardened gear tooth profiles. It shall be used to define the existence of a large number of small round or elliptical patches which under high magnification exhibit the general appearance of minute scoring occurrences.

6. Corrosive Wear

This term should not be used to define the existence of ordinary oxidation corrosion which is cause for replacement of the component. True corrosive wear occurs most generally in over-temperature operations in the presence of extremely strong EP additive lubricant of the chlorine or sodium families and therefore will be an infrequent occurrence.

7. Interference Wear

Interference wear does not occur in correctly designed, properly operating gear sets. Interference wear defines the effects of the tip of one gear tooth member contacting the fillet or root area of its mating gear tooth. If this occurs in the helicopter transmission, it will probably be accompanied by an extreme over-temperature condition or an unusual type of support bearing failure which reduces the operating clearance or backlash of the gear set.

8. Burning

Burning indicates surface tempering or softening of the tooth member. It will most probably be accompanied by a total loss of lubricant. Scoring, destructive wear, and tooth breakage may also be present. In general, burning is an advanced condition of the following term.

9. Discoloration

This term is used to locate the existence of surface temper coloring of either the active profile, the top land, or the coast side of the gear tooth. There is generally no appreciable softening of the metal to any significant depth. The condition may be indicative of marginal lubrication or excessive power operations.

10. Misalignment

Misalignment indicates operation of the gear or spline set at axes skewed from those intended by the designer. When this term is checked, at least one other term must also be checked to explain the physical result of the indicated misalignment.

11. Surface Treatment Worn Through

This term implies that the gear or spline in question was treated with an anti-wear surface coating such as Electro-Film, Dicronite, or in some instances, soft metal plating.

12. Oil Absent

This term indicates the partial or complete failure of the lubrication system either in the immediate area of concern or in the entire transmission.

13. Corrosion - Other

This term is used to define the existence of ordinary oxidation corrosion which is cause for replacement of the component. This may occur during helicopter non-operation intervals under severe moisture conditions or occur in transit, storage, or handling due to improper preservation. Indicate most likely reason under Item 12, Summary and Reworks.

<u>Surface Contact Fatigue</u>

1. Destructive Pitting

Destructive pitting shall be used to define the existence of advanced state of tooth profile deterioration. This term is used without concern as to the origin or generic identification of its beginning. It further indicates that complete loss of function of the gear tooth is imminent.

2. Spalling - Fan Shape

This term shall be used to define a pitting condition whose origin can be physically detected at the apex of the fan shape portion of the damaged area. This is a surface initiated type of fatigue which has its origin in the surface tensile cracking which leads to

the gradual erosion and exfoliation of increasingly larger pieces of gear material as the fan widens out in the direction of sliding action. The cracks will ultimately undermine the entire case of case-hardened gear teeth as the spalling approaches the extremities of the addendum.

3. Arrested Pitting

This term shall be used to indicate the existence of very small shallow pits which are not propagating into larger failure areas. A good example of this frequently occurs in the flank of the -108 planet pinions in contact with the nitrided -331 ring gears. This type of pitting has also been observed on spiral bevel gears and is frequently associated with the waviness condition referred to as "barber pole". This pitting is often considered to be corrective in that it progresses immediately to the point of relieving local compressive stress of over-load.

4. Pitch Line

Pitch line pitting belongs to the family of rolling contact fatigue and is truly subsurface in origin. It is not generally associated with a condition of lubrication distress but generally occurs at relatively high cycles of loading. In fully hardened, properly designed gears, it seldom is seen in less than 100,000 cycles of operation.

5. Addendum Origin

Checking this term merely signifies the site of origin of one of the above types of pitting or spalling.

6. Dedendum Origin

Checking this term merely signifies the site of origin of one of the above types of pitting or spalling.

7. Case Crushing

Case crushing means sheer failure of the core-case interface in case-hardened gear teeth. Generally, insufficient case depth for the load magnitude is indicated. Multiple cracking, often both transverse and longitudinal, is generally observed in the tooth face.

Breakage

1. Fatigue

   Fatigue shall be used to define high cycle repeating stress failure with a fracture surface being well defined with the customary clam shell or bench marks. Unless otherwise defined, it shall be assumed that the failure origin is in the root fillet area of the gear tooth.

2. Wear

   This term should not be used alone in the breakage category but merely serve as a modifier to indicate that some other form of breakage was accelerated by the presence of wear.

3. Overload

   In the instance of properly manufactured gears, the occurrence of overload breakage is evidenced by low cycle fatigue with few, if any, bench marks. The failure interface may in fact resemble the crystalline appearance of a static failure.

4. Misalignment

   Misalignment is operations at skewed axes, which results in a particular form of breakage defined elsewhere in this category.

5. Quench Cracks

   Quench cracks are generally cracks which occur at or near the interface of the core-case structure and result from either excessive case depth or improper location of the part relative to the quenching dies during the hardening process.

6. Grind Cracks

   Grinding cracks result from excessive temperature between the wheel and tooth interfaces during manufacture which induces a tensile stress field in excess of the elastic properties of the material. This type of crack is generally found to occur orthogonally to the direction of the grind wheel passage.

7. Impact

Impact breakage shall be that which results from sudden stoppage or debris in mesh. It will be a completely static fracture and will be accompanied by extreme deformation of the failed tooth in all cases except static fractures in nitrided gears.

Debris in Mesh

1. Moderate Damage

Moderate damage shall be defined as that level of damage which does not impair the basic functional operation of the gear tooth.

2. Heavy Damage

Heavy damage shall be defined as that level of damage which impairs the basic functional operation of the gear tooth and leads to catastrophic failure of the gear.

BEARINGS

1. Spalling

This term shall be used to define a flaking condition whose origin may be of the classical subsurface fatigue mode or a surface initiated type of fatigue.

2. Pitting

This term shall be used to indicate the existence of very small, shallow pits which are not propagating into larger failure areas.

3. Corrosion

This term is used to define the existence of ordinary oxidation corrosion which is cause for replacement of the component. This may occur during helicopter non-operation intervals under severe moisture conditions with or without the presence of highly contaminated oil.

4. Dented

Dents (indentations) in the raceway occur when foreign particles are introduced into the bearing and are

pressed between the rolling elements and the rings. Item 5 or Item 6 should be marked in conjunction with this failure mode. Denting is not to be confused with brinelling, which is explained in Item 13 below.

5. External Debris

This indicates that the debris which caused bearing damage did not originate from the bearing itself, but from another (external) failed or damaged part.

6. Internal Debris

This indicates that the debris which caused bearing damage originated within the subject bearing. For example, debris from inner race failure causing damage to the outer race.

7. Broken

This term is used to define the condition where the bearing element is fractured completely through the element crosssection. Additional information will usually be required in the Summary and Remarks section.

8. Cracked

a. Grind Cracks

Grinding cracks result from excessive temperature between the wheel and bearing element interfaces during manufacture which induces a tensile stress field in excess of the elastic properties of the material. This type of crack is generally found to occur orthogonally to the direction of the grind wheel passage.

b. Rubbing Cracks

If a hardened bearing ring under rotation rubs against a stationary part, rubbing cracks may develop. These cracks always run perpendicular to the direction of rubbing.

c. Defective Material Cracks

Cracks caused by defective material ordinarily have an easily recognizable character, but their actual cause can often be determined only by metallurgical investigation.

Any failure by cracking will require further explanation in the Summary and Remarks section.

9. Smearing

Smearing occurs because of rolling element skidding in the absence of sufficiently viscous lubrication. Smearing, as the name implies, is evidenced by a smeared-appearing deterioration of the raceway surface.

10. Glazing

This is a form of smearing whereby the affected area on the raceway becomes shiny in appearance, similar to the finish on a new ball. Metal flow has taken place during this mode of failure.

11. Wear

This is the deterioration of the bearing rolling surfaces through normal usage. Abrasives in the lubricated and/or poor lubrication accelerate the wear process.

12. Grooved

Continuous circumferential indentation on balls produced by balls running on retaining diameter of counterbored raceway.

13. Brinelled

Brinelled is a term applied to a bearing which has been statically loaded to an extent such that the raceways and rolling elements are permanently deformed. A brinelled bearing has indentions in the raceways and often has corresponding flats on the rolling elements.

14. Fretting

Fretting is generally considered to be a corrosive form of wear caused by very slight movement between two metal surfaces under very high contact pressure. The formation of an iron-oxide paste between two fretting steel members is not uncommon. It is often seen between the inner ring and the shaft.

15. Creeping

Creep is relative movement between the bearing inner ring and the shaft, caused by inadequate interference fit for the applied load. Creep causes not only undesirable ring wear but also excessive shaft wear. Creep is evidenced by circumferential scoring on the bearing bore and shaft. It may be an advanced stage of fretting.

16. Spinning

Spinning is an advanced stage of creep. The relative movement between inner ring and shaft is much greater than in creep, and the sliding surfaces may become polished. The iron-oxide from the fretting phase may still be present and assist in further wear.

17. Incorrect Installation

This term will be used when the bearing has obviously been damaged at installation or has been installed incorrectly. A common example is forcing an assembled roller bearing over the inner race with the rollers misaligned, causing marks (smeared streaks) on the inner race.

18. Disassembly Damage

This term will be used when the bearing was damaged at disassembly.

19. Discolored Due to Temperature

Discoloration of bearing elements indicates operation with marginal lubrication or at excessive power conditions.

APPENDIX II

INSTRUCTIONS FOR CREATION AND UPDATING OF GFAS AND DFAS FILES

PURPOSE

This program shall create two data tape files from input card data (or add to previously created data tape files). The input cards represent helicopter transmission overhaul data collected at ARADMAC.

INPUT

1. The first data tape file shall be created from input cards keypunched from the Gearbox Failure Analysis Sheet (GFAS). Each tape record shall consist of 80 bytes and will be created from a GFAS card. The format of the GFAS card is as follows:

Field Identification	Position in Card and Record	Field Length
GFAS Number	1 - 4	4
Last Location Code	5	1
Aircraft Type	6 - 10	5
Aircraft S/N	11 - 18	8
Date Removed (Julian)	19 - 22	4
Transmission P/N	23 - 37	15
Transmission S/N	38 - 45	8
Hours Since New	46 - 49	4
Hours Since O/H	50 - 53	4
No. of Previous O/Hs	54	1
Oil Sample Condition Code	55	1
Filter Condition Code	56	1
Quills Removed Code	57	1

Removal Reason Code	58 - 60	3
Removal Reason Remarks	61 - 76	16
Report Data (Julian)	77 - 80	4

See the enclosed GFAS for reference.

2. The second data tape file shall be created from input cards keypunched from the Detail Failure Analysis Sheet (DFAS). There are three distinct DFAS's: one for gears, one for bearings, and one for general parts. Each DFAS generates two cards, a card 1 and a card 2. The format of the first cards is unique. However, the format of the second cards depends on which DFAS the card was keypunched from. Each data file record shall consist of 160 bytes. The tape record is obtained by concatenating a card 1 and a card 2 which have identical DFAS numbers.

a. The format of the DFAS card 1 is as follows:

Field Identification	Position in Card and Record	Field Length
DFAS Number	1 - 7	7
Date (DA/MO/YR)	8 - 13	6
Part Number	14 - 28	15
Part Name	29 - 38	10
Part S/N	39 - 46	8
Ref. Data	47 - 50	4
Failure Type	51	1
Failure Identified By	52	1
Probable Short Term Effect of Failure	53	1
Continued Capability Probability	54	1
Failure Mode	55 - 79	25
Card Code	80	1

See enclosed DFAS for reference.

b. The format of the DFAS card 2 is as follows:

Field Identification	Position In Card	Position In Record	Field Length
DFAS Number	1 - 7	81 - 87	7
Failure Modes and Definitions	8 - 79	88 - 159	72
Card Code	80	160	1

Please refer to the enclosed DFAS's for card column identification of failure modes or reasons for removal of the detail part from the transmission. A letter code in column 5 of the DFAS number shall identify which set of failure mode descriptions is to apply. The code is as follows:

Code	Detail Parts
A	Gears
B	Bearings
C	General Parts

CODES AND TRANSLATION

Provisions for more information to appear on each card and record are available through the use of codes.

1. GFAS Codes

a. GFAS Number

The GFAS Number shall consist of an initial letter code and three digits. The letter code is as follows:

Code	Identification
B	Bell
F	Vertol, Forward
C	Vertol, Center
A	Vertol, Aft

The digits will be a consecutive or chronological sequence 001 through 999. (There will exist B001 and C001, etc.) Each DFAS Number will uniquely define a transmission overhaul and thus a GFAS tape record.

b. Last Location Code

This code will be a one-byte A/N code which will identify the last location using the transmission before being sent to ARADMAC. These codes will be supplied as soon as they are available.

c Oil Sample Condition Code

This code will be a one-digit numeric code indicating the condition of the oil sample taken from the transmission during overhaul. These codes are defined as follows:

Code	Description
1	Clean
2	Sludge or dirt
3	Heavy sludge or dirt
4	Contaminated with water
5	A few metal particles
6	Loaded with metal particles

d. Filter Condition Code

This code will be a one-digit numeric code indicating the condition of the oil filter removed from the transmission during overhaul. These codes will be supplied as soon as available.

e. Quills Removed Code

This code will indicate whether or not the quills were removed in the field before being sent to ARADMAC. See enclosed GFAS for codes.

f. Reason Code

This code is a three-digit numeric code and indicates the reason for removal of the transmission for overhaul. The code used will be the Army Failure Codes as used on TAERS data.

2. DFAS Codes

a. DFAS Number

The DFAS number will uniquely define a detail part removed from a transmission and the transmission that the part was removed from. The DFAS number thus uniquely determines a DFAS tape record. The first four bytes of the DFAS number will be identical to the GFAS number of the transmission from which the detail part was removed. It, therefore, established a cross reference between the two data tape files. The fifth byte is the letter code as defined in section B.2.b. The last two digits of the DFAS number represent a consecutive or chronological sequence 01 through 99.

Sample DFAS Number:

B-007-B-12

Bell Trans.	7th Bell Trans. Examined	Bearing Failure Reported	12th DFAS Processed on This Trans.

b. Failure Type

See enclosed DFAS.

c. Failure Identified by:

See enclosed DFAS.

d. Probable Short Term Effect of Failure:

See enclosed DFAS.

e. Continued Capability Probability

See enclosed DFAS.

f. Degree of Failure Condition Code

This code will indicate the degree of failure condition (e.g., the amount of bearing wear). This code will appear in one or more columns of the Failure Mode Description Field (i.e., columns 9 through 79 of the second card). The code is as follows:

Code	Degree
0	Slight
+	Moderate
#	Heavy
x	Other

Other will be used for those failures in which the degree of failure is unknown or unspecified, or in which the degree code is inapplicable (e.g., limited life).

APPENDIX III

SAMPLE CALCULATIONS

SPUR GEAR TOOTH BENDING STRESS (AGMA)

$$f_B = \frac{1.5T \left[.18 + \left(\frac{2t_{LN}}{r_f}\right)^{.15} \left(\frac{2t_{LN}}{h_{LN}}\right)^{.45} \right] \left[\frac{1}{X_{LN}} - \frac{\tan \phi_{LN}}{3t_{LN}} \right]}{\left[\frac{N}{2P} + \frac{\Delta R_{LN}}{P} \right] \left[F_e \right]}$$

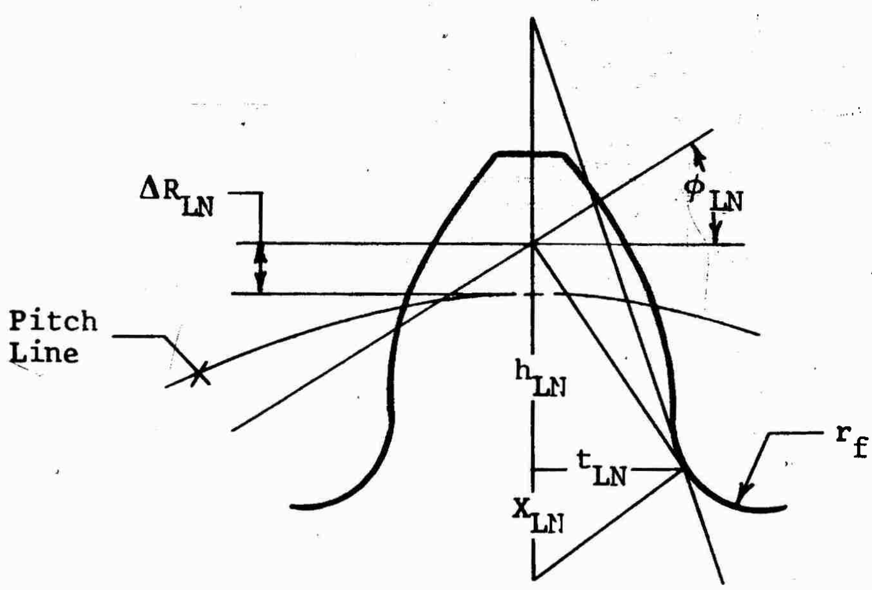

SPUR GEAR UNIT LOAD

$$U.L. = \frac{W_T P_d}{F}$$

W_T = Tangential Tooth Load

P_d = Diametral Pitch

F = Face Width

For 204-040-329 lower sun gear, UH-1 transmission:

W_T = 1731 Lbs

P_d = 8.5

F = .938

$$U.L. = \frac{(1731)(8.5)}{.938}$$

$$= 15{,}700 \text{ PSI}$$

SCORING FLASH TEMPERATURE INDEX

$$T_f = T_i + \Delta T$$

T_i = Temperature of Lubricant at Inlet Conditions

$$\Delta T = \left[\frac{W_{Te}}{F_e}\right]^{3/4} \left[\frac{50}{50-S}\right] \left[\frac{Z_T(n_p)}{(P_d)^{1/4}}\right]^{1/2}$$

W_{Te} = Effective Tangential Load, Lbs

F_e = Effective Face Width, In.

S = Surface Finish, RMS

Z_T = Scoring Geometry Factor

$$= \frac{.0175\left[\sqrt{R_p} - \sqrt{\frac{N_p}{N_g} R_g}\right]\left[P_d\right]^{1/4}}{(\cos\theta_t)^{3/4}\left[\frac{R_p R_g}{R_p + R_g}\right]^{1/4}}$$

n_p = Pinion RPM

P_d = Diametral Pitch

N_p, N_g = Number of Pinion and Gear Teeth, Respectively

R_p, R_g = Radii of Curvature, Pinion and Gear, Respectively

θ_t = Pressure Angle

The above formula is evaluated by digital computer for all power loaded gear meshes in the four transmissions studied. The results are shown in Table XII.

SURFACE COMPRESSIVE STRESS

$$f_c = 2260\sqrt{\frac{W_T}{FR'}}$$

W_T = Tangential Load

R' = Reduced Radius of Curvature

F = Face Width

For 204-040-329 lower sun gear, UH-1 transmission at pitch line.

W_T = 1731

F = .938

$$R' = \frac{.683 \times 1.256}{.683 + 1.256}$$

$$f_c = 2260\left[\frac{1731}{.938} \quad \frac{.683+1.256}{.683 \times 1.256}\right]^{1/2}$$

$$= 146{,}000 \text{ PSI}$$

LUBRICANT FILM THICKNESS (EHD) BEARINGS (Ref. 10)

$$\frac{h}{R'} = 1.13\left[\frac{P'}{E'R'}\right]^{-.091}\left[\frac{n_o\,\alpha V}{R'}\right]^{.727}$$

$$R' = \left[\frac{1}{R_1} + \frac{1}{R_2}\right]^{-1} = \text{Reduced Radius of Curvature}$$

P' = Load Per Unit Length on Max Loaded Element

E' = Reduced Modulus

V = Rolling Velocity

n_o = Lubricant Viscosity at Inlet Conditions, cs

α = Pressure Coefficient of Viscosity

The above formula has been evaluated by digital computer for each power loaded bearing in the four transmissions under investigation. Results are shown in Table XIII.

LUBRICANT FILM THICKNESS (EHD) GEARS

$$\frac{h_{min}}{R} = 2.65\ G^{.57}\ U^{.7}/W^{.13} \qquad \text{(Ref. 4)}$$

$$W = \frac{w}{E'R'}\ ,\ U = \frac{\eta_o u}{E'R'}\ ,\ G = \gamma E'$$

E' = Reduced Modulus

R' = Reduced Radius of Curvature

w = Unit Load, Lb/In.

η_o = Lubricant Viscosity, cs

u = Sun Velocity, In./Sec

γ = Pressure Coefficient of Viscosity

LUBRICANT FILM THICKNESS (EHD) GEARS (BHC)

$$h_{min} = .274\sqrt{(k/T)^2 V_S}$$

k = Constant Depending on Type of Lubricant

T = Temperature of Conjunction, Depending on Load, Lubricant Viscosity, and Coefficient of Friction at Contact Point

The above formula has been evaluated for all power loaded spur and spiral bevel gears by digital computer. The results are tabulated in Table XII.

AFBMA B_{10} BEARING LIFE

Basic Dynamic Capacity of 114DS240-2 Roller Bearing

$$C = fc\ (i\ l_{eff}\ \cos\alpha)^{7/9}\ Z^{3/4} D^{29/27}$$

i = 1 (Number of Rows)

l_{eff} = 0.936 In. (Effective Length)

α = 0 (Contact Angle)

$Z = 16$ (Number of Rollers)

$D = 1.023$ (Roller Diameter)

$$fc = (49{,}500)(fc/f); \; (fc/f) = f\left(\frac{D\cos\alpha}{dm}\right)$$

Based on line contact of roller with both inner and outer rings:

$(fc/f) = .1038$ (Ref. AFBMA)

Therefore, $C = 40{,}900$ Lbs

Bearing Load, at 100% Torque = 13,422 Lbs

B_{10} at 100% Torque $= (C/P)^4(10^6)$ Rev.

$$= \left(\frac{40{,}900}{13{,}422}\right)^4 = 85.9 \text{ MR} \quad \text{(MR = Millions of Revolutions)}$$

Unclassified
Security Classification

DOCUMENT CONTROL DATA - R & D

(Security classification of title, body of abstract and indexing annotation must be entered when the overall report is classified)

1. ORIGINATING ACTIVITY (Corporate author) Bell Helicopter Company A Division of Textron Fort Worth, Texas	2a. REPORT SECURITY CLASSIFICATION Unclassified 2b. GROUP	
3. REPORT TITLE MODE OF FAILURE INVESTIGATIONS OF HELICOPTER TRANSMISSIONS		
4. DESCRIPTIVE NOTES (Type of report and inclusive dates) Final Report		
5. AUTHOR(S) (First name, middle initial, last name) C. W. Bowen L. L. Dyson R. D. Walker		
6. REPORT DATE January 1971	7a. TOTAL NO. OF PAGES 236	7b. NO. OF REFS 24
8a. CONTRACT OR GRANT NO. DAAJ02-69-C-0061 b. PROJECT NO. Task 1G162203D14414 c. d.	9a. ORIGINATOR'S REPORT NUMBER(S) USAAVLABS Technical Report 70-66 9b. OTHER REPORT NO(S) (Any other numbers that may be assigned this report) BHC Report 299-099-479	
10. DISTRIBUTION STATEMENT This document is subject to special export controls, and each transmittal to foreign governments or foreign nationals may be made only with prior approval of Eustis Directorate, U.S. Army Air Mobility R&D Laboratory, Fort Eustis, Virginia 23604.		
11. SUPPLEMENTARY NOTES	12. SPONSORING MILITARY ACTIVITY Eustis Directorate U.S. Army Air Mobility R&D Laboratory Fort Eustis, Virginia	

13. ABSTRACT

This report presents the results of the engineering review and analysis of failed parts rejected during UH-1 and CH-47 transmission overhaul at ARADMAC. The analysis included metallurgical and metrological examinations, the identification of failure modes, the computation of operating stresses, and the correlation of calculated with observed component lives. Tribological considerations were employed in the identification of failure modes and extensive use was made of special computer programs in the generation of failure data and the correlation studies. The study revealed that overhaul life is limited by a few parts whose failure rates exceed the mean by an order of magnitude. Areas of needed research and development to improve design capabilities are identified.

DD FORM 1 NOV 65 1473 REPLACES DD FORM 1473, 1 JAN 64, WHICH IS OBSOLETE FOR ARMY USE.

Unclassified
Security Classification

Security Classification

14. KEY WORDS	LINK A		LINK B		LINK C	
	ROLE	WT	ROLE	WT	ROLE	WT
HELICOPTERS Transmissions Gearboxes TRANSMISSIONS Failure Modes Gears Bearings Reliability Overhaul GEARBOXES Analysis Wear Corrosion Design Life TRIBOLOGY Gear Conjunctions Bearing Conjunctions						

Unclassified
Security Classification